Shyam Kanhaiya
Saurabh Singh
Arohi Dixit
Atul Kumar Singh *Editors*

# Rivers of India

## Past, Present and Future

Springer

Rivers of India

Shyam Kanhaiya • Saurabh Singh
Arohi Dixit • Atul Kumar Singh
Editors

# Rivers of India

## Past, Present and Future

Springer

*Editors*
Shyam Kanhaiya
Department of Earth and Planetary Sciences
Prof. Rajendra Singh (Rajju Bhaiya)
Institute of Physical Sciences for Study and Research
VBS Purvanchal University
Jaunpur, Uttar Pradesh, India

Arohi Dixit
University of Delhi
New Delhi, India

Saurabh Singh
Department of Geology
Institute of Earth and Environmental Sciences
Dr. Rammanohar Lohia Avadh University
Ayodhya, Uttar Pradesh, India

Atul Kumar Singh
North-Eastern Hill University
Shillong, Meghalaya, India

ISBN 978-3-031-49162-7 ISBN 978-3-031-49163-4 (eBook)
https://doi.org/10.1007/978-3-031-49163-4



This Springer imprint is published by the registered company Springer Nature Switzerland AG
The registered company address is: Gewerbestrasse 11, 6330 Cham, Switzerland

Paper in this product is recyclable.

# Contents

# Geomorphological and GIS-Based Analysis of Catchment Areas in River Narmada, Central India


**Ankita Singh and Vipin Vyas**

## 1 Introduction

Evaluating landforms, sediment transport, and river flow are all aspects of the geomorphological study. In the upper course, middle course, and lower course rivers, different landforms, such as river valleys, waterfalls, river terraces, river meanders, floodplains, etc., are created by the processes of erosion and deposition. Rivers use a downward angle to transport material to their riverbeds, permitting the emergence of riverbanks, river deltas, alluvial fans, etc. The channel variations and their development are arguably the most studied platform morphology in geomorphological investigations. The study of the earth's surface's physical characteristics and how they relate to its geological structure is known as geomorphology (Pal & Pani, 2019). Morphometry is the measurement and quantitative analysis of the size, shape, and landforms of the planet (Rai et al., 2018). Understanding the dynamics of the channel planform and how it complies with floodplain regions requires an interdisciplinary approach in order to understand river morphology. In 1945, Horton developed a method for the quantitative analysis of drainage basins; in 1964, Strahler modified it. Aerial climate, regional tectonics, the slope, and the geology of the catchment area all contribute to the creation of drainage basin features. In order to determine ways of preserving and managing the environment's resources and averting natural disasters, this methodology, which is important in the field of geological studies, will evaluate the features of the drainage basins and their relationship to the terrain (Biswas et al., 1999; Pareta & Pareta, 2011). We can retrieve the geomorphological information that analysis may use to rank or list river basins by analysing numerous linear and aerial catchment area parameters. Additionally, it may assess and set up the basin to save soil and water (Mahale, 2020).

A. Singh (✉) · V. Vyas
Department of Environmental Sciences & Limnology, Barkatullah University, Bhopal, Madhya Pradesh, India



S. Kanhaiya et al. (eds.), *Rivers of India*,
https://doi.org/10.1007/978-3-031-49163-4_1

The morphometric analysis produces a quantitative representation of the seepage framework, a crucial component of the representation of catchment areas, and a crucial hydrological finding that helps to predict the behaviour of a watershed under the assumption that geomorphology and geography are correctly combined (Strahler, 1964; Chopra et al., 2005). The findings of multiple researchers' morphometric studies of river basins using remote sensing and GIS techniques, such as geomorphological characteristics of river basin used in hydrological modelling, assessment of the possibility of groundwater (Nag, 1998), and watershed prioritisation (Patel et al., 2013). The satellite pictures give a concise perspective of a wide region and are too convenient in the study of drainage basin morphometry, making remote sensing technology the ideal way for analysing morphometric features.

The majority of the issues with land and water resource planning and management may currently be controlled by spatial information technology, such as remote sensing, GIS, and GPS (Global Positioning System), in place of traditional data processing techniques (Pirasteh et al., 2010). For this type of study, the Shuttle Radar Topography Mission (SRTM) and Advanced Spaceborne Thermal Emission and Reflection Radiometer (ASTER) data are used in GIS-based analysis which has given a quick, accurate, or error-free and low-cost method through which hydrological systems can analyse (Smith & Sandwell, 2003; Grohmann, 2004). Nowadays the processed digital elevation model (DEM) data was used for creating the stream network and its supporting layers in different software for remote sensing (Magesh et al., 2011). It is simple to combine hydrological and spatial analysis with remote sensing satellite data to identify and characterise drainage areas.

The study mentioned above attempts to examine the various morphometric parameters of the three sub-basins of the river Narmada utilising remote sensing and GIS technologies in order to comprehend the peculiarities of the watershed. We account for the linear, aerial, and relief elements of the three different forms of the morphometrical study performed in this work. The drainage lines shown on the topographical map with their slopes and terrain characteristics were subjected to this study utilising a GIS-based technique. The useful results of the current investigation will be particularly practical for groundwater management, construction, and flood mitigation in the river watershed and surrounding regions. They will also aid in understanding the state of the geomorphology of the river's history and present look.

## 2 Methodology

### *2.1 Study Area*

The Narmada River is both the longest river running west in India and the largest river flowing through the state of Madhya Pradesh. It comes from the Amarkantak Plateau in Madhya Pradesh's Anuppur district, which is located on the northern

border of the Deccan Plateau between the longitudes 72°32′ and 81°45′ east and the latitudes 21°20′ and 23°45′ north. Because a large portion of the people in Madhya Pradesh relies on the Narmada River for their livelihood, the river's quality might be affected either geomorphologically or chemically. Therefore, we do geomorphological research in order to understand the status of rivers in the different catchment areas of river Narmada in a state which is shown in Fig. 2.

We choose the Dudhi River, Palakmati River, and Ganjal River as the three catchment regions of the Narmada River, which are located from Hoshangabad to Harda in the centre zone of the Narmada (Fig. 1) at latitude 22°23′N and longitude 78°45′E to latitude 22°56′N and longitude 77°21′E. The Dudhi River is a tributary of the Narmada River and is located on the left bank in the Chhindwara district of Madhya Pradesh and joins the Narmada River near Nibhora, 575 km from its source. The other tributary of the Narmada River is the Palakmati River that enters the Sohagpur Block in the Hoshangabad (Narmadapuram) district of Madhya Pradesh from the south of the hamlet of Chherka. It is situated at 22°36′35"N and 78°11′25"S. The Palakmati and Narmada rivers met in Pamli hamlet, which is located at 22°02′10″N and 78°06′55″S. The river's whole catchment area is 131.66 km$^2$. The Ganjal River is rising from the Satpura region of the Betul district of Madhya Pradesh, 800 m north of the settlement of Bhimpur, in latitudes of 22°0′N and 77°30′E. It meanders 89 km in a north-westerly direction until joining the Narmada River close to the settlement of Chhipaner.

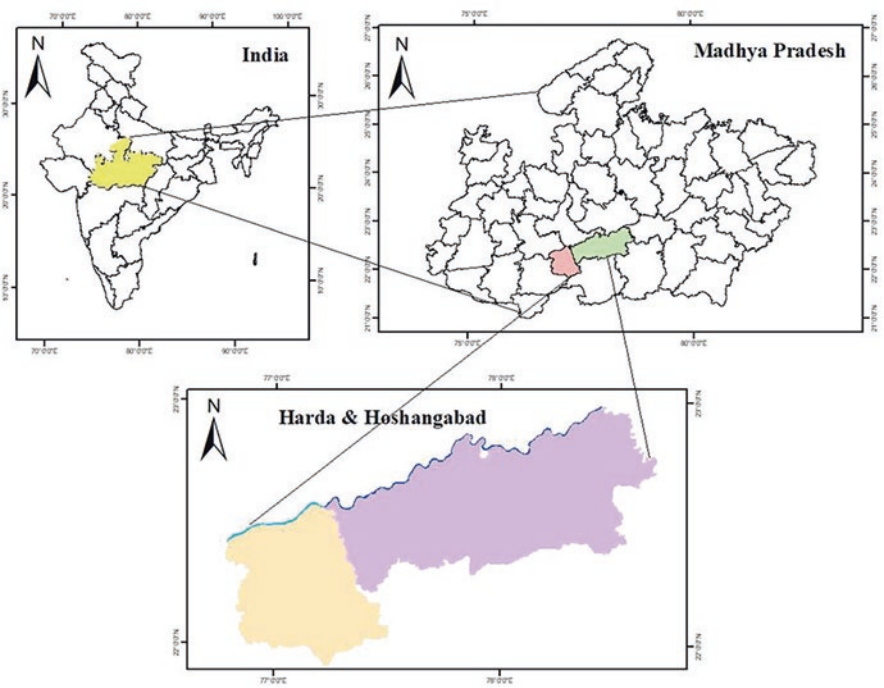


**Fig. 1** Map showing the study area

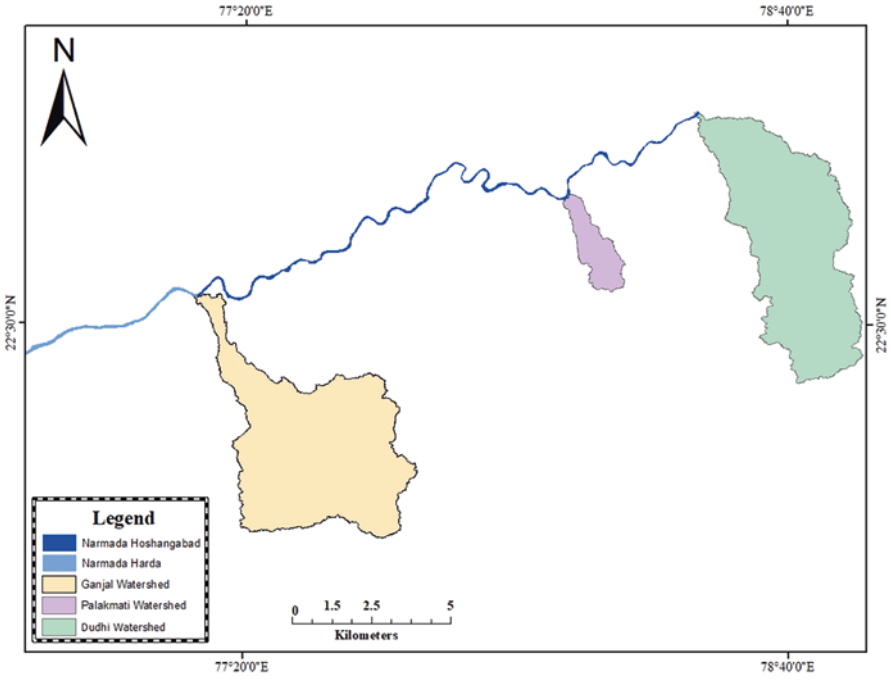


**Fig. 2** Map showing catchment areas

The climate that traverses the Narmada basin in the upper plain's region was impacted by the Tropic of Cancer, and below this line, a significant portion of the basin may be retracted. The basin has a tropical, humid climate at higher hill levels which endures four different seasons each year: cold weather, hot weather, the southwest monsoon, and post-monsoon. For the basin, the average yearly rainfall is 1178 mm. The main rainy season, the southwest monsoon, lasted from June through October and contributed to almost 94% of the annual rainfall. The months of July and August get almost 60% of the yearly rainfall. From east to west, it becomes less. The northern portions of the world have summertime maximum temperatures of around 42.5 °C and wintertime average temperatures that range from 10 to 15 °C in the south but only as low as 10 °C in the north. From lush green in the top section to dry deciduous teak forest flora in the lower part, a variety of vegetation is there. The Narmada River watershed is home to some of India's greatest hardwood forests including teak, *Terminalia arjuna*, *Syzygium cumini* (Jambul), *Syzygium heyneanum*, *Salix tetrasperma*, etc. (Fig. 2).

**Table 1** Linear, relief, and aerial morphometric parameters used for river watershed

| S. No. | Parameter | Formula |
|---|---|---|
| 1 | Stream order (U) | Hierarchical rank |
| 2 | Stream length (Lu) | Length of the stream |
| 3 | Mean stream length (Lsm) | Lsm = Lu/Nu |
| 4 | Stream length ratio (RL) | RL = Lu/(Lu − 1) |
| 5 | Bifurcation ratio (Rb) | Rb = Nu/Nu +1 |
| 6 | Mean bifurcation ratio (Rbm) | Rbm = average of bifurcation ratios of all orders |
| 7 | Drainage density (Dd) | Dd = Lu/A |
| 8 | Drainage texture (T) | T = Dd 9 Fs |
| 9 | Stream frequency (Fs) | Fs = Nu/A |
| 10 | Elongation ratio (Re) | Re = D/L = 1.128HA/L |
| 11 | Circulatory ratio (Rc) | Rc = 4pA/P2 |
| 12 | Form factor (Ff) | Ff = A/L2 |
| 13 | Length of overland flow (Lg) | Lg = 1/D 9 2 |
| 14 | Relief | R = H - h |
| 15 | Relief ratio | Rr = R/L |

## *2.2 Data and Methods*

The boundaries of the river basin or watershed and the drainage/stream network from the tributaries of the Narmada River basin have been extracted automatically using ASTER DEM data in this study to analyse the morphometric characteristics of a basin. Software utilised included ArcGIS 10.3 and ERDAS Imagine-9.1. The extracted river basin and stream networks are projected regionally, using WGS-1984 and UTM zone 44N, and Table 1 can display the various morphometric parameters that were established for this study.

### 2.2.1 Extraction of River Watershed

The georeferenced SOI toposheets at a scale of 1:50,000 are used to automatically extract the tributaries of the Narmada River basin from the DEM data which was retrieved in ArcGIS 10.3. A systematic procedure that is carried out in ArcGIS using a variety of tools creates a watershed boundary polygon from the flow direction raster data because of the automated extraction of the basin/watershed.

### 2.2.2 Extraction of Drainage Network

In ArcGIS 10.3 the tributaries are retrieved by using geoprocessing tools (Fig. 3). The outcome of this process generates a stream or drainage network with stream order following Strahler's stream order system. According to Strahler's system of categorisation, a segment without any tributaries is referred to as a stream of first order; if two first-order stream segments converge, they create a stream segment of

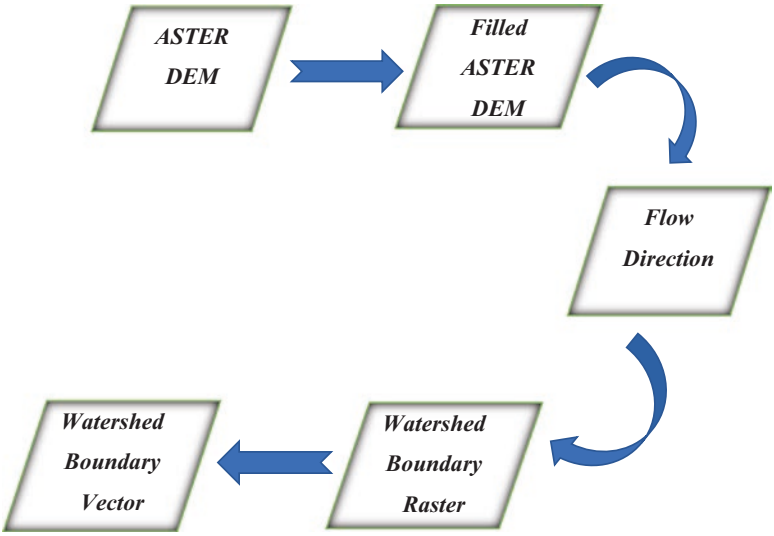


**Fig. 3** Flow chart of the methodology

second order and so on. Sixth place was found to be the highest stream order in the chosen tributary basins. We need DEM and upstream area characteristics, which are the minimum drainage area requirements for the study using this approach, in order to generate a stream segment (Magesh et al., 2013). The linear aspect, aerial aspect, and relief aspect have all been examined in order to evaluate the drainage basin morphometry using the common mathematical method shown in Table 1. We have obtained the aspect and slope map of the study region from the ASTER DEM by using hydrological tools in the ArcGIS 10.3 spatial analyst module (Figs. 4 and 6).

### 2.2.3 Terrain Status

Each landform and bedrock type has a distinctive topographic form, including a typical size and shape. Relief or terrain refers to the vertical or horizontal dimensions of the land. The geography of the area may be described in terms of big, imposing, broken-up steep hillsides, gully slopes, karst, and so on. The terrain state of the river basin's tributaries may also be examined in this study, and a clear topographic shift can be seen when two different landforms converge.

## 3 Results and Discussion

As a result, the morphometric parameters of the river basin, such as its linear aspect, relief aspect, and aerial aspect, are shown in Table 2. These parameters include the basin's area, perimeter, length, stream order and length, mean stream length, stream length ratio, bifurcation ratio, relief ratio, ruggedness number, stream frequency,

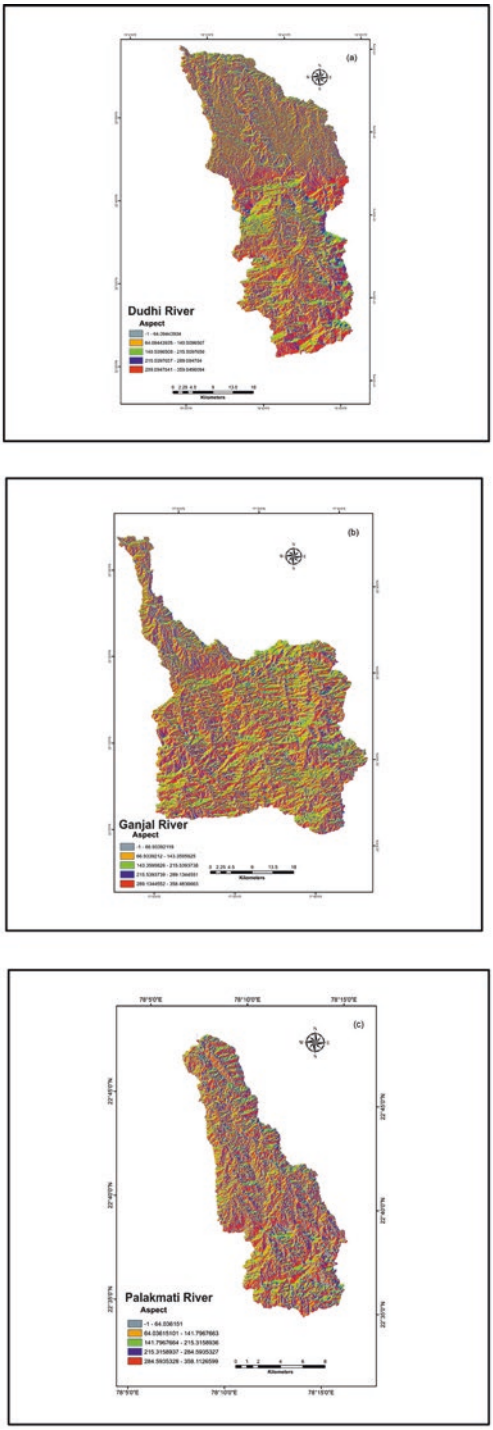


**Fig. 4** Aspect maps of river basin

**Table 2** Results of linear morphometric analysis of three rivers of the Narmada basin

| S. No | Morphometric parameters | Dudhi River | Palakmati River | Ganjal River |
|---|---|---|---|---|
| | Area of the basin ($km^2$) | 1506 | 172 | 1639 |
| 1. | Stream order (U) | V | V | VI |
| 2 | Stream no. | I: 390, II: 91, III:25, IV: 7, and V: 1 | I: 358, II: 105, III: 20, IV: 3, and V: 1 | I: 420, II: 110, III: 22, IV: 3, V: 2, and VI: 1 |
| 3 | Stream length (Lu) | I: 617.205, II: 356.606, III: 188.582, IV: 114.825, and V: 10.084 | I: 206.597, II: 98.244, III: 40.473, IV: 52.639, and V: 26.199 | I: 695.282, II: 307.542, III: 121.425, IV: 183.671, V: 52.217, and VI: 33.813 |
| 4 | Mean stream length (Lsm) | I: 2.12, II: 3.91, III: 7.54, IV: 16.40, and V: 10.084 | I: 0.57, II: 0.93, III: 2.02, IV: 17.54, and V: 26.199 | I: 2.17, II: 2.79, III: 5.51, IV: 61.22, V: 26.10, and VI: 33.81 |
| 5 | Stream length ratio (RL) | II/I = 0.57; III/ II = 0.52; IV/ III = 0.60; and V/ IV = 0.08 | II/I = 0.47; III/ II = 0.41; IV/ III = 1.30; and V/ IV = 0.49 | II/I = 0.44; III/ II = 0.39; IV/III = 1.51; V/IV = 0.28; and VI/V = 0.64 |
| 6 | Bifurcation ratio (Rb) | I and II = 3.18; II and III = 3.64; III and IV = 3.57; and IV and V = 7.00 | I and II = 3.40; II and III = 5.25; III and IV = 6.66; and IV and V = 3.00 | I and II = 2.90; II and III = 5.00; III and IV = 7.33; IV and V = 1.50; V and VI = 2.00 |
| 7 | Mean bifurcation ratio (Rbm) | 4.34 | 4.57 | 3.74 |

elongation ratio, etc. This work places a strong focus on the use of satellite remote sensing for morphometric analysis in order to avoid the traditional laborious technique. Below are the results in more detail.

## *3.1 Aspect*

The topographic feature reveals the potential slope orientation, which can have a big impact on the local climate (Kanhaiya et al., 2019). An aspect of the Dudhi, Palakmati, and Ganjal rivers, showing the basin's north, northwest, south, and southwest-facing slopes, is shown in Fig. 4. This slope's characteristics, which include its higher moisture content and lower evaporation than other basin areas, are crucial for maintaining the study's biodiversity, forests, and flora.

### 3.1.1 Slope

The analysis of the basin's slope is a crucial component of geomorphological research since it depends on the types of rocks in its catchment region, each of which has a different resistance (Magesh et al., 2011). Because they are closely tied to run-off of the water that creates the network of the river basin, slope factors are influencing the amount of time that rain must fall before reaching the river beds. Using the analytical features of ArcGIS 10.3, which is depicted in Fig. 4, the slope map in this study is produced in a percent increase and is based on DEM data. Dudhi River's slope ranges from 0 to 59,700,00; Palakmati River's slope is between 0 and 55,100,000; and Ganjal River's slope is between 0 and 54,100,000. The planning for watershed management, agricultural processes, reforestation/deforestation, water harvesting, civil engineering purposes, and morpho-conservation methods in river basins may all be outlined using this slope map (Sreedevi et al., 2005).

### 3.1.2 Terrain Status

In this study, Dudhi, Palakmati, and Ganjal rivers' terrain were calculated as tributaries of the Narmada River. These three tributaries are between 60.556 and 1213 m in elevation. According to Fig. 9, the Dudhi River has the highest height (1213 m), while the Palakmati River has the lowest elevation (545 m).

## *3.2 Linear Aspect*

This aspect contains the following variables, which were computed, and the results are shown in Table 2.

### 3.2.1 Stream Order

Strahler (1964) suggested a hierarchical ordering system for all three catchments, the Dudhi, Palakmati, and Ganjal rivers, where all have streams that reach the fifth and sixth orders, respectively. According to Strahler, the tributaries of the smallest fingerprint were assigned a first-order number. A second-order stream forms when two first-order streams collide. When two second-order streams meet, a third-order stream is generated and so on. The channel, which was designated as one of any drainage basin's top rank streams, was where most of the water was dumped. The flow sequence is influenced by the basin's shape, size, and relief characteristics of this type of basin (Maurizio Lazzari, 2020).

### 3.2.2 Stream Number

According to Horton's law from 1945 the "number of stream segments of each order forms an inverse geometric sequence with an order number" (Shah et al., 2021). Most first-order streams are found in the Ganjal River, which implies a less permeable formation and soft lithology, whereas the fewest first-order streams are found in the Palakmati River.

### 3.2.3 Stream Length

Using GIS software, we measured the length of the stream from the river mouth to the drainage split and then conducted this analysis based on Horton's law (1945) for the research region. The greatest length of streams is in first order over the course of this research, and it diminishes as stream order grows, as shown in Table 2.

These findings are the consequence of streams flowing from high elevations, changes in rock types, such as when bedrock is porous, a few longer streams are generated, and, vice versa, smaller streams are formed; lithological variety; relatively steep slopes; and maybe uplift across the basin (Rudraiah et al., 2008).

### 3.2.4 Mean Stream Length

A characteristic attribute of drainage network components and their related basin surfaces is mean stream length, which is computed by the division of the total stream length of a specific stream order and the number of streams of that order (Strahler, 1964). Table 2 provides information on the mean stream lengths of the Ganjal, Palakmati, and Dudhi rivers. Between 0.57 and 61.22 km, the Lsm's value ranges. In accordance with the definition, the Lsm of an order is greater than its lower order and less than its next higher order up to the fifth-order stream. However, due to variations in slope and topography for the fifth- and sixth-order streams in the Ganjal River, the values are lower than the lower-order stream (Figs. 5, 6 and 7).

### 3.2.5 Stream Length Ratio

The stream length ratio (RL), which is affected in some way by the slope and regional topography through which the discharge and erosional activity of the specific watershed or basin will be controlled, is the result of the mean stream length of a given order, i.e. Lu and the mean stream length of the next higher order, i.e. Lu + 1 (Horton, 1945). Table 2 provides the average stream length ratio values for each of the three tributaries. Changes in RL are seen in the Dudhi, Palakmati, and Ganjal rivers, which may be related to changes in terrain and slope. This suggests that the research area's streams are in a late juvenile stage of geomorphic development.

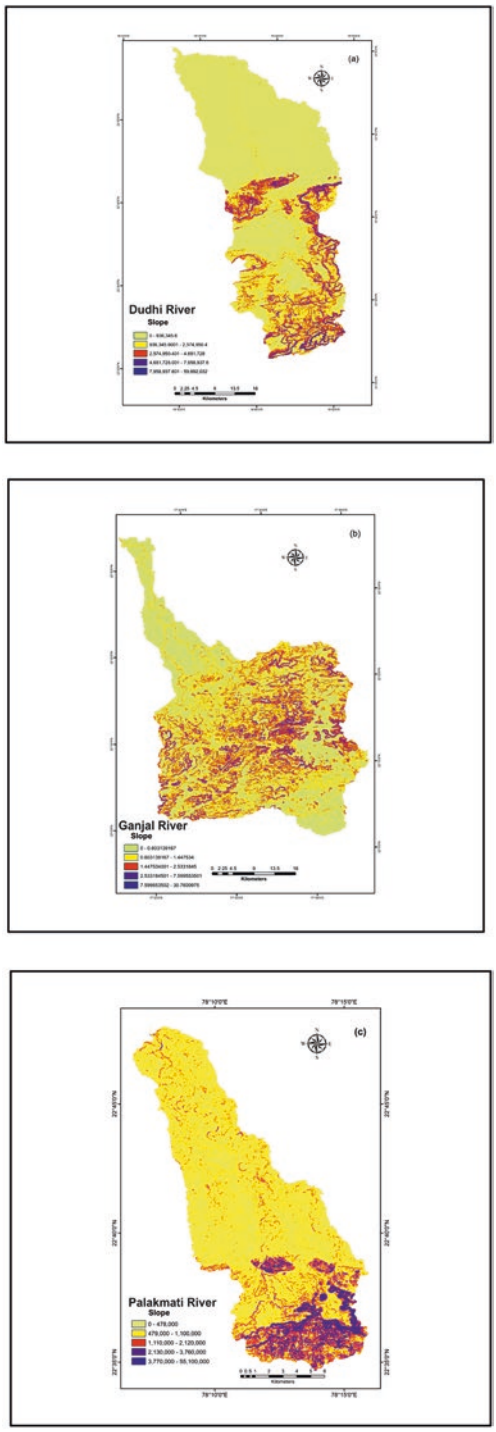


**Fig. 5** Slope maps of river basins

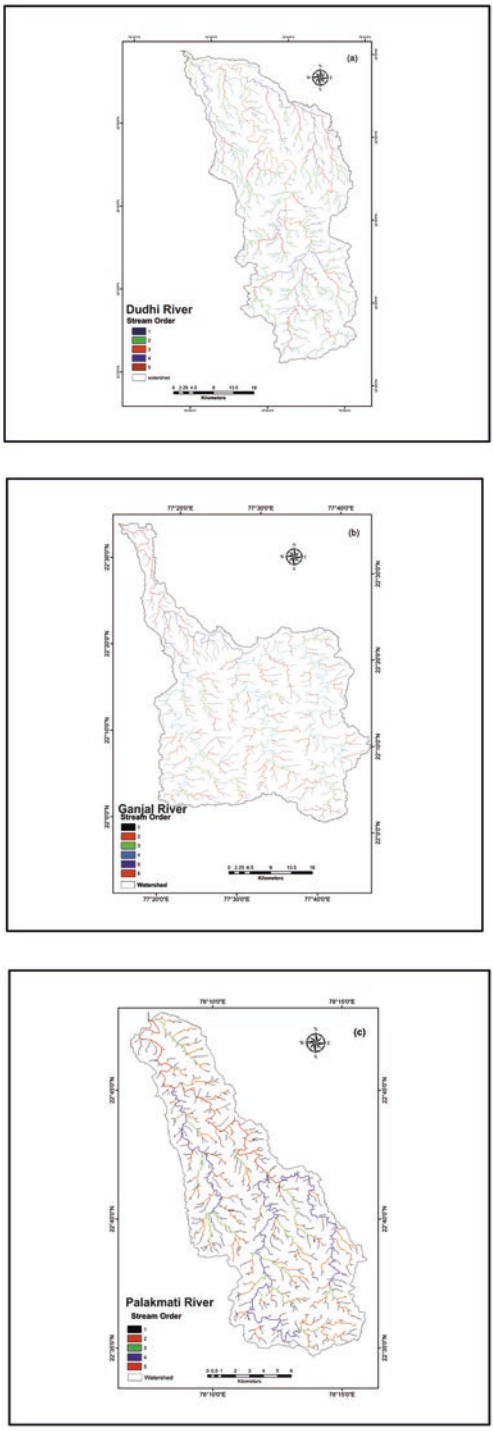


**Fig. 6** Drainage network maps of river basins

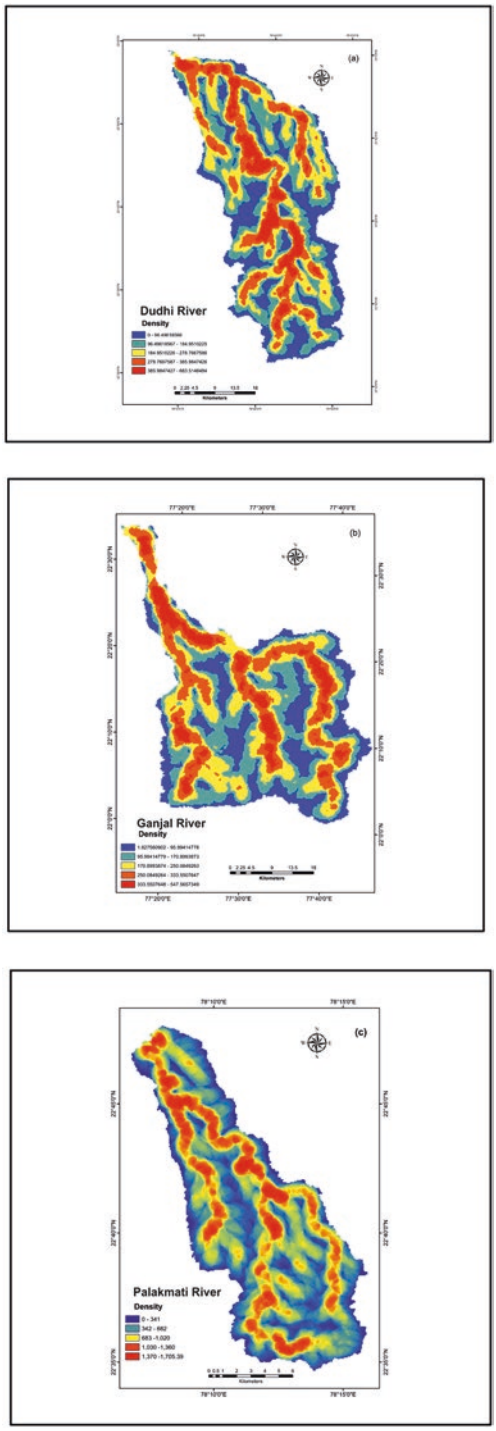


**Fig. 7** Drainage density maps of river basin

### 3.2.6 Bifurcation Ratio

In 1956, Schumm coined the term bifurcation ratio which shows the correlation between the number of stream segments of a given order and the number of segments of the next higher orders that exhibit a condensed range of variation for various places or environments when the potent geological influence is disregarded (Strahler, 1957). Table 2's values for Rb in the research region show that they vary from one order to the next and that these variations are influenced by the drainage basin's geological and lithological evolution. Rb values in the research region varied from 1.50 to 7.00, indicating that certain streams belong under the category of normal basins while others fall under the category of disturbing tributaries (Strahler, 1957). The sub-watershed is less impacted by structural disturbances, which may be anthropogenic or natural, according to the lowest value of Rb. The greatest value of Rb shows a significant structural control on the drainage pattern (Srinivasa Vittala et al., 2004).

## *3.3 Aerial Aspects*

Different morphometric metrics parameters are involved in aerial aspects (Lg) which values are listed in Table 3 and explored more below.

### 3.3.1 Drainage Density

By dividing the entire length of a stream by the area of a drainage basin, one may calculate drainage density (Dn), which is defined as the length of streams per unit of drainage area (A) (Horton, 1945). Analysis of drainage density, which demonstrates a strong association between drainage density, precipitation, and evaporation, was done to consider the interplay between the climate and the geological setting (Horton, 1932). Drainage density measures the distance between drainage ways, and a greater value indicates a closer spacing between the channels. The areas with extremely permeable subsurface, extensive vegetative cover, and low relief indicate that the catchment area's coarse drainage density is present. The range of drainage density in the current research is between 0.82 and 2.46 km/km$^2$, suggesting low drainage density (Table 3). In the Western Ghats studies, Magesh and Chandrasekar (2014) found that the range of drainage density reveals that the nature of subsurface strata is permeable. The low drainage density of the catchment area also indicates that the region has dense vegetation cover, low relief, and a highly permeable subsoil (Bansod & Ajabe, 2018).

**Table 3** Results of aerial morphometric analysis of three rivers of the Narmada basin

| S. No | Morphometric parameters | Dudhi River | Palakmati River | Ganjal River |
|---|---|---|---|---|
| 1 | Drainage density (Dd) | 0.84 | 2.46 | 0.85 |
| 2 | Stream frequency (Fs) | 0.27 | 2.83 | 0.27 |
| 3 | Drainage texture (T) | 0.22 | 6.96 | 0.22 |
| 4 | Infiltration no. (If) | 0.05 | 19.69 | 0.05 |
| 5 | Length of overland flow (Lg) | 2.38 | 0.81 | 2.35 |
| 6 | Circulatory ratio (Rc) | 0.25 | 1.11 | 0.39 |
| 7 | Form factor (Ff) | 0.26 | 0.22 | 0.25 |
| 8 | Elongation ratio (Re) | 2.52 | 1.40 | 2.55 |

### 3.3.2 Drainage Frequency

Horton (1945) defined drainage frequency as the entire stream segments of all orders per unit area. The values of Fs for all three tributaries specify a productive relationship with the values of drainage density, indicating an increment in stream population with respect to an increase in drainage density (Table 3). The Dudhi and Ganjal rivers also exhibit equal frequency.

### 3.3.3 Drainage Texture

One of the key geomorphology concepts, RT specifies the relative spacing of drainage lines which is indicated as the entire stream segment numbers of all sorts per perimeter of the area, according to Horton (1945). In Smith's 1950 classification of drainage density, there were five distinct textures: extremely coarse (2), coarse (2–4), moderate (4–6), fine (6–8), and very fine (>8). According to Table 3, the drainage density values for the catchment area ranged from 0.22 to 6.96, indicating a very coarse to fine drainage texture (Lombana & Martínez-Graña, 2021).

### 3.3.4 Form Factor

According to Horton (1932), Rf is a quantitative statement of the contour of a drainage basin which is explained as the ratio of the basin's area to the square of its length, with a value of 0 denoting a severely elongated form and a value of 1 denoting a circular shape (Bera et al., 2018). According to Table 3, the research region's form factor in the current study spans from 0.22 to 0.26. This shows that the tributaries' morphology is extended.

### 3.3.5 Circulatory Ratio

It is the ratio of the basin's area to a circle area whose circumference is equal to its perimeter (Miller, 1953), which is impacted by the extent of streams, the structures of the basin's geological features, the basin's land use and land cover, the basin's climate, its relief, and its slope (Shekhar et al., 2021). This ratio, which varies in the study area between 0.25 and 1.11, is shown in Table 3. Maximum and minimum values were found in the Palakmati and Dudhi rivers, respectively, indicating that they are roughly circular and have high to moderate relief, all of which imply that the drainage system has been organisationally examined.

### 3.3.6 Elongation Ratio

Schumn (1956) established the elongation ratio (Re) of a river basin as the ratio between the diameter of the circle with the same area as the basin and the greater length of the basin. This value indicates favourable infiltration and run-off conditions. According to Strahler (1964), values in the range of 0.6–0.8 are comparable to high relief and steep ground slope, whereas values close to approximately 1.0 are indicative of locations with very low relief. There are many different climatic and geologic types represented by the following groups of Re values: circular (>0.9), oval (0.9–0.8), and less elongated (0.7). The Dudhi River's measured elongation ratio is 2.52, Palakmati's is 1.40, and Ganjal's is 2.55, indicating very little relief, little run-off, and the basin's circular form.

### 3.3.7 Length of Overland Flow

The length of overland flow (Lg), as defined by Horton in 1945, is the amount of time that water spends above the ground before it is concentrated into specific stream channels, which affects the hydrological and physiographic aspects of the basin. The Lg value in the current study basin varies from 0.81 to 2.38, indicating a rather advanced level of drainage development.

## *3.4 Relief Aspect*

The relief measurements like relief ratio, total relief, and ruggedness number are given in Table 4.

**Table 4** Results of relief morphometric analysis of three rivers of the Narmada basin

| S. No | Morphometric parameters | Dudhi River | Palakmati River | Ganjal River |
|---|---|---|---|---|
| 1 | Relief | 0.107 | 0.484 | 0.702 |
| 2 | Relief ratio | 0.001 | 0.017 | 0.008 |
| 3 | Ruggedness no. (Rn) | 0.0000084 | 0.000041 | 0.000068 |

### 3.4.1 Basin Relief

The relief tributaries range in height from the catchment mouth by 322 to 624 m. According to Table 4, the calculated relief of the tributaries ranges from 0.107 to 0.702 m. Figure 8 shows the basin's generalised relief map.

### 3.4.2 Relief Ratio

The relief ratio (Rh) is calculated by dividing the basin's total relief by the length of the basin (Qadir et al., 2020), and the calculated value for the tributaries is between 0.001 and 0.017 m/km as shown in Table 4. The relief ratio is defined as the response of horizontal distance between two points (H) to the vertical difference between the same two points (Lb) (Fig. 9).

### 3.4.3 Ruggedness Number

In 1958, Strahler calculated the ruggedness number (Rn), which reflects the variance in slope and relief in the basin, is the product of basin relief and drainage density, which ranges from 0.000041 to 0.0000084 indicating the low value, suggesting that the basin region is less likely to experience soil erosion and lacks inherent structural complexity in relation to the relief of the basin and drainage density (Thomas et al., 2010) given in Table 4.

## 4 Conclusion

In the modern day, remote sensing and GIS are magnificent tools that are utilised in many fields for better study and to get a comprehensive understanding of the past and present on a single platform, on the basis of which we can quickly develop forecasts for our desired item. Since precise river structures will be available, models may be laid out for investigations of river behaviour. The middle zone of the Narmada basin's tributaries has undergone effective morphometric investigation using remote sensing and GIS techniques.

1. In the catchment regions, a dendritic drainage pattern was found, and variations in the stream length ratio may have been caused by changes in the terrain's slope.

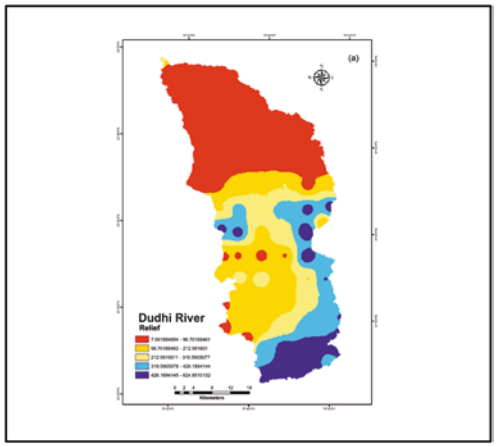


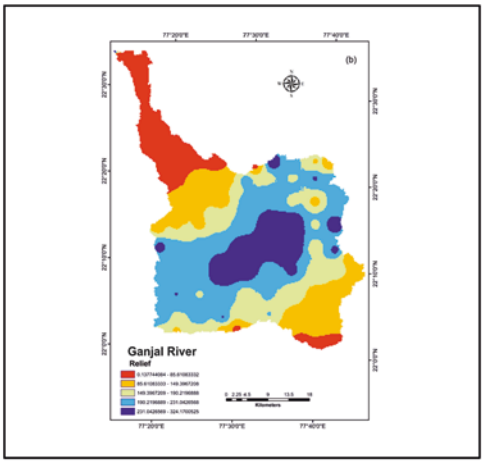


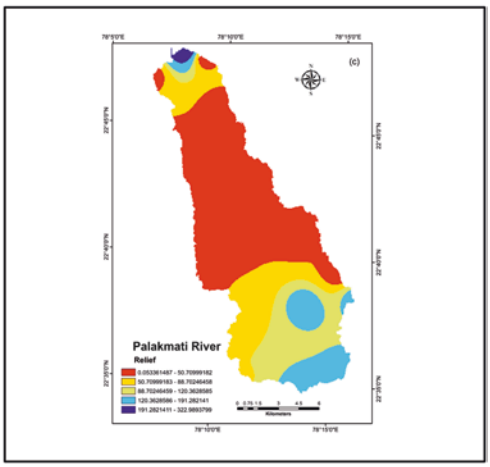


**Fig. 8** Relief maps of river basin

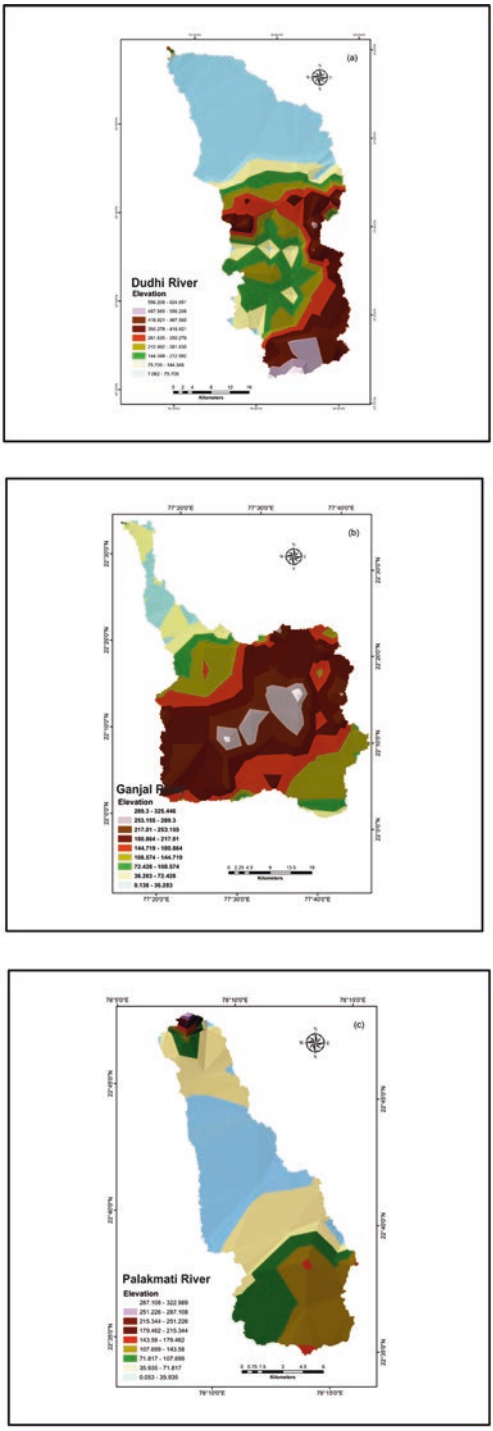


**Fig. 9** Triangular irregular network (TIN) model of river basins

2. The bifurcation ratio values for all stream orders vary between catchment regions, and this variation is linked to variations in topography, geometric development, and features of the sub-humid zone of tropical environments.
3. As the stream population expands in response to higher drainage densities, stream frequencies for the catchment area show a positive correlation with drainage density values.
4. The relief characteristics show a mild to moderate slope that permits little run-off and strong infiltration, while lower values are characterised by being very susceptible to erosion and sediment load.
5. Indicating a porous subsurface and dense plant cover in the examined region, the sub-watershed drainage texture ranges from extremely coarse to fine.
6. According to the elongation ratio, all three tributaries are circular. Higher values of the elongation ratio show strong infiltration capability and little run-off, whereas lower values are more prone to erosion and sediment load.

## References

Bansod, R. D., & Ajabe, G. S. (2018). Determination of geomorphological characteristics of Karpri-Kalu watershed using GIS techniques. *Journal of Pharmacognosy and Phytochemistry, 7*(1), 1940–1944.

Bera, A., Mukhopadhyay, B. P., & Das, D. (2018). Morphometric analysis of Adula River Basin in Maharashtra, India using GIS and remote sensing techniques. *Geo-spatial Data in Natural Resources*, 13–35.

Biswas, S., Sudhakar, S., & Desai, V. R. (1999). Prioritisation of sub watersheds based on morphometric analysis of drainage basin: A remote sensing and GIS approach. *Journal of the Indian Society of Remote Sensing, 27*(3), 155–166.

Chopra, R., Dhiman, R. D., & Sharma, P. K. (2005). Morphometric analysis of sub-watersheds in Gurdaspur district, Punjab using remote sensing and GIS techniques. *Journal of the Indian Society of Remote Sensing, 33*(4), 531–539.

Grohmann, C. H. (2004). Morphometric analysis in geographic information systems: Applications of free software GRASS and R. *Computers & Geosciences, 30*(9–10), 1055–1067.

Horton, R. E. (1932). Drainage-basin characteristics. *Transactions, American Geophysical Union, 13*(1), 350–361.

Horton, R. E. (1945). Erosional development of streams and their drainage basins; hydrophysical approach to quantitative morphology. *Geological Society of America Bulletin, 56*(3), 275–370.

Kanhaiya, S., Singh, B. P., Singh, S., Mittal, P., & Srivastava, V. K. (2019). Morphometric analysis, bedload sediments, and weathering intensity in the Khurar River Basin, Central India. *Geological Journal, 54*(1), 466–481.

Lazzari, M. (2020). GIS application in fluvial geomorphology and landscape changes. *Water, 12*(12), 3481.

Lombana, L., & Martínez-Graña, A. (2021). Multiscale hydrogeomorphometric analysis for fluvial risk management. Application in the Carrión River, Spain. *Remote Sensing, 13*(15), 2955.

Magesh, N. S., & Chandrasekar, N. (2014). GIS model-based morphometric evaluation of Tamiraparani subbasin, Tirunelveli district, Tamil Nadu, India. *Arabian Journal of Geosciences, 7*(1), 131–141.

Magesh, N. S., Chandrasekar, N., & Soundranayagam, J. P. (2011). Morphometric evaluation of Papanasam and Manimuthar watersheds, parts of Western Ghats, Tirunelveli district, Tamil Nadu, India: A GIS approach. *Environmental Earth Sciences, 64*(2), 373–381.

Magesh, N. S., Jitheshlal, K. V., Chandrasekar, N., & Jini, K. V. (2013). Geographical information system-based morphometric analysis of Bharathapuzha river basin, Kerala, India. *Applied Water Science, 3*(2), 467–477.

Mahale, A. (2020). The significance of morphometric analysis to understand the hydrological and morphological characteristics in two different morpho-climatic settings. *Applied Water Science, 10*(1), 1–16.

Miller, V. C. (1953). *A quantitative geomorphic study of Drainage Basin characteristics in the Clinch Mountain area Virginia and Tennessee*. Columbia University.

Nag, S. K. (1998). Morphometric analysis using remote sensing techniques in the Chaka sub-basin, Purulia district, West Bengal. *Journal of the Indian Society of Remote Sensing, 26*(1), 69–76.

Pal, R., & Pani, P. (2019). Remote sensing and GIS-based analysis of evolving planform morphology of the middle-lower part of the Ganga River, India. *The Egyptian Journal of Remote Sensing and Space Science, 22*(1), 1–10.

Pareta, K., & Pareta, U. (2011). Hydromorphogeological study of Karawan watershed using GIS and remote sensing techniques. *International Scientific Research Journal, 3*(4), 243–268.

Patel, D. P., Gajjar, C. A., & Srivastava, P. K. (2013). Prioritization of Malesari mini-watersheds through morphometric analysis: A remote sensing and GIS perspective. *Environmental Earth Sciences, 69*(8), 2643–2656.

Pirasteh, S., Safari, H. O., Pradhan, B., & Attarzadeh, I. (2010). Lithomorphotectonics analysis using Landsat ETM data and GIS techniques: Zagros Fold Belt (ZFB), SW Iran. *International Geoinformatics Research and Development Journal, 1*(2), 28–36.

Qadir, A., Yasir, M., Abir, I. A., Akhtar, N., & San, L. H. (2020, July). Quantitative morphometric analysis using remote sensing and GIS techniques for Mandakini River Basin. In *IOP conference series: Earth and environmental science* (Vol. 540, No. 1, p. 012021). IOP Publishing.

Rai, P. K., Chandel, R. S., Mishra, V. N., & Singh, P. (2018). Hydrological inferences through morphometric analysis of lower Kosi River basin of India for water resource management based on remote sensing data. *Applied Water Science, 8*(1), 1–16.

Rudraiah, M., Govindaiah, S., & Vittala, S. S. (2008). Morphometry using remote sensing and GIS techniques in the sub-basins of Kagna river basin, Gulburga district, Karnataka, India. *Journal of the Indian Society of Remote Sensing, 36*(4), 351–360.

Schumm, S. A. (1956). Evolution of drainage systems and slopes in badlands at Perth Amboy, New Jersey. *Geological Society of America Bulletin, 67*(5), 597–646.

Shah, A. K., Morya, J. S., & Majethiya, H. V. (2021). Morphometric analysis of Kaswali River Basin, Kachchh, Gujarat, western India using remote sensing and GIS.

Shekhar, S., Mawale, Y. K., Giri, P. M., Jaipurkar, R. S., & Singh, N. (2021). Remote sensing and GIS based extensive morphotectonic analysis of Tapti River Basin, Peninsular India. *Journal of Scientific Research, 65*(3), 23.

Smith, B., & Sandwell, D. (2003). Accuracy and resolution of shuttle radar topography mission data. *Geophysical Research Letters, 30*(9), 1467.

Sreedevi, P. D., Subrahmanyam, K., & Ahmed, S. (2005). Integrated approach for delineating potential zones to explore for groundwater in the Pageru River basin, Cuddapah District, Andhra Pradesh, India. *Hydrogeology Journal, 13*(3), 534–543.

Srinivasa Vittala, S., Govindaiah, S., & Honne Gowda, H. (2004). Morphometric analysis of subwatersheds in the Pavagada area of Tumkur district, South India using remote sensing and GIS techniques. *Journal of the Indian Society of Remote Sensing, 32*(4), 351–362.

Strahler, A. N. (1957). Quantitative analysis of watershed geomorphology. *Eos, Transactions American Geophysical Union, 38*(6), 913–920.

Strahler, A. N. (1964). Part II. Quantitative geomorphology of drainage basins and channel networks. In *Handbook of applied hydrology* (pp. 4–39). McGraw-Hill.

Thomas, J., Joseph, S., & Thrivikramaji, K. P. (2010). Morphometric aspects of a small tropical mountain river system, the southern Western Ghats, India. *International Journal of Digital Earth, 3*(2), 135–156.

# Role of Multipurpose River Valley Projects in the Agricultural Development of India Since Independence


**NikhatBano, SyedKausar Shamim, and Ateeque Ahmad**

## 1 Introduction

In India, irrigation has been used for centuries. The Rigveda makes the first mention of it, followed by the Mughal emperors. In Assam, Bihar, Orissa, Punjab, and Uttar Pradesh, the British constructed a sizable number of canals and irrigation systems by 1940 (Singh, 2003a; Charlesworth, 1981; Stone, 2002; D'Souza, 2006). Due to 48% of India's total area being irrigated, there was only modest advancement in the field of irrigation throughout World War II and the depression of the 1930s. While at the time of partition, Pakistan received a 31% share of the major canal systems, including the Sutlej and Indus systems (Bano, 2013).

The largest consumer of water, irrigation accounts for over 80% of all water used for irrigation globally (in India, irrigation accounts for 85% of all water resources). With an average annual rainfall of 1170 mm and a total area of 3.3 million kilometres, India receives 4000 $km^3$ of water, over half of which is lost through evaporation, percolation, and subsurface flows to the oceans, with just 1953 billion cubic metres (BCM) being directly responsible. Only 1086 BCM of the available water may be used, and 1700 BCM of water per person per year is considered safe due to regional and temporal variations in water supply (Phansalkar & Verma, 2005; Falkenmark & Lindh, 1976). India's Annual Water Resource (AWR) was 2214 $m^3$ in 1996; by 2025, it is predicted to be 1496 $m^3$. Although the AWR is high right now, the developed water resource (DWR), which makes up only 25% of the AWR, is what determines the actual availability of water (Gulati et al., 2005). Additionally, because water is a local issue and there are many parts of India where water availability per capita is below the acceptable limit, national averages do not convey the whole story. In addition to the environment and industry, the other major users of water—drinking water in both urban and rural areas—show an increase in demand.

NikhatBano (✉) · S. Shamim · A. Ahmad
Faculty of Science, Department of Geography, Aligarh Muslim University, Aligarh, India



S. Kanhaiya et al. (eds.), *Rivers of India*,
https://doi.org/10.1007/978-3-031-49163-4_2

## 2 Materials and Methods

The chapter, which comprehensively discusses the various aspects of irrigation with special reference to multipurpose projects covering the development of irrigation facilities through major and medium irrigation projects, is the result of various publications by the Planning Commission, Ministry of Agriculture, Central Water Commission Report, Central Ground Water Board Ministry of Water Resources, Minutes of Working Group Reports of the Government of India, blogs, and other related agencies.

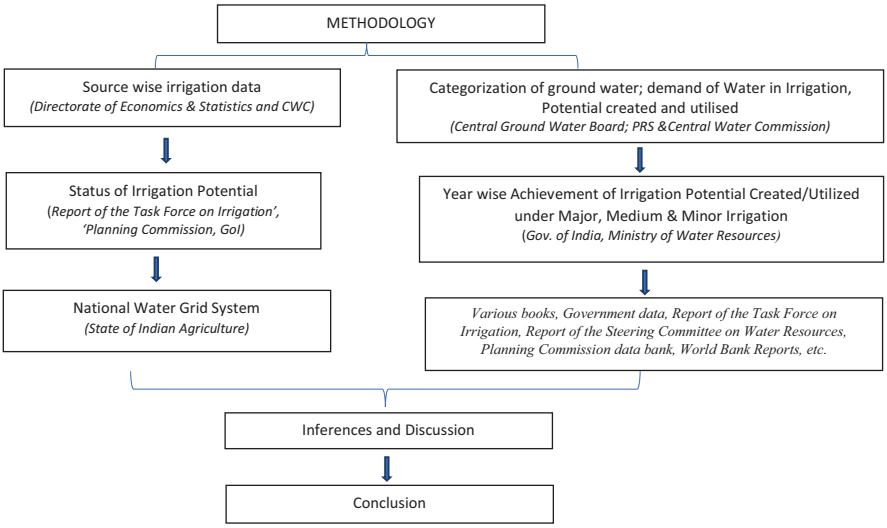


## 3 Irrigation Development as per Sources in India

The amount of agricultural output and productivity is largely dependent on the availability of water for irrigation, which depends on the presence of irrigation infrastructure, which are severely lacking in India (Seth, 2018). For instance, in 1950–1951, only 17% of the total land was grossly wetted. Although there have been significant investments made in irrigation projects over the planning period, the gross irrigated area as a percentage of gross cropped area was only 44.6% in 2007–2008 (87.26 million hectares (Mha) out of 195.83 Mha), currently, 63 Mha (45%) of net cropped area is irrigated (Economic Survey of India, 2013), and even now, 60% of gross cropped area depends on rain; therefore, Indian agriculture is called a bet (Hantal, 2018). The available moisture is insufficient to support numerous crops, even in regions with high annual precipitation totals. The anticipated amount of irrigated land is only 66 Mha, or 47.6% of the net sown area. In order to

boost agricultural productivity and output, more cropped land must be placed under assured irrigation. The country's entire ultimate irrigation potential has been estimated at 140 Mha, of which 64 Mha comes from groundwater sources and 76 Mha from surface water sources, according to a report released by the Directorate of Economics and Statistics (Garg, 2017).

The biggest portion of India's 68.38 Mha total irrigation area, or 46.22%, is shared by tube wells, followed by canals and wells (Table 1), according to the Agricultural Census 2014–2015 (Provisional). In terms of the expansion of irrigated land in India, the net irrigated area has consistently increased from 20.58 Mha in 1950–1951 to 63.66 Mha in 2010–2011 and 68.10 Mha in 2013–2014. The gross irrigated area of the nation has increased significantly from 22.56 Mha in 1950–1951 to 88.93 Mha in 2010–2011 and up to 95.77 Mha in 2013–2014 as a result of diverse irrigation development through big, medium, and small irrigation projects.

On a global scale, irrigation projects have grown at an unparalleled rate over the past century. From 50 Mha in 1900, irrigated land now covers 267 Mha worldwide. Groundwater costs have been reduced by adopting tube well irrigation, and food security has been attained by subsidizing big reservoirs and canals. India has made significant financial investments in both large- and medium-scale irrigation projects since the post-independence era, making it one of the world's leading practitioners of large-scale irrigation. The disparity between potentially developed and utilized, however, has grown over time. Three of the states have already reached 70% or more of their potential for irrigation, with Tamil Nadu having reached 100%, Punjab 84%, and Rajasthan 74% (Palanisami et al., 2007).

Through the intensive agriculture development program (IADP) and high yielding variety program (HYVP), the central and state governments are constantly pursuing various actions to expand irrigation potential in India in all directions and utilize it. Prior to 1951, India's irrigation potential through the major and medium (M&M) sectors was 9.70 Mha; this increased to 22.6 Mha in 1951 and to 102.77 Mha by the end of the Tenth Five Year Plan Period (2002–2007). By the end of March 2009, an irrigation potential of 7.3 Mha has been produced during the XI Plan. Thus, by the end of March 2009, the nation's total cumulative potential reached 110.07 Mha. However, it is predicted that the 58.47 Mha objectives would be met under major and medium projects by the end of the XII Plan (Muthyam et al., 2013). By the end of the X Plan, India's total irrigation potential had been developed to the extent of 102.8 Mha, with 42.4 Mha under major and medium irrigation and the remaining 60.4 Mha under minor irrigation. This analysis shows that the irrigation potential developed through various major, medium, and minor irrigation projects has not been fully utilized. In 1980–1981, out of the total irrigation potential of 58 Mha, the actual utilization was 54 Mha. The potential that has been created has, however, not been fully used. At the end of the X Plan, the overall amount of irrigation potential that had been used was 87.2 Mha, while the total amount of potential that had been developed was 102.8 Mha, leaving a 15.6 Mha deficit. The primary causes of this underutilization of created potential are the length of time it takes

**Table 1** Source-wise development of irrigated area in India (1950–2014)

| | | | | | | | | (000 hectares) |
|---|---|---|---|---|---|---|---|---|
| | Source of irrigation | | | | | | | |
| | Canals | | | Tanks | Tube wells | Other wells | Other sources | Net irrigated area |
| Year | Government | Private | Total | | | | | |
| 1950–1951 | 7158 | 1137 | 8295 | 3613 | (a) | 5978 | 2967 | 20,853 |
| 1955–1956 | 8025 | 1360 | 9385 | 4423 | (a) | 6739 | 2211 | 22,758 |
| 2001–2002 | 14,993 | 209 | 15,202 | 2196 | 23,245 | 11,952 | 4342 | 56,936 |
| 2002–2003 | 13,867 | 206 | 14,073 | 1811 | 25,627 | 8727 | 3658 | 53,897 |
| 2003–2004 | 14,251 | 206 | 14,458 | 1916 | 26,691 | 9693 | 4299 | 57,057 |
| 2004–2005 | 14,553 | 214 | 14,766 | 1734 | 25,235 | 9956 | 7538 | 59,229 |
| 2005–2006 | 16,490 | 227 | 16,718 | 2083 | 26,026 | 10,044 | 5966 | 60,837 |
| 2006–2007 | 16,802 | 224 | 17,027 | 2078 | 26,942 | 10,698 | 5999 | 62,744 |
| 2007–2008 | 16,531 | 217 | 16,748 | 1973 | 28,497 | 9864 | 6107 | 63,189 |
| 2008–2009(p) | 16,686 | 195 | 16,881 | 1981 | 28,367 | 10,389 | 6020 | 63,638 |
| 2009–2010(p) | 14,789 | 188 | 14,978 | 1587 | 28,371 | 9992 | 7008 | 61,936 |
| 2010–2011(p) | 15,472 | 171 | 15,643 | 1980 | 28,543 | 10,629 | 6864 | 63,659 |
| 2011–2012(p) | 15,833 | 172 | 16,005 | 1919 | 29,943 | 10,595 | 7236 | 65,697 |
| 2012–2013(p) | 15,506 | 165 | 15,672 | 1753 | 30,543 | 10,763 | 7536 | 66,266 |
| 2013–2014(p) | 16,115 | 163 | 16,278 | 1842 | 31,126 | 11,312 | 7542 | 68,100 |
| 2014–2015(p) | 16,020 | 163 | 16,182 | 1723 | 31,606 | 11,354 | 7519 | 68,383 |

Source: Directorate of Economics & Statistics, Ministry of Agriculture and Farmers Welfare, Govt. of India (ON1393) & Past Issues

Note: (a): Included under "other wells" as separate figures were not collected for these years; Abbr: *p* provisional

farmers to transition to new cropping practices, such as moving from dry farming to irrigated farming, as well as delays in developing on-farm tasks like building field channels, shaping or levelling the land, and adopting the Warabandi system (Kwat, 2018).

### *3.1 Types and Sources of Irrigation*

Since the end of World War II, irrigation activities have dramatically increased which has greatly boosted agricultural output and allowed mankind to feed its doubling population. There must be a distinction made between the overall beneficial effects of irrigation and water on agricultural productivity and economic welfare and the significant resource mismanagement that has accompanied the growth of irrigation, according to Schoengold and Zilberman (2004) and Apoorva, (2007).

## 4 Water Resources in India

There are two types of water resources: dynamic and static. Water resources must be measured in terms of their flow rates due to their dynamic and regenerative character and the enduring requirement for their use. Water resources which are either fixed or found everywhere (ubiquitous) vary in accordance with characteristics of volume size or area they cover.

### *4.1 Water Bodies*

The nation's inland water resources are divided into rivers, canals, reservoirs, tanks, lakes, ponds, abandoned water features, and brackish water. There are 195,210 Mha for rivers and canals (length in km) and other water bodies (area in Mha) in India's inland water resources. A total of 7.36 Mha is covered by all bodies of water other than rivers and canals. According to CWC (2013), "reservoirs" have the largest area of these water bodies (2.91 Mha), followed by tanks, lakes, and ponds (2.41 Mha), flood plain lakes and derelict water (0.80 Mha), and brackish water (1.24 Mha).

It is not possible to estimate the size of the nation's rivers and canals. However, the length of them all throughout the nation is close to 2 lakh km. According to the theoretical allocation of the nation's water resources, the yearly water availability per person was 1816 $m^3$ in 2001 and 1544 $m^3$ in 2011. While it was as low as 263 $m^3$ in the Sabarmati Basin, the Ganga-Brahmaputra-Meghna system estimated average per capita availability for the year 2010 was 2045 $m^3$. The country's per capita availability will drop from 1608 $m^3$ in 2010 to 1140 $m^3$ in 2050. International authorities classify any situation with availability of less than 1000 $m^3$ per person as a scarcity.

Out of the total 1869 BCM in the nation, the Ganga-Brahmaputra-Meghna River Basin has an annual water resource potential of 1111 BCM. In terms of utilizable surface water, smaller basins have a very high ratio of utilizable surface water resources to potential water resources. The total consumption surpasses the annual availability of natural flows in Pennar and some other river basins. The ratio of utilizable surface water to average water resources potential is found to be highest in

the Ganga-Brahmaputra sub-basins, which share 59.4% of the total water resources potential of the various rivers and 39.7% of utilizable surface water resources, whereas Indus (up to the border), Godavari, Krishna, and Maharashtra share the smallest percentages of utilizable surface water to average water resources potential.

Under major and medium irrigation projects, the nation now has a total storage capacity of around 253.4 BCM. There will be an additional 51 BCM from the ongoing projects. Therefore, once the ongoing projects are finished, there will likely be 304.3 BCM of storage available. The country's groundwater potential has been estimated as 431 BCM, which contributes more than 79% of the total ultimate potential through minor irrigation. This is less, but it has provided assured irrigation in significant areas, extended the supply of drinking water to remote areas, and ensured water supply to hydro and thermal power plants. Due to major and medium irrigation projects, Uttar Pradesh and Bihar are two of the states with the greatest potential. About 54% of the nation's total ultimate potential for major and medium irrigation is accounted by these two states followed by Madhya Pradesh, Andhra Pradesh, and Maharashtra. Uttar Pradesh has the greatest UIP for groundwater minor irrigation. The potential for minor irrigation (surface water) is significantly larger in Andhra Pradesh and Madhya Pradesh than in the other states. However, thanks to a variety of programs, Uttar Pradesh ranks first among the states with the greatest potential (CWC, 2013; Water and Related Statistics, 2015).

## *4.2 Types of Water Sources*

The sources of water are classified as surface water and groundwater.

### 4.2.1 Surface Water

Rivers and streams, reservoirs, tanks, ponds, and lakes are the sources of surface water. River is the naturally flowing water that flows freely in perennial and non-perennial channels. The majority of towns and cities get their water from rivers. As a result of sewage, industrial waste, animal and human waste, and other contaminants, rivers nowadays are unfit for drinking without treatment. Reservoirs are lakes that have been created intentionally by damming rivers or building brick structures. The water in reservoirs is clear, pleasant, soft, and pathogen-free. But it might become contaminated by habitations for people or animals. Tanks are substantial excavations used to hold water and are a vital supply of water for many Indian settlements. They get heavily contaminated by anthropogenic activity, aquatic vegetation, colloidal particles, silt, and regular defecation, making them unfit for human consumption.

### 4.2.2 Groundwater

It is naturally filtered water drawn from springs or wells. Wells are hollow pits dug out several metres below the surface in the aquifer zone. In many Indian villages and cities, wells are the primary sources of water. They are divided into dug wells and tube wells based on the building method. The most prevalent type of well in India is a dug well. It could be a brick or stone-lined puck well or an uncovered ketch well. The puck well is referred to as a step well if it has steps. Two types of tube wells exist, both shallow and deep tube wells. An iron pipe that has been driven into the water-bearing stratum and has a strainer at the bottom and a hand pump at the top is a shallow tube well. Deep tube wells are mechanically bored to a depth of several hundred feet using equipment with an electric motor to retrieve water. Springs are pressure-driven natural discharges of groundwater with variable quality and poor production. There are four different types of springs as follows: shallow springs, deep springs, mineral springs, and thermal springs (Lisha, 2022; Bano, 2013).

## 5 Different Types of Irrigation

Irrigation systems are often designed to maximize efficiencies and minimize labour and capital requirements. There are three broad classes of irrigation system:

(a) Pressurized distribution.
(b) Gravity flow distribution.
(c) Drainage flow distribution.

(a) *Pressurized distribution:* In pressurized systems water is distributed over the fields through pressurized pipe networks, for example, sprinkler and trickle.
(b) *Gravity flow distribution:* This system bears overland flow regime, and water is distributed at the field level by a free surface.
(c) *Drainage flow distribution:* Using a controlled drainage system, it is workable to raise the level of groundwater so that the roots of the crops are within reach by regulating the water flow at key spots.

There should be a consistent water supply throughout the entire field in order to give each plant enough water. As a result, there are many different types of irrigation strategies for distributing water over the field using different mechanisms, which are as indicated below.

## *5.1 Surface Irrigation*

This irrigation method relies on simple gravity flow, in which water runs over and across the soil to moisten it and allow for soil infiltration. Furrow, border strip, and basin irrigation are different types of surface irrigation.

## *5.2 Ditch Irrigation*

It is still widely used around the world and is the simplest and oldest type of irrigation system. The only technological input required is labour or equipment to create ditches or furrows between plant rows, and water is fed to these furrows using gravity flow, pumps, and siphons.

## *5.3 Localized Irrigation*

This system uses a modest flow of water that is distributed via network of pipes at low pressure and according to a predetermined pattern.

## *5.4 Drip Irrigation*

This form of irrigation, also known as trickling irrigation, is said to be the most effective since water is applied drop by drop at or close to the root zone of plants.

## *5.5 Overhead Irrigation*

The method of artificially watering crops from above using central pivot systems equipped with sprinklers spaced along extremely long pipes made of either aluminium or steel that extends in two directions from a central supply point is most commonly utilized in places with flat terrain.

## *5.6 Sub-irrigation*

This technique, which is sometimes known as seepage irrigation, has been employed for many years in farms with high water tables. In this technique, the soil is allowed to become moistened from below the plants' root zone artificially raising the water table.

## *5.7 Manual Irrigation*

Instead of large labour inputs through the use of watering cans or buckets, this technique requires modest infrastructure and technical equipment. According to various irrigation sources, there are two main divisions, as listed below.

### 5.7.1 Flow Irrigation

Flow irrigation refers to the process where water from a reservoir or tank automatically flows into a channel to serve as an irrigation canal when the reservoir or tank is connected to a field.

### 5.7.2 Lift Irrigation

Lift irrigation is the practice of using motorized pumps to lift water for irrigation when the level of the field is higher than the level of any tanks or canals (Ghosh, 2012).

## *5.8 Sources of Irrigation*

Moreover, half of the total irrigated area relies on minor irrigation works, while the remaining area relies on medium and major irrigation works.

Accordingly, the primary irrigation sources in various sections of the nation are:

5.8.1. Canals
5.8.2. Wells and tube wells
5.8.3. Tanks
5.8.4. Other sources (Dongs, Kuhls, Springs, etc.)

### 5.8.1 Canal Irrigation

In India, wells and tube wells replaced irrigation canals as the second-most significant source of irrigation in the 1970s, which had been canals up until that point. In places with low relief, a reliable source of water, rich soil, and a large area, canals are an efficient irrigation method. Because of the stony terrain, canal irrigation is concentrated more in the northern lowlands than in the peninsular plateau region, with the exception of a few coastal and delta regions in the south.

Canals come in two varieties.

#### 5.8.1.1 Inundation Canals

Canals that have been cut off from rivers without any kind of control mechanism at the top. These canals are useful for irrigation when there is too much water in the river during the rainy season, such as the Satluj canal in Punjab. Since irrigation from these types of canals is doubtful, they have been transformed into perennial canals.

#### 5.8.1.2 Perennial Canals

By building a barrage across the river, these canals are separated from perennial rivers. Currently, India has a majority of perennial canals (Mondal, 2022a). Less than 25% of the country's total irrigated land is now irrigated by canals, down from a high of nearly 40% in 1950–1951. In the northern Indian states of Uttar Pradesh, Punjab, Haryana, Rajasthan, and Bihar, canal irrigation covers over 60% of the land.

### 5.8.2 Wells and Tube Well Irrigation

This is a well-known irrigation technique in India. Through a variety of techniques, including reht, charas or mot, the Persian wheel and dhinghly (the lever), etc., groundwater from the well is hoisted. The use of wells for irrigation is common in areas with abundant groundwater and few canals. The major portions of the Northern Plain, the Mahanadi delta, the Godavari, the Krishna, and the Cauvery, the weathered strata of the Deccan trap, and the peninsular crystalline rocks and sedimentary zones are among these areas. However, a greater area of peninsular India is not suited for well irrigation due to its stony nature, uneven surface, and absence of subsurface water. Brackish groundwater makes the larger arid plains of Rajasthan, as well as the neighbouring regions of Punjab, Haryana, Gujarat, and some areas of Uttar Pradesh unsuitable for well irrigation. There were approximately five million wells in 1950–1951; today, there are approximately 12 million. Currently more than 60% of the country's net irrigated land is supplied by wells and tube wells, compared to 29.2% by canal and only 4.6% by tank irrigation. The majority of the

country's well-irrigated land, 28% of it, is in the state of Uttar Pradesh, and Rajasthan (10%), Punjab (8.65%), Madhya Pradesh (8%), and Gujarat (7.3%) are the next states in line. About 82% of the net irrigated area in Gujarat is irrigated by wells; other states with well irrigation include Punjab (80%), Uttar Pradesh (74%), Rajasthan (71%), and Maharashtra (65%). About three-fourths of the entire well-irrigated area is made up of the states of Uttar Pradesh, Rajasthan, Punjab, Madhya Pradesh, Gujarat, Bihar, and Andhra Pradesh.

India's first tube well was dug in Uttar Pradesh in 1930, and the nation had only 2500 of them by 1951. Between 1995 and 1996, the number of electrical pump sets expanded from 2.3 lakh to over 4 million, while the number of dieselized pump sets went from 2.3 lakh to over 3 million. There are already 28 million irrigation pumps in our nation, including electric and diesel (Mondal, 2022b; Garg, 2017; Anonymous, 2015).

### 5.8.3 Tank Irrigation

In order to save monsoon water for later use and irrigation, streams are blocked to create a type of tiny lake, pool, or reservoir known as a tank. In peninsular India, where Tamil Nadu and Andhra Pradesh are the top two states for irrigation, tank irrigation is common and accounts for around 3% of the net irrigated area of the nation. With 29% of its territory irrigated by tanks, Andhra Pradesh is the state with the most tank-irrigated land. In the state tanks cover about 16% of the total irrigated land. Many tanks are present in the Godavari and its tributaries drainage basins. The two districts that use tank irrigation the most are Nellore and Warangal. With 23% of its land under tank irrigation, Tamil Nadu is the second-largest state. The expansion in well and tube well irrigation is largely to blame for the fall in the proportion of tank-irrigated land to the nation's total irrigated area, which fell from 14% in 1960–1961 to roughly 3.1% in 2008–2009. Tank irrigation is used in West Bengal, Bihar, the Bundelkhand region of Uttar Pradesh, Rajasthan, and Gujarat in addition to the Peninsular Plateau.

Tank irrigation is practised in peninsular region mainly due to the following:

- The presence of hard rocks and undulating relief make it difficult to dig canals and wells.
- The hard rock structure allows sizable percolation of water, and groundwater is not available in large quantities.
- Peninsular rivers are mostly seasonal, and most of the streams become torrential only during the rainy season, as if the only way to use this water is to retain it by constructing bunds and building tanks, and it is also easy to collect rainwater in natural or artificial pits due to impermeable nature of rocks.
- The agricultural fields are scattered (Civilsdaily, 2017; Directorate of Economics & Statistics, 2014).

# 6 Development of Underground Sources of Irrigation in India

According to the CWC Report from April 2015, the nation has an annual water availability or water resource potential of 1869 BCM per year based on natural river discharge. However, due to topographic limitations and an uneven distribution of the resource across different river basins, the country's accessible water resources have been assessed to be 1123 BCM per year, making it challenging to extract the full 1869 BCM per year that is available. The share of surface water and groundwater, respectively, is 690 BCM per year and 433 BCM per year of the total 1123 BCM per year available. The net annual groundwater availability for the entire country is 398 BCM after allowing 35 BCM for natural outflow. The country's yearly groundwater resource is primarily comprised of rainfall, which contributes 68% of the total. The other resources, which include return flow from irrigation, recharge from tanks, canal seepage, ponds, and water conservation buildings, collectively make up 32%. The national yearly water availability per person has decreased 15% from 1816 $m^3$ in 2001 to 1544 $m^3$ in 2011 as a result of the country's growing population.

The degree of groundwater development, which is exceptionally high in the states of Delhi, Haryana, Punjab, and Rajasthan where groundwater development is more than 100%, can be used to estimate the amount of groundwater that is readily available for all uses. This shows that annual groundwater use in certain states exceeds annual groundwater recharging. The states of Himachal Pradesh, Tamil Nadu, and Uttar Pradesh, as well as the Union Territory of Puducherry, have groundwater development levels of 70% or more, whereas the other states have levels below 70%. In regions where the resource are easily accessible, groundwater use has grown through time. Fig. 1 shows how this led to a rise in groundwater development overall, which went from 58% in 2004 to 62% in 2011.

## *6.1 Groundwater Irrigation*

The extraction of groundwater is mostly used for irrigation with canals, tanks, and wells including tube wells, being other significant irrigation methods in the nation. Groundwater makes up the largest portion of all of these sources. Surface water usage has been trending downward over the years, whereas groundwater use for irrigation has been steadily rising. The primary irrigation sources usage patterns are shown in Fig. 2. Additionally, the proportion of tube wells has grown rapidly, indicating that farmers are using more groundwater for irrigation. With the introduction of the green revolution, which depended on heavy use of inputs like water and fertilizers to promote farm productivity, the dependence on groundwater for irrigation has increased (Suhag, 2016). However, excessive water usage has caused a significant fall in water tables. Despite growing scarcity, India's groundwater irrigation system is still very inefficient from a technical standpoint. For instance, the third

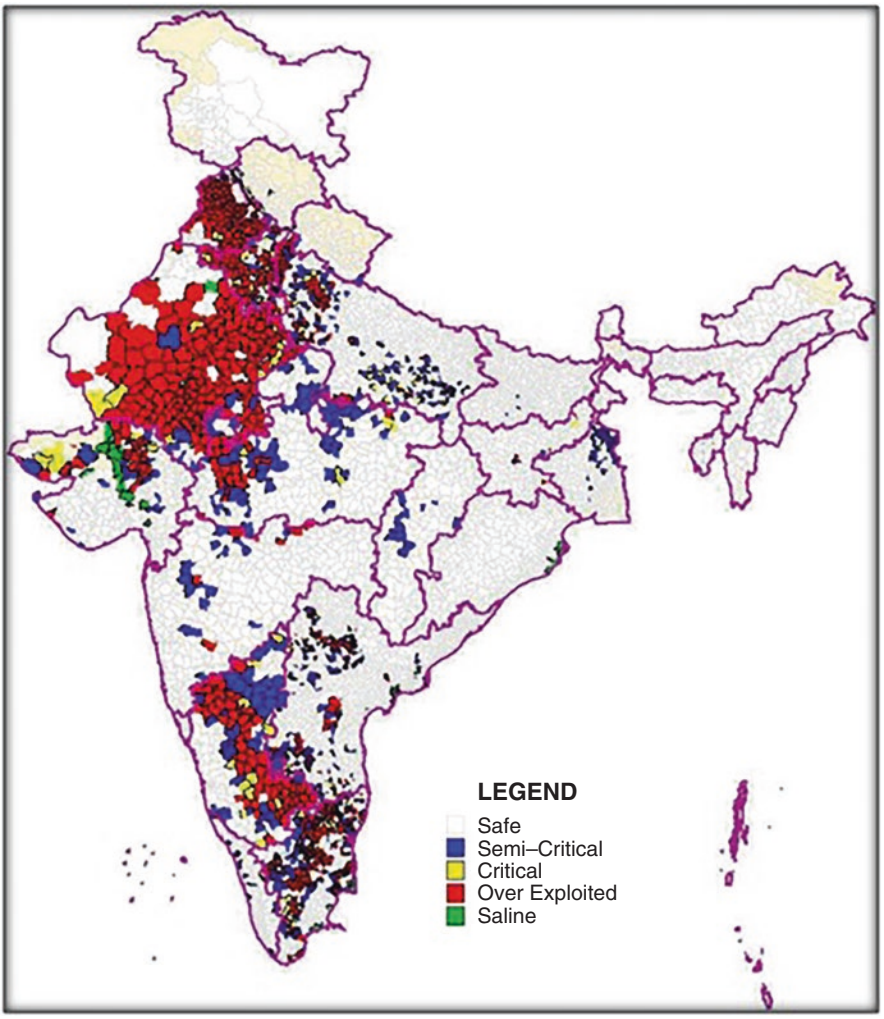


**Fig. 1** Categorization of groundwater assessment units. (Source: Ground water scenario in India, November 2014, Central Ground Water Board; PRS. Note: Data as of 2011)

Minor Irrigation Census of India in 2001 found that only 3% of India's 8.5 million tube well owners used drip or sprinkler irrigation while 88% flooded open channels to distribute water to their crops.

By evaluating about 39% of the wells, the Central Ground Water Board indicated a drop in groundwater level. Out of 6607 assessment units across the nation, 1071 (in 15 states and 2 union territories) have been labelled as "over-exploited" as a result of the stage of groundwater depletion and long-term reduction in groundwater level. According to NASA GRACE Satellite data, the aquifers in North West India's underdeveloped and densely populated areas are most stressed.

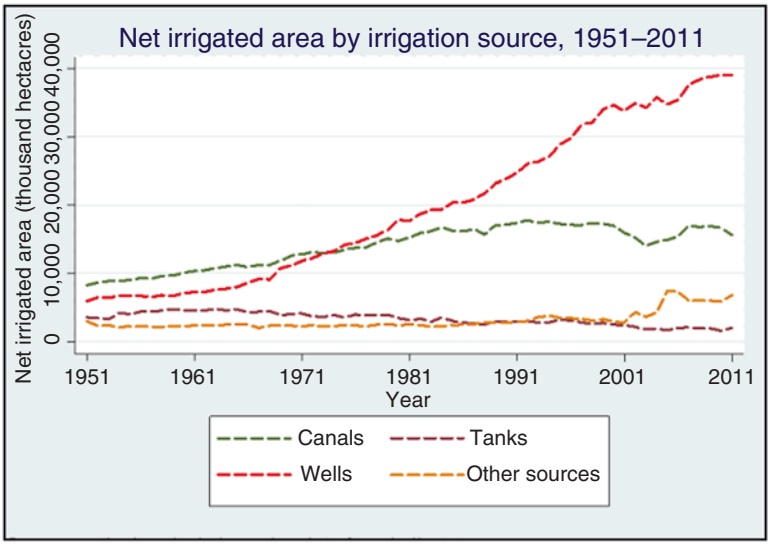


**Fig. 2** Tube wells increasingly being the main source of irrigation. (Source: http://www.waternexussolutions.org)

The second-most stressed aquifer in the world is located in the Indus River Basin, which is shared by Pakistan and India. India is currently planning on ways to reform irrigation departments so they can become capable of improving the water delivery system. The current policy thinkers and planners will benefit from a thoughtful understanding of other nations' interventions and India's own community-based intervention models in order to improve governance structures and understand key indicators that will help them make data-driven decisions (Dhawan, 2017).

## 7 Intensity of Irrigation and Agricultural Development

The ratio of net irrigated area to net seeded area has been used to describe irrigation intensity. Since 55% of the population in India depends on agriculture, many state governments are providing incentives and subsidies to ensure the availability of water for irrigation purposes. For example, the Punjab government in Northern India has been providing free electricity for groundwater pumping, while the Western Indian states of Gujarat and Maharashtra have generously subsidized solar pumps. In India, different regions have varying geographical characteristics, which have led to variances in irrigation intensity. Because water extraction is an expensive endeavour in hilly terrain, deep aquifers, and sandy deserts, there are very few irrigation systems available.

**Table 2** Season-wise area, production, and yield of food grains

| | Kharif | | | Rabi | | | Total | | |
|---|---|---|---|---|---|---|---|---|---|
| Year | A | P | Y | A | P | Y | A | P | Y |
| 2004–2005 | 72.26 | 103.31 | 1430 | 47.82 | 95.05 | 2004 | 120.08 | 198.36 | 1652 |
| 2013–2014 | 69.05 | 128.69 | 1864 | 55.99 | 136.35 | 2435 | 125.04 | 265.04 | 2120 |
| 2014–2015 | 68.77 | 128.06 | 1862 | 55.53 | 123.96 | 2232 | 124.30 | 252.02 | 2028 |
| 2015–2016[a] | 68.76 | 124.01 | 1804 | 53.89 | 128.21 | 2379 | 122.65 | 252.22 | 2056 |

Source: Directorate of Economics & Statistics, DAC&FW
Note: *A* area in million hectares, *P* production in million tonnes, *Y* yield in Kg/ha
[a]Fourth advance estimates

On the other hand, regions with productive alluvial plains, potable groundwater, perennial rivers, and regions with less than 125 cm of rainfall stand out as being regions with a high percentage of irrigation. The Kashmir Valley, the Ganga-Yamuna Doab of Uttar Pradesh, greater portions of Punjab and Haryana, the western half of the South Bihar Plain, Birbhum (West Bengal), Lakhimpur (Assam), the Godavari-Krishna Delta, and Chengalpattu (Tamil Nadu) are among the areas with the highest intensity of irrigation, while in some regions of Punjab the intensity of irrigation exceeds 75%. However, it is impossible to raise crops without irrigation in dry locations like the Spiti and Lahaul districts in Himachal Pradesh and the Ladakh district in Jammu and Kashmir.

Despite the lack of precise statistics, the northern plain and east coastal plains' larger regions record average intensities that fluctuate between 30% and 60%. Parts of the Brahmaputra plain, Chambal Valley, and peninsular plateau have low-intensity irrigation ranging from 15% to 30%. The areas with low intensity of irrigation, almost 0%, are seen along the coasts of Kerala, Manipur, Mizoram, and Tripura, as well as the Andaman and Nicobar Islands. These regions do not require irrigation because they receive high and consistent rainfall throughout the year or they have been unable to develop irrigation facilities because of unfavourable geographic conditions like infertile soils, rugged topography, a lack of surface and groundwater, etc., like parts of the Bihar plain and areas (Dhawan, 2017).

Table 2 analyses show that seasonally adjusted area, yield, and food grain production grew from 198.40 million tonnes in 2004–2005 to an all-time high of 265.04 million tonnes in 2013–2014, a favourable monsoon year, from 198.40 million tonnes in 2004–2005.

However, pre-monsoon rainfall in 2014–2015 was only 99% of the long-term normal, and both monsoon and post-monsoon rainfall were insufficient, which had an impact on the production of both kharif and rabi crops that year.

The states of Punjab, Uttar Pradesh, and Haryana have the highest irrigation intensity, measured as the ratio of net area irrigated to net area sown, according to data cited by the *Directorate of Economics and Statistics, Ministry of Agriculture and Farmers Welfare.* These states are followed by Madhya Pradesh (61.31%), West Bengal (59.21%), Tamil Nadu (56.83%), Bihar (55.85%), Uttarakhand (46.79%), Andhra Pradesh (46.74%), Telangana (46.14%), and Jammu and Kashmir (43.59%), whereas the states of Assam (10.74%), Mizoram (14.04%), Jharkhand (15.68%),

Sikkim (16.88%), Manipur (18.30%), Maharashtra (18.70%), and Kerala (19.36%) have the lowest irrigation intensity. Comparatively speaking, the all-India figure of 48.15% is extremely low.

According to a report from the *Directorate of Economics and Statistics, Ministry of Agriculture and Farmers Welfare*, Uttar Pradesh has the most government canals (2557), followed by Rajasthan (1859), Madhya Pradesh (1625), Andhra Pradesh (1429), Karnataka (1253), Haryana (1210), Punjab (1122), Maharashtra (1081), Bihar (914), and Chhattisgarh (874); Mizoram has the few union territories that also have government canals, including Dadra and Nagar Haveli (1), Delhi (2), and Puducherry (4). There are some states, including Arunachal Pradesh, Manipur, Nagaland, West Bengal, and Sikkim, where no public canals are visible. Private canals are also found in the states of J&K, Kerala, Meghalaya, Mizoram, and Uttarakhand.

Tamil Nadu has the most tanks (378), followed by Andhra Pradesh (340), Karnataka (196), Madhya Pradesh (264), Telangana (230), Karnataka (154), Uttar Pradesh (119), Rajasthan (67), Bihar (58), Jharkhand (52), Chhattisgarh (50), and Gujarat (45); Tripura has the fewest tanks of two.

The number of tube wells and wells is largely distributed in the states of Uttar Pradesh (9984 and 836), Rajasthan (3402 and 264), Madhya Pradesh (3109 and 2986), Punjab (3022 and 0), Maharashtra (2167 and 20), Bihar (1830 and 20), and Haryana (1721 and 0); aside from this, Karnataka, Andhra Pradesh, Gujarat, and Telangana have good proportion of tube wells, whereas Assam and Tripura have least number of wells.

West Bengal has the most sources (3099) compared to other states, followed by Madhya Pradesh (1347), Orissa (1245), Karnataka (416), Rajasthan (162), Assam (140), Andhra Pradesh (124), Kerala (116), Gujarat (114), and Bihar (112). The lowest are Goa and Tamil Nadu, with scores of 6 and 2, respectively. Punjab, Meghalaya, Meghalaya, Haryana, and Maharashtra have all registered very few sources under this heading.

## 8 Demand of Water in the Irrigation Sector

The National Commission for Integrated Water Resources Development and the Indian Planning Commission estimate that by 2050, the world will need 1191 BCM of water for irrigation alone and 1681 BCM overall, including water for other uses (Table 3).

**Table 3** Water requirement for the irrigation sector as determined by the standing sub-committee and NCIWRDP

| Year | 2010 | 2025 | 2050 |
|---|---|---|---|
| Standing sub-committee of MoWR | 688 | 910 | 1072 |
| NICWRD | 557 | 611 | 807 |

Source: Vankar (2015)

## 9 Irrigation Development in the Country During Different Plan Periods

As indicated earlier irrigation projects are classified as major, medium, or minor irrigation projects. The minor irrigation projects (schemes) are further divided into two categories, viz., surface water schemes and groundwater schemes. Major and medium irrigation projects are generally surface water projects.

Irrigation potential has expanded from 22.6 Mha in the pre-plan era to 101.7 Mha by the end of the X Plan (2002–2007), according to an analysis of data on potential developed and exploited across various plan eras. It is likely that the 108.91 Mha of irrigation potential produced by the XI Plan's 2010–2011 period was achieved; of this, 45.3 Mha came from major and medium schemes, and the remaining 63.6 Mha came from smaller schemes. In terms of irrigation potential used, it can be seen that the whole potential developed was utilized to the tune of 22.6 Mha during the pre-plan period and 87.4 Mha by the end of 2010–2011. Up until the VIII Plan, the IPU to IPC ratio stayed at 90% or higher. However, in later plans, the percentage began to fall. It was close to 80% in the XI Plan (from 2010 to 2011). The potential established towards the end of the X Plan (2002–2007) for big and medium-sized projects across the states is highest for Uttar Pradesh with 8.8 Mha, followed by Andhra Pradesh and Maharashtra with 3.6 and 3.5 Mha, respectively. These three states contributed around 38% of the overall irrigation potential in their combined total. At the national level, the percentage of potential developed through major and medium irrigation projects up until the end of the X Plan to ultimate potential is 71% (GoI, 2000, 2007) (Table 4).

According to data analysis on the potential usage at the end of the X Plan, major and medium irrigation projects at the level of all India used roughly 81% of the potential created. With a 99.6% consumption rate, Tamil Nadu was the most utilized state, followed by Punjab, Orissa, Jammu and Kashmir, and Andhra Pradesh, all of which had 90% or above utilization (Table 2).

The country's overall potential for minor irrigation is 81.4 Mha, while the amount of potential that was created and used during the X Plan at the all-India level was 60.1 Mha and 51.5 Mha, respectively. At the national level, the percentage of potential developed up until the X Plan to ultimate potential is 73.8. In summary, by the end of the X Plan, 72.7% of the 140 Mha of ultimate potential have been generated, of which 83.8% have been used at the national level, when all big, medium, and minor plans are taken into account cumulatively.

**Table 4** Achievements of irrigation potential created/utilized for major and medium irrigation

| | | | | ('000 ha) | |
|---|---|---|---|---|---|
| States | Ultimate irrigation potential (UIP) | Potential created up to the X Plan (IPC) | Potential utilized up to the X Plan (IPU) | % of IPC to UIP | % of IPU to IPC |
| Andhra Pradesh | 5000 | 3600.2 | 3244.6 | 72.0 | 90.1 |
| Haryana | 3000 | 2193.7 | 1893.3 | 73.1 | 86.3 |
| J&K | 250 | 187.3 | 174.6 | 74.9 | 93.2 |
| Karnataka | 2500 | 2637.7 | 2119.7 | 105.5 | 80.4 |
| Orissa | 3600 | 1974.4 | 1878.7 | 54.8 | 95.2 |
| Punjab | 3000 | 2574.7 | 2510.5 | 85.8 | 97.5 |
| Rajasthan | 2750 | 2861.6 | 2526.1 | 104.1 | 88.3 |
| Tamil Nadu | 1500 | 1562.6 | 1556.9 | 104.2 | 99.6 |
| West Bengal | 2300 | 1754.8 | 1573.6 | 76.3 | 89.7 |
| *All India* | *58,465* | *41637.9* | *33739.6* | *71.2* | *81.0* |

Source: Central Water Commission, 2013

There were 260 large projects that were finished up until the X Plan (2002–2007), and 35 more were finished in the XI Plan (2007–2012). There are 149 large projects that have overrun in the XII Plan, of which 49 are in Maharashtra and 30 in Andhra Pradesh. Up till the completion of the X Plan, Uttar Pradesh had the most significant projects completed among the states (57), followed by Maharashtra (26) and Gujarat (19). Madhya Pradesh was found to have the most recent major projects, with 16, while Maharashtra has the most active major projects, with 49. Up until the X Plan, 956 medium-sized projects were finished, and 62 more were finished during the XI Plan period. In the XII Plan, 138 additional medium projects have been added. Madhya Pradesh had the most new projects (12), according to the analysis. Maharashtra has the most active medium-sized projects (71), followed by Madhya Pradesh (13). There are extension, renovation, and modernization (ERM) projects in addition to major and medium projects. Up until the X Plan, 121 of these projects were finished, while 19 projects have been finished in the XI Plan. In contrast, there are 27 new ERM projects in the XII Plan and 3.9 ongoing ERM projects in the plan (CGW, 2013; GoI, 2011; CGW & GoI, 1999).

## 10 Status of Irrigation Potential and Its Likely Phasing

The status of irrigation potential of the country that remains to be created and its likely phasing overtime is summarized in Table 5.

The overall irrigation potential created up until the X plan was 102.77 Mha, and there will be an additional 16 Mha, 21 Mha, and 2.66 Mha irrigation potential created in the XI, XII, and XIII plans, respectively. Major and medium-sized projects have a greater impact on irrigation potential in India than smaller projects do (GoI, 2013b).

**Table 5** Status of irrigation potential and its likely phasing

| Plan | Major and medium irrigation | Minor irrigation | | Inter-basin water transfer (IBWT) | Total |
|---|---|---|---|---|---|
| | | Surface | Ground | | |
| Ultimate irrigation potential | 58.47 | 17.38 | 64.05 | 35.1 | 175.00 |
| Developed till the end of the X Plan | 42.35 | 14.31 | 46.11 | – | 102.77 |
| Expected addition in: | | | | | |
| XI Plan | 9.0 | 2.50 | 4.50 | – | 16.0 |
| XII Plan | 9.0 | 0.50 | 11.50 | – | 21.0 |
| XIII Plan | | 0.07 | 1.94 | 0.65 | 2.66 |
| XIV Plan | – | – | – | 0.38 | – |
| Subsequent Plans | – | – | – | 34.1 | – |

Source: Government of India (2009), "Report of the Task Force on Irrigation", "Planning Commission", Government of India, May 2009

## 11 Year-Wise Achievement of Irrigation Potential Created/ Utilized Under Major, Medium, and Minor Irrigation of the XI Plan in India

During the XI Plan, irrigation potential of 12643.32 thousand hectares (Th.ha) was intended to be created, and 1536.36 Th.ha of irrigation potential was intended to be used from major and minor irrigation projects. In terms of small irrigation projects, 7188.75 Th.ha of irrigation potential was intended for creation and 2274.03 Th.ha for utilization. It is likely that out of 12643.32 Th.ha, only 3701.01 Th.ha of irrigation potential was developed, and that as of 2011, major and medium projects had used 925.06 Th.ha of irrigation potential. When taking into account the minor irrigation projects, it becomes clear that it was likely that 3465.82 Th.ha of the total targeted irrigation potential (7188.75 Th.ha) would have been created and that 1246.47 Th.ha of the irrigation potential had been used up until 2011 from the minor irrigation projects (Table 6).

According to information now available, the VII Plan sought to reach an irrigation potential total of 13 Mha; however, the Indian government has succeeded in achieving irrigation potential up to 11.31 Mha, demonstrating that there was not much of a gap. However, the following VIII, IX, and X plans showed a gaping hole in the government's ability to accomplish the desired irrigation potential (Table 4).

The development of irrigation has received the majority of the agricultural investment. Despite a rise in plan spending on irrigation from Rs. 441.8 crore in the Ist Plan to Rs. 100,106 crore in the X Plan, the share of total plan spending has declined from 23% in the Ist Plan to 6% in the X Plan (Gov. of India, Ministry of Water Resources, 2011).

According to the Report of the Steering Committee on Water Resources for Eleventh Five Year Plan (2007–2012) of the Government of India Planning Commission, there is a physical gap between potential created (4.604) and potential

**Table 6** Plan-wise potential creation targets vs. achievements

| | | | | (In Mha) | | |
|---|---|---|---|---|---|---|
| | Targets | | | Achievements | | |
| Plan | MMI[a] | MI[b] | Total | MMI | MI | Total |
| VII | 4.3 | 8.6 | 13 | 2.22 | 9.09 | 11.31 |
| VIII | 5.087 | 10.71 | 15.8 | 2.21 | 2.96 | 5.17 |
| IX | 9.81 | 7.24 | 17.05 | 4.1 | 3.59 | 7.69 |
| X | 9.936 | 6.807 | 16.74 | 5.3 | 3.52 | 8.82 |

Source: Government of India (2013b), "Water and Related Statistics, Water Resources Information System, Directorate Information System Organization, Water Planning & Project Wing, Central Water Commission", New Delhi, Delhi, December, 2013

[a]Major and medium irrigation projects

[b]Minor irrigation projects

utilized (1.360) during the indicated years in India despite an increase in expenditure from 29390.64 crore to 68735.3* crore in the 2007 to 2010–2011 period November 2011 in New Delhi (GoI, 2003, 2007, 2009, 2011, 2013a, b).

In India, there are now 219 medium irrigation projects and 169 major ones. The state of Maharashtra stands out as having the most active major (56) and medium (95) irrigation projects, followed by the states of Karnataka, Jharkhand, and Andhra Pradesh. When comparing the numbers of major and minor projects started and finished during various plan eras, it can be seen that a total of 488 major irrigation projects were started up until the XI plan, of which 305 were finished.

In a similar manner, 1282 medium irrigation projects were started, of which 1023 were finished; likewise, 261 ERM projects were started, of which 122 were finished (Ministry of Water Resource, Government of India, 2015), Out of the 2031 total projects (major, medium, and ERM) taken on, 1450 have been finished.

## 12 Post-Independence Irrigation Development in India

According to the Department of Agriculture and Cooperation and Statistics (2014), the agriculture sector in India is regarded as the foundation of the country's economy because it accounts for about 18% of the country's total GDP and provides a living for more than 70% of the population in rural areas. It is also the country's largest employer, employing 49% of the total labour force. In addition to providing jobs, the agriculture sector is crucial for ensuring food security. According to an analysis by the NSSO from 2013, an ordinary Indian still spends more than half of their income on food security. However, due to the fact that Indian agriculture is heavily dependent on rainfall, as a result the majority of its growth rates have fluctuated since independence 1950–2013 (Giri, 2016; Dev, 2013; GoI, 2005, 2009).

The early years of independence had a negative growth rate in the agricultural sector. Except for 2002–2003 due to a severe drought, growth rates after 1958 have been positive. With the onset of the green revolution between 1960 and 1970, the

agriculture industry grew at an astonishing rate. Even though agriculture's growth rate has fluctuated, it continues to contribute less and less to India's overall GDP, despite the reality that the bulk of the labour force has been underutilized. Even though at the time of independence, agriculture made up over half of the total GDP, it has since decreased to 18% from more than 45% in 1954–1955, according to Giri (2016) and Arjun (2013). Due to the availability of the most recent technology, developed seeds, improved irrigation facilities, and new production techniques, the total amount of rice production has increased dramatically from about 20 million tonnes in 1950 to almost 106 million tonnes in 2013–14. With new production techniques and technologies, wheat production as a whole increased after independence during the first phase of the green revolution. The total yield rose from 11 million tonnes in 1966–1967 to 88.94 million tonnes in 2014–2015 (Department of Agriculture and Cooperation & Statistics, 2014; Ryan & Asokan, 1977). Since the start of the green revolution, the yield curve has improved. In 1967–1968, 1 ha of wheat produced 1103 kg; today, per-hectare production has been steadily improving, indicating that wheat production has been rising (Ministry of Agriculture, 2015; Sebby, 2011). When compared to 1950–1951, when the total production was 5.50 million tonnes, the total agricultural yield of jowar has been steadily declining, with a total production of 5.39 million tonnes being recorded in 2013–2014. This decrease is due to the jowar cultivated area declining from 15.57 to 5.82 Mha in 2013–2014, as well as a change in attitude from the traditional product to the modern commercial crops (Giri, 2016; Ministry of Agriculutre, 2015; Zalkuwi et al., 2014).

## *12.1 Present Status of Irrigation Development in India*

India's construction of huge storage-based irrigation systems during this century, especially after independence, has been made possible by government's effort and funding. Major and medium (M&M) projects have received more than 60% of irrigation funds since independence (Satyajit, 1997). From a time of severe droughts and susceptibility to food shortages, Indian agriculture has come a long way to being a key exporter of agricultural products. This has been made feasible by ongoing work to maximize the potential of available land and water resources for agricultural use. In the 50 years leading up to independence, Indian agriculture expanded at a rate of approximately 1% annually; in the 50 years following freedom, it expanded at a rate of around 3% annually (Abrol, 1995; NSSO, 2013)

The long-awaited inter-basin water transfer, which aims to increase India's irrigated area by 35 Mha, has recently seen some encouraging moves taken. Depending on the priorities of the government, the inter-basin water transfer link plans are implemented in stages. The links Ken-Betwa, Parbati-Kalisindh-Chambal, Godavari-Krishna (Vijayawada), Damanganga-Pinjal, and Par-Tapi-Narmada have been identified as priority links for reaching an agreement among the concerned states to begin preparing detailed project reports (Shirsath, 2009).

### *12.2 Irrigation in Twelfth Plan Period*

By 2050, the demand gap for irrigation might be in the range of 250 BCM if the XII Plan is taken into account. Even if a significant portion of this increased demand is met by groundwater, surface irrigation will still need to be expanded by 150 BCM in order to reach self-sufficiency by 2050. It is clear that the country needs and wants to create greater storage through its major and medium irrigation sector. Many of the efforts intended to provide a sustainable solution for food security and agricultural expansion have their roots in the major and medium irrigation sector.

The Working Group estimated that there would be a total of 583 projects listed in the XII plan, including 236 major, 265 medium, 65 ERM, and 17 special category projects involving various tasks such dam safety and specific maintenance. A total of 327 active projects, comprising 154 major, 139 medium, and 34 ERM projects, are anticipated to require financial inputs in the XII plan for their implementation based on the current financial and physical state. According to estimates, 130 projects were started in the XI Plan, of which 116 are said to have been finished, including 45 large, 66 medium, and 5 ERM projects, while 37 have obligations for the XII Plan (8 major, 28 medium, and 1 ERM project). In the XII plan, there are suggestions for 28 major, 32 medium, and 25 ERM new projects. There are 337 projects in total that are anticipated to spill over into the XII Plan, including 155 large, 147 medium, and 35 ERM initiatives (Government of India and Confederation of Indian Industry, 2005).

## 13 National Water Grid System

Only 4% of the world's renewable water resources are found in India. The average yearly precipitation in India is thought to be 4000 BCM, of which 3000 BCM is thought to fall during the monsoon season (June–September). The rivers receive 1869 BCM on average each year, according to estimates. The anticipated amount of surface water that can be used out of the aforementioned is 690 BCM. The total utilizable groundwater resource, excluding the aforementioned, is 431 BCM. As a result, 1121 BCM is thought to represent the nation's total yearly utilizable water supply (State of Indian Agriculture, 2016).

In India, the idea of interconnecting rivers has a long history. Arthur Cotton proposed a plan to connect India's major rivers in the nineteenth century, during the period of British colonial rule, in order to speed up the import and export of goods from the South Asian colony and to address water shortages and droughts in the region's south-east (Andhra Pradesh and Orissa) (Srivastava, 2016).

Significant attention was paid to the river interlinking concept for moving water from surplus basins to shortage basins. The famed "National Water Grid" or "Ganga-Cauvery Link", with a 2640 km connection canal, was proposed by Dr. K. L. Rao, the then Union Minister of State for Irrigation and Power (now the Ministry of

Water Resources), in 1972. Similar to Captain D. J. Dastur, who proposed the "Garland Canal", which consists of the 9300-km Central Indian and Southern Garland Canal and the 4200-km Himalayan Canal (Desai et al., 2012). Rao suggested that the Brahmaputra and Ganga basins are water surplus regions and central and south India are water-deficit regions on this ground, but his proposal has not been furthered by the government as they were not techno-economically feasible (Singh, 2003). Rao's primary concern was to deal with severe water shortages in the south and consistent flooding in the north every year.

A National Perspective Plan (NPP) for water resources development was created in 1980 by the Central Water Commission and the Ministry of Water Resources (formerly the Ministry of Irrigation). The NPP consists of two parts, Peninsular Rivers Development and Himalayan Rivers Development, and calls for building storage facilities on a number of river systems as well as connecting canal networks to move water from areas with water surpluses to those with shortages (Srivastava, 2016). The Government of India (GoI) established the National Water Development Agency (NWDA) in 1982 to carry out studies on a realistic and scientific basis for the viability of inter-basin water transfer projects and give NPP a tangible form. Finally, in 1990, in addition to the already designated mission of Peninsular Rivers Development, NWDA was also given the task of Himalayan Rivers Development. NWDA has found 30 linkages based on a number of studies (16 Peninsular and 14 Himalayan) (NWDA, 2003, 2014; MoWR, 2011).

The consent of the involved states, their collaboration, and the agreements with the neighbouring countries are necessary for the interlinking of rivers to take place in the nation. In order to supply irrigation in the water-scarce/arid districts of Madhya Pradesh and Rajasthan in the Chambal basin, one of the links, namely, Parbati-Kalisindh-Chambal, has been considered under NPP (Desai et al., 2012). However, this link cannot be implemented due to various ecological problems in the Panna Biosphere Reserve. Additionally, on June 28, 2006, the NWDA Society's functions were modified to include the creation of DPR for link projects and prefeasibility/feasibility reports for intra-basin links as suggested by states. NWDA's duties were further expanded to include the creation of DPRs for intra-state lines (NWDA, 2017).

## *13.1 Himalayan Component*

The Himalayan Rivers Development envisioned building reservoirs on the Ganga, the Brahmaputra, and their principal tributaries in India and Nepal, as well as a network of interconnected canals to transfer excess water from the eastern tributaries of the Ganga to the west and connect the main Brahmaputra with the Ganga. This system will generate around 30 million kilowatts of hydropower and add irrigation to nearly 22 Mha, helping to significantly reduce flood damage in the Ganga-Brahmaputra basin (NWDA, 2022b).

### *13.2 Peninsular Component*

The Peninsular River Development Scheme has four major parts.

1. The Mahanadi-Godavari-Krishna-Palar-Pennar-Kaveri interlinking.
2. The west-flowing rivers, north of Bombay, and south of Tapi interlinking.
3. Ken with Chambal interlinking.
4. Deviation of some water from west-flowing rivers.

Figure 3 depicts the beginning of the peninsular and Himalayan components. In addition to benefits for improved flood control and regional transportation, the Peninsular component held the potential to irrigate an extra 25 Mha through surface waters, 10 Mha through increased use of groundwaters, and generate hydropower (NWDA, 2022a, b).

### *13.3 Intra-state Interlinking of Rivers*

In June 2005, India gave the National Water Development Agency permission and a commission to find and finish feasible studies of intra-state projects intended for the interlinking of rivers inside the state. However, a sizable number of states responded that they have no intra-state river connection proposals, including Nagaland, Meghalaya, Kerala, Punjab, Delhi, Sikkim, Haryana, the Union Territories of Puducherry, Andaman and Nicobar Islands, Daman and Diu, and Lakshadweep. The Pennaiyar-Sankarabarani Link was proposed by the Puducherry government, despite the fact that it is not an intra-state project. The governments of Bihar and Maharashtra have each proposed interlinking six projects between their respective rivers, while Gujarat has proposed one project, Orissa has proposed three, Rajasthan has proposed two, Jharkhand has proposed three, and Tamil Nadu has proposed one. Since 2005, NDWA has completed feasibility studies on the projects, determining that 20 of them are practicable, 1 was withdrawn by the Maharashtra government, and 1 was deemed to be infeasible (NWDA, 2013, 2014).

## 14 Present Status of Interlinking of Rivers Program

The National Water Development Agency (NWDA) has identified 30 links under the National Perspective Plan (NPP) for water resources development through inter-basin transfer of water prepared by the Ministry of Irrigation in August 1980 for the purpose of preparing feasibility reports (FRs), as the pre-feasibility reports of those links have already been distributed to the concerned states (16 under the Peninsular Component and 14 under the Himalayan Component). Following surveys and investigations, FRs for 2 connections in the Himalayan component and 14 links

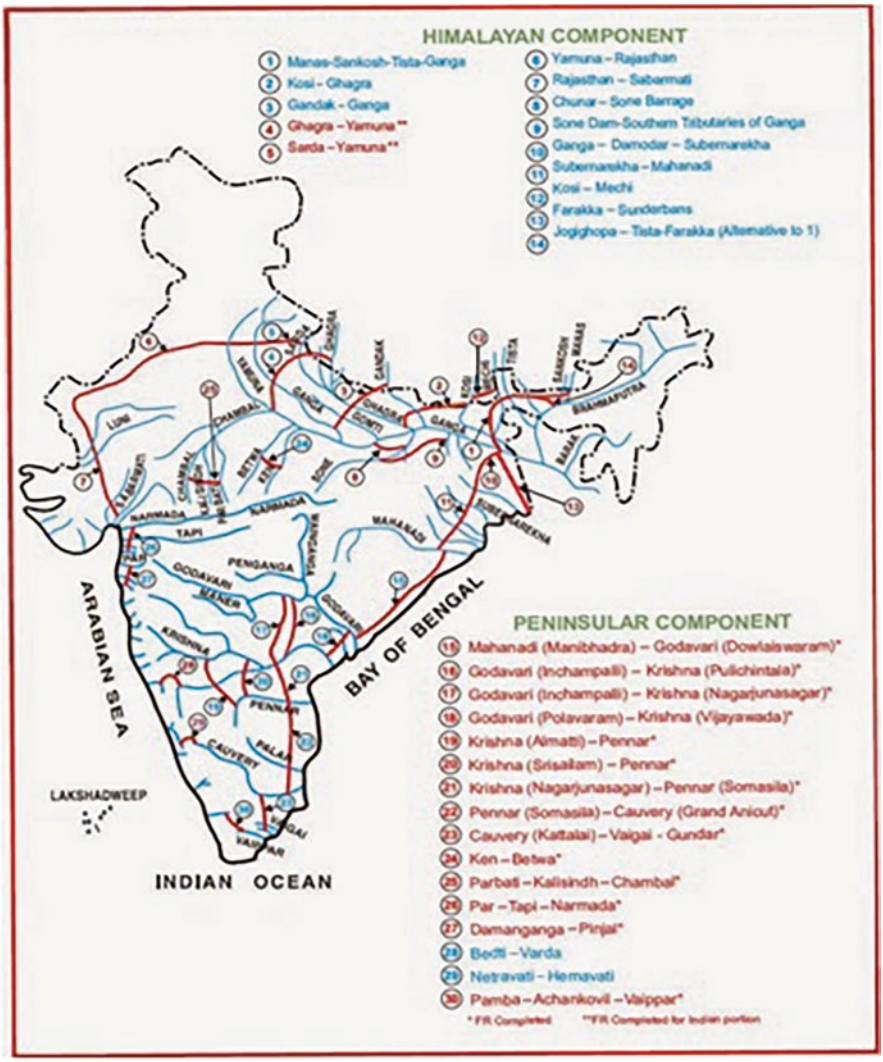


**Fig. 3** Proposed inter-basin water transfer links. (Source: NWDA, 2014)

under the Peninsular Component were created. Four priority links have been identified for the development of detailed project reports (DPRs) based on the agreement of the involved states, namely, the Ken-Betwa Link Project (KBLP) Phases I and II, the Damanganga-Pinjal Link, the Par-Tapi-Narmada Link, and the Mahanadi-Godavari Link. The relevant states have received the DPRs for the KBLP Phase I and II, Daman-Ganga-Pinjal, and Par-Tapi-Narmada. For KBLP Phase I, numerous statutory clearances have also been received. The Bundelkhand region in Uttar Pradesh and Madhya Pradesh, which is prone to drought, will gain from the project.

Additionally, the Damanganga-Pinjal Link project has received techno-economic clearance, pending to statutory clearances. The Central Water Commission has received the DPR of Par-Tapi-Narmada for technical evaluation. Due to the significant submergence caused by the Manibhadra Dam, the Government of Odisha refused to support the Mahanadi-Godavari Link, the mother link of the nine-link system, which also includes the Krishna, Pennar, Palar, Cauvery, Vaigai, and Gundar. A preliminary revised proposal for the Mahanadi-Godavari Link Project with reduced submergence has been prepared by NWDA and presented to the State Government of Odisha based on recommendations from WRD (Press Information Bureau, 2018).

The interlinking of rivers in India is one of the most expansive projects ever put out to deal with the country's difficulties with water scarcity and floods. The proposed water infrastructure project, which is divided into two phases, calls for numerous connections between the nation's major rivers in an effort to both enhance India's hydropower capacity and find a long-term solution to the country's frequent floods and droughts. A task force was established by the minister of water resources, river development, and Ganga rejuvenation to further the project. The project will have a significant impact on the future of our nation in many areas and will spark enormous ecological issues that will contaminate natural habitats. India may or may not carry out the ILR project as envisioned now that the Union Government has given it top priority and established a powerful task force for quick and meticulous implementation of the project. However, it appears vital to spend heavily in water infrastructure on a comparable or bigger scale, as the population that is affected by water scarcity or flooding may increase owing to population expansion. The country's future water demand must also be taken into account while developing the medium-term water sector (Langar, 2017).

## *14.1 Pros and Cons of River Interlinking*

There are several benefits to linking rivers together, including the potential to increase agricultural production by an additional 100% over the following 5 years, prevent crop losses due to extreme drought or flooding (which cost $550 million in 2002), conserve foreign exchange by avoiding oil export, and, more, enlist every Panchayat as a stakeholder and implement agency to unify the nation. By adding a second line of defence, you may increase the country's security and create 10 lakh jobs over the next 10 years of eradication of the yearly flooding issues in the northeast and the north. Through the use of alternate perennial water resources, the water crisis situation can be resolved, allowing for inland shipping, sufficient food production, and an increase in farmers' yearly average revenue.

The project's drawbacks include negative environmental effects (deforestation, soil erosion, etc.), the difficulty of rehabilitation, social unrest/psychological harm brought on by the forcible resettling of locals (such as the Sardar Sarovar Project),

political consequences including tense relations with neighbours (Pakistan, Bangladesh), increased evaporation losses, and a pricey undertaking for the upkeep of built-in canals (Mehta & Mehta, 2013).

### 14.1.1 Conclusion

In India and around the world, irrigation is being rapidly expanded due to the pressure of survival and the need for more food supply. The availability of irrigation water for crops is crucial to the production and productivity of agricultural fields. In India, achieving sustainable growth and effective water management is becoming a more difficult task. Competing claims for water are created by rising agricultural productivity, expanding urbanization, growing urbanization, and rapid industrialization.

India's agriculture has been reliant on the monsoons since ancient times. A shift in monsoon patterns has a significant impact on agriculture. Indian agriculture is being impacted even by the rising temperature. Rain-fed or unirrigated crops, which are grown on approximately 60% of cropland, will be most affected by climate change. The implementation of major and minor irrigation schemes has greatly benefited the nation; however, the sustainability objectives have not yet been met. New irrigation opportunities have been made possible by the relatively recent action of joining rivers, which may mark a win in increasing production and productivity as well as eradicating regional imbalance.

## References

Abrol, I. P. (1995). *Agriculture in India*. Centre for Advancement of Sustainable Agriculture.

Anonymous. (2015). *Different types of irrigation and irrigation systems storage*. Retrieved from https://selfstudyhistory.com/2015/10/06/gs-paper-3-different-types-of-irrigation-and-irrigation-systems-storage/ on 8 Feb. 2018

Apoorva, O. (2007). *Irrigation: Achievements and challenges* (India infrastructure report) (pp. 178–196). Irrigation and Water Resources.

Arjun, K. M. (2013). Indian agriculture-status, importance and role in Indian economy. *International Journal of Agriculture and Food Science Technology, 4*(4), 343–346.

Bano, N. (2013). *Sources of irrigation and agricultural development in India*. LAP LAMBERT Academic Publishing.

Central Ground Water Board website. (1999). FAQs, http://www.cgwb.gov.in/faq.html

Central Water Commission. (2013, December). *Water and related statistics*. Water Resources Information System Directorate, Information System Organisation, Water Planning & Project Wing.

Charlesworth, N. (1981). *British rule and the Indian economy, 1800–1914* (pp. 23–37). Springer.

Civilsdaily. (2017). *Sources and methods of irrigation (Part I)*. Retrieved on 8 Feb 2018 from http://www.civilsdaily.com/blog/sources-and-methods-of-irrigation-tank-irrigation-wells-and-tubewells-canals-ultimate-irrigation-potential-net-irrigated-area-irrigation-intensity/

D'Souza, R. (2006). Water in British India: the making of a 'colonial hydrology'. *History Compass, 4*(4), 621–628.

Department of Agriculture and Cooperation, & Directorate of Economics and Statistics. (2014). *Agricultural statistics at a glance 2014*. Directorate of Economics and Statistics.

Desai, V., Ghosh, S. N., & Patro, J. (2012). National water grid—Its objective and challenge. *ISH Journal of Hydraulic Engineering, 12*, 131–132. https://doi.org/10.1080/09715010.2006.10514824

Dev, S. M. (2013). *Small farmers in India: Challenges and opportunities*. Indira Gandhi Institute of Development.

Dhawan, V. (2017). *Water and agriculture in India "status, challenges and possible options for action"* (Background paper for the South Asia expert panel during the Global Forum for Food and Agriculture (GFFA)). Federal Ministry of Food and Agriculture.

Economic Survey of India (2013) https://www.indiabudget.gov.in/budget2014-2015/es2013-14/estat1.pdf

Falkenmark, M, & Lindh, G. (1976). *Impact of water resources on population*. Submitted by the Swedish delegation to the UN world population conference, Bucharest, 19–30 August.

Garg, V. (2017). *Sources and methods of irrigation: Part 1*. Retrieved from https://www.civilsdaily.com/sources-and-methods-of-irrigation-tank-irrigation-wells-and-tubewells-canals-ultimate-irrigation-potential-net-irrigated-area-irrigation-intensity/ on 11 Jan 2018.

Ghosh, A (2012). *Impact of Mayurakshi irrigation canal system on the socio-economic aspects of its command area*. Thesis submitted at Department of Geography, Visva-Bharati, Santiniketan, West Bengal, India.

Giri, I. (2016). *Overview of the agriculture sector in India since independence*. Retrieved from https://www.projectguru.in/agriculture-sector-india/ on 18 Jan 2018.

Government of India. (1999). *Water resources development plan of India: Policy and issues*. National Commission for Integrated Water Resources Plan, Ministry of Water Resources, GOI.

Government of India. (2000). Report of the task force on irrigation. Planning Commission, Government of India.

Government of India. (2005). Report of the task force on irrigation. Planning Commission, Government of India.

Government of India. (2003, May). *Report of the task force on irrigation* (p. 2009). Planning Commission, Government of India.

Government of India. (2007, May). *Report of the steering Committee on Water Resources for Eleventh Five Year Plan (2007–2012)*. Planning Commission.

Government of India. (2009, May). *Report of the task force on irrigation*. Planning Commission, Government of India.

Government of India. (2011). *Final report of minor irrigation and watershed management for the Twelfth Five Year Plan (2012–2017)*. Planning Commission, Government of India.

Government of India. (2013a). *Twelfth Five Year Plan (2012–2017), faster, more inclusive and sustainable growth* (Vol. I). Sage Publication, Planning Commission, Government of India.

Government of India. (2013b, December). *Water and related statistics*. Water Resources Information System, Directorate Information System Organization, Water Planning & Project Wing, Central Water Commission.

Government of India and Confederation of Indian Industry. (2005). *Irrigation*. National conference on Bharat Nirman, Bharat Nirman, pp. 17–21.

Gulati, A., Meinzen-Dick, R., & Raju, K. V. (2005). *Institutional reforms in Indian irrigation*. Sage Publications.

Hantal, B. (2018). *Importance of irrigation in India*. Retrieved from http://www.yourarticlelibrary.com/essay/importance-of-irrigation-in-india/42581 on 8 Jan 2018.

Kwat, N. (2018). *Irrigation potential and it's utilization in India*. Retrieved from http://www.economicsdiscussion.net/india/irrigation/irrigation-potential-and-its-utilization-in-india/19049 on 8 Jan 2018.

Langar, S. Z. (2017). *Behind India's ambitious plan to create the world's longest river*. Retrieved from https://www.archdaily.com/877423/behind-indias-ambitious-plan-to-create-the-worlds-longest-river on 12 Oct 2022.

Lisha. (2022). *What are the various sources of water available in India*. Retrieved from https://www.preservearticles.com/articles/what-are-the-various-sources-of-water-available-in-india/5481 on 8 Oct 2022.
Mehta, D., & Mehta, N. K. (2013). Interlinking of rivers in India: Issues & challenges. *Geo-Eco-Marina, 19*, 137–143.
Ministry of Agriculutre. (2015). *Agricultural situation in India*. Ministry of Agriculutre.
Ministry of Water Resources (MoWR). (2011). *Report of working group on major, medium and command area development for the XII Five Year Plan (2012–2017)*. Government of India.
Ministry of Water Resources (MoWR), Govt. of India. (2015). http://wrmin.nic.in
Mondal, P. (2022a). *Canals irrigation in India*. Retrieved from https://www.yourarticlelibrary.com/irrigation/canals-irrigation-in-india-with-maps-an-pictures/21102 on 8 Oct 2022.
Mondal, P. (2022b). *Wells and tubewells irrigation in India: Merits and demerits*. Retrieved from https://www.yourarticlelibrary.com/irrigation/wells-and-tube-wells-irrigation-in-india-merit-and-demerits/21109 on 9 Oct 2022.
Muthyam, S., Suresh, B. A. V., Rao, B. S., & Rao, V. (2013). *Monitoring of irrigation projects using high resolution cartosat satellite data*. NNRMS Bulletin.
National Water Development Agency (NWDA). (2003). *Inter-basin water transfer proposals*. NWDA.
National Water Development Agency (NWDA). (2013). Ministry of Water Resources, Govt of India.
National Water Development Agency (NWDA). (2014). Ministry of Water Resources, Govt of India.
National Water Development Agency (NWDA). (2017). *Note on interlinking of rivers projects in the country details and status*. Retrieved from http://www.nwda.gov.in/upload/uploadfiles/files/File423.pdf on 11 Oct 2022.
National Water Development Agency (NWDA). (2022a). *Intra-state river link proposals received from the state governments, Government of India*. Retrieved from http://www.nwda.gov.in/content/innerpage/intra-state-links.php on 12 Oct 2022.
National Water Development Agency (NWDA). (2022b). *National perspectives for water resources development*. Retrieved from http://www.nwda.gov.in/content/innerpage/click-more.php on 11 Dec 2022.
NSSO. (2013). National Sample Survey Office. New Dellhi.
Palanisami, K., Karthikeyan, C., & Venkatesapalanichamy, N. (2007). *India: Water management – An overview*. Proceeding paper in Indo-US workshop on innovative e-technologies for distance education and extension/outreach for efficient water management, March 5–9, 2007, ICRISAT, Patancheru/Hyderabad, Andhra Pradesh, India.
Phansalkar, S., & Verma, S. (2005). *Silver bullets for the poor: Off the business mark?* Mimeo. International Water Management Institute.
Press Information Bureau. (2018, March). *Inter-linking of rivers*. Ministry of Water Resources, River Development and Ganga Rejuvenation. Retrieved from https://pib.gov.in/PressReleasePage.aspx?PRID=1523256 on 12 Oct 2022.
Ryan, J. G., & Asokan, M. (1977). Effect of Green Revolution in wheat on production of pulses and nutrients in India. *Indlan Journal of Agricultural Economics, 32*(3), 8–15.
Satyajit (1997) Taming the waters: the political economy of large dams in India, Oxford University Press, copyright 1997 (published 2002).
Schoengold, K., & Zilberman, D. (2004). *Water and development: The importance of irrigation in developing countries*. Retrieved on February 12, 2018, from http://are.berkeley.edu/courses/ARE253/2004/handouts/Bretton_Woods.pdf
Sebby, K. (2011). *The Green Revolution of the 1960's and its impact on small farmers in India*. University of Nebraska-Lincoln.
Seth, T. (2018). *Irrigation: Importance, sources, development and limitations*. Retrieved on February 7, 2018, from http://www.economicsdiscussion.net/essays/irrigation-importance-sources-development-and-limitations/2108

Shirsath, P. B. (2009). *Irrigation development in India: History and impact*. Retrieved on January 16, 2018, from http://indiairrigation.blogspot.in/2009/01/history-of-irrigation-development-in_01.html
Singh, P. (2003a). *Colonising the rivers: Colonial technology, irrigation and flood control in North Bihar, 1850–1950.* PhD thesis. Jawaharlal Nehru University, pp. 198–261.
Singh, A. K. (2003b). *Inter-linking of rivers in India: A preliminary assessment*. New Delhi, The Other Media (www.landportal.org).
Srivastava, S. (2016). *What is the difference between National Water Grid and National River Linking Project? Or are both the same?* Retrieved on January 23, 2018, from https://www.quora.com/What-is-the-difference-between-National-Water-Grid-and-National-River-Linking-Project-Or-are-both-the-same
State of Indian Agriculture. (2016). Ministry of Agriculture & Farmers Welfare, Department of Agriculture, Cooperation & Farmers Welfare.
Stone, I. (2002). *Canal irrigation in British India: Perspectives on technological change in a peasant economy* (pp. 278–280). Cambridge University Press.
Suhag, R. (2016). *Overview of ground water in India*. Retrieved on February 8, 2018, from http://www.prsindia.org/administrator/uploads/general/1455682937~~Overview%20of%20Ground%20Water%20in%20India.pdf
Vankar, S. P. (2015). *A socio-economic study of irrigation projects in Maharashtra state with special reference to Marathwada region*. Thesis submitted at Department of Economics, Dr. Babasaheb Ambedkar Marathwada University, Aurangabad, India.
Water and Related Statistics. (2015, April). Central Water Commission. http://www.cwc.gov.in/main/downloads/Water%20&%20Related%20Statistics%202015.pdf
Zalkuwi, J., Singh, R., Bhattarai, M., Singh, O., & Dayakar, B. (2014). Profitability analysis of sorghum production in India. *International Journal of Commerce, Business and Management, 3*(5), 707–714.

## *Bibliography*

Data.gov.in. (2016). *Agriculture production stock yield*. Retrieved August 1, 2016, from https://data.gov.in/catalog/agriculture-production-stock-yield
http://india-wris.nrsc.gov.in/wrpinfo/index.php?title=CGWB_Ground_water_resources
http://nwda.gov.in/writereaddata/mainlinkfile/File423.pdf
http://planningcommission.nic.in/aboutus/committee/wrkgrp12/wr/wg_major.pdf
http://water-atlas.blogspot.in/p/chapter-1-andhra-pradesh-in-india.html
http://wrmin.nic.in/forms/list.aspx?lid=380
http://www.preservearticles.com/201105257067/what-are-the-various-sources-of-water-available-in-india.html
https://ecoursesonline.icar.gov.in/mod/page/view.php?id=128515
India-2008, Publications Division, Ministry of Information and Broadcasting, Government of India, rrtd.nic.in/India_2008.pdf
NNRMS Bulletin – December 2013.
Planning Commission. (2015). *Data bank on agriculture and allied sectors*. Retrieved January 8, 2016, from http://planningcommission.gov.in/sectors/agri_html/DataBank.html
World Bank. (1991). *India irrigation sector review* (Vol. II). The World Bank.
World Bank. (1995). *Tamil Nadu water resources consolidation project: Staff appraisal report*. the World Bank.

# Response of the River Jhelum to Active Tectonics, NW Himalaya

**Reyaz Ahmad Dar, Yasir Manhas, Khalid Omar Murtaza, Waseem Qader, Jehangeer Ahmad Mir, and Omar Jaan Paul**

## 1 Introduction

Alluvial rivers flow on the sediments deposited by them and are sensitive to slight changes in geomorphic, tectonic, and anthropogenic processes occurring within the basin (Achyuthan, 2003; Joshi & Kotlia, 2014, 2018; Kale et al., 2014; Kothyari et al., 2016a; Dubey et al., 2017; Dar et al., 2019). In view of their sensitivity and quick response to various disturbing processes, alluvial rivers provide a vital opportunity to comprehend the tectonic deformation of an area (Seeber & Gornitz, 1983; Ouchi, 1985; Holbrook & Schumm, 1999; Jain & Sinha, 2005; Turowski et al., 2006; Amos & Burbank, 2007). The response of alluvial rivers to active tectonics can be inferred from varied channel dimensions, including channel sinuosity, channel avulsions, aggradation, and degradation (Willett & Brandon, 2002). According to Schumm et al. (2000) any deformation on a scale of few millimeters (2–3 mm annually) may induce morphological changes in a river basin. Besides, climate, lithology, folding, faulting, incision, etc., can result in the formation of various channel patterns and alluvial landforms (Schumm, 1986; Keller & Pinter, 1996; Whipple et al., 2013; Kothyari, 2014; Kothyari et al., 2016b, 2018; Taloor et al., 2017).

The Kashmir Valley located in the NW Himalaya is sandwiched between the Great Himalayan Range to the northeast and Pir Panjal Range to the southwest (Fig. 1). The geomorphic setting of the valley suggests that due to the tectonic uplift of the Pir Panjal Range, the ancient drainage got impounded and formed a vast lake (Dar et al., 2014; Paul et al., 2021). This lake, known as Karewa Lake, later on

R. A. Dar (✉) · Y. Manhas · W. Qader · J. A. Mir · O. J. Paul
Department of Earth Sciences, University of Kashmir, Srinagar, India

K. O. Murtaza
Department of Geoinformatics, University of Kashmir, Srinagar, India



S. Kanhaiya et al. (eds.), *Rivers of India*,
https://doi.org/10.1007/978-3-031-49163-4_3

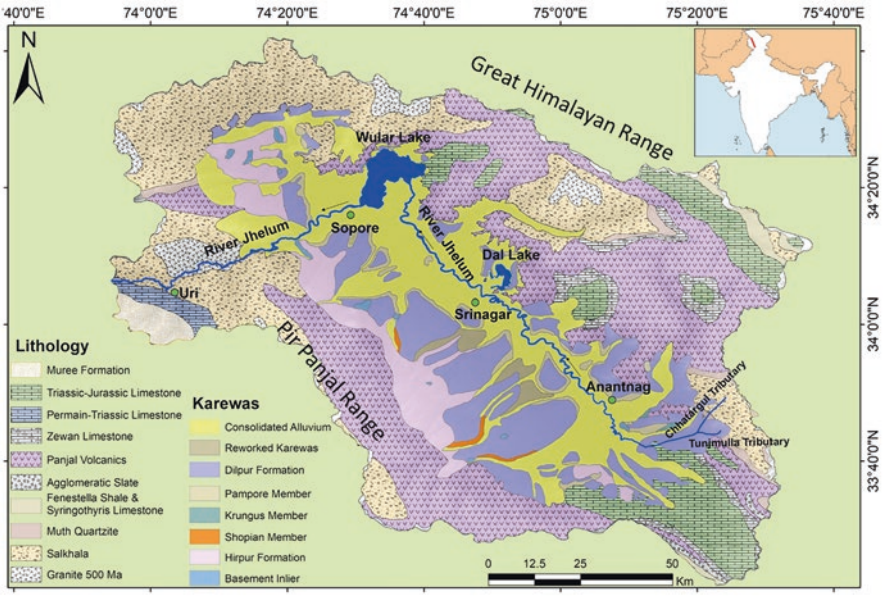


**Fig. 1** Lithological and Karewa distribution map of the Kashmir Valley modified after Dar et al., (2014) and Bhatt (1982) respectively. The course of the River Jhelum and the major lakes (Wular and Dal Lake) are also shown in the map

drained out through the Baramulla gorge giving rise to the River Jhelum and its tributaries. Flowing through the axial part of the tectonically active Kashmir Valley, the river is characterized by diverse morphology manifested in channel width variations, meandering bends, braid bars, channel avulsions, unpaired terraces, and perturbations in longitudinal profile. The river continuum extends from partly confined to laterally unconfined (alluvial) to confined variants. To ascertain the causes of this anomalous geomorphology, we divided the river into different reaches and used various techniques and river geomorphic indices to evaluate the river response to disturbing forces. The geomorphic indices used in this study have previously been tested in comprehending the role of active tectonics in triggering river geomorphic changes (Silva et al., 2003; El Hamdouni et al., 2008; Della-Seta et al., 2008; Dehbozorgi et al., 2010). It is good to mention here that the tectonic-geomorphic study of the Srinagar reach of the River Jhelum has previously been published (Dar et al., 2019), and the current chapter extends that work to the entire course of the river in the Kashmir Valley.

## 2 Tectonic-geomorphic Setting of the Kashmir Valley

Geologically, the Kashmir Valley encompasses a complete stratigraphic record of lithologies of all ages ranging from Archean to recent (Gansser, 1964; Dar et al., 2015; Stojanovic et al., 2016). Recent alluvium and Quaternary sediments occupy almost all of the valley floor (Dar et al., 2017, 2021). The valley is bounded by a complex fault pattern, namely, the imbrication of northward rooted basal decollement branded as the Main Himalayan Thrust (Schelling & Arita, 1991). The Suring-Mustgarh anticline fold represents the southern-most deformation front extending between the River Jhelum in NE and Beas in SE (Ahmad et al., 2015). The other fault systems that are associated with the Kashmir Valley include the Himalayan Frontal Thrust, Main Boundary Thrust, Kotli Thrust, Riasi Thrust, Balapur Thrust, and Bagh-balakot Fault. It is believed that the Kashmir Valley evolved in the Late Miocene with the shifting of NE thrust complex to the SW front of Pir Panjal from the base of Great Himalayan side (Burbank, 1983; Burbank & Johnson, 1983). Owing to this shifting the existing structural system basement complexes of the Main Boundary Thrust/Main Central Thrust replaced the NE thrust complex (Ahmad et al., 2015). Nevertheless, there are some studies that propose that the evolution of the Kashmir Valley is a result of dextral strike slip fault accompanied by pull-apart character in NW Himalaya (Alam et al., 2015a, b). These fault systems along with other local faults have affected the geomorphology and the drainage of the entire NW Himalaya encompassing the Kashmir Valley.

## 3 Methodology

To study the alluvial river response to prevailing tectonics, the calculation of geomorphic indices occupies the central place (Jaan et al., 2015). In the present study we employed geomorphic indices to infer the impact of tectonic activity on the River Jhelum, in the Kashmir Himalaya. We employed an integrated approach using remote sensing and extensive field expeditions to study the influence of tectonic activity on the River Jhelum. Google Earth imagery and ALOS PALSAR DEM of 12.5 m resolution were used to calculate different geomorphic indices. Measurements of geomorphic indices and other related parameters were carried out in ArcGIS environment followed by the interpretation of river geomorphic features and geomorphic indices in terms of tectonic activity and/or lithological variation. The various geomorphic indices used include sinuosity index (SI), lateral entrenchment ratio (ER), stream length gradient index (SL), braided index (BI), and mountain front sinuosity (Smf) augmented with river width profile and river terrace analysis. The impact of channel sinuosity on channel erosion and channel shifting was validated from lateral entrenchment (ER) ratio which was measured as a ratio between the length of the two banks of a river along the corresponding reach (Goswami et al., 1999). The stream length gradient index of the River Jhelum was calculated

using the formula SL = ($\Delta H/\Delta L$) L of Hack (1973), where $\Delta H/\Delta L$ is the gradient of the reach or channel slope, $\Delta H$ is the elevation change along the reach, $\Delta L$ is the length of the reach, and $L$ is the total channel length from the midpoint of the reach of computation. Braided index (Bi) is a measure of the degree to which bars and/or islands separate multiple flow paths and is measured as a ratio between twice the length bar and reach length (Goswami et al., 1999). Similarly, mountain front sinuosity (Smf) of the fronts (wherever necessary) was calculated as a ratio of straight-line length of the mountain front (Ls) to the length of mountain front along the mountain foot (Lmf) (Bull, 1977). The observations derived from the geomorphic indices were augmented by river terrace observations and width changes of the river. Besides, river reaches with anomalous river response were selected, and intensive field work was carried out for validation of the results. The motivation behind using geomorphic indices is that most of the Jhelum basin is covered by thick alluvium and Quaternary sediments (Dar & Zeeden, 2020) and the direct surface expressions of geological structures and their impact on river geomorphology are difficult to trace using conventional methods.

## 4 Results and Discussion

### *4.1 Sinuosity Index*

For the calculation of sinuosity index (SI), the River Jhelum was divided into various reaches (Fig. 2a). Few of the tributaries, joining the river from Chhatargul and Tunj Mulla localities, (hereafter referred as Chhatargul and Tunj Mulla tributaries), were also studied for SI (Fig. 2a). The reaches located on the main River Jhelum are from Sheikh Gund to Nai Basti (Anantnag), from Anantnag to Wular Lake, and from Sopore town to Uri. The reaches of tributaries and main river were further subdivided into sub-reaches to determine the SI and other parameters discussed in the following sections.

The sinuosity index values (Fig. 2b) calculated for Chhatargul tributary (CT) are 1.08 (reach 1), 1.12 (reach 2), and 1.23 (reach 3). Similarly, for Tunj Mulla tributary (TT) the SI values are 1.14 (reach 1), 1.10 (reach 2), 1.17 (reach 3), and 1.18 (reach 4). The values lie between 1.06 and 1.30, suggesting low sinuosity. The SI values calculated for the main river from Sheikh Gund to Nai Basti (SN) along various reaches are 1.29 (reach 1), 1.37 (reach 2), 1.18 (reach 3), and 1.59 (reach 4). The values fall with the sinuous/meandering degree of sinuosity (Schumm, 1963). Similarly, the SI values from Nai Basti (Anantnag) to Wular Lake (NW) are 1.87, 1.33, 1.33, 1.64, 1.80, 1.37, and 1.28 for reaches 1, 2, 3, 4, 5, 6, and 7, respectively. These values again fall within the sinuous/meandering degree class of channel sinuosity. After its exit from the Wular Lake near the Sopore town, the river heads toward Baramulla town and finally leaves the Kashmir Valley, traversing through

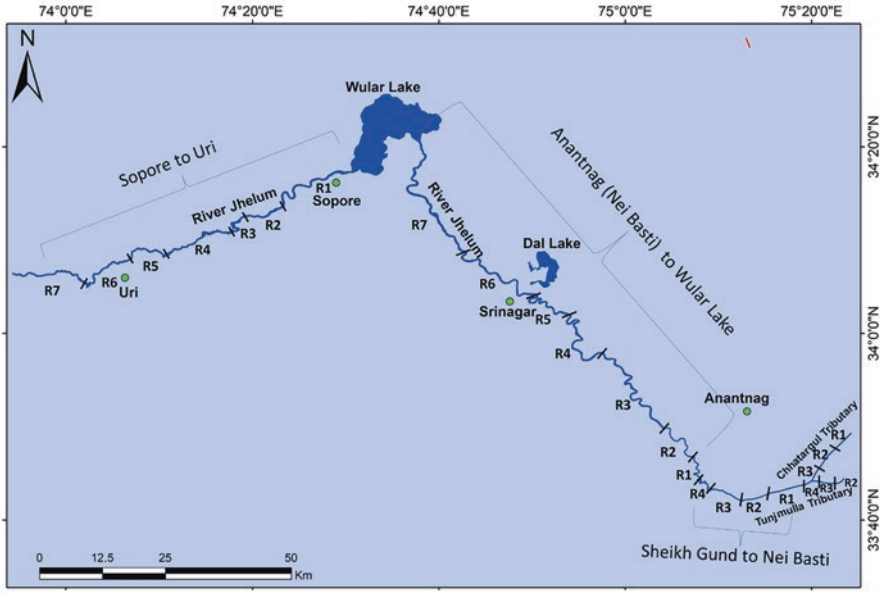


**Fig. 2a** Map showing the course of the River Jhelum. The tributaries (Chhatargul and Tunj Mulla) and reach scheme are also shown in the map

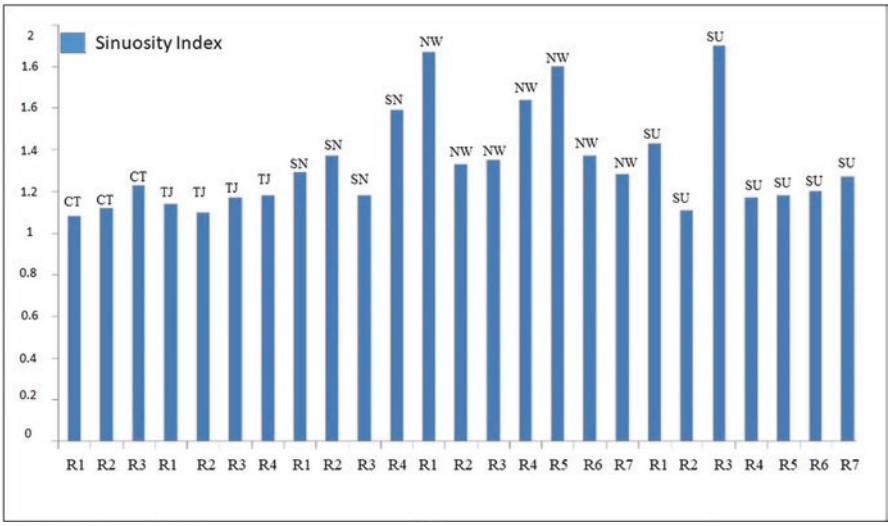


**Fig. 2b** Bar chart showing the sinuosity index of the River Jhelum along different reaches. *CT* Chhatargul tributaries, *TT* Tunj Mulla tributaries, *SN* Sheikh Gund to Nai Basti, *NW* Main River Jhelum (Nai Basti to Wular Lake), *SU* Sopore to Uri

the Pir Panjal Range near Uri. The SI values of the River Jhelum from Sopore town to Uri (SU) are 1.43, 1.11, 1.87, 1.17, 1.18, 1.85, and 1.27 for reaches 1, 2, 3, 4, 5, 6, and 7, respectively, referring to a low river sinuosity. Thus, from the above results it is suggested that the River Jhelum sinuosity ranges from low sinuosity to sinuous/meandering degree.

## *4.2 Lateral Entrenchment Ratio*

Similar to sinuosity index, the lateral entrenchment ratio (ER) was calculated for the sub-reaches of the River Jhelum. It is good to mention here that ER values <1 indicate left bank erosion and >1 right bank erosion (Rosgen, 1994). For Chhatargul and Tunj Mulla reaches, the ER values are 0.99, 0.99, 1.02, 0.99, 1.02, 0.98, and 0.95 respectively. These values indicate that in reaches 1 and 2 of Chhatargul stretch, the value is close to 1 reflecting negligible river bank shifting. However, the right bank of the river has experienced slightly more incision relative to the left bank in the reach 3 as is reflected by the ER value of 1.02. The ER value for Tunj Mulla stretch reveals that the right bank has experienced slightly more incision and consequently has shifted toward right.

The ER calculated for the reaches from Sheikh Gund to Wular Lake (total 11 reaches; Sheikh Gund to Nai Basti = 4 reaches, and Nai Basti to Wular Lake = 7 reaches) are 1.0, 1.03, 1.02, 1.01, 1.06, 0.98, 0.97, 0.96, 1.02, 1.01, and 0.99 respectively. Analysis of the ER of these reaches suggests that the right bank has experienced more incision relative to the left bank. The meander growth and the slightly higher incision on the right side of the river could be attributed to the general tilt of the valley toward northeast owing to higher uplift of the Pir Panjal Range compared to the Greater Himalayan Range (Dar et al., 2014). This observation is substantiated by the presence of several meanders with wide concave bends on the right bank of the river.

However, the ER values in some reaches suggest that the left bank incision is comparatively higher than the right bank. Since a large number of fault/lineaments are observed in the valley floor (Ali & Ali, 2020), few of which trend along, and others cut across the river at several locations (Fig. 3a). The deformation associated with these faults/lineaments and the unconsolidated nature of the bank material lead to substantive erosion of the river banks. Besides the diversity in the river bank lithology with hard rocks forming one bank and alluvium the other bank (e.g., downstream from Baramulla town), the alluvial bank erosion outpaces the hard rock bank.

ER values calculated from Sopore town to Uri are 0.97, 1.01, 1.0, 0.98, 0.97, 1.07, and 1.04 for the reaches 1, 2, 3, 4, 5, 6, and 7, respectively. The results suggest that reaches 1, 4, and 5 have experienced more incision in the left bank in comparison to the right bank, while reaches 2, 6, and 7 show that incision is more in the right banks of river. In case of reach 1 (from Wular to Sherwani Abad), the right bank of

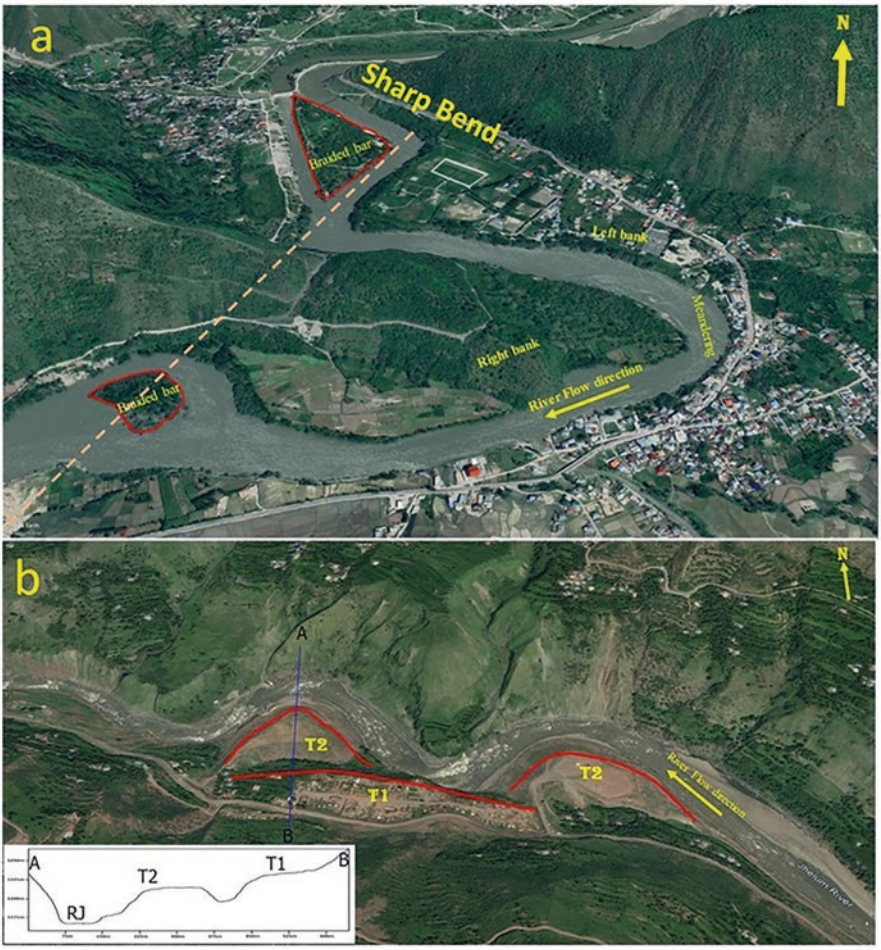


**Fig. 3** (**a**) Google Earth imagery showing entrenched meandering of Jhelum near Baramulla. The dashed line shows the possible fault, and the sharp bend and two braid bars are also associated with this fault. (**b**) Google Earth image showing the presence of terrace (T1, T2) on the left bank. AB represents the elevation profile showing the course of the River Jhelum (RJ) and the river terraces. Note the absence of terraces along the right bank

river is closer to a mountain with hard rock lithology, and in the left side it is bounded mainly by recent alluvium, so a chance of erosion and lateral migration toward left is more than right side. Also, mass wasting from the mountain has played an important role in confinement of the right bank and erosion of the left bank. Overall, the ER values are nearly close to 1 in all reaches of this stretch of the River Jhelum. This could be because of the presence of a fault that runs parallel to the river course, promoting down-cutting or confinement of the river valley due to the presence of hard rocks on both sides of the river. The preservation of older terraces along reaches 4 and 5 suggests more vertical erosion along the right bank and lateral

erosion along the left. At reach 7, the ER values suggest slightly more erosion of the right bank. This is well substantiated by the presence of river terraces along the left bank (Fig. 3b). Overall, the river course shows a combined effect of lineaments/faults and lithology downstream from the Sopore town.

### *4.3 Stream Length Gradient Index*

The SL values calculated for different reaches of the River Jhelum are shown in Figs. 5 and 6. The abnormality in SL of a river results from a variety of factors including river bed lithology, geological structures, slope, etc. (Dar et al., 2022). However, the drainage scaled upward is related to regional tectonic uplift (Chen et al., 2003; Dehbozorgi et al., 2010). The SL values for Chhatargul to Anantnag stretch of the River Jhelum range from 57 to 130 (Fig. 4). The relatively low values are due to the absence of hard rock lithology as the river here flows over alluvium with almost homogenous physical properties. The water elevation profile shows an almost constant decrease in slope. However, few perturbations are observed on the elevation profile which may be associated with the presence of lineaments/faults as indicated by the knickpoints with SL values of 88.6, 104.8, and 130. It is good to mention here that the SL values for the Srinagar reach of the River Jhelum are already published (Dar et al., 2019) and therefore were not incorporated in this study.

Similarly, the SL values of the River Jhelum from Sopore to Uri range from 43.5 to 850 (Fig. 4). The values are comparatively higher than the upstream reaches of the River Jhelum from Chhatargul to Anantnag. Numerous convexities are observed on the elevation profile. Here, the river mostly flows over the hard rocks which may be responsible for the anomalous SL values. Besides, many lineaments are also observed, some of which cut across the river in this reach which might be responsible to the higher SL values in these locations (Ali & Ali, 2020). Therefore, both the hard rocks and the presence of lineaments/faults result in higher SL values for this stretch of the River Jhelum. Moreover, the change in valley confinement configuration downstream and anthropogenic activities like dam construction for hydropower generation also alter the SL values.

### *4.4 Braided Index (BI)*

The BI values for reaches 1, 2, and 3 of Chhatargul tributary are 0.37, 0.25, and 0.19, respectively, with <5% degree of braiding for all reaches. However, the BI values for reaches 1, 2, 3, and 4 of Tunj Mulla tributary are 1.33, 0.79, 0.32, and 0.96, respectively, with degree of braiding ranging from 5% to 34% for reaches 1, 2, and 4 and <5% for reach 2. Downstream, the BI values for reaches 1, 2, 3, 4, and 5 of the main River Jhelum from Sheikh Gund to Anantnag are 0.42, 0.45, 0.71, 0.10, and 0.73, respectively, with degree of braiding <5% for reaches 1 and 2 and

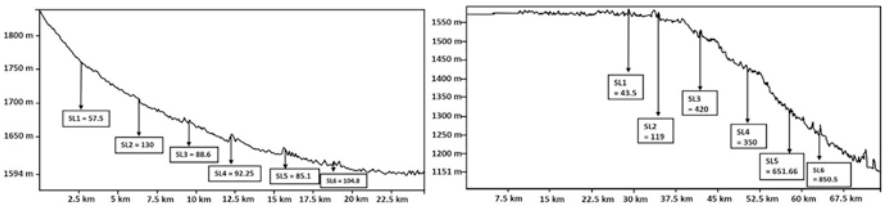


**Fig. 4** Stream length gradient index values of the River Jhelum from Sheikh Gund to Anantnag (left) and from Sopore to Uri (right). Note the increase in the SL values as the river here passes through the Baramulla gorge and finally exits the valley.


**Fig. 5** (**a**) Google Earth image showing braided bars in the course of the River Jhelum near Tail Wani (**b**) showing island bars at Thaji Wara

5–34% for reaches 3, 4, and 5. The results suggest that braiding is less in the tributaries than in the main channel. The comparatively higher gradient of tributaries than the main river prevents braid bar formation, for example, in the Chhatargul tributary. However, owing to low gradient of the main River Jhelum, the deposition of the bedload takes place, thus resulting in the formation of braided channels, as observed in the Sheikh Gund to Anantnag reach of the river (Fig. 5). From Anantnag to Wular Lake the River Jhelum shows meandering character rather than the braided pattern as it is not fulfilling the prerequisite conditions (abundant sediment supply) for the formation of braid bars although occasionally some small braid bars are observed. These braid bars have been related to the presence of lineaments/faults by Dar et al. (2019). Further downstream from Sopore to Uri, the river is narrow and confined by hard rocks which decreases the chances of braid bar formation. Overall, the braiding decreases toward the downstream reaches of the River Jhelum due to the decrease in sediment load, occasional narrowing of the river course due to vertical incision along faults/lineaments, and the confinement of river by hard rocks.

### *4.5 River Width Profiling*

Geomorphic studies carried out in the Kashmir Valley reveal numerous lineaments/faults running parallel, along, or cutting across the River Jhelum (Ganju & Khar, 1984; Alam et al., 2015b; Dar et al., 2019). The lineaments/faults running along the river course result in down-cutting instead of side-cutting, causing narrowing and deepening of the river channel. However, widening occurs where lineaments/faults cut across the river course (Dar et al., 2019). The narrow and long stretch of the river near Anantnag suggests the presence of fault that forced the river to incise deep and maintain a narrow course. The Google Earth image (Fig. 6) of the stretch shows that the river is confined from the right side by an elevated topography, a potential fault scarp that have constricted the lateral cutting. This part of the river also shows less sinuous behavior and follows a nearly straight course in this reach.

Downstream, laterally unconfined settings have resulted in greater sideward erosion. The low slope of the valley floor also favors more lateral cutting and less vertical incision, resulting in river widening and meandering. Overall, the width profile from Sheikh Gund to Wular Lake shows narrowing for the initial 30 miles with widening in few narrow strips, but thereafter the river shows overall widening (Fig. 7a). This could be because of the high river gradient in initial course which favors vertical incision. Downstream, the river enters the valley floor, and the gradient decreases which increases lateral erosion and results in the overall widening of the river channel. The negligible gradient, less confined conditions, and erodible banks augment more side cutting, less vertical incision, and hence more channel width. In its Srinagar reach, the river exhibits high variability in width. Google Earth imagery and field survey reveal that in few places the narrowing is due to anthropogenic encroachments of the river banks, thus making the district more vulnerable to flooding (Romshoo et al., 2018).


**Fig. 6** Google Earth image showing a fault scarp near Anantnag town and the course of the River Jhelum in its proximity

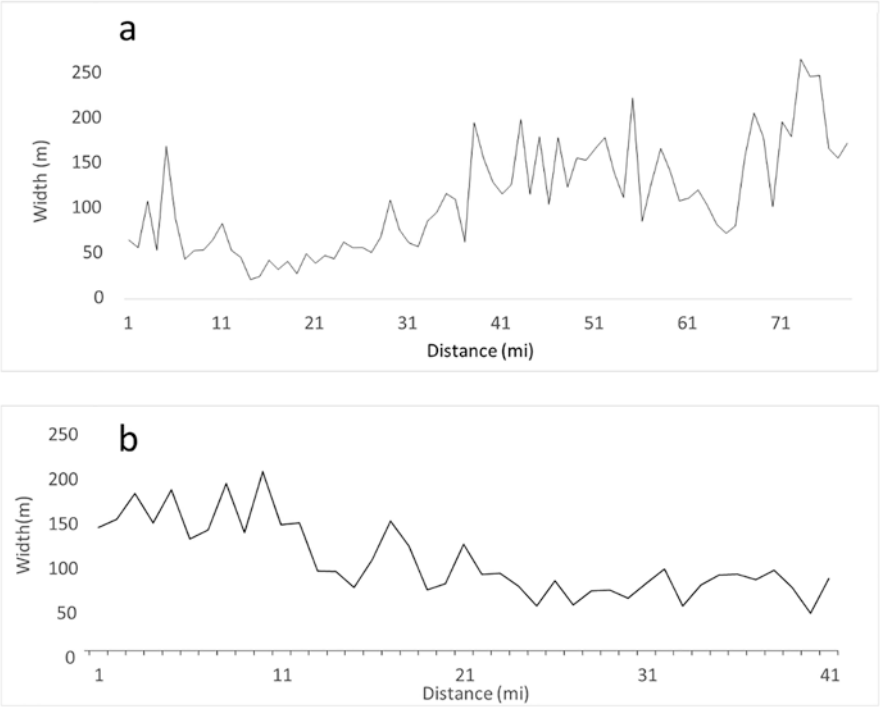


**Fig. 7** (**a**) Channel width profile of the River Jhelum between Sheikh Gund and Wular Lake and (**b**) from Sopore to Uri

The width of the River Jhelum from Sopore town to Uri shows an overall decrease in width (Fig. 7b). Near Sopore town, the river is wide and exhibits meandering because of low gradient and unconfined settings. The river width decreases downstream owing to the confined valley setting, hard rock lithology, and presence of geological structures. The river narrowing has resulted in increased stream power and vertical incision.

## *4.6 River Terraces*

Analysis of the river geomorphology reveals the occasional preservation of river terraces along the course of the River Jhelum. However, along most of the river reaches, step features of river terraces were difficult to distinguish due to human settlement and anthropogenic activities on the river banks. The river terraces observed along the Sopore to Uri stretch of the River Jhelum are well preserved and occur along reaches 4, 5, 6, and 7. Field observations suggest that terraces are predominantly unpaired along this stretch (Fig. 8), as the right bank terraces are


**Fig. 8** Field photograph showing unpaired terraces and braid bar near Baramulla town

preserved while few of the left bank terraces are absent. However, along reaches 1 and 2, step features of river terrace are difficult to differentiate due to human settlements. Along reach 3 near the Baramulla gorge, the river has deeply incised, thus minimizing the chances of alluvial terrace formation. Downstream from Uri along reach 7, the River Jhelum changes its overall trend from SE to NW. Along this reach, the river terraces are also unpaired but well preserved along the left bank, showing uplift of the left and erosion along the right bank. Slow and continuous river incision with associated lateral erosion may have played a role in unpaired terraces formation as observed during field work. Therefore, the presences of unpaired terraces indicate that the river has responded to the structural deformations or/is still responding to tectonic activities.

## 5 Summary and Conclusion

The tributaries and the main channel of the River Jhelum cut and flow over the alluvium in Kashmir Valley, NW Himalaya. The tributaries, coming from the surrounding mountain ranges, possess high gradient and usually follow low sinuous paths, bringing water and sediments to the trunk stream. The sediment load deposited in the main River Jhelum is transported and redeposited downstream, thus affecting the river course especially in the middle part of the basin where the slope is very low. Sediment deposition and lateral erosion along with low slope have resulted in meandering and increase in the river width. However, high variability in width is found with low carrying capacity in few middle reaches as compared to the lower and upper reaches. The right bank experiences more incision relative to the left bank with meandering growth on the right side due to higher rate of uplift of the Pir Panjal Range than the Greater Himalayan Range. Wherever, the river flows along the trend of the faults/lineaments, vertical incision, channel narrowing, straight channel course, and high water velocity have been observed. For example, an E-W trending fault reported from Baramulla has produced about 55 m high scarp in the area (Bilham & Bali, 2014). Traversing through this fault zone, the river exhibits

incised activity into the bedrock and has carved a huge meandering loop and bifurcated the river into two parts, with one part flowing through the trace of the faults. Downstream from Baramulla town, the River Jhelum enters the confined valley setting with hard rock lithology. Before its exit from the valley through the Pir Panjal Range near Uri, confined valley setting, geological structures, and hard rock lithology result in low river sinuosity. The confined settings also control channel planform and width, thus increasing stream power and vertical incision. Further, the unpaired terraces observed show signs of tectonic uplift and slow and continuous river incision indicating valley floor deformations and river response to active tectonics.

Overall, the ongoing tectonic activity and the associated slow deformation of the valley floor have affected the fluvial systems of the Kashmir Valley. Besides, the rapid uplift of the Pir Panjal Range has also affected the climate of the valley shifting the climate toward temperate from subtropical type. Hence, it can be concluded that the comparatively higher degree of uplift of the valley towards the left side of the River Jhelum has produced a general tilt to erode and shift the river action toward the right bank. Our observations of the change in the intensity and the direction of river erosion and the consequent varying ER and SI ratios reflect that the geology, structure, and slope have played an important role in determining the course of the River Jhelum in the Kashmir Valley.

## References

Achyuthan, H. (2003). Bedrock Channel incision in the arid tracts of Jaisalmer, Rajasthan. *Proceedings-Indian National Science Academy Part A, 69*(2), 241–250.

Ahmad, S., Alam, A., Ahmad, B., Bhat, M. I., & Bhat, M. S. (2015). Geomorphic evidence of unrecognized Balapur fault segment in the Southwest Kashmir basin of Northwest Himalayas. *Geomorphology, 250*, 159–172.

Alam, A., Ahmad, S., Bhat, M. S., & Ahmad, B. (2015a). Tectonic evolution of Kashmir basin in Northwest Himalayas. *Geomorphology, 239*, 114–126.

Alam, A., Ahmad, S., Bhat, M. S., & Ahmad, B. (2015b). Response to the commentary by Shah AA (2015) and further evidence supporting the dextral strike–slip pull-apart evolution of the Kashmir basin along the Central Kashmir fault (CKF). *Geomorphology, 253*, 558–563.

Ali, U., & Ali, S. A. (2020). Comparative response of Kashmir Basin and its surroundings to the earthquake shaking based on various site effects. *Soil Dynamics and Earthquake Engineering, 132*, 106046.

Amos, C. B., & Burbank, D. W. (2007). Channel width response to differential uplift. *Journal of Geophysical Research: Earth Surface, 112*(F2). https://doi.org/10.1029/2006JF000672

Bilham, R., & Bali, B. S. (2014). A ninth century earthquake-induced landslide and flood in the Kashmir Valley and earthquake damage to Kashmir's Medieval temples. *Bulletin of Earthquake Engineering, 12*(1), 79–109.

Bhatt, D. K., 1982. A review of the stratigraphy of the Karewa Group (Pliocene/Quaternary), Kashmir. Man Env. 6, 46–55.

Bull, W. B. (1977). *Tectonic geomorphology of the Mojave Desert* (188p.). US Geological Survey Contract Report 14-08-001-G-394. Office of Earthquakes, Volcanoes, and Engineering.

Burbank, D. W. (1983). The chronology of intermontane-basin development in the northwestern Himalaya and the evolution of the northwest Syntaxis. *Earth and Planetary Science Letters, 64*(1), 77–92.

Burbank, D. W., & Johnson, G. D. (1983). The late Cenozoic chronologic and stratigraphic development of the Kashmir intermontane basin, northwestern Himalaya. *Palaeogeography, Palaeoclimatology, Palaeoecology, 43*(3–4), 205–235.

Chen, Y. C., Sung, Q., & Cheng, K. Y. (2003). Along-strike variations of morphotectonic features in the Western Foothills of Taiwan: Tectonic implications based on stream-gradient and hypsometric analysis. *Geomorphology, 56*(1–2), 109–137.

Dar, R. A., & Zeeden, C. (2020). Loess-palaeosol sequences in the Kashmir Valley, NW Himalayas: A review. *Frontiers in Earth Science, 8*, 113.

Dar, R. A., Romshoo, S. A., Chandra, R., & Ahmad, I. (2014). Tectono-geomorphic study of the Karewa Basin of Kashmir Valley. *Journal of Asian Earth Sciences, 92*, 143–156.

Dar, R. A., Chandra, R., Romshoo, S. A., Lone, M. A., & Ahmad, S. M. (2015). Isotopic and micromorphological studies of late quaternary loess–paleosol sequences of the Karewa Group: Inferences for palaeoclimate of Kashmir Valley. *Quaternary International, 371*, 122–134.

Dar, R. A., Jaan, O., Murtaza, K. O., & Romshoo, S. A. (2017). Glacial-geomorphic study of the Thajwas glacier valley, Kashmir Himalayas, India. *Quaternary International, 444*, 157–171.

Dar, R. A., Mir, S. A., & Romshoo, S. A. (2019). Influence of geomorphic and anthropogenic activities on channel morphology of River Jhelum in Kashmir Valley, NW Himalayas. *Quaternary International, 507*, 333–341.

Dar, R. A., Paul, O. J., Murtaza, K. O., & Romshoo, S. A. (2021). Late quaternary glacial geomorphology of Kashmir Valley, NW Himalayas: A case study of the Sind Basin. In *Water, cryosphere, and climate change in the himalayas: A geospatial approach* (Vol. 145). Springer.

Dar, R. A., Murtaza, K. O., Paul, O. J., Nisa, A. U., Akhter, N., Dar, F. A., & Mir, R. A. (2022). River response to melting cryosphere since late quaternary in the pir panjal range of NW Himalaya. *Frontiers in Water, 4*, 879001.

Dehbozorgi, M., Pourkermani, M., Arian, M., Matkan, A. A., Motamedi, H., & Hosseiniasl, A. (2010). Quantitative analysis of relative tectonic activity in the Sarvestan area, central Zagros, Iran. *Geomorphology, 121*(3–4), 329–341.

Della-Seta, M., Del Monte, M., Fredi, P., Miccadei, E., Nesci, O., Pambianchi, G., & Troiani, F. (2008). Morphotectonic evolution of the Adriatic piedmont of the Apennines: An advancement in the knowledge of the Marche-Abruzzo border area. *Geomorphology, 102*(1), 119–129.

Dubey, R. K., Dar, J. A., & Kothyari, G. C. (2017). Evaluation of relative tectonic perturbations of the Kashmir Basin, northwest Himalaya, India: An integrated morphological approach. *Journal of Asian Earth Sciences, 148*, 153–172.

El Hamdouni, R., Irigaray, C., Fernández, T., Chacón, J., & Keller, E. A. (2008). Assessment of relative active tectonics, southwest border of the Sierra Nevada (southern Spain). *Geomorphology, 96*(1–2), 150–173.

Ganju, J. L., & Khar, B. M. (1984). Tectonics and hydrocarbon prospects of Kashmir valley-possible exploration targets. *Petroleum Asian Journals, 7*, 207–216.

Gansser, A. (1964). Geology of the Himalayas. Interscience Publishers John Wiley and Sons Ltd., London, New York, Sydney, pp. 1–289.

Goswami, U., Sarma, J. N., & Patgiri, A. D. (1999). River channel changes of the Subansiri in Assam, India. *Geomorphology, 30*(3), 227–244.

Hack, J. T. (1973). Stream-profile analysis and stream-gradient index. *Journal of Research of the US Geological Survey, 1*(4), 421–429.

Holbrook, J., & Schumm, S. A. (1999). Geomorphic and sedimentary response of rivers to tectonic deformation: A brief review and critique of a tool for recognizing subtle epeirogenic deformation in modern and ancient settings. *Tectonophysics, 305*(1–3), 287–306.

Jaan, O., Lone, S., Malik, R., Lone, A., Wasim, M., & Nissa, A. (2015). Morphotectonic and morphometric analysis of Vishav basin left bank tributary of Jhelum River SW Kashmir Valley India. *International Journal of Economic and Environmental Geology, 6*, 17–26.

Jain, V., & Sinha, R. (2005). Response of active tectonics on the alluvial Baghmati River, Himalayan foreland basin, eastern India. *Geomorphology, 70*(3–4), 339–356.

Joshi, L. M., & Kotlia, B. S. (2014). Neotectonically triggered instability around the palaeolake regime in Central Kumaun Himalaya, India. *Quaternary International, 371*, 219–231.

Joshi, L. M., & Kotlia, B. S. (2018). Tectonic footprints and landscape evaluation along Kulur River Valley, Kumaun lesser Himalaya, India. *Journal of Asian Earth Sciences, 162*, 121–136.

Kale, V. S., Sengupta, S., Achyuthan, H., & Jaiswal, M. K. (2014). Tectonic controls upon Kaveri River drainage, cratonic peninsular India: Inferences from longitudinal profiles, morphotectonic indices, hanging valleys and fluvial records. *Geomorphology, 227*, 153–165.

Keller, E. A., & Pinter, N. (1996) *Active tectonics* (338pp.). Prentice-Hall.

Kothyari, G. C. (2014). Morphometric analysis of tectonically active Pindar and Saryu River basins: Central Kumaun Himalaya. *Zeitschrift für Geomorphologie, 59*(4), 421–442.

Kothyari, G. C., Rastogi, B. K., Morthekai, P., & Dumka, R. K. (2016a). Landform development in a zone of active Gedi Fault, Eastern Kachchh rift basin, India. *Tectonophysics, 670*, 115–126.

Kothyari, G. C., Rastogi, B. K., Morthekai, P., Dumka, R. K., & Kandregula, R. S. (2016b). Active segmentation assessment of the tectonically active south Wagad fault in Kachchh, western peninsular India. *Geomorphology, 253*, 491–507.

Kothyari, G. C., Singh, A. P., Mishra, S., Kandregula, R. S., Chaudhary, I., & Chauhan, G. (2018). Evolution of drainage in response to brittle-ductile dynamics and surface processes in Kachchh Rift Basin, Western India. In *Tectonics: A problem of regional settings* (p. 10). Books on Demand.

Ouchi, S. (1985). Response of alluvial rivers to slow active tectonic movement. *Geological Society of America Bulletin, 96*(4), 504–515.

Paul, O. J., Dar, R. A., & Romshoo, S. A. (2021). *Paleo-glacial and paleo-equilibrium line altitude reconstruction from the Late Quaternary glacier features in the Pir Panjal Range*. Quaternary International.

Romshoo, S. A., Altaf, S., Rashid, I., & Dar, R. A. (2018). Climatic, geomorphic and anthropogenic drivers of the 2014 extreme flooding in the Jhelum basin of Kashmir, India. *Geomatics, Natural Hazards and Risk, 9*(1), 224–248.

Rosgen, D. L. (1994). A classification of natural rivers. *Catena, 22*(3), 169–199.

Schelling, D., & Arita, K. (1991). Thrust tectonics, crustal shortening, and the structure of the far-eastern Nepal Himalaya. *Tectonics, 10*(5), 851–862.

Schumm, S. A. (1963). Sinuosity of alluvial rivers on the Great Plains. *Geological Society of America Bulletin, 74*(9), 1089–1100.

Schumm, S. A. (1986). Alluvial river response to active tectonics. In *Active tectonics* (pp. 80–94). National Academies Press.

Schumm, S. A., Dumont, J. F., & Holbrook, J. M. (2000). *Active tectonics and alluvial rivers* (Vol. 276). Cambridge University Press.

Seeber, L., & Gornitz, V. (1983). River profiles along the Himalayan arc as indicators of active tectonics. *Tectonophysics, 92*(4), 335–367.

Silva, P. G., Goy, J. L., Zazo, C., & Bardajı, T. (2003). Fault-generated mountain fronts in Southeast Spain: Geomorphologic assessment of tectonic and seismic activity. *Geomorphology, 50*(1–3), 203–225.

Stojanovic, D., Aitchison, J. C., Ali, J. R., Ahmad, T., & Dar, R. A. (2016). Paleomagnetic investigation of the early Permian Panjal traps of NW India; regional tectonic implications. *Journal of Asian Earth Sciences, 115*, 114–123.

Taloor, A. K., Ray, P. K. C., Jasrotia, A. S., Kotlia, B. S., Alam, A., Kumar, S. G., & Roy, S. (2017). Active tectonic deformation along reactivated faults in Binta basin in Kumaun Himalaya of North India: Inferences from tectono-geomorphic evaluation. *Zeitschrift für Geomorphologie, 61*(2), 159–180.

Turowski, J. M., Lague, D., Crave, A., & Hovius, N. (2006). Experimental channel response to tectonic uplift. *Journal of Geophysical Research: Earth Surface, 111*(F3), F03008.

Whipple, K. X., Dibiase, R. A., & Crosby, B. T. (2013). Bedrock rivers. In *Fluvial geomorphology* (pp. 550–573). Elsevier.

Willett, S. D., & Brandon, M. T. (2002). On steady states in mountain belts. *Geology, 30*(2), 175–178.

# Current Status of Pollution in Major Rivers and Tributaries of India and Protection-Restoration Strategies


**Shreyosi Dey and Arnab Majumdar**

## 1 Introduction

The river has a significant impact on humanity. All of the earliest civilizations arose near the river. In this modern-day world too, all industries are near the river for easy availability of water. This, in turn, results in water pollution. Water pollution is defined as the contamination of water bodies in such a manner that it interferes with their legitimate uses (Majumdar, 2021). A list of rivers and their tributaries (Table 1) has been given here with the path lines that cross over through different states of the Indian subcontinent (Singh, 2007; Singh et al., 2014). These rivers are treated as the open pit for dumping wastes without adequate treatment resulting in several toxic elemental contents to be traced in the river water as presented in Table 2. Due to this, the health of the aquatic organisms get affected (Majumdar et al., 2020a; Upadhyay et al., 2020). Water is contaminated by a variety of reasons, the most significant of which are industrial pollutants. Other concerns, in addition to industrial waste, include herbicides, insecticides, and air pollution. Humans are afflicted by pathogens found in dirty water. Water pollution has a negative impact on the entire ecology of water bodies (Owa, 2013; Upadhyay & Majumdar, 2022). All sectors must work together to protect our water environment, which is a component of sustainable development (Secretariat of the United Nations Commission for Europe, 1994). It is also important to note that even if sewage is completely cleaned, continuous discharge of treated sewage into Indian rivers would not raise river water to bathing

S. Dey
Department of Ecological Studies, University of Kalyani, Kalyani, West Bengal, India

A. Majumdar (✉)
Department of Earth Sciences, Indian Institute of Science Education and Research Kolkata, Mohanpur, West Bengal, India

School of Environmental Studies, Jadavpur University, Kolkata, India



S. Kanhaiya et al. (eds.), *Rivers of India*,
https://doi.org/10.1007/978-3-031-49163-4_4

**Table 1** List of rivers and tributaries of Indian subcontinent with cross-over of states

| Sl. no. | Name of the river | States passing through |
|---|---|---|
| 1 | Ganga | Uttarakhand, Uttar Pradesh, Bihar, Jharkhand, West Bengal |
| 2 | Yamuna | Uttarakhand, Himachal Pradesh, Uttar Pradesh, Haryana, Delhi |
| 3 | Brahmaputra | Assam, Arunachal, Tibet |
| 4 | Mahanadi | Chhattisgarh, Odisha |
| 6 | Godavari | Maharashtra, Telangana, Chhattisgarh, Andhra Pradesh, Puducherry |
| 6 | Krishna | Maharashtra, Telangana, Karnataka |
| 7 | Narmada | Madhya Pradesh, Maharashtra, Gujarat |
| 8 | Tapti | Madhya Pradesh, Maharashtra, Gujarat |
| 9 | Gomti | Uttar Pradesh, Gujarat |
| 10 | Koshi | Shigatse Prefecture, Janakpur, Sagarmatha, Koshi, Mechi Zones, Bihar |
| 11 | Gandaka | Madhya Pradesh, Uttar Pradesh, Jharkhand, Bihar |
| 12 | Betwa | Madhya Pradesh, Uttar Pradesh |
| 13 | Son | Madhya Pradesh, Uttar Pradesh, Jharkhand, Bihar |
| 14 | Sutlej | Himachal Pradesh, Punjab |
| 15 | Ravi | Himachal Pradesh, Punjab |
| 16 | Beas | Himachal Pradesh, Punjab |
| 17 | Chenab | Himachal Pradesh, Punjab |
| 18 | Jhelum | Jammu and Kashmir, Punjab |
| 19 | Kaveri | Karnataka, Tamil Nadu |
| 20 | Ghaggar | Himachal Pradesh, Rajasthan |
| 21 | Hugli | Kolkata |
| 22 | Damodar | Jharkhand, Bengal |
| 23 | Indus | Gilgit-Baltistan, Jammu and Kashmir, Khyber Pakhtunkhwa, Punjab, Sindh, Tibet |
| 24 | Tungabhadra | Karnataka, Andhra Pradesh, Telangana |
| 25 | Mahi | Madhya Pradesh, Vindhyas |
| 26 | Bhagirathi | Uttarakhand |
| 27 | Sabarmati | Aravalli Range, Jaipur |
| 28 | Alaknanda | Uttarakhand |
| 29 | Teesta | Sikkim, West Bengal, India, Rangpur, Bangladesh |
| 30 | Indravati | Odisha, Chhattisgarh, Maharashtra |
| 31 | Bheema | Maharashtra, Karnataka, Telangana |
| 32 | Subarnarekha | Jharkhand, Odisha, West Bengal |
| 33 | Konya | Maharashtra |
| 34 | Ramganga | Uttarakhand, Uttar Pradesh |
| 35 | Penna | Andhra Pradesh, Karnataka |
| 36 | Brahmani | Odisha |
| 37 | Periyar | Kerala, Tamil Nadu |
| 38 | Mahananda | West Bengal, Bihar |
| 39 | Benas | Rajasthan, Uttar Pradesh |

(continued)

**Table 1** (continued)

| Sl. no. | Name of the river | States passing through |
|---|---|---|
| 40 | Vaigai | Tamil Nadu |
| 41 | Sharda | Uttarakhand and Uttar Pradesh |

quality levels during the lean season. As a result, it is essential to keep a minimal flow throughout the year in order to support the river ecosystem and aquatic life. It would be prudent to build more water storage facilities for the riverine system and release water during dry periods in order to efficiently maintain a minimum flow in the river (CPCB, 2013). While effective wastewater treatment has the potential to save the water environment, incorporating environmental policies into the core objectives of the actor firms, as well as continuous periodical enlightenment on the present and future consequences of water pollution, will greatly aid in water conservation (Chowdhury et al., 2022; Majumdar et al., 2022a).

## 2 Causes of Pollution

Several reasons attribute to river water pollution in India at different extents, and Fig. 1 summarizes some of the major reasons in a pictorial form. These aspects are then discussed below with some case reports given. The overall scenario poses serious environmental as well as human health risk issues that need to be attended to.

### *2.1 Natural Causes*

1. Algal blooms: An algal bloom occurs when the population of algae in freshwater or marine water systems rapidly increases or accumulates. The coloring in the water caused by the algae's colors is commonly used to identify it. Algal blooms occur when a nutrient, such as nitrogen or phosphorus, from fertilizer runoff enters the aquatic system and causes excessive algae growth. An algal bloom has a wide-ranging impact on the ecology (Afsal et al., 2020; Majumdar et al., 2020b). Due to this massive growth, negative impacts like light blockage to the bottom layer of the water body, reduction of the dissolved oxygen level, and disturbed feeding of higher trophic organisms are frequent (Majumdar et al., 2018a, 2021). Eutrophication is the process of an excess of nutrients leading to algae growth and oxygen deprivation. When humans ingest marine species that feed on algae, the blooms become fatal. In 1981, incidents of paralytic shellfish poisoning were reported in Tamil Nadu, Karnataka, and Maharashtra as a result of an algal bloom. In Tamil Nadu, 3 people were killed, and 85 were hospitalized. In a similar occurrence in Vizhinjam, Kerala, in 1997, 7 people were killed,

**Table 2** Concentration of heavy metals in rivers and their tributaries (µg/L)

| Sl. no. | Rivers | As | Cd | Cr | Cu | Co | Fe | Hg | Mn | Ni | Pb | Zn | References |
|---|---|---|---|---|---|---|---|---|---|---|---|---|---|
| 1 | Ganga | | 13,100 | 1090 | 2000 | 26.70 | 6870 | 950 | 2800 | 1120 | 26,900 | 15,320 | Paul (2017) and Chaudhary et al. (2017) |
| 2 | Yamuna | 6.0 | 110.1 | 362.7 | 4791.1 | – | 19,467.2 | 206.6 | 581.5 | 851.5 | 255.3 | 3518.5 | Bhardwaj et al. (2017) and Sehgal et al. (2012) |
| 3 | Brahmaputra | 27.67 | 10 | 10 | 6800 | 4800 | 19,043 | BDL | 2500 | 34 | 20 | 20 | Rahman et al. (2016), Baruah et al. (2021) and Bhuyan et al. (2019) |
| 4 | Mahanadi | | 1.30 | 3.67 | 8.39 | 5.81 | 223.3 | – | 22.04 | 15.75 | 19.13 | 29.28 | Sundaray et al. (2012) |
| 6 | Godavari | 7.61 | 0.99 | 10.12 | 42.80 | – | 0.60 | – | | 17.29 | 4.11 | 0.094 | Hussain et al. (2017) and Ghorade et al. (2014) |
| 7 | Narmada | 0.6 | 0.06 | 2.62 | 80.80 | 0.05 | 55.95 | – | 13.68 | 1.68 | 8.81 | 22.77 | Mishra and Kumar (2021) |
| 8 | Tapti | – | 0.18 | | 0.091 | 0.93 | – | – | – | – | – | – | |
| 9 | Gomti | 29 | 54 | 23.9 | 1.30 | BDL | 339 | – | 99 | 9 | 176 | 28.5 | Khan et al. (2020) and Singh et al. (2005) |
| 12 | Betwa | – | BDL | BDL | 30 | BDL | 720 | – | 270 | BDL | BDL | 570 | Kori et al. (2006) |
| 13 | Son | – | | | | | | – | – | – | – | – | |
| 14 | Sutlej | 20 | 16 | 67 | 354 | 30 | 1919 | – | 1158 | 87 | 630 | 2867 | Singh et al. (2014) and Setia et al. (2020) |
| 16 | Beas | – | 8 | 80 | 60 | – | – | – | 1290 | – | 750 | 610 | Kumar et al. (2020a, b) |
| 17 | Chenab | – | – | – | – | – | – | – | – | – | – | – | |
| 18 | Jhelum | 190 | 2060 | 1270 | 1330 | – | – | 1390 | – | 1320 | 1420 | 1250 | Ullah et al. (2018) |
| 19 | Kaveri | – | – | – | – | – | – | – | – | – | – | – | |
| 20 | Ghaggar | 0 | 45 | 50 | 50 | | 2200 | 18 | – | 40 | 45 | 1890 | Pareek et al. (2018) |
| 21 | Hugli | 2030 | 40 | 40 | 2940 | – | – | – | – | 7420 | | 43,910 | Mokarram et al. (2020) |
| 22 | Damodar | 0.30 | 300 | 11,550 | 3950 | | 480 | | | 63 | 0.99 | 113 | Chatterjee et al. (2010), Tiwari et al. (2017) and Mahato et al. (2017) |
| 23 | Indus | – | 5920 | – | 4230 | – | 3520 | – | 590 | – | 30 | 4230 | Imran et al. (2019) |
| 24 | Tungabhadra | – | BDL | – | BDL | – | 3500 | – | 460 | BDL | BDL | 1500 | Siddaramu et al. (2009) |
| 25 | Mahi | – | 24 | 11 | 202 | | 25,990 | 5529 | 1141 | 58 | 45 | 175 | Pandey et al. (2020) |

| Sl. no. | Rivers | As | Cd | Cr | Cu | Co | Fe | Hg | Mn | Ni | Pb | Zn | References |
|---|---|---|---|---|---|---|---|---|---|---|---|---|---|
| 26 | Bhagirathi | | | | | | | | | | | | |
| 27 | Sabarmati | BDL | BDL | 309 | 386 | BDL | BDL | – | BDL | 289 | BDL | 103 | Kumar et al. (2013) |
| 28 | Alaknanda | | – | – | | – | – | – | – | | – | – | |
| 29 | Teesta | BDL | – | – | BDL | – | – | – | – | BDL | BDL | 30,000 | Saha et al. (2017) |
| 30 | Indravati | | – | – | | – | – | – | | | | | |
| 31 | Bheema | 500 | 40 | 500 | 2500 | | 500 | 100 | 300 | 10 | 500 | 4000 | Waghmare et al. (2017) |
| 32 | Subarnarekha | BDL | 0.02 | 0.80 | 4.84 | 0.27 | 83.60 | – | 7.04 | 3.03 | 0.38 | 0.421 | Giri and Singh (2014) and Banerjee et al. (2016) |
| 34 | Ramganga | – | 303 | 1331 | 190 | 624 | – | – | 1360 | – | 2245 | 105.8 | Mazhar and Ahmad (2020) and Khan et al. (2017) |
| 35 | Penna | – | | | | | | | | | | | |
| 36 | Brahmani | – | 8 | 10.89 | 6.67 | 8.67 | 481 | – | 303.30 | 24.78 | 1.67 | 31.56 | Sundaray (2010) and Dey et al. (2005) |
| 37 | Periyar | – | 13.33 | – | 4.50 | – | 517.42 | – | – | – | 16.58 | 257.92 | Kumar et al. (2011) |
| 38 | Mahananda | – | 73 | – | 456 | – | – | – | – | – | 343 | 217 | Kumar et al. (2020a, b) |

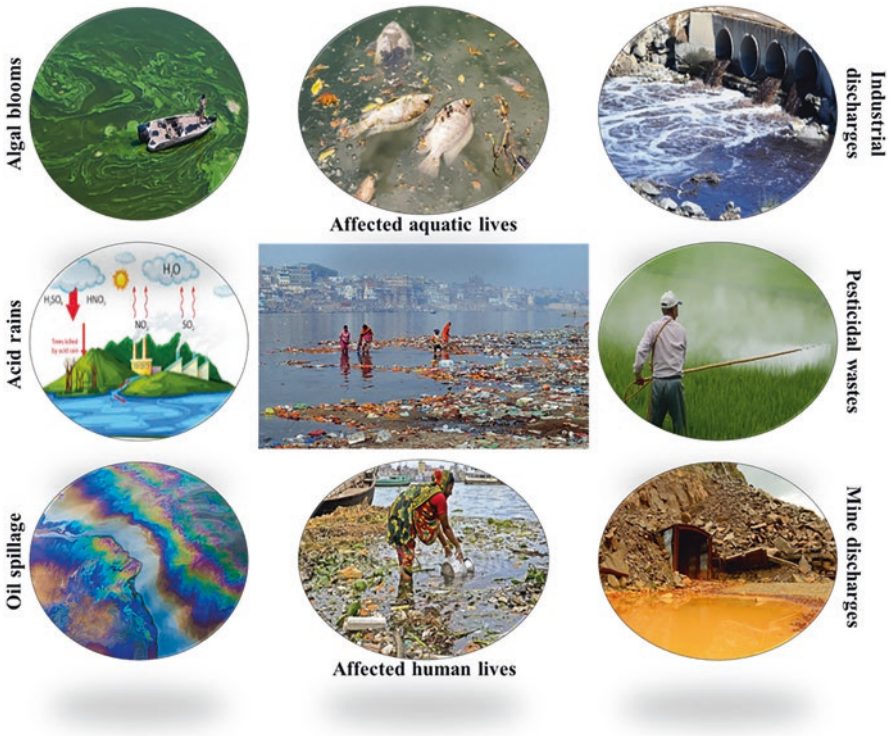


**Fig. 1** River pollution sources and their effects on environmental well-being

and 500 were hospitalized. These folks had eaten a mussel that had eaten deadly algae. Another bloom that affected Kerala in 2004 caused sickening odors to emanate from the coastal waters from Kollam to Vizhinjam. Due to the terrible odor, more than 200 people experienced nausea and shortness of breath for a short period of time. According to experts, the bloom caused widespread fatalities in the area. Over 30 nations, including India, have reported toxic blooms. In India, the first observation of algal blooms was made in 1908. The peak major algal blooms were caused by high fertilizer concentrations, low flows, warm water, and intense solar radiation in the Kali and Ramganga rivers, which had a significant influence on the Ganga (Bowes et al., 2020; Majumdar et al., 2022a, b). According to study data produced by a team of marine life experts, including K.B. Padmakumar and V.N. Sanjeevan of the Centre for Marine Living Resources and Ecology, Kochi, and N.R. Menon of the Cochin University of Science and Technology, as part of the Centre's national program between 1998 and 2010, there were 80 hazardous blooms in the Indian Ocean, compared to 38 between 1958 and 1997. According to experts, there were just 12 such blooms between 1917 and 1957. Harmful algal blooms (HAB), which are dangerous to both humans and marine ecosystems, are becoming more prevalent in Indian seas.

Toxic blooms in Indian waters have grown by almost 15% in the previous 12 years, according to researchers.

2. Acid rain: Chemical substances like sulfuric or nitric acids in the atmosphere get precipitated on the soil/water surface, termed acid rain (Singh and Agrawal, 2007). The form of these chemicals is mixed with rain, fog, snow, hail, and condensed dusts. Wind and air currents carry sulfur dioxide ($SO_2$) and nitrogen oxides (NOX), which are released in the atmosphere due to growing pollution, and mixed with aerosols and water droplets in the air, resulting in acid rain (Majumdar et al., 2020a). As a natural source of $SO_2$ and NOX, volcanoes release these chemicals into the atmosphere, although a major input comes from the combustion of fossil fuels. The burning of fossil fuels to produce power, cars and heavy equipment, and manufacturing, oil refineries, and other sectors are the principal contributors to SO2 and NOX in the atmosphere. Mumbai received rains with a pH of 3.5. Air pollution is progressively increasing in major cities like Kolkata, Delhi, and Mumbai. In Delhi, the average pH of rainwater was 9.1 in 1963 and 6.2 in 1984 (Khemani et al., 1989). The World Meteorological Organization forecasts a significant increase in acidity in cities such as Hyderabad, Chennai, Pune, and Kanpur. Acid rain causes water bodies to become acidic. Streams and lakes typically exhibit visible symptoms of acidification because they have less capacity to buffer acid inputs than soils and plants, resulting in water pollution (Singh, 2007; Tyagi et al., 2022).
3. Weathering of rocks: Weathering is the breakdown of rocks caused by interaction with water, atmospheric gases, and biological organisms. Chemical weathering is most common in soil, where water and minerals are constantly in touch (Majumdar et al., 2018b, 2019b). Water, carbonic acid, strong acids, oxygen, and air pollution are some of the weathering agents. As a part of the chemical weathering, these factors react with rock-infused minerals to generate clays, iron oxides, and salts. Water is extremely essential in chemical weathering in three ways. First, it reacts with carbon dioxide in the soil to generate carbonic acid, a weak acid. Microbe respiration produces a large amount of soil carbon dioxide, while precipitation (which also contains atmospheric carbon dioxide) percolates through the soil to give water (Majumdar et al., 2022b). Carbonate minerals found in limestone and marble are slowly and gradually dissolved by carbonic acid. The weak acid dissolves the insoluble rock into water-soluble by-products that enter the groundwater. These dissolved minerals can also result in water pollution by increasing the requisite amount of minerals needed in that water (Gupta et al., 2022). Weathering of rock-forming minerals dominated the major ion chemistry of the aquatic system, with only a minor contribution from atmospheric sources (Majumdar et al. 2019a; 2022d). Sulfate concentrations are high in the ground and mine water from the Jharia mining belt and other coal mining locations of India (Tiwary, 2001). The majority of chloride in water is considered to come from either atmospheric sources or sea water. The observed high fluoride levels at Koderma may be ascribed to the weathering product of fluorite-containing minerals connected with the area's geological formation. Excavation and dumping procedures connected with mining activities expose new surfaces

for weathering and hasten the dissolving processes and rate of ion release in solution, resulting in a rise in TDS and other dissolved ion concentrations (Singh et al., 2008; Sarkar et al., 2017).

4. Oil spills: The discharge of a liquid petroleum hydrocarbon into the environment, particularly marine ecology, is referred to as an oil spill (Michel and Fingas, 2016). Oil spills can occur as a result of crude oil leakages from tankers, offshore oil storages, drilling rigs within the sea, and spills of gasoline and diesel (types of refined petroleum products), heavier fuels such as bunker fuel, or waste oil. Natural seeps from undersea rocks account for 40–50% of all oil spilt into the oceans. On a worldwide scale, this equates to around 600,000 tons every year. In the course of evolution, the ecosystem has developed a maintenance process toward oil spillages from natural seeps, although these are the single most source of natural oil leakage. Ocean microorganisms, for example, have developed to break down oil molecules around natural oil leaks (Burgherr, 2007). The damage inflicted by the MV Wakashio, which went aground on a coral reef off Mauritius' southeastern coast and began spewing heavy fuel oil into the biodiversity hotspot, might take decades to repair and recover. Around Mauritius, the blue seas have turned dark. After a Japanese ship's cargo of 4000 tons of heavy fuel oil leaked into the Indian Ocean, the country's mangrove wetlands were damaged, and reptiles and waterbirds were covered in sticky fuel oil (Sivadas et al., 2008). The 2017 Ennore oil leak happened in Chennai, Tamil Nadu, India, outside the Kamarajar Port. A departing empty tanker BW Maple collided with an inbound full oil tanker Dawn Kanchipuram around 04:00 local time on January 28, 2017, causing a leak. Oil and fuel from land-based sources can reach the seas as oil and fuel (Michel et al., 2005). Runoff oil and oil from rivers are thought to be responsible for 11% of all oil contamination in the oceans. Oil on roads from land vehicles may also cause pollution, which is subsequently washed into the waters during rainstorms (Burgherr, 2007). Land-based oil spills vary from maritime oil spills in that oil does not spread as rapidly on land as it does on water, hence the impacts are limited.
5. Marine dumping and volcanic eruption: The deliberate disposal of wastes or other hazardous stuff from carrying vessels, planes, satellite debris, offshore platforms, or other man-made structures into the sea has been marked as marine dumping. But there is no such report of the pollution caused by marine dumping. A volcanic eruption occurs when a volcano releases lava and gas, sometimes explosively. Several historical eruptions were detected on Barren Island, an abandoned Indian property in the Andaman Sea, between 1787 and 1832. There was no more sign of activity until 1991, when ash plumes, Strombolian explosions, and lava flows reaching the sea were discovered. Significant quantities of chemically recognized Toba eruption debris may be discovered around 700 m east of Dhaba, near Ghogara, on the northern bank of the Son river, and in cliff parts on the east bank of the Rehi River (Petraglia et al., 2012). There is not much evidence to conclude the river pollution generated by volcanic eruptions in India.

## 2.2 Anthropogenic Causes

1. Industrial waste: Waste created by manufacturing or industrial activities is referred to as industrial waste. The acids and bases, solvents, organic wastewater coming from chemical manufacturers, heavy metal solution, waste inks, solvents coming from printing industries, benzene and other hydrocarbon-containing sludge from petroleum refining industries, toluene and benzene from leather products manufacturing industry, strong acids and bases of the construction industry, and cyanide and heavy metal-containing wastes of metal industry are all examples of industrial wastes (Mishra & Rhee, 2010). Industrial wastes also include asbestos, lead, mercury nitrates, phosphates, sulfur, petrochemicals, and other oily compounds. Asbestos poses a major health risk and is carcinogenic. Asbestosis, mesothelioma, lung cancer, intestinal cancer, and liver cancer can all be caused by inhaling its fibers. Lead is a metallic element that may be harmful to one's health and the environment. Because it is a nonbiodegradable chemical, it is difficult to remove once the environment has been affected (Shrivastava et al., 2020). It is toxic to the health of many animals, including humans, since it inhibits the function of biological enzymes. Mercury is a metallic element that may be hazardous to one's health and the environment. Because it is a nonbiodegradable chemical, it is difficult to remove once the environment has been affected. It is also hazardous to animal health since it can lead to disease due to mercury, lead, or arsenic toxicity (Majumdar & Bose, 2017, 2018). Sulfur, a nonmetallic chemical produced as a by-product in many industries, is toxic to marine life. Petroleum is a hazardous substance that is made from gas or petrol and can harm marine life. A writ suit was filed at the Supreme Court in 1989 against Hindustan Agro Chemicals Limited for damaging the land and water in Bichhri village, Udaipur district, Rajasthan. The hazardous untreated wastewater was permitted to run freely, and because the untreated toxic sludge was dumped out in the open in and around the complex, the toxic compounds percolated deep into the earth's bowels, poisoning the aquifers and subterranean water supplies. In 1990, over 20 villages got polluted for their soil and water sources due to industrial dumping of untreated chemical waste by a group of 224 industrial units in Telangana's Patancheru-Bollaram. The Periyar River in Kerala, which runs between Eloor and Edayar, has been seriously contaminated by the suspected dumping of untreated hazardous waste and effluents by 400 companies. The Eloor-Edayar region began to industrialize in the 1950s, with the establishment of Hindustan Insecticides Limited. Antipollution protests began in the area in the early 1990s. A Supreme Court-appointed High-Power Committee was established in 1997 to investigate all problems connected to hazardous waste and violations of environmental regulations. In 2004, while hearing a case filed the same year, the Supreme Court chastised the Kerala State Pollution Control Board (KSPCB) for the river's poor state.
2. Agricultural wastes: Agricultural waste is waste that is generated as a result of various agricultural processes. Manure and other wastes from farms, poultry

houses, and slaughterhouses are included, as well as harvest waste, fertilizer runoff from fields, pesticides that enter the water, air, or soils, and salt and silt drained from fields (Majumdar et al., 2019b). Agriculture, which accounts for 70% of global water withdrawals, is a major contributor to water contamination (Barla et al., 2017; Upadhyay et al., 2021). In most high-income nations and many emerging economies, agricultural pollution has already surpassed contamination from cities and industry as the leading cause of inland and coastal water pollution. Agriculture-derived nitrate is the most frequent chemical contamination in the world's groundwater aquifers. Pesticides and fertilizers, which include compounds not found in nature, have been the primary source of contamination. After being sprayed, the chemical reacts with the water and penetrates into the ground. The remainder is absorbed by the plant. As a result, the groundwater-fed streams in the area become poisoned. Due to inefficient farming practices, the topmost layer of the soil gets eroded which gets eroded by water or wind resulting in sedimentation in the water bodies (Majumdar et al., 2019c). It can also reduce light penetration in water, harming aquatic life forms, and the turbidity that results can interfere with aquatic fish-eating patterns. The usage of heavy metal-containing fertilizers, manure, and other organic wastes, such as arsenic, cadmium, mercury, and lead, can lead to heavy metal buildup in the soil. Irrigation practices, for example, can contribute to selenium buildup. Irrigation can promote salinization by mobilizing salts stored in soils (leaching fractions), which are subsequently carried to receiving water bodies by drainage water. Excessive irrigation can also elevate water tables in salty aquifers, causing saline groundwater to flow into waterways. Post-harvest losses and waste deplete precious resources and have a negative impact on the ecosystem, including water quality deterioration (Mateo-Sagasta et al., 2017).

3. Municipal discharge: Municipal discharge is a major cause of environmental deterioration due to household wastes, as well as eutrophication due to nutrient overloading. Apart from natural development, the rapid expansion of the urban population is attributable to massive population movement (mainly from rural regions and small towns to major cities) and the integration of newer rural areas in nearby metropolitan settings. Sewerage and sewage treatment services are not available in the majority of towns and cities. Many cities have grown beyond municipalities, but the new urban agglomerations are still administered by rural governments, which lack the ability to handle sewage. In smaller communities, sewage management is worse. Sewage is either discharged directly into rivers or lakes (Kamyotra & Bhardwaj, 2011). According to research conducted by the Central Pollution Control Board (CPCB), India has 269 sewage treatment facilities (STPs), of which only 231 are active, implying that the existing treatment capacity is just 21% of the current sewage production. Untreated sewage is the primary source of pollution in rivers and lakes. The majority of STPs built under central funding programs like the Ganga Action Plan and the Yamuna Action Plan of the National River Action Plan are not completely operational.
4. Animal husbandry: Animal husbandry is the field of agriculture that deals with animals produced for meat, fiber, milk, or other purposes. Water quality can be

harmed by grazing animals and pasture production due to erosion and sediment movement into surface waterways, nutrients from the animals' urine and feces, fertility methods connected with the creation of high-quality pasture, and diseases from the wastes. Fecal bacteria infiltrate waterbodies by direct feces deposition and cattle migration. Aquaculture has grown dramatically and quickly in marine, brackish water, and freshwater habitats across the world. Fish excreta as well as leftover feds from aquaculture can harm the water quality. Increased production has been accompanied by increased usage of antibiotics, fungicides, and antifouling chemicals, which may contaminate downstream ecosystems (FAO, 2016).

5. Construction site: Any type of detritus from the building process is referred to as construction waste or rubbish. Construction and demolition materials are formed when a new building or structure is built or when an old structure is renovated or demolished. Concrete, steel, wood, asphalt, and gypsum are examples of heavy materials utilized in vast quantities in modern buildings. Construction site sediment contamination contaminates drinking water, has an impact on recreational waterways, reduces commercial fishing, and raises the danger of flooding. Other contaminants can be carried into rivers by dirty runoff from construction projects. Though there are cases of water pollution in Indian rivers due to construction sites, still no such study had been done for its proper analysis.
6. Mining activities: The extraction of minerals from different ores or natural elements in their raw state from the deep sites of the earth is generally termed as mining. Direct and indirect mining operations can have environmental consequences on a local, regional, and global scale. Spill erosion, sedimentation, acid mine drainage, lowering of the water table, subsidence, disruption of the hydrological cycle, and rainfall are all effects of mining on the surface and groundwater. Mine drainage is metal-rich water that results from a chemical interaction between water and sulfur-bearing minerals in rocks. Sulfuric acid and dissolved iron are substances that end up in the water. Some or all of this iron can be solidified, forming the red, orange, or yellow deposits found at the bottom of mine drainage streams. Heavy metals such as copper, lead, and mercury are further dissolved by the acid discharge and end up in groundwater or surface water. Water pollution due to coal mining is reported near Talcher Coalfield, Umaria Coalfields, Damodar River basin, Makum Coalfields, Bijolia mining areas, etc.

## 3 Current Status of Pollution in Major Rivers

In 2018, India's Central Pollution Control Board (CPCB) recognized 351 contaminated river sections. The study of water quality for identifying contaminated river sections discovered that rivers and streams in 31 states and union territories (UT) did not fulfil the water quality requirements. These states/UTs must submit their action plans in order to be considered. The state with the most contaminated river is Maharashtra (53), followed by Assam (44), Madhya Pradesh (22), Kerala (21),

**Table 3** Categorical divisions of biological oxygen demand in river waters with priority levels

| Category | BOD |
|---|---|
| Priority 1 | Greater than 30 mg/L |
| Priority 2 | 20–30 mg/L |
| Priority 3 | 10–20 mg/L |
| Priority 4 | 6–10 mg/L |
| Priority 5 | 3–6 mg/L |

**Table 4** Water quality criteria for basic usability with expected rationales

| Criteria | | Rationale |
|---|---|---|
| Fecal coliform MPN/100 mL | 500 (desirable) 2500 (maximum permissible) | Fecal coliform and fecal streptococci are regarded to assure low sewage pollution since they represent bacterial pathogenicity |
| Fecal streptococci MPN/100 mL | 100 (desirable) 500 (maximum permissible) | To account for variations in environmental variables such as seasonal fluctuations, changes in flow conditions, and so on, the ideal and allowable limits are given. Fecal coliform and fecal streptococci are regarded to assure low sewage pollution since they represent bacterial pathogenicity |
| pH | Between 6.5 and 8.5 | The range protects the skin as well as vital organs such as the eyes, nose, and ears, which are immediately exposed while outdoor bathing |
| Dissolved oxygen | 5 mg/L or more | The 5 mg/L dissolved oxygen content guarantees reasonable independence from oxygen-consuming organic pollutants upstream, which is required to avoid the generation of anaerobic gases (noxious gases) from sediment |
| Biochemical oxygen demand 3-day, 27 °C | 3 mg/L or less | A biochemical oxygen demand of 3 mg/L or less of water guarantees acceptable independence from oxygen-demanding contaminants and avoids the formation of toxic gases |

Gujarat (20), Odisha (19), West Bengal (19), and Karnataka (17). Polluted rivers are detected and classified into five priority classifications if they do not match the requirements. Polluted river sections are routinely categorized into five groups based on biological oxygen requirement concentration as given in Table 3.

According to the CPCB, the most important parameters for bathing water quality are included in Table 4 below, along with their rationale.

**The Ganga** The Ganga basin is the country's largest river basin, covering slightly more than a quarter of the country's total geographical area (26.3%). The Ganga gets its name from the Gangotri Glaciers in the Himalayas, which are located in the Uttarkashi district of Uttarakhand, India. The Ganga River travels through the rest of the mountain range until emptying into the plains at Haridwar. In its 2525-km journey to the Bay of Bengal, it is joined by a significant number of tributaries on both sides (Singh, 2007). On the Ganga, the Central Pollution Control Board maintains a network of 57 water quality monitoring stations that regularly measure 9

fundamental criteria. The river Ganga was found to be under the required BOD levels from its source to Rishikesh, as well as in the Bihar portion of the network. However, water quality surpasses the threshold in terms of BOD in the Rishikesh downstream to Garhmukteshwar and Kannauj upstream to Trighat stretches, as well as a few spots in West Bengal (Dakshineswar, Uluberia, and Diamond Harbour). Nearly all of the monitoring stations for dissolved oxygen and pH fulfil the criterion, while most of the monitoring locations for fecal coliform do not match the criteria from Kanpur downstream to Diamond Harbour (Trivedi, 2010). The Ganga has a slew of issues, the most serious of which is the lack of flow during the dry season. Untreated and/or partly treated sewage and industrial wastewater discharge into the river are major problems (Matta et al., 2022). Even with treated sewage, dilution is difficult due to the diversion of river water through the Upper and Lower Ganga canals, leaving almost no flow in the main river stream. In Uttar Pradesh, sewage treatment is required, as is the presence of a functional sewage transportation infrastructure. In the state of Uttar Pradesh, the Ganga needs a minimal ecological flow to survive. Because a river is a living ecosystem, the ultimate objective should be to safeguard the river's ability to operate. The Ramganga and Kali-East tributaries of the Ganga require rapid care since they carry the industrial and domestic pollution burden of Uttarakhand and Uttar Pradesh. Ganga and its tributaries are getting polluted from the constant release of wastes coming out of sugar and distilleries, tanneries, and paper mills. There is an immediate need for strict environmental surveillance to ensure that they are adhering to environmental regulations. Even though treated sewage has a BOD level of 30 mg/L, continuous discharge of treated sewage (BOD level of 30 mg/L) cannot bring river water to bathing quality in the lean season. As a result, a minimum flow must be maintained throughout the year to support the river ecosystem and aquatic life. To efficiently maintain minimal flow in the river, it would be prudent to build more water storage facilities for the Ganga riverine system and release water during the dry season.

**The Yamuna** The Yamuna River Table is the Ganga River's largest tributary. The Yamunotri Glacier, located at Bandar Punch (38°59′N 78°27′E) in the Mussorie Range of the lower Himalayas at a height of around 6320 m above mean sea level in the district Uttarkashi, is the source of the Yamuna River's primary tributary (Uttaranchal). The Yamuna River's catchment area includes sections of Uttaranchal, Uttar Pradesh (U.P.), Himachal Pradesh, Haryana, Rajasthan, Madhya Pradesh, and Delhi itself. The Yamuna River flows over the plain for roughly 1370 km from Uttar Pradesh's Saharanpur district to Allahabad, where it joins the Ganga. Tons, Betwa, Chambal, Ken, and Sindh are the river's primary tributaries, accounting for 70.9% of the catchment area, with the remaining 29.1% coming from direct drainage of the main river and lesser tributaries (Central Water Commission, 2007). About 85% of the river's pollution comes from domestic sources. Raw manure, industrial effluents, the disposal of waste and deceased bodies, idol worship, and pollution due to in-stream water consumption are the primary sources of contamination in the Yamuna (CPCB, 2006; Asim & Nageswara Rao, 2021). Diffuse sources of pollution, such as farmland contamination and a range of in-stream water uses, such as

cattle wading, bathing, open defecation, and textile washing, contribute to the deterioration of river water quality (Sengupta, 2006). The presence of pathogens in the river is aided by the presence of household waste. Industrialized release, natural material discharge into water, residential waste, and other factors have resulted in a drop in oxygen levels and are a major source of eutrophication (CPCB, 2003). It has been noticed that a 500-km section of the river is in poor condition, with water quality that is frequently below the necessary threshold for "designated best use." During the dry season, the river stretch between Wazirabad and Etawah exhibits four different gradients of pollution load. The length between Wazirabad and Okhla is the filthiest, as it carries a large amount of effluent from Delhi. This input has triggered a cascade of chemical and biological processes in the water downstream. This stretch is distinguished by a large bacterial population, a hazy appearance, a high BOD level, and a strong foul odor, all of which indicate a general lack of oxygen. Masses of gaseous muck emerging from the bottom are frequently seen floating near the water's surface. During the monsoon, the muck accumulated in this stretch is flushed and remains suspended, causing an increase in oxygen absorption in the downstreams. Every year, this causes a large number of fish deaths during the initial flushing after the start of the monsoon. The length from Agra to the confluence with the Chambal River at Etawah is distinguished by the self-purification processes of the Agra effluents. The confluence with the comparatively clean Chambal River is extremely beneficial in reducing the pollution load of the Yamuna before it enters the Ganga at Allahabad. During the monsoon season, due to the massive amount of water flowing down the river, the barrages are opened, resulting in a more or less continuous system. The heavy load of untreated biodegradable material causes multiple gradients in saprobic and eutrophic conditions; the majority of the Yamuna can rarely meet its specified usage.

**The Brahmaputra** The Brahmaputra River is a trans-Himalayan River that originates in south Tibet from the glaciers of Mount Kailash at an elevation of around 5150 m at 30°31′ North, 82°10′ East. The river is known in Tibet as Tsangpo, and it runs eastward for nearly 1600 km across southern Tibet, almost parallel to the Great Himalayan range (Rao, 1975). It is a significant ecosystem with significant aquaculture potential, and it plays a critical role in reducing rural poverty and delivering food to the impoverished fishing community as well as the local population. Continuous fluctuations in the river's course are a crucial aspect of Brahmaputra hydrology (Bhuyan et al., 2018). Toxic metal contamination has plagued the Old Brahmaputra River as a result of fast agricultural, urban, and industrial expansion on the river's banks (Barbulescu et al., 2021). Furthermore, the Brahmaputra River, which flows through China, India, and Bangladesh, is one of the most important transboundary rivers in South Asia. As a result, upstream water may contribute to trace metal contamination in downstream river segments (Shorna et al., 2021). In terms of pH and conductivity, the water quality of the Brahmaputra River meets water quality guidelines. Conductivity varies between 68 and 278 μmhos/cm. DO ranges from 4.4 to 9 mg/L. BOD value ranges from 0.3 to 9.2 mg/L. Total coliform (TC) values range from 0 to 1500 MPN/100 mL, whereas fecal coliform (FC) values

range from 0 to 15,000 MPN/100 mL. The abundance of microplastics in the Antu and Beijing rivers, which flow through densely populated areas with high economic and business activity, as compared to the Brahmaputra River, indicates that rivers in the Indian Himalayas are highly polluted with microplastics regardless of lower anthropogenic activity (Rodrigues et al., 2018; Tsering et al., 2021). According to a report, the river water is becoming increasingly contaminated as a result of unplanned industrialization, urbanization, and agricultural operations (Bhuyan et al., 2018). The water of the Old Brahmaputra River was found to be unsafe for aquatic species, irrigation, and other uses. Furthermore, dangerous concentrations of several water characteristics can endanger fish and human settlements living in and around the Old Brahmaputra River. To reduce the contamination of the Old Brahmaputra River's water, adequate development planning and river management should be implemented (Bhuyan et al., 2018).

**The Mahanadi** The Mahanadi River system is the third biggest in India's peninsula and the largest in Orissa state. The basin (80°300′–86°500′E and 19°200′–23°350′N) has an area of roughly 141,600 $km^2$, with a total length of 851 km, an annual runoff of 50,109 $m^3$, and a total length of 851 km (Konhauser et al., 1997). A large population in the Mahanadi drainage system, like all other river systems, is dependent on the river for drinking water, irrigation, industrial usage, fisheries, and other social necessities. It is essentially the state of Odisha and Chhattisgarh's lifeblood (Samanta et al., 2020). Dhamtari, Nawapara Nagar, Bilaspur, Raigarh, Sheorinarayan, Sambalpur, Chipilima, Sonepur, Boudh, Athmallik, Baudhgarh, Kantilo, Cuttack, and Paradeep are among the cities and towns that dump sewage and industrial waste directly or indirectly into the river. The river absorbed raw/partially treated sewage, various effluents from industry, agricultural runoff, and other contaminants that may have increased the metal concentrations in the river system (Nanda & Tiwari, 2001). Its pH ranges from 7.1 to 8.6. Conductivity varies between 90 and 13,190 μmhos/cm. DO ranges from 4.9 to 10.5 mg/L. BOD value ranges from 0.6 to 3.6 mg/L. Total coliform (TC) values range from 76 to 160,000 MPN/100 mL, whereas fecal coliform (FC) values range from 10 to 160,000 MPN/100 mL. Pollutants are caused by the discharge of effluents from various sources into the estuary, which produces major changes in water quality and, in the long term, has a negative impact on the mangrove environment. The urgent need is to keep current sewage treatment plants running so that effluent discharge contains as few suspended particulates as possible. As a result, it is critical that the Mahanadi mangrove health in the coastal environment be monitored as soon as possible (Behera et al., 2014).

**The Narmada** The Narmada River is the biggest west-flowing peninsular perennial river in central India. It rises in the Maikala Ranges near Amarkantak in the Anuppur District of Madhya Pradesh, flows through the Deccan traps toward the west, and is bounded by the Satpura and Vindhyan hills. The Narmada basin is located between latitudes 21°20'N and 23°45′N and longitudes 72°32′E and 81°45′E. Significantly, the Narmada River is a lifeline for Madhya Pradesh, draining

a huge land area of 85,938 km$^2$ (87% of the entire river basin area) from east to west (Jain et al., 2008). The rapid growth in the human population, which has resulted in urbanization, changes in land use and land cover, excessive water extraction, shrinkage of river width, and direct discharge of untreated wastewater, has contributed to the deterioration of water quality in the Narmada. The input wastewater is contaminated with a high number of organic and inorganic pollutants, posing a serious biotic danger, influencing the biogeochemical cycle, and decreasing the river's ecological health (Mishra & Kumar, 2021). Its pH ranges from 7.1 to 8.5. Conductivity varies between 217 and 651 μmhos/cm. DO ranges from 6.2 to 9.9 mg/L. BOD value ranges from 0.8 to 5.0 mg/L. Total coliform (TC) values range from 4 to 1600 MPN/100 mL, whereas fecal coliform (FC) values range from 0 to 17 MPN/100 mL. When compared to the water quality in 2012 and 2013, it is possible to infer that pollution levels have dropped as a result of the Clean Narmada Green Jabalpur initiative, and the water is healthy owing to the existence of healthy aquatic life and fewer contaminants (Purnima, 2013).

**Other River Systems** The water quality of tributary streams of Suswa, Gola, Ramganga, Kalindi (east), Varuna, Sai, Gomti, Rapti, Saryu, Ghaghara, Rihand, Sone, Gandak, Sikrana, Burhi Gandak, Harbora, Kamla, Manusmar, Koshi, Daha, Dhous, Farmar, Ram Rekha, and Sirsa are in accordance to water quality criteria with respect to pH and conductivity throughout its length except in River Kalindi (east) at Kannauj, River Gandak at Rewaghat (Mujaffarpur), River Manusmar at Riga, (Sitamarhi), River Suswa at Mothrawala, River Daha at Itwa Bridge (Siwan), River Sai at Unnao after drain outfall, and River Sikrana at Lal Parse, Bittiah, where pH is observed higher than the desired criteria. In the rivers indicated, the DO ranges from 0.0 to 11.5 mg/L. DO is found to be low in relation to desirable water quality standards in the rivers Suswa at Mothrawala (1.6 mg/L), Gomti at Lucknow downstreams (2.5 mg/L), Sirsa at Raxaul (0.0 mg/L), Ram Rekha at Harinagar (2 mg/L), and Rihand at Renukut downstream (1.5 mg/L). In the tributary streams listed above, BOD levels range from 1 to 161 mg/L. Total coliform (TC) values vary from 160 to 11 × 108 MPN/100 mL, whereas fecal coliform (FC) values range from 40 to 46 × 107 MPN/100 mL. At all locations, the water quality of the Ashwani, Pabbar, Kali Sindh, Sindh, Kalindi, Hindon, Tons, Betwa, Chambal, Parvati, Khan, Kshipra, Bichia, Sankh, Banas, Kaliasot, Kolar, Chhapi, Batta, Giri, and Ujad tributary streams meet water quality criteria in terms of pH and conductivity. The conductivity of the River Chambal at Nagda downstreams does not satisfy the necessary water quality requirements (9880 mhos/cm). At their limited monitoring stations, the pH of the rivers Betwa, Parvati, Govind Sagar, Chhapi, Ashwani, Kali Sindh, Giri, Banas, Kolar, Chambal, Gohad, Kshipra, and Sone is somewhat higher than the acceptable requirement. Dissolved oxygen concentrations vary from nil to 19.7 mg/L. DO is nil in the Hindon River downstream of Ghaziabad. BOD concentrations vary from 0.1 to 369 mg/L. The highest concentration of BOD (369 mg/L) is found downstream of Muzaffarnagar in the River Kalindi. Total coliform (TC) values range from 2 to 11 × 108 MPN/100 mL, whereas fecal coliform (FC) values range from 2 to 11 × 107 MPN/100 mL. In the Muzaffarnagar downstreams of the

River Kalindi, the highest value of fecal coliform and total coliform is recorded. Nitrate-nitrite concentrations vary from 0.0 to 17.6 mg/L. The highest concentration of nitrate is found in the River Betwa in Charantirghat, Vidisha. In terms of pH, DO, and conductivity, the tributary streams Barakar, Konar, Dwarakeshwar, Silabati, Jalangi, Kansi, Mayurkashi, Mahananda, Bokaro, and Jumar fulfil the water quality standards. The BOD ranges from 0.2 to 90 mg/L. The fecal coliform (FC) value varies between 2 and 5 × 106 MPN/100 mL, whereas the total coliform (TC) value varies between 4 and ×106 MPN/100 mL which creates further enteric disturbances.

## 4 Impacts of Water Pollution

Water pollution frequently has a negative impact on aquatic life. Animals and plants in polluted water sources may perish or fail to reproduce normally. Heavy metals and chemicals from municipal and industrial wastewater are instances of water pollution that impair the life spans and reproduction ability of aquatic creatures. Furthermore, algal blooms in lakes and marine settings, caused by excess nutrients such as nitrates and phosphates from agricultural runoff, have a significant impact on aquatic life. These algal blooms can be seen in eutrophic waterbodies. Debris and litter, which may smother and harm many aquatic animals, are also a hazard to marine life.

***Effects on Aquatic Biodiversity*** Pollution is a severe concern in aquatic habitats because it may induce changes in environmental circumstances to which aquatic creatures are sensitive Majumdar et al. (2023a). Aquatic species adapt to significant changes in their environment by migrating to other appropriate habitats or, in extreme circumstances, simply dying off. In less severe situations, just the reproductive potential and metabolism of aquatic creatures are harmed. However, in the long term, this may have a detrimental impact on their population. A food web's complicated interactions between species are critical. Fish populations may begin to decline as a result of food chain disturbance and loss or degradation of variety. The impact of increased water temperature and low oxygen levels on common mayfly species, which are considered cool water insects are employed as bioindicators to help evaluate biologically essential aspects of freshwater environments.

***Effects on Human Health*** Water pollution incidents, which are mainly caused by severe rainfall, floods, or drought, frequently overrun inadequate wastewater storage and treatment facilities. These occurrences can result in the release of industrial effluent or sewage overflows, as well as a reduction in the amount of freshwater available to dilute contaminants. The deteriorating state of much of the surface water resources, along with a lack of cooperation between public health protection and water quality management, poses major dangers to human health (Upadhyay et al., 2019). Low levels of sewage treatment have led to widespread pollution of

drinking water sources, leading to severe outbreaks of sickness. Sewage is the major source of pollution in water sources (piped water, surface water, and groundwater), and sewage contamination causes more illnesses than chemical and pesticide contamination. Untreated sewage typically includes a high concentration of dangerous microorganisms such as schistosomula eggs cercaria and parasitic fluke and worm ova; hepatitis A, bacterial dysentery, infectious diarrhea, paracholera, and typhoid are also frequent. Aside from infectious illnesses, increased rates of cancer mortality in cities have been linked to a lack of effective sewage treatment systems. Infant mortality rates in less-developed nations are positively related to the intensity of industrial organic water pollution, after controlling for economic development, health expenditures, fertility rates, and other characteristics. Understanding the socioeconomic structural origins of water pollution and other types of pollution is crucial, given their empirically verifiable human health repercussions (Schwarzenbach et al., 2010; Wu et al., 1999; Reddy & Behera, 2006).

## 5 Strategies to Control Pollution

1. Use of chemical-free products: Increased chemical use has become a curse with respect to water pollution (Srivastava et al., 2021). To reduce pollution, cutting down of chemicals is a necessity. It can be done by (i) replacing hazardous cleansers with nontoxic and biodegradable cleaners and pesticides, (ii) components drawn from renewable plants rather than nonrenewable petroleum, (iii) refillable containers, and (iv) packaging produced from larger percentages of recycled plastic. The use of phosphate-free detergents is a must to prevent pollution in households. Along with that, the use of dishwashers should be checked so as to prevent chemical pollution (Helmer & Hespanhol, 1997).
2. Use of organic products: Though organic products are a little costly, still usage of such products must be encouraged so as to prevent water pollution. The use of bio-enzymes in lieu of cleaners must be encouraged (Majumdar et al. 2023b; Schwarzenbach et al., 2010).
3. Less usage of plastic: Plastic, of course, is particularly troublesome since it is nonbiodegradable and hence persists for far longer (up to 1000 years longer) than other types of rubbish. Animals can become entangled in this rubbish or consume it, either because they mistake it for prey or because saltwater has broken it down into small particles. To safeguard the waterways, the greatest thing that can be done is to keep as much plastic as possible out of the waste stream in the first place. Some of the ways to prevent plastic use are to carry one own bottle, boycott microplastic-containing products, carrying own bag, recycle and reuse, etc. (Derraik, 2002).
4. Proper disposal of wastes: Wastes should be disposed of in a proper way to prevent riverine pollution. The rivers often get stuck by the wastes that are being directly disposed of in the rivers. The Ganga and the Yamuna are perfect examples

of it. Proper disposal methods should be implemented for distinguished wastes so as to segregate them before disposing of (Owa, 2013).

5. Checking sedimentation: Site-specific sites would be chosen to limit sediment deposition outside the building zones, perhaps including silt barriers, hay bales, vegetation coverings, and diversions, to reduce damage to river water (Yang & Liu, 2010).
6. Stringent action against polluters: Polluter must pay principle must be applied to all. Strict laws should be implemented to control water pollution. Industrial water must to be monitored before being disposed into the river bodies. Cooling tower blowdown, process effluents, and runoff from anticipated activities would be discharged to wastewater management and reuse systems. There would be no release of process effluent into any river flows. Proper precautions must be taken to reduce the possibility of unintentional spills and to define the necessary processes to be followed in the event of an accidental leak. To the greatest degree possible, the proposed mining design will safeguard the project area's hydrologic balance and limit damage to streams (Helmer & Hespanhol, 1997).
7. Afforestation: Planting trees not only prevents soil pollution but also can check water pollution to some extent.
8. Cleaning of waterside area: Once the water body is already polluted, it is the responsibility of the citizens as well as the government to clean it up. Many non-governmental organizations are already working on this matter (Vorobiev et al., 2014). As a possible option, nanotechnology can be opted for (Majumdar et al., 2022c, 2023b, c).

## 6 Conclusion

The rivers are the lifeline of a majority of the population in cities, towns, and villages. It is a vital supply of surface water for agriculture, households, and industry. However, contamination of river water is growing as a result of increasing human population, industrialization, intensive agricultural practices, and enormous wastewater discharges into the river. In underdeveloped nations, an estimated 90% of all wastewater is dumped untreated directly into rivers, lakes, or the seas. The major rivers of India including Ganga, Yamuna, Brahmaputra, Mahanadi, and their tributaries are highly polluted due to uncontrolled waste discharge into these water bodies. The government organizations are making action plan to clean up these lifelines, although the rate of the pollution spread is much greater than the cleanup rate. Such discharges contribute to the fast eutrophication in rivers. Therefore, to prevent this pollution, proper mitigation measures must be taken, and regular monitoring of water bodies on a periodic basis is an important component of the protection strategy in this area. This chapter tried to confine the pollution status in these river systems and related health population awareness issues with probable controlling strategies to implement further.

**Acknowledgments** The authors are thankful to the IISER Kolkata, Kalyani University library facilities, for the collection of articles and database availability. AM is thankful to the Ministry of Earth Sciences, India (MoES/P.O. (Geosci)/56/2015), for providing JRF, and IISER Kolkata for providing SRF. AM is also thankful to SERB, Govt. of India, for the Postdoctoral Fellowship and research grant (File no – PDF/2022/001418/LS).

## References

Afsal, F., Majumdar, A., Kumar, J. S., & Bose, S. (2020). Microbial inoculation to alleviate the metal toxicity in crop plants and subsequent growth promotion. In *Sustainable solutions for elemental deficiency and excess in crop plants* (pp. 451–479). Springer.

Asim, M., & Nageswara Rao, K. (2021). Assessment of heavy metal pollution in Yamuna River, Delhi-NCR, using heavy metal pollution index and GIS. *Environmental Monitoring and Assessment, 193*, 1–16.

Banerjee, S., Kumar, A., Maiti, S. K., & Chowdhury, A. (2016). Seasonal variation in heavy metal contaminations in water and sediments of Jamshedpur stretch of Subarnarekha river, India. *Environmental Earth Sciences, 75*(3), 265.

Barbulescu, A., Barbes, L., & Dumitriu, C. S. (2021). Assessing the water pollution of the Brahmaputra River using water quality indexes. *Toxics, 9*, 297.

Barla, A., Shrivastava, A., Majumdar, A., Upadhyay, M. K., & Bose, S. (2017). Heavy metal dispersion in water saturated and water unsaturated soil of Bengal delta region, India. *Chemosphere, 168*, 807–816.

Baruah, S. G., Ahmed, I., Das, B., Ingtipi, B., Boruah, H., Gupta, S. K., Nema, A. K., & Chabukdhara, M. (2021). Heavy metal (loid)s contamination and health risk assessment of soil-rice system in rural and peri-urban areas of lower brahmaputra valley, northeast India. *Chemosphere, 266*, 129150.

Behera, B. C., Mishra, R. R., Patra, J. K., Dutta, S. K., & Thatoi, H. N. (2014). Physico chemical properties of water sample collected from mangrove ecosystem of Mahanadi River Delta, Odisha, India. *American Journal of Marine Science, 2*(1), 19–24.

Bhardwaj, R., Gupta, A., & Garg, J. K. (2017). Evaluation of heavy metal contamination using environmetrics and indexing approach for River Yamuna, Delhi stretch, India. *Water Science, 31*(1), 52–66.

Bhuyan, M., Bakar, M., Sharif, A. S. M., Hasan, M., & Islam, M. (2018). Water quality assessment using water quality indicators and multivariate analyses of the old Brahmaputra River. *Pollution, 4*(3), 481–493.

Bhuyan, M. S., Bakar, M. A., Rashed-Un-Nabi, M., Senapathi, V., Chung, S. Y., & Islam, M. S. (2019). Monitoring and assessment of heavy metal contamination in surface water and sediment of the Old Brahmaputra River, Bangladesh. *Applied Water Science, 9*(5), 1–13.

Bowes, M. J., Read, D. S., Joshi, H., Sinha, R., Ansari, A., Hazra, M., Simon, M., Vishwakarma, R., Armstrong, L. K., Nicholls, D. J., & Wickham, H. D. (2020). Nutrient and microbial water quality of the upper Ganga River, India: Identification of pollution sources. *Environmental Monitoring and Assessment, 192*(8), 1–20.

Burgherr, P. (2007). In-depth analysis of accidental oil spills from tankers in the context of global spill trends from all sources. *Journal of Hazardous Materials, 140*(1–2), 245–256.

Central Water Commission. (2007). *Yamuna Basin organization*. Central Water Commission.

Chatterjee, S. K., Bhattacharjee, I., & Chandra, G. (2010). Water quality assessment near an industrial site of Damodar River, India. *Environmental Monitoring and Assessment, 161*(1), 177–189.

Chaudhary, M., Mishra, S., & Kumar, A. (2017). Estimation of water pollution and probability of health risk due to imbalanced nutrients in River Ganga, India. *International Journal of River Basin Management, 15*(1), 53–60.

Chowdhury, N. R., Das, A., Joardar, M., Mridha, D., De, A., Majumder, S., Mandal, J., Majumdar, A., & Roychowdhury, T. (2022). Distribution of arsenic in rice grain from West Bengal, India: Its relevance to geographical origin, variety, cultivars and cultivation season. In *Global arsenic hazard: Ecotoxicology and remediation* (pp. 509–531). Springer.

CPCB. (Central Pollution Control Board). (2003). *Chapter on corporate responsibility for environmental protection, distillery*. http://www.cpcb.nic.in/Charter/charter5.htm

CPCB. (2006). *Status of sewage treatment in India, Central Pollution Control Board*. Government of India: Control of Urban Pollution Series: CUPS/37/ 2005–2006

CPCB. (2013). Specifications and Guidelines for Continuous Emissions Monitoring Systems (CEMS) for PM Measurement with Special Reference to Emission Trading Programmes, New Delhi: Central Pollution Control Board, Ministry of Environment and Forests, Government of India.

Derraik, J. G. (2002). The pollution of the marine environment by plastic debris: A review. *Marine Pollution Bulletin, 44*(9), 842–852.

Dey, K., Mohapatra, S. C., & Misra, M. B. (2005). Assessment of water quality parameters of the river Brahmani at Rourkela. *Journal of Industrial Control Pollution, 21*(1), 299–304.

FAO. (2016). *The state of world fisheries and aquaculture 2016. Contributing to food security and nutrition for all* (p. 200). FAO.

Ghorade, I. B., Lamture, S. V., & Patil, S. S. (2014). Assessment of heavy metal content in Godavari river water. *International Journal of Research in Applied, Natural and Social Sciences, 2*(6), 23–26.

Giri, S., & Singh, A. K. (2014). Assessment of surface water quality using heavy metal pollution index in Subarnarekha River, India. *Water Quality, Exposure and Health, 5*(4), 173–182.

Gupta, A., Majumdar, A., & Srivastava, S. (2022). Approaches for assisted phytoremediation of arsenic contaminated sites. In *Assisted Phytoremediation* (pp. 221–242). Elsevier.

Helmer, R., & Hespanhol, I. (1997). *Water pollution control: A guide to the use of water quality management principles*. CRC Press.

Hussain, J., Husain, I., Arif, M., & Gupta, N. (2017). Studies on heavy metal contamination in Godavari river basin. *Applied Water Science, 7*(8), 4539–4548.

Imran, U., Ullah, A., Shaikh, K., Mehmood, R., & Saeed, M. (2019). Health risk assessment of the exposure of heavy metal contamination in surface water of lower Sindh, Pakistan. *SN Applied Sciences, 1*(6), 1–10.

Jain, C. K., Gupta, H., & Chakrapani, G. J. (2008). Enrichment and fractionation of heavy metals in bed sediments of River Narmada, India. *Environmental Monitoring and Assessment, 141*(1), 35–47.

Kamyotra, J. S., & Bhardwaj, R. M. (2011). *Municipal wastewater management in India* (p. 299). India infrastructure report. Scientific Research Publishing.

Khan, M. Y. A., Gani, K. M., & Chakrapani, G. J. (2017). Spatial and temporal variations of physicochemical and heavy metal pollution in Ramganga River—A tributary of River Ganges, India. *Environmental Earth Sciences, 76*(5), 231.

Khan, R., Saxena, A., & Shukla, S. (2020). Evaluation of heavy metal pollution for River Gomti, in parts of Ganga Alluvial Plain, India. *SN Applied Sciences, 2*(8), 1–12.

Khemani, L. T., Momin, G. A., Rao, P. P., Safai, P. D., Singh, G., Chatterjee, R. N., & Prakash, P. (1989). Long-term effects of pollutants on pH of rain water in North India. *Atmospheric Environment, 23*(4), 753–756.

Konhauser, K. O., Powell, M. A., Fyfe, W. S., Longstaffe, F. J., & Tripathy, S. (1997). Trace element geochemistry of river sediment, Orissa State, India. *Journal of Hydrology, 193*(1–4), 258–269.

Kori, R., Shrivastava, K. P., Upadhyay, N., & Singh, R. (2006). Studies on presence of heavy metals and halogenated hydrocarbons in river Betwa (MP), India. *Поволж. экол. журн, 2/3*, 147–153.

Kumar, A. A., Dipu, S., & Sobha, V. (2011). Seasonal variation of heavy metals in cochin estuary and adjoining Periyar and Muvattupuzha rivers, Kerala, India. *Global Journal of Environmental Research, 5*(1), 15–20.

Kumar, R. N., Solanki, R., & Kumar, J. N. (2013). Seasonal variation in heavy metal contamination in water and sediments of river Sabarmati and Kharicut canal at Ahmedabad, Gujarat. *Environmental Monitoring and Assessment, 185*(1), 359–368.

Kumar, A., Kumar, A., & Jha, S. K. (2020a). Distribution and bioaccumulation of heavy metal in water, sediment and fish tissue from the River Mahananda in Seemanchal zone, North Bihar, India. *International Journal of Aquatic Biology, 8*(2), 109–125.

Kumar, V., Sharma, A., Kumar, R., Bhardwaj, R., Kumar Thukral, A., & Rodrigo-Comino, J. (2020b). Assessment of heavy-metal pollution in three different Indian water bodies by combination of multivariate analysis and water pollution indices. *Human and Ecological Risk Assessment: An International Journal, 26*(1), 1–16.

Mahato, M. K., Singh, G., Singh, P. K., Singh, A. K., & Tiwari, A. K. (2017). Assessment of mine water quality using heavy metal pollution index in a coal mining area of Damodar River Basin, India. *Bulletin of Environmental Contamination and Toxicology, 99*(1), 54–61.

Majumdar, A. (2021). *Arsenic bio-regulation management and altered plant physiology under different irrigation regime.* Doctoral dissertation. Indian Institute of Science Education and Research Kolkata.

Majumdar, A., & Bose, S. (2017). Toxicogenesis and metabolism of arsenic in rice and wheat plants with probable mitigation strategies. In *Arsenic: Risks of exposure, behavior in the environment and toxicology* (pp. 149–166). Nova Science Publishers.

Majumdar, A., & Bose, S. (2018). A glimpse on uptake kinetics and molecular responses of arsenic tolerance in Rice plants. In *Mechanisms of arsenic toxicity and tolerance in plants* (pp. 299–315). Springer.

Majumdar, A., Pradhan, N., Sadasivan, J., Acharya, A., Ojha, N., Babu, S., & Bose, S. (2018a). Food degradation and foodborne diseases: A microbial approach. In *Microbial contamination and food degradation* (pp. 109–148). Academic Press.

Majumdar, A., Barla, A., Upadhyay, M. K., Ghosh, D., Chaudhuri, P., Srivastava, S., & Bose, S. (2018b). Vermiremediation of metal (loid)s via Eichornia crassipes phytomass extraction: a sustainable technique for plant amelioration. *Journal of Environmental Management, 220*, 118–125.

Majumdar, A., Upadhyay, M. K., Kumar, J. S., Barla, A., Srivastava, S., Jaiswal, M. K., & Bose, S. (2019a). Ultra-structure alteration via enhanced silicon uptake in arsenic stressed rice cultivars under intermittent irrigation practices in Bengal delta basin. *Ecotoxicology and Environmental Safety, 180*, 770–779.

Majumdar, A., Upadhyay, M. K., Srivastava, S., Jaiswal, M. K., & Bose, S. (2019b). Arsenic-silicon dynamics in soil and bacterial biotransformation under altered irrigation practice induces plant anatomy. In *AGU fall meeting abstracts* (Vol. 2019, p. B44B-04). American Geophysical Union.

Majumdar, A., Barla, A., Bose, S., Upadhyay, M. K., & Srivastava, S. (2019c). Alleviation of altered ultrastructure in arsenic stressed rice cultivars under proposed irrigation practice in Bengal Delta Basin. In *Environmental arsenic in a changing world* (pp. 543–544). CRC Press.

Majumdar, A., Kumar, J. S., & Bose, S. (2020a). Agricultural water management practices and environmental influences on arsenic dynamics in rice field. In *Arsenic in Drinking Water and Food* (pp. 425–443). Springer.

Majumdar, A., Shrivastava, A., Sarkar, S. R., Sathyavelu, S., Barla, A., & Bose, S. (2020b). Hydrology, sedimentation and mineralisation: A wetland ecology perspective. *Climate Change and Environmental Sustainability, 8*(2), 134–151.

Majumdar, A., Upadhyay, M. K., Giri, B., Srivastava, S., Srivastava, A. K., Jaiswal, M. K., & Bose, S. (2021). Arsenic dynamics and flux assessment under drying-wetting irrigation and enhanced microbial diversity in paddy soils: A four year study in Bengal delta plain. *Journal of Hazardous Materials, 409*, 124443.

Majumdar, A., Afsal, F., Pathak, S., Upadhayay, M. K., Roychowdhury, T., & Srivastava, S. (2022a). Molecular aspects of arsenic responsive microbes in soil-plant-aqueous triphasic systems. In *Global arsenic hazard: Ecotoxicology and remediation* (pp. 291–312). Springer.

Majumdar, A., Upadhyay, M. K., Dubey, P. K., Giri, B., Srivastava, A. K., & Srivastava, S. (2022b). *Effect of combined dry-wet irrigation and microbial dynamics on soil nutrient bioavailability*.

Majumdar, A., Upadhyay, M. K., Ojha, M., Afsal, F., Giri, B., Srivastava, S., & Bose, S. (2022c). Enhanced phytoremediation of Metal (loid)s via spiked ZVI nanoparticles: An urban clean-up strategy with ornamental plants. *Chemosphere, 288*, 132588.

Majumdar, A., Kumar Upadhyay, M., Srivastava, A. K., Srivastava, S., & Bose, S. (2022d, July). *Soil geochemical dynamics of arsenic and nutrients affects microbial diversity, elemental release and plant-microbe interactions: A long-term study from field to genomics*. In 2022 Goldschmidt conference. Goldschmidt.

Majumdar, A., Dubey, P. K., Giri, B., Moulick, D., Srivastava, A. K., Roychowdhury, T., Bose, S., & Jaiswal, M. K. (2023a). Combined effects of dry-wet irrigation, redox changes and microbial diversity on soil nutrient bioavailability in the rice field. *Soil and Tillage Research, 232*, 105752.

Majumdar, A., Upadhyay, M. K., Giri, B., Karwadiya, J., Bose, S., & Jaiswal, M. K. (2023b). Iron oxide doped rice biochar reduces soil-plant arsenic stress, improves nutrient values: An amendment towards sustainable development goals. *Chemosphere, 312*, 137117.

Majumdar, A., Upadhyay, M. K., Giri, B., Moulick, D., Sarkar, S., Thakur, B., Yadav, P., Sahu, K., Srivastava, A. K., Buck, M., & Tibbett, M. (2023c). Sustainable irrigation reduces arsenic bioavailability in fluvio-alluvial soils promoting microbial responses, high rice productivity and economic profit. 1, 1–90.

Mateo-Sagasta, J., Zadeh, S. M., Turral, H., & Burke, J. (2017). *Water pollution from agriculture: A global review*. Executive summary.

Matta, G., Kumar, A., Nayak, A., & Kumar, P. (2022). Appraisal of spatial–temporal variation and pollution source estimation of Ganga River system through pollution indices and environmetrics in Upper Ganga basin. *Applied Water Science, 12*, 1–11.

Mazhar, S. N., & Ahmad, S. (2020). Assessment of water quality pollution indices and distribution of heavy metals in drinking water in Ramganga aquifer, Bareilly District Uttar Pradesh, India. *Groundwater for Sustainable Development, 10*, 100304.

Michel, J., & Fingas, M. (2016). Oil Spills: Causes, consequences, prevention, and countermeasures. In *Fossil Fuels: Current Status and Future Directions* (pp. 159–201). World Scientific.

Michel, J., Gilbert, T., Etkin, D. S., Urban, R., Waldron, J. & Blocksidge, C. T. (2005). May. Potentially polluting wrecks in marine waters. In *Annals of the 2005 International Oil Spill Conference, Maio* (Vol. 16, pp. 1–84).

Mishra, S., & Kumar, A. (2021). Estimation of physicochemical characteristics and associated metal contamination risk in the Narmada River, India. *Environmental Engineering Research, 26*(1). https://doi.org/10.4491/eer.2019.521

Mishra, D., & Rhee, Y. H. (2010). Current research trends of microbiological leaching for metal recovery from industrial wastes. *Current Research, Technology and Education Topics in Applied Microbiology and Microbial Biotechnology, 2*, 1289–1292.

Mokarram, M., Saber, A., & Sheykhi, V. (2020). Effects of heavy metal contamination on river water quality due to release of industrial effluents. *Journal of Cleaner Production, 277*, 123380.

Nanda, S. N., & Tiwari, T. N. (2001). Effect of discharge of municipal sewage on the quality of River Mahanadi at Sambalpur. *Indian Journal of Environmental Protection, 21*(4), 336–343.

Owa, F. D. (2013). Water pollution: Sources, effects, control and management. *Mediterranean Journal of Social Sciences, 4*(8), 65.

Pandey, H., Senthilnathan, S., & Thivakaran, G. (2020). Heavy metal contamination in water, sediment and fish of Mahi estuary, Gujarat, India. *Pollution Research, 39*, 326–333.

Pareek, R. K., Khan, A. S., Srivastava, P., & Roy, S. (2018). A study of heavy metal pollution of Ghaggar River. *International Journal of Theoretical and Applied Sciences, 10*(1), 66–70.

Paul, D. (2017). Research on heavy metal pollution of river Ganga: A review. *Annals of Agrarian Science, 15*(2), 278–286.

Petraglia, M. D., Ditchfield, P., Jones, S., Korisettar, R., & Pal, J. N. (2012). The Toba volcanic super-eruption, environmental change, and hominin occupation history in India over the last 140,000 years. *Quaternary International, 258*, 119–134.

Purnima, B. (2013). A comparative study on the pollution status of the Narmada river. *Asian Journal of Environmental Science, 8*(2), 136–138.

Rahman, M. M., Islam, M. A., & Khan, M. B. (2016). Status of heavy metal pollution of water and fishes in Balu and Brahmaputra rivers. *Progressive Agriculture, 27*(4), 444–452.

Rao, K. L. (1975). *India's water wealth* (255pp.). Orient Longman.

Reddy, V. R., & Behera, B. (2006). Impact of water pollution on rural communities: An economic analysis. *Ecological Economics, 58*(3), 520–537.

Rodrigues, M. O., Abrantes, N., Gonçalves, F. J. M., Nogueira, H., Marques, J. C., & Gonçalves, A. M. M. (2018). Spatial and temporal distribution of microplastics in water and sediments of a freshwater system (Antuã River, Portugal). *Science of the Total Environment, 633*, 1549–1559.

Saha, M., Sengupta, S., Sinha, B., & Mishra, D. K. (2017). Assessment of physico-chemical properties, some heavy metals and arsenic of river teesta in Jalpaiguri district, West Bengal, India. *Asian Journal of Research in Chemistry, 10*(3), 399–404.

Samanta, S., Kumar, V., Nag, S. K., Raman, R. K., Saha, K., Bandyopadhyay, S., et al. (2020). Metal contaminations in sediment and associated ecological risk assessment of river Mahanadi, India. *Environmental Monitoring and Assessment, 192*(1), 1–17.

Sarkar, S. R., Majumdar, A., Barla, A., Pradhan, N., Singh, S., Ojha, N., & Bose, S. (2017). A conjugative study of Typha latifolia for expunge of phyto-available heavy metals in fly ash ameliorated soil. *Geoderma, 305*, 354–362.

Schwarzenbach, R. P., Egli, T., Hofstetter, T. B., Von Gunten, U., & Wehrli, B. (2010). Global water pollution and human health. *Annual Review of Environment and Resources, 35*, 109–136.

Secretariat of the United Nations Commission for Europe. (1994). Protection and use of transboundary watercourses and international lakes in Europe. In *Natural resources forum* (Vol. 18, No. 3, pp. 171–180). Blackwell Publishing Ltd.

Sehgal, M., Garg, A., Suresh, R., & Dagar, P. (2012). Heavy metal contamination in the Delhi segment of Yamuna basin. *Environmental Monitoring and Assessment, 184*(2), 1181–1196.

Sengupta, B. (2006). *Water quality status of Yamuna River (1999–2005)* (Assessment and development of river basin series: ADSORBS/41/2006-07). Central Pollution Control Board.

Setia, R., Dhaliwal, S. S., Kumar, V., Singh, R., Kukal, S. S., & Pateriya, B. (2020). Impact assessment of metal contamination in surface water of Sutlej River (India) on human health risks. *Environmental Pollution, 265*, 114907.

Shorna, S., Quraishi, S. B., Hosen, M. M., Hossain, M. K., Saha, B., Hossain, A., & Habibullah-Al-Mamun, M. (2021). Ecological risk assessment of trace metals in sediment from the Old Brahmaputra River in Bangladesh. *Chemistry and Ecology, 37*(9–10), 809–826.

Shrivastava, A., Barla, A., Majumdar, A., Singh, S., & Bose, S. (2020). Arsenic mitigation in rice grain loading via alternative irrigation by proposed water management practices. *Chemosphere, 238*, 124988.

Siddaramu, D., Harish Babu, K., Naik Prakash, S., & Puttaiah, E. T. (2009). Heavy metal concentration in surface and sub-surface waters along Tungabhadra River in Karnataka, India. *Nature Environment and Pollution Technology, 8*(4), 649–655.

Singh, I. B. (2007). The Ganga River. In *Large rivers: Geomorphology and management* (pp. 347–371). Wiley.

Singh, A., & Agrawal, M. (2007). Acid rain and its ecological consequences. *Journal of Environmental Biology, 29*(1), 15.

Singh, K. P., Malik, A., Sinha, S., Singh, V. K., & Murthy, R. C. (2005). Estimation of source of heavy metal contamination in sediments of Gomti River (India) using principal component analysis. *Water, Air, and Soil Pollution, 166*(1), 321–341.

Singh, A. K., Mondal, G. C., Kumar, S., Singh, T. B., Tewary, B. K., & Sinha, A. (2008). Major ion chemistry, weathering processes and water quality assessment in upper catchment of Damodar River basin, India. *Environmental Geology, 54*(4), 745–758.

Singh, C. K., Rina, K., Singh, R. P., & Mukherjee, S. (2014). Geochemical characterization and heavy metal contamination of groundwater in Satluj River Basin. *Environmental Earth Sciences, 71*(1), 201–216.

Sivadas, S., Gregory, A., & Ingole, B. (2008). How vulnerable is Indian coast to oil spills? Impact of MV Ocean Seraya oil spill. *Current Science, 95*, 504–512.

Srivastava, A. K., Pandey, M., Ghate, T., Kumar, V., Upadhyay, M. K., Majumdar, A., Sanjukta, A. K., Agrawal, A. K., Bose, S., Srivastava, S., & Suprasanna, P. (2021). Chemical intervention for enhancing growth and reducing grain arsenic accumulation in rice. *Environmental Pollution, 276*, 116719.

Sundaray, S. K. (2010). Application of multivariate statistical techniques in hydrogeochemical studies—A case study: Brahmani–Koel River (India). *Environmental Monitoring and Assessment, 164*(1), 297–310.

Sundaray, S. K., Nayak, B. B., Kanungo, T. K., & Bhatta, D. (2012). Dynamics and quantification of dissolved heavy metals in the Mahanadi river estuarine system, India. *Environmental Monitoring and Assessment, 184*(2), 1157–1179.

Tiwari, A. K., Singh, P. K., & Mahato, M. K. (2017). Assessment of metal contamination in the mine water of the West Bokaro Coalfield, India. *Mine Water and the Environment, 36*(4), 532–541.

Tiwary, R. K. (2001). Environmental impact of coal mining on water regime and its management. *Water, Air, and Soil Pollution, 132*(1), 185–199.

Trivedi, R. C. (2010). Water quality of the Ganga River – An overview. *Aquatic Ecosystem Health and Management, 13*(4), 347–351.

Tsering, T., Sillanpää, M., Sillanpää, M., Viitala, M., & Reinikainen, S. P. (2021). Microplastics pollution in the Brahmaputra River and the Indus River of the Indian Himalaya. *Science of the Total Environment, 789*, 147968.

Tyagi, N., Upadhyay, M. K., Majumdar, A., Pathak, S. K., Giri, B., Jaiswal, M. K., & Srivastava, S. (2022). An assessment of various potentially toxic elements and associated health risks in agricultural soil along the middle Gangetic basin, India. *Chemosphere, 300*, 134433.

Ullah, R., Asghar, R., Tanveer, Z., Aziz, S., Babar, M., Ali, S., & Mahmood, A. (2018). Determination of heavy metals levels in water of River Jhelum in the State of Azad Jammu and Kashmir, Pakistan. *International Journal of Biosciences, 12*, 267–274.

Upadhyay, M. K., & Majumdar, A. (2022). Heavy metals' stress responses in field crops. In *Response of field crops to abiotic stress* (pp. 45–54). CRC Press.

Upadhyay, M. K., Majumdar, A., Barla, A., Bose, S., & Srivastava, S. (2019). An assessment of arsenic hazard in groundwater–soil–rice system in two villages of Nadia district, West Bengal, India. *Environmental Geochemistry and Health, 41*(6), 2381–2395.

Upadhyay, M. K., Majumdar, A., Suresh Kumar, J., & Srivastava, S. (2020). Arsenic in rice agroecosystem: Solutions for safe and sustainable rice production. *Frontiers in Sustainable Food Systems, 4*, 53.

Upadhyay, M. K., Majumdar, A., Barla, A., Bose, S., & Srivastava, S. (2021). Thiourea supplementation mediated reduction of grain arsenic in rice (Oryza sativa L.) cultivars: A two year field study. *Journal of Hazardous Materials, 407*, 124368.

Vorobiev, D. S., Merzlyakov, O. E., & Noskov, Y. A. (2014). Oil decontamination of bottom sediments: past, present and future. *Procedia Chemistry, 10*, 158–161.

Waghmare, T., Bhandare, P., & Belldal, B. (2017). Acute toxicity of heavy metals from Bheema River water and effects on albino rat. *Trends in Biosciences, 10*, 2246–2252.

Wu, C., Maurer, C., Wang, Y., Xue, S., & Davis, D. L. (1999). Water pollution and human health in China. *Environmental Health Perspectives, 107*(4), 251–256.

Yang, S. Q., & Liu, P. W. (2010). Strategy of water pollution prevention in Taihu Lake and its effects analysis. *Journal of Great Lakes Research, 36*(1), 150–158.

# Geochemistry and Mineralogy of Peninsular Indian River Sediments with Special Reference to Godavari and Krishna Rivers

**Syed Masood Ahmad, Waseem Raza, and Archana Bhagwat Kaotekwar**

## 1 Introduction

Understanding the geochemical cycling of the elements and the erosional characteristics of the river basins requires knowledge of the chemical and mineralogical composition of riverine sediments (Martin & Meybeck, 1979; Milliman & Meade, 1983; Cullers et al., 1988). Since a few decades ago, eroded material's transit via rivers has drawn considerable study (Nesbitt, 1979; Cullers et al., 1987; Ross et al., 1995; Singh & Rajamani, 2001; Sharma et al., 2013). A number of physical and chemical factors regulate the ability of rivers to transfer weathered materials to oceans. According to Milliman and Meade (1983), the Indian subcontinent accounts for around 30% of the sedimentary load carried by rivers around the world. The suspended sediments in a river's water, which carry pollutants and nutrients, regulate the water quality. Certain metals can be effectively scavenged by the discharge of heavy metals caused by human activity and transported by suspended particles. Weathering of rocks is influenced by local geology, climate, topography, and human activity (Subramanian et al., 1985; Sharma & Rajamani, 2001; Das et al., 2005; Tripathi et al., 2007; Rajamani et al., 2009; Sharma et al., 2013). The type of source rock, the degree of weathering, physical sorting during transportation, and the environment of deposition all play a substantial role in determining the geochemistry of the sediments (Taylor & Mclennan, 1985; Nesbitt & Young, 1996). Rocks and minerals are converted into sediments and soil through symbiotic physical, chemical, and microbiological processes known as weathering.

S. M. Ahmad (✉)
Inter-University Accelerator Centre, New Delhi, India

W. Raza · A. B. Kaotekwar
CSIR-National Geophysical Research Institute, Hyderabad, India



S. Kanhaiya et al. (eds.), *Rivers of India*,
https://doi.org/10.1007/978-3-031-49163-4_5

According to various researchers (Cullers et al., 1987; Biksham et al., 1991; Singh & Rajamani, 2001; Rengarajan & Sarin, 2004; Singh, 2009; Sharma et al., 2013), the effect of weathering on major, trace, and rare-earth elements in eroded particles has been reported. As sediments obtain their elemental composition from the parent rocks, rare-earth elements are helpful to understand the sedimentary settings (Alexander & Gibson, 1977; Ross et al., 1995; Sensarma et al., 2008; Shynu et al., 2011). Peninsular Indian river sediments have unique textural, chemical, and mineralogical characteristics that can be employed as diagnostic indicators of their provenance and movement history. Some researchers (Singh & Rajamani, 2001; Das & Krishnaswami, 2007; Singh, 2009) have provided evidence of the value of chemical and isotopic signatures as fingerprints of source rocks and transport pathways of detrital particles. The Godavari and Krishna River systems, which deposit a significant amount of sediment into the BoB, record the history of rock weathering and erosion in their drainage basins (Kaotekwar et al., 2019). In order to understand the behavior of numerous main and trace elements during chemical weathering and transit, investigations on sediments from the Godavari and Krishna River basins have been conducted.

## 2 Geological Settings and Climate

The Godavari and Krishna Rivers are two of Peninsular India's few biggest rivers. Before releasing their sedimentary load and water fluxes into the BoB, they flow in easterly and southeasterly directions and originate in the Deccan Traps (Fig. 1). The Deccan Traps of the Cretaceous period dominate the upper portions of the Godavari basin, while a diverse variety of rocks, including Archaean granites, quartzites, amphiboles, phyllites, and gneisses, may be found in the middle portion. The Deccan Traps, 11% Precambrian and Gondwana sediments, and 2–3% modern alluvium make up almost 48% of the River Godavari's bedrock. Nearly 8% of India's total land area, or 258,948 $km^2$, is made up by the Krishna River basin. The basin's maximum dimensions are around 701 km in length and 672 km in width. The Deccan Traps in the northwest, undifferentiated crystallines in the center, Cuddapah Group in the east, Dharwar in the southwest, and Vindhyan in the east central region make up the majority of the Krishna basin's geology. Around 80% of the rocks in the Krishna basin are Archean or newer crystalline rocks, 20% are Tertiary Deccan Traps, and 2% are recent alluvial. Sediments from the Pleistocene to more recent times make up the bottom portions of the Godavari and Krishna basins.

The majority of the tholeiitic lavas that make up the upper portions of the Deccan Basalt are composed primarily of the minerals plagioclase, pyroxene, and olivine. Augite and pigeonite are more prevalent among pyroxenes (Das & Krishnaswami, 2007). Zeolites have reportedly been found in basalt cavities as crystalline specimens. According to Das et al. (2005) and Jeffery et al. (1988), there have been reports of the presence of calcite as a minor phase in some basalts and calcium carbonate as a component of bed sediments in the Krishna basin. Many Deccan

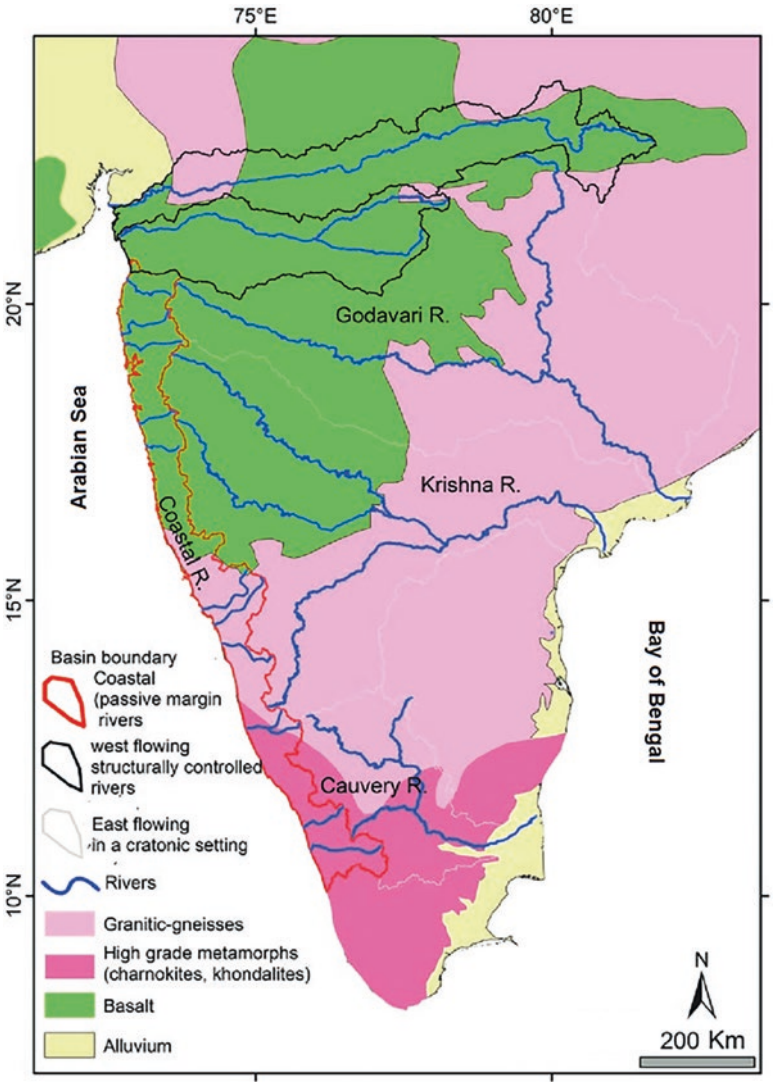


**Fig. 1** Location map of Godavari and Krishna Rivers

Trap areas have soils that are mainly lateral and black in hue. Due to the continental leaching of parent basalts, black soils tend to be fine textured with high smectite clay content and low Ca, Na, and Mg concentrations. Zones of damaged and new rock surfaces define the catchment areas of the Godavari and Krishna basins. In comparison to the sediments of the Himalayan River, sediments from both of these rivers tend to be finer grained and more flexible in character. Godavari and Krishna basins have a subtropical climate with semiarid conditions. Rainfall in catchment

areas varies greatly, averaging between 60 and 85 cm per year and falling primarily between June and September during the southwest monsoon season.

## 3 Geochemistry

### *3.1 Major and Trace Elements*

Chemical patterns of riverbed sediments typically mimic those of their source rocks but more frequently. During the weathering process, the parent rock's chemical and mineralogical compositions go through significant changes. The chemical and mineralogical makeup of the parent rock, the physical and chemical characteristics of the operative agents during weathering, transportation, and deposition, the duration of processes, the presence of initial pathways within the parent rock, and the type of the local climate are the main factors that control a rock's elemental behavior. Therefore, two competing processes compete to control the elemental concentrations of sediments: (a) the leaching of cations from primary minerals constituting the protolith's original source rock (protolith) during the early weathering stages and (b) the fixation of these cations by exchange and adsorption onto secondary clay minerals during the advanced weathering stages before breakdown and deposition as sediments (occurring in water bodies). For instance, the order of elemental mobility during the early stages of basalt weathering is Si>K, Na:Mg> Ca>K, Na: Mg>Fe, Al, and Ti, whereas during the late stages of chemical weathering it is Si>Ca>K, Na: Mg> Fe, Al, and Ti.

Numerous researchers have conducted in-depth geochemical and mineralogical analyses on the bed and suspended sediments of Peninsular Indian rivers to better understand the mobility of major, minor, and trace elements during weathering and transportation processes (Subramanian et al., 1985; Ramesh et al., 1989; Dekov et al., 1998; Sharma & Rajamani, 2000; Andersson et al., 2005; Kaotekwar et al., 2019). The chemical and hydrodynamic behavior of the main mineral phases can be understood by using chemically immobile components like $TiO_2$, $Al_2O_3$, and $SiO_2$. In order to deduce the behavior of major and trace elements during weathering of old crustal rocks like gneisses and charnockites, Rajamani et al. (2009) performed thorough geochemistry of Cauvery River sediments from southern India. To better understand the nature of chemical weathering and the mobility of elements, Das and Krishnaswami (2007) analyzed the geochemical features of sediments from rivers flowing through the Deccan Traps. The lower Godavari River sediments' elemental compositions show that they were primarily created by the weathering of minerals acquired from the surrounding Precambrian rocks (Fig. 2).

Sediments from the lower (downstream) Godavari River exhibit exceptionally high $SiO_2$ concentration (range from 71.52% to 74.23%) and comparatively little $Al_2O_3$ (between 8.65% and 9.45%). Because of their great mobility during the chemical weathering process, the concentrations of other important oxides

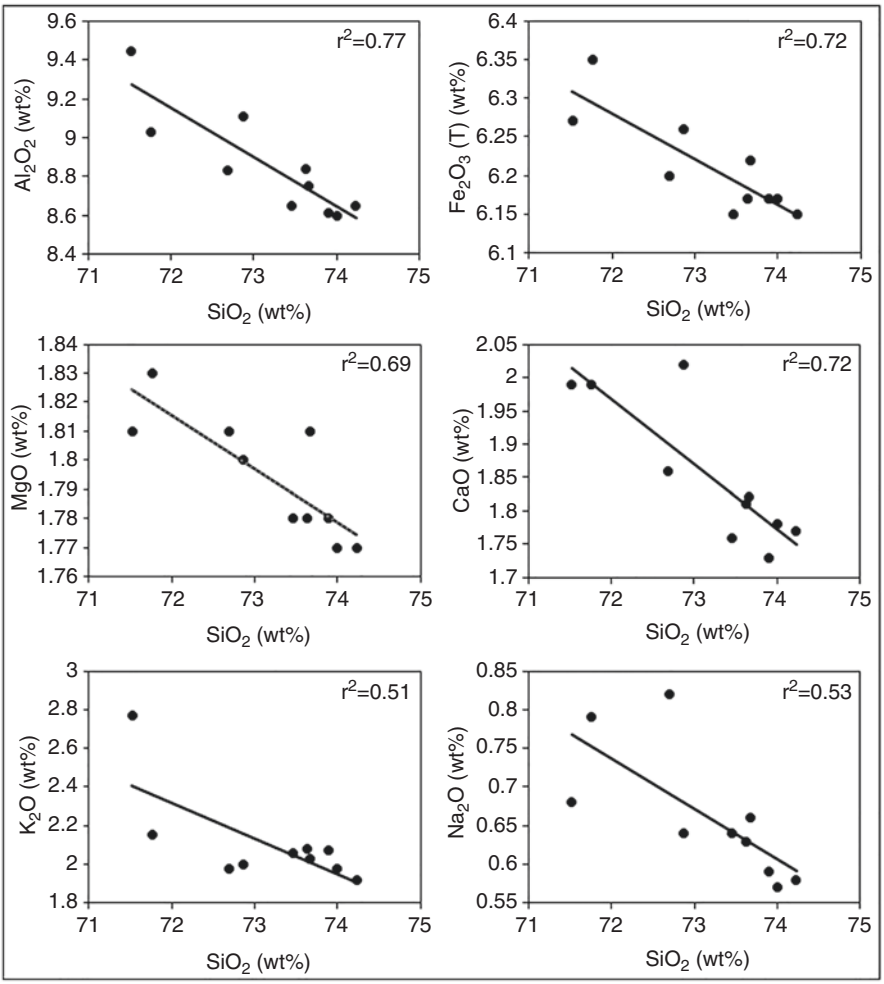


**Fig. 2** Correlation of $SiO_2$ with other major oxides in downstream sediments of Godavari River

including $Na_2O$, CaO, and MgO in lower Godavari and Krishna River sediments were observed to be quite low. Strong to moderate correlations between $SiO_2$ and $Al_2O_3$, $Fe_2O_3$, MgO, CaO, $K_2O$, and $Na_2O$ in these rivers' sediments suggest that the geochemistry and mineralogical composition of source rocks are controlled by particle size (Fig. 2). Due to the presence of K-feldspar, high potassium concentrations have been interpreted in some Krishna River sediment areas (Kaotekwar et al., 2019). It's interesting to note that lower Godavari sediments and lower Krishna River sediments have differing elemental compositions (Kaotekwar et al., 2019). Due to their interaction with rock-forming minerals, the $SiO_2$ content in Krishna River sediments, for instance, was observed to be rather low, ranging from 40.59% to 51.87%, with substantial correlations to several other major oxides. Because

titanite mineral is present in source rocks at Krishna's drainage basin, the lower Krishna River sediments often have higher quantities of titanium than lower Godavari sediments. Additionally, there are large fluctuations in Ca contents in the upper Krishna River sediments, which may indicate different degrees of calcium carbonate precipitation or weathering of the parent rock (Das & Krishnaswami, 2007; Sharma et al., 2013).

Due to their co-occurrence in weathering-resistant minerals and/or the scavenging of titanium by iron oxy-hydroxides during the weathering of source rocks, $Fe_2O_3$ and $TiO_2$ in sediments of the lower reaches of the Godavari and Krishna Rivers have been shown to have a strong relationship (Kaotekwar et al., 2019). Because of their affiliation with iron minerals and/or their sequestration with iron oxy-hydroxides, trace metals like vanadium (V) and nickel (Ni) also show a strong link with $Fe_2O_3$. Due to changes in the mineralogy of the source rock, the abundance of other trace elements, such as Cr, Cu, and Zn, exhibits considerable dispersion with larger concentrations in upstream sediments. In comparison to silicic igneous rocks, mafic to ultramafic igneous rocks often have higher concentrations of trace elements such Cu, Cr, Ni, and Co (Sharma et al., 2013). Sediments in the upper reaches of the Godavari and Krishna basins have higher quantities of trace elements because sediments in large volcanic provinces like the Deccan basalts contain significant amounts of mafic minerals. In-depth geochemical analyses of sediments from the Cauvery River in southern India have demonstrated that mineral breakdown is not the cause of the depletion and enrichment of various elements but rather the leaching of primary minerals, particularly mafic minerals, by meteoric water (Sharma & Rajamani, 2000). The suspended particles of the Krishna River were more enriched in heavy metals than the bed sediments (Ramesh et al., 1989). They also note significant fluctuations in heavy metal contents between sediments in the upstream and downstream due to alterations in subbasin geology and human influence. Lower Godavari and Krishna River sediments exhibit high chemical index of alteration (CIA) values, ranging from 61.0 to 67.0, indicating a moderate to vigorous chemical weathering environment. It should be noted that CIA values can vary greatly depending on the level and intensity of weathering and are sensitive to land surface temperature and latitude at river mouth. However, the highly varying CIA values in the sediments of the upper Godavari and Krishna basins (ranging from 37.0 to 60.2) indicate that there is a great deal of regional variation in the rate of chemical weathering of the parent rocks. It has been established that samples with reduced Ca concentration exhibit higher CIA values, whereas sediments with a high Ca content exhibit substantially lower CIA values. Basaltic fragments found in some areas of the upper Godavari River basin reflect an environment that is only beginning to weather under a semiarid climate.

## 3.2 *Rare-Earth Elements*

The amount of source rock weathering, transit, and deposition processes has a significant impact on rare-earth elements in riverine sediments (Cullers et al., 1987; Elderfield et al., 1990). Due to similarities in their electrical architecture, these elements have a distinct behavior during chemical weathering. When compared to heavy rare-earth elements (HREEs), light rare-earth elements (LREEs) typically exhibit more fractionation and therefore offer extremely helpful information on the origin and mobility of sediment. River sediments often exhibit a consistent REE pattern with enrichment of LREEs and depletion of HREEs (Goldstein & Jacobson, 1988; Sholkovitz, 1995; Galy & France-Lanord, 2001). The LREEs are preferentially scavenged during weathering, while the HREEs are kept in a dissolved

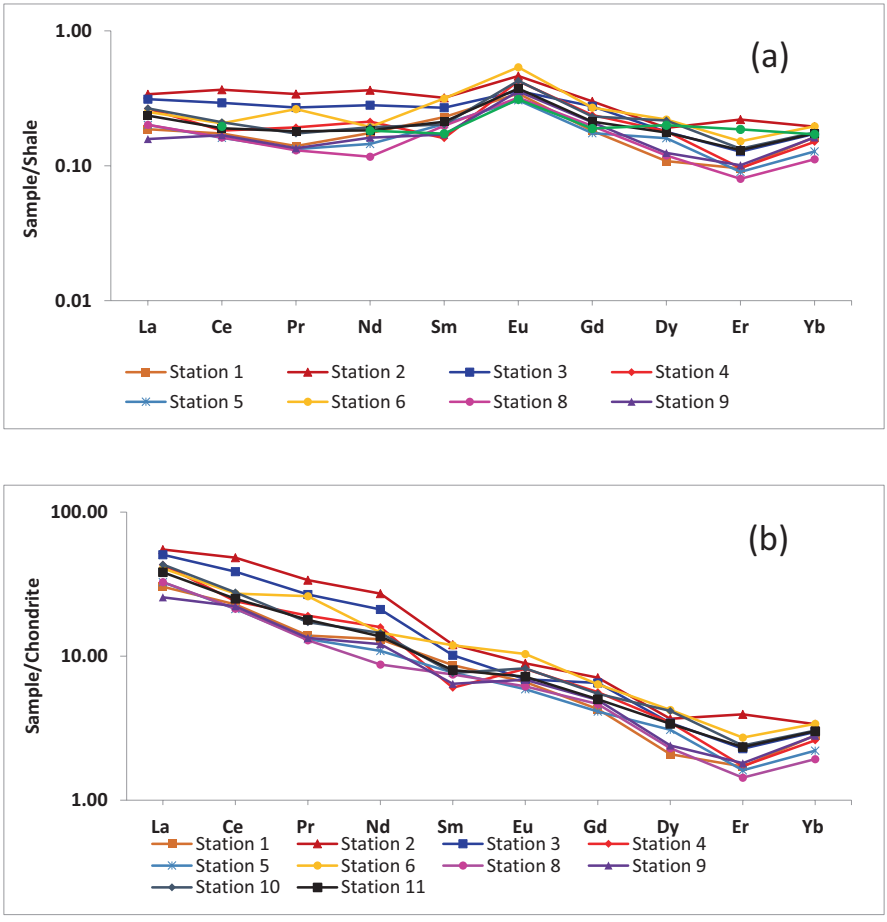


**Fig. 3** (**a**) Shale-normalized REE pattern of lower Godavari River sediments and (**b**) chondrite-normalized REE pattern of lower Godavari River sediments

condition. Additionally, REEs entering rivers are fractionated due to the removal of specific components as a result of intricate chemical processes. When the pH is neutral or alkaline, these elements become adsorbed on worn tiny particles and precipitate. These elements are often mobilized in an acidic environment. The flatness of the curve with a positive Eu anomaly, as illustrated in Fig. 3a, is a distinguishing quality of the lower Godavari sediments' shale-normalized REE pattern. Kaotekwar et al. (2019) discovered a similar pattern with a positive Eu anomaly in the bed sediments of the lower Krishna River basin. Plagioclase feldspar or anthropogenic organic input may be present, which could result in such a positive Eu anomaly (Tang & Johannesson, 2003). In contrast, due to low plagioclase concentration or a lack of human organic input, sediments formed by chemical weathering of basaltic rocks in upstream Godavari River do not exhibit any positive Eu anomaly. The downstream Godavari sediments' chondrite-normalized REE pattern (Fig. 3b) has a steep shape, which is typical of sediments formed by weathering mostly older crustal rocks such granites and gneisses (Taylor & Mclennan, 1985). The lower Krishna River sediments' chondrite-normalized REE pattern demonstrates that basalt and other mixed-rock types were chemically weathered to produce them. Remarkably, the upper Godavari sediments' REE pattern displays a weak to strong Ce anomaly, which indicates an oxidizing environment during sediment deposition.

Kaotekwar et al. (2019) conducted a thorough analysis of the behavior of REEs in various size fractions of Krishna River sediments. They have noted clearly distinct patterns in the sediment size fractions of clay, silt, and sand, as well as established relationships between a few trace elements and REEs. As shown by their higher $(La/Yb)_N$ ratios, the clay fractions of the Krishna River sediments contain much higher amounts of LREEs than the bed sediments. According to certain findings, coarser sand fractions contain less REE than silt and clay size fractions (Singh & Rajamani, 2001). These authors have shown that, with the exception of the Eu anomaly, REE trends in various size fractions are comparable. When compared to sediments with lower sand contents or larger silt or clay size fractions, sediments with higher sand contents exhibit a more dramatic positive Eu anomaly. Ti and Ce were shown to have a significant positive connection in sediments from the Godavari and Krishna Rivers (Kaotekwar et al., 2019). Additionally, a favorable association between Ti and REEs shows that titaniferous minerals have a significant influence on the chemistry of REEs. Southern Indian sediments from the Cauvery River showed a similar link between REEs and Ti concentrations (Singh & Rajamani, 2001). It should be mentioned that the weathering of ancient crustal rocks containing the mineral titanite has resulted in much greater quantities of REEs and Ti in the sediments of the Cauvery floodplain (Singh & Rajamani, 2001). The lower Godavari samples may have been created by weathering biotite and magnetite minerals due to their low REE and Ti concentrations. Lower Godavari and Krishna sediments show a positive correlation between REEs and Zr, indicating zircon control over REE geochemistry.

### 3.3 Strontium and Neodymium Isotopes

Strontium ($^{87}Sr/^{86}Sr$) and neodymium ($^{143}Nd/^{144}Nd$) isotopic ratios, which depend on the age and geological history of the parent rock, offer extremely useful information regarding the provenance of sediments (Goldstein & Jacobson, 1987; Krishnaswami et al., 1992; Andersson et al., 2005). Peninsular Indian rivers' bed sediments contain distinctive Sr and Nd isotope compositions (Ahmad et al., 2009). In comparison to sediments generated from younger crust, river sediments formed by weathering of older rocks include more radiogenic Sr and non-radiogenic Nd (Goldstein et al., 1984; Kessarkar et al., 2003). The amount of chemical weathering and erosion of authigenic precipitates, however, can have an impact on $^{87}Sr/^{86}Sr$. Nd isotopes, on the other hand, are thought to be a more accurate indicator of source rock because they are less impacted by differences in grain size and do not vary much during the processes of weathering, transportation, and winnowing. It should be mentioned that the Brahmaputra River's very varying Sr and Nd isotope ratios were explained by the diverse origins of sediments in its drainage basin.

The $^{87}Sr/^{86}Sr$ ratios in the sediments of the Godavari, Krishna, and Pennar Rivers range significantly from 0.719 to 0.761 with $\varepsilon_{Nd}$ values ranging from −12.0 to −23.7 (Ahmad et al., 2009). The Pennar River basin has produced the highest $^{87}Sr/^{86}Sr$ ratios (ranging from 0.753 to 0.761) and the lowest $\varepsilon_{Nd}$ values (ranging from −21.7 to −23.7). This is a result of the old crustal rocks in the Pennar River basin, which include schist, granite, gneisses, and migmatite, chemically weathering (Ahmad et al., 2009). Medium- to high-grade Dharwar metamorphic rocks with high $^{87}Sr/^{86}Sr$ and low $\varepsilon_{Nd}$ values are among the several types of rocks found in the Pennar basin. According to Ahmad et al. (2009), the $^{87}Sr/^{86}Sr$ and $\varepsilon_{Nd}$ values of the Godavari sediments vary from 0.719 to 0.721 and − 15.3 to −18.2, respectively. The Godavari and Krishna Rivers' downstream sediments typically contain high $^{87}Sr/^{86}Sr$ ratios and low $\varepsilon_{Nd}$ values, which suggests that older crustal rocks may have a stronger impact on the Sr and Nd isotopic compositions than younger rocks like Deccan basalts. Additionally, the Peninsular Indian river sediments' noticeably high $^{87}Sr/^{86}Sr$ ratios and low $\varepsilon_{Nd}$ values may have had a substantial impact on the Sr and Nd isotopic compositions of the BoB sediments. According to a previous study by Krishnaswami et al. (1992), the erosional by-products of older rocks transported by significant river systems into the BoB may have had a significant impact on the evolution of seawater $^{87}Sr/^{86}Sr$.

### 3.4 Clay Mineralogy

In contrast, less smectite content in downstream sediments of these rivers may be due to absence of black cotton soil. Other clay minerals in lower Godavari sediments consist of illite (19–32%), kaolinite (15–26%), and chlorite (5–19%) (Table 1).

**Table 1** Clay mineralogical composition of sediments at lower, middle, and upper parts of Godavari River (Vuba, 2015)

| Station | Smectite % | Illite % | Kaolinite % | Chlorite % | S/I % | K/C % |
|---|---|---|---|---|---|---|
| *(a) Clay mineralogical compositions in <2 μm fraction of lower Godavari sediments* | | | | | | |
| 1 | 40.84 | 24.86 | 27.55 | 6.75 | 1.64 | 4.08 |
| 2 | 37.02 | 18.42 | 27.95 | 16.59 | 2.01 | 1.69 |
| 3 | 36.87 | 35.79 | 18.02 | 9.32 | 1.05 | 1.93 |
| 4 | 54.00 | 30.00 | 10.05 | 5.95 | 1.8 | 1.69 |
| 5 | 45.91 | 22.28 | 25.34 | 6.47 | 2.06 | 3.92 |
| 6 | 37.40 | 29.12 | 21.78 | 11.71 | 1.28 | 1.86 |
| 7 | 51.53 | 20.96 | 20.82 | 6.69 | 2.46 | 3.11 |
| 8 | 24.55 | 40.51 | 27.72 | 7.23 | 0.61 | 3.84 |
| 9 | 27.02 | 43.49 | 19.68 | 9.81 | 0.62 | 2.01 |
| 10 | 34.66 | 32.33 | 24.79 | 8.23 | 1.07 | 3.01 |
| *(b) Clay mineralogical compositions of lower middle Godavari sediments* | | | | | | |
| 30 | 37.5 | 24.6 | 19.3 | 18.6 | 1.52 | 1.03 |
| 31 | 34.7 | 32.2 | 21.5 | 11.6 | 1.08 | 1.84 |
| 32 | 29.1 | 25.5 | 26.3 | 19.1 | 1.14 | 1.38 |
| 33 | 48.9 | 29.0 | 16.3 | 5.7 | 1.69 | 2.84 |
| 34 | 50.4 | 19.5 | 14.5 | 15.7 | 2.58 | 0.92 |
| 35 | 47.1 | 19.3 | 23.1 | 10.5 | 2.44 | 2.19 |
| *(c) Clay mineralogical compositions in <2 μm fraction of upper Godavari sediments* | | | | | | |
| 19 | 85.2 | – | 8.9 | 5.9 | 1.51 | 94.1 |
| 20 | 90.6 | – | 5.3 | 4.1 | 1.29 | 95.9 |
| 21 | 90.3 | – | 4.1 | 5.6 | 0.72 | 94.4 |
| 23 | 88.6 | – | 4.2 | 7.3 | 0.57 | 92.8 |
| 24 | 85.9 | – | 5.7 | 8.4 | 0.68 | 91.6 |
| 25 | 88.6 | – | 7.3 | 4.1 | 1.77 | 95.9 |
| 27 | 88.3 | – | 7.6 | 4.1 | 1.86 | 95.9 |
| 29 | 89.5 | – | 5.6 | 4.9 | 1.13 | 95.1 |

District differences can be seen in the clay mineralogical compositions of sediments from the upper and lower sections of the Godavari and Krishna Rivers. The smectite content of upstream sediments is significantly higher than that of downstream sediments. In the higher sections of these rivers, the kaolinite content was observed to be extremely low, indicating the beginning of weathering under a semi-arid climate. Table 1 gives specifics on the clay mineral makeup of the Godavari deposits. High smectite concentrations seen in the higher portions of the Godavari and Krishna sediments may have resulted from the chemical weathering of black cotton soil and Deccan basalts. In contrast, the absence of black cotton soil may be the cause of the lower smectite content in the downstream sediments of these rivers. Table 1 lists the percentages of illite (19–32%), kaolinite (15–26%), and chlorite (5–19%) in the lower Godavari sediments.

Na, K, and Ca are primarily removed by surface fluid as ions during chemical weathering to produce primarily smectite clay mineral. The sedimentary load of the

Godavari and Krishna Rivers is anticipated to have a high percentage of smectite because these rivers flow through regions with black cotton soils and dense vegetation. The soils formed from Deccan Traps typically contain more than 80% smectite with low amounts of kaolinite and illite clay minerals (Rao, 1991). Deccan Traps are typically transformed by weathering to laterite or bauxite. Weathering of rocks like the khondalites, charnockites, gneisses, and granites may have produced clays like kaolinite, illite, and chlorite in the middle and lower sections of the Godavari and Krishna Rivers. As a result, variations in the source rock composition, level of alteration, type of vegetation, and regional topography can be used to explain variations in the relative abundances of clay minerals in upstream and downstream deposits.

## 4 Conclusions

Sediments from the upper portions of the Godavari and Krishna basins have geochemical features that point to weathering of basaltic rocks from the Deccan volcanic province as their primary source of origin. However, the chemical and mineralogical compositions of sediments from the lower reaches of these rivers indicate that they are mostly the result of the chemical weathering of felsic rocks in the surrounding area. Due to their co-occurrence in weathering-resistant minerals and/or the scavenging of titanium by iron oxy-hydroxides during the weathering process, $Fe_2O_3$ and $TiO_2$ have a strong connection in sediments. In comparison to their source rock, the amounts of $Na_2O$, $K_2O$, and MgO in upstream sediments are relatively lower. Significant scatter can be seen in the concentration of trace elements including V, Cr, Cu, and Zn in both upstream and downstream sediments. Due to their interaction with iron minerals or their sequestration with iron oxy-hydroxides, the concentrations of vanadium and nickel significantly correlate with $Fe_2O_3$. The mineralogy and level of source rock weathering have a significant impact on the REEs pattern. When sediments are weathered and transported, light rare-earth elements (LREEs) exhibit more fractionation than heavy rare-earth elements (HREEs). In upstream sediments, the chemical index of alteration varies considerably, showing significant geographical diversity in the rate of chemical weathering of parent rock. Higher CIA values, on the other hand, indicate a moderate to extreme chemical weathering environment in downstream sediments. High levels of smectite in upstream sediments appear to have resulted from the chemical weathering of black cotton soil and Deccan basalt. When compared to downstream sediments, upstream sediments have significantly less kaolinite, which indicates that basaltic rocks are beginning to weather in a semiarid climate.

## References

Ahmad, S. M., Padmakumari, V. M., & Babu, A. G. (2009). Strontium and neodymium isotopic compositions in sediments from Godavari, Krishna and Pennar rivers. *Current Science, 97*, 1766–1769.

Alexander, P. O., & Gibson, I. L. (1977). Rare earth abundances in Deccan Trap basalts. *Lithos, 10*, 143–147.

Andersson, K., Dahlqvist, R., Turner, D., Stolpe, B., Larsson, T., Ingri, J., & Andersson, P. (2005). Colloidal rare earth elements in a boreal river: Changing sources and distribution during the spring flood. *Geochimica et Cosmochimica Acta, 70*, 3261–3274.

Biksham, G., Subramanian, V., Ramanathan, A. L., & Grieken, R. V. (1991). Heavy metal distribution in the Godavari River basin. *Environmental Geology and Water Sciences, 17*, 117–126.

Cullers, R. L., Barret, T., Carlson, R., & Robinson, B. (1987). Rare earth element and mineralogical changes in Holocene soil and stream sediments: A case study in the Wet Mountains, Colorado, U.S.A. *Chemical Geology, 63*, 275–297.

Cullers, R. L., Basu, A., & Suttner, L. J. (1988). Geochemical signature of provenance in sand size materials in soils and stream sediments near the Tobacco Root Batholith, Montana, U.S.A. *Chemical Geology, 70*, 335–348.

Das, A., & Krishnaswami, S. (2007). Elemental geochemistry of river sediments from the Deccan Traps, India: Implications to sources of elements and their mobility during basalt-water interaction. *Chemical Geology, 242*, 232–254.

Das, A., Krishnaswami, S., Sarin, M. M., & Pande, K. (2005). Chemical weathering in the Krishna Basin and Western Ghats of the Deccan Traps, India: Rates of basalt weathering and their controls. *Geochimica et Cosmochimica Acta, 69*(8), 2067–2084.

Dekov, V. M., Subramanian, V., & Van Grieken, R. (1998). Chemical composition of suspended matter and sediments from the India sub-continent: A fifteen-year research survey. In *Recent trend in environmental biogeochemistry* (pp. 81–92). ENVIS Center, School of Environmental Sciences, Jawaharlal Nehru University.

Elderfield, H., Upstill-Goddard, R., & Sholkovitz, E. R. (1990). The rare earth elements in rivers, estuaries and coastal seas and their significance to the composition of ocean waters. *Geochimica et Cosmochimica Acta, 54*, 971–991.

Galy, A., & France-Lanord, C. (2001). Higher erosion rates in the Himalaya: Geochemical constraints on riverine fluxes. *Geology, 29*, 23–26.

Goldstein, S. J., & Jacobson, S. B. (1987). The Nd and Sr isotopic systematic of river water dissolved material: Implications for sources of Nd and Sr in seawater. *Chemical Geology, 66*, 245–272.

Goldstein, S. J., & Jacobson, S. B. (1988). Rare earth elements in river waters. *Earth and Planetary Science Letters, 89*, 35–47.

Goldstein, S. L., O'Nions, R. K., & Hamilton, P. J. (1984). A Sm/Nd isotopic study of atmospheric dust and particulates in major river systems. *Earth and Planetary Science Letters, 70*, 221–236.

Jeffery, K. L., Henderson, P., Subbarao, K. V., & Walsh, J. N. (1988). The zeolites of the Deccan basalt – A study of their distribution. Deccan Flood Basalts. *Memoirs of the Geological Survey of India, 10*, 151–162.

Kaotekwar, A. B., Ahmad, S. M., Satyanarayanan, M., & Krishna, A. K. (2019). Geochemical investigations in bulk and clay size fractions from lower Krishna river sediments, southern India: Implications of elemental fractionation during weathering, transportation and deposition. *Geosciences Journal*. https://doi.org/10.1007/s12303-019-0002-2

Kessarkar, P. M., Rao, V. P., Ahmad, S. M., & Anil Babu, G. (2003). Clay minerals and Sr-Nd isotopes of the sediments along the western margin of India and their implications for sediment provenance. *Marine Geology, 202*, 55–69.

Krishnaswami, S., Trivedi, J. R., Sarin, M. M., Ramesh, R., & Sharma, K. K. (1992). Strontium isotope and rubidium in the Ganga-Brahmaputra river system: Weathering in the Himalaya, fluxes to the Bay of Bengal and contribution to the evolution of oceanic 87Sr/86Sr. *Earth and Planetary Science Letters, 109*, 243–253.

Martin, J. M., & Meybeck, M. (1979). Elemental mass-balance of material carried by major world rivers. *Marine Chemistry, 7*, 173–206.

Milliman, J. D., & Meade, R. H. (1983). World-wide delivery of river sediment to the oceans. *The Journal of Geology, 91*, 1–21.

Nesbitt, H. W. (1979). Mobility and fractionation of REE during weathering of granodiorite. *Nature, 279*, 206–210.

Nesbitt, H. W., & Young, G. M. (1996). Petrogenesis of sediments in the absence of chemical weathering: Effects of abrasion and sorting on bulk composition and mineralogy. *Sedimentology, 43*, 341–358.

Rajamani, V., Tripathi, J. K., & Malviya, V. P. (2009). Weathering of lower crustal rocks in the Kaveri river catchment, southern India: Implications to sediment geochemistry. *Chemical Geology, 265*, 410–419.

Ramesh, R., Subramanian, V., Van Grieken, R., & Van'tdack, L. (1989). The elemental chemistry of sediments in the Krishna River basin, India. *Chemical Geology, 74*, 331–341.

Rao, V. P. (1991). Clay mineral distribution in the continental shelf sediments from Krishna to Ganges River mouth, east coast of India. *Indian Journal of Marine Sciences, 20*, 7–12.

Rengarajan, R., & Sarin, M. M. (2004). Distribution of rare earth elements in the Yamuna and the Chambal rivers, India. *Geochemical Journal, 38*, 551–569.

Ross, G. R., Guevara, S. R., & Arribere, M. A. (1995). Rare earth geochemistry in sediments of the Upper Manso River Basin, Rio Negro, Argentina. *Earth and Planetary Science Letters, 133*, 47–57.

Sensarma, S., Rajamani, V., & Tripathi, J. K. (2008). Petrography and geochemical characteristics of the sediments of the small River Hemavati, southern India: Implications for provenance and weathering processes. *Sedimentary Geology, 205*, 111–125.

Sharma, A., & Rajamani, V., (2000). Weathering of gneissic rocks in the upper reaches of Cauvery river, south India: implications to neotectonics of the region. *Chemical Geology, 166*(3–4), 203–223, ISSN 0009-2541, https://doi.org/10.1016/S0009-2541(99)00222-3

Sharma, A., & Rajamani, V. (2001). Weathering of charnockites and sediment production in the catchment area of the Kaveri River, southern India. *Sedimentary Geology, 143*, 169–184.

Sharma, A., Sensarma, S., Kumar, K., Khanna, P. P., & Saini, N. K. (2013). Mineralogy and geochemistry of the Mahi River sediments in tectonically active western India: Implications for Deccan large igneous province source, weathering and mobility of elements in a semi-arid climate. *Geochimica et Cosmochimica Acta, 104*, 63–83.

Sholkovitz, E. R. (1995). The aquatic chemistry of rare earth elements in rivers and estuaries. *Aquatic Geochemistry, 1*, 1–34.

Shynu, R., Rao, V. P., Kessarkar, P. M., & Rao, T. G. (2011). Rare earth elements in suspended and bottom sediments of the Mandovi estuary, central west coast of India: Influence of mining. *Estuarine, Coastal and Shelf Science, 94*, 355–368.

Singh, P. (2009). Major, trace and REE geochemical of the Ganga River sediments: Influence of provenance and sedimentary processes. *Chemical Geology, 266*, 242–255.

Singh, P., & Rajamani, V. (2001). REE geochemistry of recent clastic sediments from the Kaveri floodplains, southern India: Implications to source weathering and sedimentary processes. *Geochimica et Cosmochimica Acta, 65*, 3093–3108.

Subramanian, V., Dack, L. V., & Grieken, R. V. (1985). Chemical composition of river sediments from the Indian sub-continent. *Chemical Geology, 48*, 271–279.

Tang, J., & Johannesson, K. H. (2003). Speciation of rare earth elements in natural terrestrial waters: Assessing the role of dissolved organic matter from the modelling approach. *Geochimica et Cosmochimica Acta, 67*, 2321–2339.

Taylor, S. R., & Mclennan, S. M. (1985). *The continental crust: Its composition and evolution* (301p.). Blackwell.

Tripathi, J. K., Ghazanfari, P., Rajamani, V., & Tandon, S. K. (2007). Geochemistry of sediments of the Ganges alluvial plains: Evidence of large-scale sediment recycling. *Quaternary International, 159*, 119–130.

Vuba, S., Ahmad, S. M., Anipindi, N. R., (2015). Geochemical and mineralogical studies in recent clastic sediments from upper Godavari river in peninsular India. *Journal of the Geological Society of India, 86*(1),107–114, https://doi.org/10.1007/s12594-015-0286-4

# Sand Mining: A Silent Threat to the River Ecosystem


**Neeta Kumari, Soumya Pandey, and Gaurav Kumar**

## 1 Introduction

The survival of humanity depends on surface water resources (Chandra et al., 2014; Stajkowski et al., 2020). Throughout their length, the river bodies possess sufficient energy to weather, crush, and move the sediments (Gutiérrez et al., 2018; Otvos, 2020). Rivers gather and spread tons of sediment and crushed stones over their basin area on their way from source to submergence (Sengani & Zvarivadza, 2019). Higher lands typically include larger, coarser sediments, aggregates, or rocks, and lower lands contain finer sediments like sand, silt, and clay (Addis & Klik, 2015; Sathya et al., 2021). From their tributaries and surface rainfall-runoff flow, rivers receive an increased amount of sediments (Sathya et al., 2021). The chemicals and toxins that are added to this water through runoff, waste discharge, mine drains, and industrial effluents may or may not be abundant (Ndimele et al., 2021; Sathya et al., 2021). The sediments accumulate on the riverbed as a result of gravity acting on the sediment bulk or a reduction in flow velocity. Metals and chemicals frequently adhere to soil particles like clay and silt. Given their coarse, naturally refined structure and high mineral content, the deposited sand (both coarser and finer) is a great source of soil material used for building, electroplating, ceramics, glass, etc. As a result, sand is frequently extracted from river beds and banks for a variety of uses (Meng et al., 2021).

According to Abidin et al. (2018) and Doloksaribu et al. (2020), sand mining is the process of extracting sand that has collected over many years as a result of erosion and sedimentation. According to Subha Dharani et al. (2010), the extraction is typically done from river bottoms, ocean beds, dunes, and beaches. The

N. Kumari (✉) · S. Pandey · G. Kumar
Civil and Environmental Engineering, Birla Institute of Technology, Mesra, Ranchi, Jharkhand, India



S. Kanhaiya et al. (eds.), *Rivers of India*,
https://doi.org/10.1007/978-3-031-49163-4_6

contemporary economy is thought to be built on elements like sand, sediment, and gravel (McCarroll et al., 2020). Sand, crushed stone, and gravel make up the biggest volume of solid material mined or removed globally, according to the United Nations Environment Program (UNEP-GEAS, 2014; Peduzzi, 2014). Especially the rate of extraction, particularly in developing countries, is between 32 and 50 billion. The construction industry or infrastructure sector uses these solid materials most frequently, particularly alluvial or eolian sand, as a component of concrete, mortars, plasters, in roofs, grouts, paint, skid resistance surfaces, asphalt, stucco, etc. (Surendar et al., 2021; Cavaleri et al., 2017; Gencel et al., 2021). According to Kumar et al. (2021) and Vandana et al. (2020), pure sand (quartz) is also a crucial component for many other sectors, including electroplating, glass, ceramics, glass production, metal casting, steel and foundries, sanitary ware, tiles, packaging material, water purifiers, and oil and gas recovery. Throughout this chapter, "sand mining" refers to any type of river soil product, regardless of size.

Sand mining is typically allowed in accordance with government-issued tenders, but due to a lack of adequate legislation, oversight, and evaluation, illicit sand mining takes place on a large scale in practically all major and minor river bodies (Ashraf et al., 2011). Construction activities are one of the main causes of illegal sand mining (Damodhara Reddy et al., 2020; Sathya et al., 2021). The river-mined sand is preferred by the construction industry because it has qualities that are almost ideal for its procedures, such as concrete mix and asphalt, cement strength, plasters, filling basements and under floors. Sand that is inexpensively accessible aids in reducing building costs, while jeopardizing the water body's ecology (Kaufmann, 2020). Sand beds are also home to minerals such rutile, ilmenite, and zircon (Huo et al., 2021). These minerals, which are a significant source of zirconium and titanium, are less accessible due to sand extraction (Fitzpatrick & Chittleborough, 2018). This has an impact on the numerous businesses, including electroplating and aircraft that use these minerals as a primary raw material. A later portion of the chapter goes into greater detail about these difficulties.

Sand mining has a negative impact on the river environment in addition to the economy. Sand mining requires the continual movement of ships and equipment on the riverbed and channel while sand is being extracted. Due to this, aquaculture is harmed (Xu et al., 2020), the coast erodes, breeding grounds are harmed, there is excessive turbidity, and minerals and soil particles that are frequently enriched with heavy metals in water are moved around (Wang et al., 2012). The sandpits that have been made, however, are like blind spots with an undetermined depth. Residents have reportedly died after falling into the pit (Ramya & Kumari, 2020). When the rate of extraction far outpaces the rate at which the layers of the sand bed are formed, sand mining becomes problematic. Sand mining has significantly altered the riverine environment and its sediment layers, according to the Geological Survey of India (GSI) (Chen et al., 2018). The World Wildlife Fund (WWF) reported in 2018 that numerous microbial species had died or become extinct as a result of sand

mining (WWF, 2018; Arsyad et al., 2020; Atejioye & Odeyemi, 2018; Chandra et al., 2014; Juen & De Marco, 2011). This process immediately influences the river morphology, alteration of channel width and depth, explosion of flood plains, pollution from the plume and ship oil, and increased turbidity and pH. Intake structures, water retention structures, and bridge piers are also damaged, endangering the stability of these structures (Ndimele et al., 2021).

In recent years, environmental impact assessment tools and techniques have made it easier to understand the situation (Elmayel et al., 2019). Geographic information systems (GIS) and remote sensing are two examples of these essential newly developed tools that aid in the visual or geospatial analysis. The data from satellites such as LANDSAT, Modis/Aqua, and VIIR, are freely provided by government organisations such as USGS, BHUVAN, and NASA. At the same time, their processing can be easily done through Geographic information system (GIS) based software such as ArcGIS, Quantum-GIS (QGIS), SAGAGIS, JUMPGIS, AUTOCAD for the assessment of accessible sand resources and loss due to extraction in the variable time frame (Upgupta & Singh, 2020; Wang et al., 2019). Additionally, evaluations of the region's flora, fauna, sediment, and accessible contaminants (Eslamian et al., 2020; Ahamad et al., 2020) provide a clear picture of the damage that sand mining has caused to the river water ecosystem (Filho et al., 2021). Additional validation and prediction can be performed using statistical tools like multivariate statistics principal component analysis (PCA), correlation coefficient analysis, regression analysis, cluster analysis, etc. (Khadija et al., 2021; Mishra et al., 2021; Pandey et al., 2021) and neural networking models using the soil and water assessment tool (SWAT), artificial neural networking (ANN), convolutional neural network (CNN), fuzzy logic, etc. (Liang et al., 2020; Zhang et al., 2017).

Sand is also believed to be a plentiful resource that will never run out by miners, including both professionals and villagers (Mahadevan, 2019). They support the exploitation since they see it as a cheap source of revenue. Illegal sand mining has been reported to be a significant problem in nations like China and India (Bhattacharya et al., 2019; Park et al., 2021). Correct resource estimation and legal usage become much more challenging in the absence of monitoring and assessment (UNEP-GEAS, 2014). According to reports, Indonesia is experiencing significant losses along its international coastline borders as a result of ongoing sand mining (Goh, 2019). The process and motivations behind sand mining have been reviewed in this chapter, along with how it affects various elements of the river ecology (Ali, 2019). The use of contemporary approaches and their function in assessment and monitoring have also been discussed. This chapter aids in raising awareness of the underappreciated damage that this issue is causing to riverine biomes, which is made worse by the villagers' and the government's deliberate ignorance of the issue.

## 2 Factors Affecting Sand Mining

### *2.1 Civil Construction: The Major Driver of Sand Mining*

Any country's economic growth has a major impact on reducing poverty, and this is especially true for infrastructure development. The cost of labor and raw materials determines the majority of building costs (Yue et al., 2019). Sand and aggregate are the most frequently and widely utilized raw materials; they make up over 80% of concrete roads and 90% of asphalt pavements. Even greater quantities of sand and aggregates are needed as the raw material for large projects like dams, retaining structures, high rise buildings, embankments, coastline development, land reclamation, etc. (Chakrabarti, 2019; Okeke et al., 2021; Sahoo et al., 2021). Depending on the design mix used during construction, every ton of cement would require approximately eight times more sand and aggregate for a mortar mix in a traditional building (UNEP-GEAS, 2014). This alone can provide a sense of how heavily the building industry depends on sand and aggregate as a source of raw materials. Sand and aggregates are mined annually at a global rate of around 50 billion tons, of which 70–80% is river products (Tsymbarovich et al., 2020; UNEP-GEAS, 2014) (Fig. 1).

A boom in the building industry has resulted from Asia's rapid economic growth due to urbanization and population change. Sand consumption is currently expanding quickly in China and India, which is encouraging illegal mining. The Ganga has changed its path in the last 30 years, moving 5–6 km away from Patna. Sand mining and brick kilns have been two of the main causes (Datta & Litt, 2020; Pathak et al.,


**Fig. 1** Properties of river sand that make it ideal for construction

2018; Singh et al., 2002). China's construction industry has had a tremendous boom, and it is now worth roughly 1049 billion US$ dollars (Jiang et al., 2021). It represents 20% of the world's building expenditure, and by 2030, it is anticipated to spend about 13 trillion US$ dollars on infrastructure. Sand is needed for building in Sri Lanka on an annual basis in the range of 7–7.5 million cubic meters (Piyadasa, 2011). After the tsunami of 2004, construction for rehabilitation is at its peak. According to a UN report (Hackney et al., 2021; Park et al., 2021), nations like Cambodia, Vietnam, and Indonesia have a significant supply of aggregates (fine and coarse) from legal and illicit mining, particularly for economic development and land reclamation projects. LikNilwala and Ginganga rivers in Sri Lanka (Piyadasa, 2011), Poyang Lake in China (Teng et al., 2021), Sa'dang River in Indonesia (Arsyad et al., 2020), Ganga in India, and others are some of the commonly mentioned surface water bodies that have suffered greatly. Due to its idealistic qualities, the construction industry prefers river sand (Surendar et al., 2021). These kinds of sand hardly need any preprocessing, such as washing, crushing, etc., as rivers naturally clean and crush the fine aggregate (sand) as they go along their courses. According to Ben Othman et al. (2019), river sand has a better shape (rakish) and a different mineral makeup, and it works better in concrete than other types of sand (Soutsos et al., 2011). Due to the high quality of the fine aggregate, the compressive strength of the concrete mix is likewise strong (Cavaleri et al., 2017). The material is easily accessible and even cuts construction site costs, particularly for projects near riverbodies. Sand is utilized in a variety of other industries besides building, including water filtration, plastics, glassware, dams, oil extraction, electronics, etc. (Filho et al., 2021).

## 3 Formation and Characteristics of River Sand

Hence, under the action of gravity (Zhao et al., 2018), coarser particles being heavy are loosely packed and usually found on the highlands while the finer particles like small stones and coarser sand are found downstream, whereas fine sand, silt, and clays are found in the plains (Pal & Debanshi, 2018).

Different types of weathered boulders from inland are hauled and transported throughout the river to generate sand or river soil (Fig. 2). While the sediment bed depends on the size and structure of the sediments, sediment movement is influenced by the grain size, mobility, and transport rate. Due to the effects of gravity and the interactions of various particles during the movement of sediments under stream hydraulics, a natural gradation is present (Bhattacharya et al., 2019). Numerous point and non-point sources provide additional silt to the river body (Varekar et al., 2021). Additionally, the irregular terrain of the river channel (Arabameri et al., 2018) leads to significant soil abrasion and weathering, which are transmitted throughout the river (Doloksaribu et al., 2020). As the river's flow intensity drops, heavier soil and rock particles are deposited (Gutiérrez et al., 2018; Kaufmann, 2020; Otvos, 2020). The finer and lighter particles flow along the water to the lower

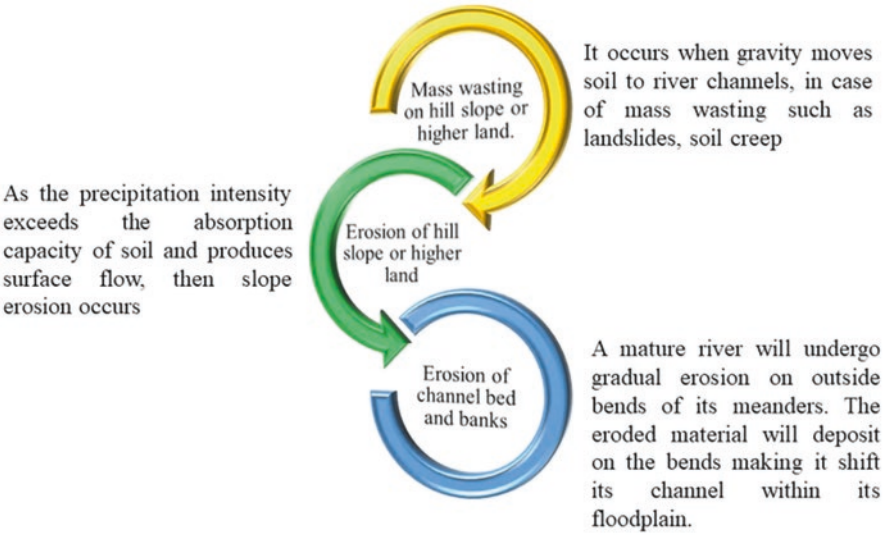


**Fig. 2** Process of sand formation

or downstream section, and the process keeps happening for decades (Arsyad et al., 2020; Ma et al., 2020). As a result, finer particles like small stones and coarser sand are typically found downstream, whereas fine sand, silt, and clays are found in the plains (Pal & Debanshi, 2018). This is because under the influence of gravity, coarser particles are heavy and loosely packed (Zhao et al., 2018).

In the monsoon season, surface runoff transports pollutants (such as metals, plastics, chemicals, organic compounds, heavy metals, etc.) from point source (Aydin et al., 2021; Ranjith et al., 2019) and nutrients (such as fertilizers, agriculture waste, organic chemicals, pesticides, etc.) as well as soil fines from non-point sources to the river bodies and its tributaries (Jaiswal & Pandey, 2019; Pavlidis & Tsihrintzis, 2018). By settling with soil fines on the surface, contaminants and nutrients added to the soil contaminate it. Therefore, the monsoon season is another time when soil masses are eroded (Park et al., 2021). Additionally, this adds sediments around everyone. However, erosion is influenced by the soil's shear strength, the amount and length of rainfall, and the slope (Gutiérrez et al., 2018; Zhao et al., 2018). A sufficient shear strength would prevent soil from easily separating from its parent source. Despite this, there is a higher need for mineral-rich, well-formed sand particles (Aminuddin et al., 2021; Miheretu & Yimer, 2018).

Quartz and silica make up the majority of the sand and sediments found in river bodies (Chandrasekaran et al., 2021). Research has also frequently identified minerals such feldspar, clay (Kaolinite, gibbsite), (Hussain & Ali, 2021), carbonate, organic carbon, calcite, zircon, aragonite, magnetite (Usman et al., 2021), and kyanite. Modern tools such as X-ray diffraction (XRD) (Deb & Sahu, 2010; Omar et al., 2021), scanning electron microscope (SEM) (Shalini Tirkey et al., 2013), field emission scanning electron microscopy (FESEM) (Benchaa et al., 2021; Omar

**Table 1** Properties of fine (sand) and coarse aggregate as per Indian Standard code

| IS code | Properties |
|---|---|
| (IS 383:2016) | Characteristics of sediments |
| (IS 2386 (Part 1): 1963) Fine aggregate (size between 4.75–0.075 mm) | Cohesion, rakish and coarser features, sharp grains, chemically inert, strong, and durable. It should be free from organic matter, hygroscopic salt, silt, and clay |
| (IS 2386 (Part 1): 1963) Coarse aggregate (size >4.75 mm) | The material should be chemically inert, durable (resistant to weathering), free of impurities, organic matter, salts, silts, and clays |
| (IS 2386 (Part 4):1963) | In general, aggregates (fine and coarse) should have adequate mechanical strength, determined by aggregate impact value, aggregate abrasion value, and aggregate crushing value |
| (IS 2386 (Part 5):1963) | The material should have adequate soundness |

Source: Literature survey

et al., 2021), etc. are used to examine the mineralogy of soil. By presenting peaks, this equipment aids in identifying the component that is present in the silt or soil. Every compound has a peak, making it simple to distinguish between them. Use of inductively coupled plasma mass spectroscopy (ICP-MS) (Bibak et al., 2020; Leventeli & Yalcin, 2021), inductively coupled plasma optical emission spectrometry (ICP-OES) (Gallo et al., 2018; Kumar & Acharya, 2021; Kumar et al., 2017), etc. is done by digestion of soil and sediments (wet digestion mostly using aqua regia) and then studying the number of metals present in the sediments. According to the Indian Standard Code, Table 1 presents the characteristics of fine and coarse aggregate.

The actual query is why, given the quantity of different forms of sand, such as desert sand, marine or sea sand, etc., they are not more popular than other varieties of river sand. The features and development of sand (Damodhara Reddy et al., 2020; Kondolf, 1994; Okur & Erturaç, 2021; Tamura et al., 2020) provide the solution to this query. For instance, materials used in the construction industry should have the necessary geotechnical characteristics, such as being pure, coarser or rakish, clean, durable, and having high mechanical strength, permeability, and shear strength (Donovan & Monaghan, 2021; Rezaei et al., 2009; Yoobanpot et al., 2020). They should also be compacted. If the sand is coarse, it enhances the workability of concrete and produces greater friction and cohesiveness (Evans et al., 2022; Li et al., 2015). Sand particle form impacts particle arrangement and density. Unlike desert or marine sand, river sand has several characteristics. Sand from deserts has a very fine structure (Gencel et al., 2021). They have a more open structure due to their rounder and finer shape. Due to their limited bearing capacity, inability to form linkages or cohesive bonding in concrete mixtures, and lack of strength, they do not contribute to the strength of final concrete structures (Diago et al., 2018; Evans et al., 2022). Furthermore, the chemical makeup of desert sand is difficult to determine, thus preparation may be necessary before usage. The same is true of marine

sands. They are exceedingly fine for any engineering purpose and have an unknown soil chemical composition, but they are typically high in ion carbonates, sulfates, chlorides, etc. (Sathya et al., 2021; Tamura et al., 2020). The salts in them react with the concrete and diminish the strength (compressive and tensile) of the concrete by causing fractures, shrinkage, and corrosion in the concrete and reinforcement, respectively (Diago et al., 2018; Kaufmann, 2020).

## 4 Monitoring of Sand Mining Activities

Although mining has greatly harmed the ecosystem, nature still survives for the sake of economic development (Chauhan, 2010). Legal sand mining generates billions of dollars in revenue each year in the United States, while sand mafias mostly extract other riverine products illegally in nations like China and India (Mahadevan, 2019; UNEP-GEAS, 2014). Although numerous regulations have been passed to regulate unlawful sand mining operations, nothing glaring has ever surfaced.

India (Sathya et al., 2021; Singh et al., 2018), Indonesia (Ali, 2019; Doloksaribu et al., 2020), and other developing nations have experienced this issue more frequently since residents support sand mafias and government authorities are unable to keep the situation under control. Since sand is believed to be infinitely available and there is a great lack of understanding regarding the damage it does to the river ecology (Koehnken et al., 2020), illegal sand mining is not always a terrible solution when faced with poverty (Okur & Erturaç, 2021). This results in losses to the socio-economic system as well as the environment (Xie et al., 2020; Zheng et al., 2022). Dredging and an open pit are used in the mining of sand (Duan et al., 2019; Tetsopgang et al., 2020). To collect the sand from rivers, open pits are dug, and over time, these pits grow into steep slopes with unknown volumes (Koehnken et al., 2020; Xie et al., 2020). The scour that was produced moved upstream and downstream in the stream. According to Angillieri (2012) and Hackney et al. (2020), the process alters the river bed, the banks, the slopes of the bed, the aquatic ecosystem, the breeding grounds, the erosion, and the flooding. A lack of monitoring and evaluation data has been posing a barrier to the rigorous rules that are needed to be designed and enacted in order to manage the illicit mining activities (Duncan & De Vries, 2018).

Recently, the assessment and monitoring of sand mining activities have been made easier because of the use of remote sensing and geographic information systems (GIS). A summary of a few of these works can be found in Table 2. Geospatial study of the land and water surfaces is aided by data from satellites like Modis, Sentinel, Landsat, etc. (Bagwan & Gavali, 2021; Shrestha et al., 2019; Sun et al., 2021). Ship movement increases the quantity of pits, amount of sedimentation, slope of the river bed, etc. (Tamura et al., 2020). This makes it possible to monitor all of the actions occurring in the area. The change in land use and land cover, water quality and quantity, slope, streamline order, etc. can all be determined from spectral indices such as (NDWI) normalized difference water index (Al Kafy et al.,

**Table 2** Recent reported research on sand mining activities using GIS and satellite data

| Year | Methodology | Findings | References |
|---|---|---|---|
| 2018 | The researchers developed the Web GIS application to obtain the geographical location of mining sites in Lumajang | Excessive damage to the shoreline was found due to mining at WacoPecak beach, whereas agricultural land was also affected as the sea water entered the farms. Noise pollution and vehicle pollution were also found significantly with the movement of the vehicle from the chemical sites | Nurhasan and Saputra (2018) |
| 2018 | Using Landsat 5 thematic mapper data and 8 OLI data were used and processed using ALOS PALSAR and tasseled cap transformation (TCT) using the SAR interferometry (InSAR) method | The TCT AND InSAR method showed 352.92 ha were mined, and in the 7-year study, period deformation has been up to 7 m | Indriasari et al. (2018) |
| 2019 | A study on Hongze Lake of China used the satellite data from MODIS/aqua, LANDSAT, and VIIRS day/night band nighttime light | The study revealed that the mining activities started around February 2012, and a massive increase was seen in terms of the monthly average in 2016. Also, the change in the suspended particulate matter was found to be consistent with the movement of the vessel | Duan et al. (2019) |
| 2019 | A study on the Nzhelele River in Limpopo province, South Africa, has been done to study the sand mining impacts on the riverine environment identified the adverse factors. The study was done based on data obtained from field observation, analysis of water and soil quality, particle size analysis, survey (questionnaire), and GIS data obtained from LANDSAT (ETM+) and NDVI | Research demonstrated that sand mining has been contributing to erosion, worsening of water quality, reduction in grassland and agricultural land | Sengani and Zvarivadza (2019) |
| 2020 | In the Swarnamukhi watershed, in the Chittoor district of Andhra Pradesh, the sand mining activities were mapped by identifying mining sites in the region. The sites were identified using GIS tools like ArcGIS and Google Earth Engine (GEE) | The study found that river mining activities have led to the deterioration of groundwater and the riverine environment. Similarly, the river morphology is studied using GIS tools and software, with help of satellite and GEE data | Reddy et al. (2020) |

(continued)

**Table 2** (continued)

| Year | Methodology | Findings | References |
|---|---|---|---|
| 2020 | A study on Sa'dang River, Indonesia, studied the change in river morphology, in varying years (2006, 2014, 2017, and 2019) impacted by sand mining activities. The authenticity of the satellite data is obtained by observing the ground truth from field data. River morphology can also be studied using the various spectral indices, like Normalized Difference Vegetation Index (NDVI), Normalized Difference Water Index (NDWI), etc. | The study found that channel width is inversely proportional to the river water body in case the sediment deposits decrease. The most authenticated study of the impact of sand mining on river morphology and ecosystem should generally include field study along with experimental and software-based analysis. These spectral indices help in identifying the quality of water, surrounding vegetation, erosion of banks, sedimentation in downstream areas, pollution, reduction in farmlands, etc. through a spatial-temporal analysis, identifying the change patterns in river morphology, water flow pattern, sand mining zones, ecological deterioration, air, land, and water pollution levels can all be monitored | Arsyad et al. (2020) |
| 2021 | The study on slope stability of river morphology was done using UAV's multitemporal image. In the study, aerial photography was carried out with UAVs. DEM (digital elevation model) was developed by processing the multitemporal aerial images for slope geometry analysis, while the field sampling was done to obtain soil samples for experiments like shear parameters and bulk density | The data was analyzed using the Bishop slope stability method, and the slopes were found unstable | Darmajati et al. (2021) |
| 2021 | A study on dams of Cambodia based on the Mekong River revealed that the volume of the lake has decreased in a four-decade period (1980–2018) and the water storage has also decreased | The shrinkage of the lake has been attributed to the intensification of sand mining which is promptly done for construction, landfilling, and export of sand to other areas | NG and Park (2021) |

Source: Literature survey

2020; Serrano et al., 2019), (NDVI) normalized difference vegetation (Hamzah et al., 2020), (NDBI) normalized difference built-up index (Halder et al., 2021; Nguyen et al., 2019), (NDMI) normalized difference built-up index, LULC (Kamaraj & Rangarajan, 2021), etc. Use of unnamed aerial vehicles (UAV) (Abidin et al., 2018; Nowak et al., 2019) is also preferred by many researchers as they give a clearer picture of the area with a short range.

For instance, a study conducted in 2006 on the Vembanad lake and the Chalakudy, Periyar, and Muvattapuzha rivers, which are home to Kochi, Kerala, India, revealed that approximately 11.527 million tons of sand were mined annually (8.764 in-stream and 2.763 floods plain sand) (Padmalal et al., 2008; Sreebha & Padmalal, 2011). This rate of extraction was concerning because it would permanently harm the hydraulics of the river and the stability of the channel because the rate of replenishment is much lower than the rate of extraction (Kondolf, 1994; Sreebha & Padmalal, 2011). Table 2 displays studies that are comparable. Due to their greater capacity for extraction, modern technologies like power shovels, draglines, dredging boats, suction pumps, and others can quickly create instability to banks and coastlines (Duan et al., 2019; McCarroll et al., 2020). Furthermore, the depths of the pits dug and their locations are known, although sand mining does make water more murky. As a result, this poses a challenge for the inhabitants, particularly those who depend on river water for everyday needs. For instance, in India, sand mining caused 193 fatalities between 2019 and 2020 (Arulbalaji & Padmalal, 2020; Ghosh & Jana, 2021).

## 5 Impact of Sand Mining on the River Ecosystem

### *5.1 Morphology and Sediment Beds of Rivers*

Sand mining generally causes serious ecological and socioeconomic problems in the area where it occurs (Fig. 3). In recent decades, several rivers have lost or altered their course (Singh et al., 2018). Mining has a direct impact on the physical

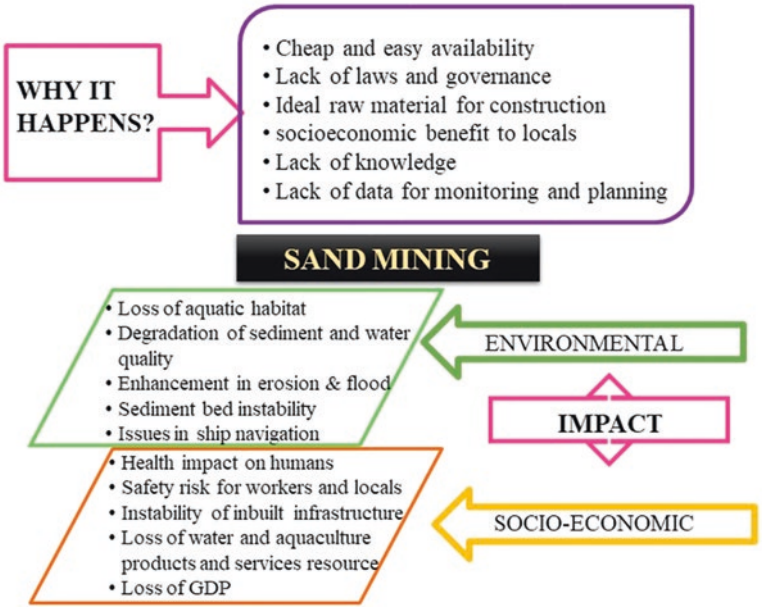


**Fig. 3** Environmental and socioeconomic impact of sand mining in river biomes

composition of the soil (Uniyal et al., 2020). As mining takes place, it affects the physical structure and chemical composition of the sediment beds, which fractures the layering of the sediments and causes chemicals to leach onto the surface effects (Zheng et al., 2022). Minerals are released after the silt material is broken down (Zhang et al., 2018). As a result, the pH is changed, the turbidity rises, and the water quality is disrupted also; increased turbidity prevents sunlight from penetrating the bed and renders benthic organisms blind (Bhattacharya et al., 2019). Aquatic vegetation succumbs to the lack of sunlight. Additionally, aquatic species may die if they swallow metals released in the water, especially heavy metals (Ahamad et al., 2020; Madhav et al., 2018). If taken in excess by living things, heavy metals have the potential to be lethal; they also have the tendency to bioaccumulate and biomagnify throughout the food chain (Pandey et al., 2021; Sarath & Puthur, 2021). Numerous incidences of heavy metal poisoning of aquatic life in zones have been documented globally. Sand mining has significantly altered the properties of river beds and sediment morphology such as channel widening, channel narrowing, variations in sediment transport, channel hydraulics, flow intensity, flood control, and channel incision (0.5–30 m reported channel incision) (Marco et al., 2021; Padmalal et al., 2018; Sreebha & Padmalal, 2011).

One of the main reasons for this change is the usage of heavy machinery, which tends to seriously disrupt the infrastructure in coastal areas, water intake structures, and shoreline protection (McCarroll et al., 2020; Tamura et al., 2020). Sand mining has a more detrimental effect in basins with older geomorphology (Evans et al., 2022). For instance, Himalayan river basins are more susceptible to erosion than Deccan plateau river basins since the mountains are younger (Das et al., 2021; Dimri et al., 2021; Purushothaman & Chakrapani, 2007). A few centimeters of soil strata are developed by rivers over ages. The formation rate and the mining rate ought to work together. According to research, the harm done to the river environment persists long after the mining is stopped (Sathya et al., 2021). Sand mining has an impact on groundwater as well since it frequently dehydrates the land and prevents groundwater recharging (Masindi et al., 2021; Sahoo et al., 2018). Additionally, the region has increasing water stress as a result of the declining water table. River sand mining is more prevalent in the midlands and lowlands (Sreebha & Padmalal, 2011). Sand mining by hand is more prevalent in the middlelands, where Bar skimming is employed. Pit excavation is more common in lowlands, where it is done both manually and mechanically (with high power suction pumps). Due to a sixfold increase in mining activity compared to lowlands, the midlands are more affected than lowlands (Padmalal et al., 2008; Sreebha & Padmalal, 2011). The ecosystem of the river has been harmed by both pit excavation and bar skimming. Comparatively speaking, bar skimming causes less harm than an excavated pit. The pits resemble blind spots with undetermined volume and position because of increased turbidity, which also affects visibility. Locals drowning incidents are becoming more frequent.

### *5.2 Impact on Water Quality and Aquatic Life*

Aquatic biomes and water quality are significantly impacted by sand mining. According to Abidin et al. (2018) and Ben Ameur et al. (2019), pollution from oil spills and vehicle smoke are results of ships' constant movement. All year round, ships and boats operate (Teo et al., 2017). Consequently, pollution and turbidity are year-round issues. Additionally, the movement of ships causes significant damage to the sediment bed and banks (Balogun et al., 2020). Aquatic creatures breed in sediment beds, but ongoing turbulence damages the surface, making breeding nearly impossible (Duan et al., 2019; Kondolf, 1994). Even the extraction equipment themselves compact the sediment bed and eliminate the habitat for plant development and spawning (Safiur Rahman et al., 2021). There have been numerous instances where sand mining has caused the region's aquaculture to fail and fish species to disappear (Thakur et al., 2020). The socioeconomic growth of the inhabitants who depend on aquaculture for their subsistence is also impacted by this, which not only damages the river ecosystem (Ouma et al., 2020). Fuel exhaustion lowers water quality in the area by causing metal and surface pollution (Deng et al., 2020). The oil spill prevents sunlight and oxygen from reaching the water's surface, which lowers the amount of both in the body of water. Aquatic life, including both plants and animals, perishes as a result (Balogun et al., 2020; Saha et al., 2021).

Heavy metal pollution is a different type of contamination (Nazneen et al., 2018; Nazneen & Raju, 2017). Heavy metal has a propensity to bind to soil particles. Although there are heavy metals in the sediments from geogenic sources, more anthropogenic activity in the watershed causes a greater influx of contaminants (Nazneen et al., 2019; Zhang et al., 2018). However, sand mining creates turbulence in the river water, which causes soil fines and heavy metals to start rising to the top (Aminuddin et al., 2021; Marco et al., 2021). The pollutant often settles down on the sediment bed. These heavy metals are consumed by aquatic plants and animals alike (Delang, 2018). According to Nodefarahani et al. (2020), the main issue with heavy metals is their propensity to biomagnify, accumulate throughout the food chain, and be hazardous to all species of living things. The riverine environment continues to be harmed by the heavy metal poisoning as a result of the flowing water. Given all the problems, it is essential to sustain both the pace of replenishing and mining (Hackney et al., 2020).

## 6 Remediation Alternatives

The extraction and use of sand in many industries has been reduced, thanks to the efforts of scientists from all over the world who are searching for innovative and cutting-edge materials and methods. Sand is mostly used in the building industry, as is obvious. The biggest consumer and producer of it both are China. However, in recent years, different materials have been utilized in concrete in place of sand,

including M-sand, quarry rock dust, recycled sand and aggregate, coconut shell, etc. The majority of these tests have produced fruitful outcomes. These waste materials, which pollute water, air, and soil, can be appropriately disposed of in the construction industry in an affordable and environmentally responsible way. Additionally, this will lessen the burden on landfills and forbid other ecological problems like leaching and water resource poisoning. Quarry stone dust boosts the durability of concrete by 10%, according to a study on the usage of quarry dust as a sand substitute. Quarry dust was produced in large quantities as a by-product of the aggregate industry and also produces significant air pollution and large carbon emissions. According to Indian Codal requirements, hard granite rock is crushed to a fineness of 4.75 mm to create M-sand, also known as manufactured sand. In areas without access to river sand, M-sand works well as a replacement for fine aggregate in concrete. The qualities of concrete made with M-sand and electronic waste sand (E-sand) were investigated by Mane et al. (2020) by adjusting the proportion of replacement from 0% to 40%, with an increment of 10%. The research revealed that the highest strength in concrete was achieved when 20% of the M-sand was replaced by E-sand. For the purpose of replacing aggregate in concrete mixtures, numerous such alternative material combinations have been used (Table 1).

Many countries, including the USA and China, have realized the potential of "crushed rock" as a substitute for aggregate in concrete. However, the main issue is that it would take a lot of manpower and money to blast, mine, and process rocks into construction-ready aggregates. For both small and large building projects, this might not be suitable. Additionally, not every nation has access deposits of rock bed with a high compressive strength and the right chemical composition. Additionally, concerns with the environment like noise, air, and water pollution, leaching, and the loss of valuable topsoil are also brought on by the extraction of rock. The many pieces of mining and extraction equipment would need a comparable amount of expensive, still insufficiently supplied electricity.

## 7 Summary

Resources made of sand are precious natural resources. The majority favor river sand over other available sand types including desert and coastal sand because of its greater quality. Sand is an expensive and scarce resource. It is readily available, has a wide range of qualities, and serves as the raw material for numerous sectors including building, glass, electroplating, etc. As a result, sand mining has started and grown rapidly during the past few decades. The effects of sand mining are now quite obvious, particularly in growing nations like China and India. Sand resources have been heavily exploited due to the growth of sprawling, enormous urban areas. The origin and effects of sand mining on the riverine environment were identified in this study. Sand mining operations disrupt sediment flow and unbalance sediment deposition brought about by years of riverine system erosion and sedimentation. The riverbed was altered as a result of excessive sand mining, altering the river's path and contributing to bank erosion. Saline water results from rivers and river

mouths being deeper. Additionally, it harms fisheries productivity, habitats for wildlife, and timber resources in rivers. The aquifer's thickness decreases as the sandbed is reduced. Overall, the harmonious operation of many elements of the riverine ecosystem is a prerequisite for the negative effects of mining. Changes in river morphology and sediment properties, such as channel incision, river channel narrowing and deepening, bank erosion, slope instability, etc., were shown to be some of the negative effects.

The study revealed that there is an immediate need for monitoring the sand mining activities and taking strict actions to conserve our environment. The field study is also required for better assessment and detailed monitoring of sand mining activities based on which region-specific remediation and awareness programs could be developed.

Previously, it was challenging to monitor and evaluate sand mining activities, but the application of GIS and remote sensing techniques has provided a distinct benefit. Various geographical features or geological features can be easily researched with the aid of instruments like satellite data processed from MODIS, LANDSAT, BHUVAN, Google Earth Engine, etc. UAVs and spectral indices like NDVI, NDWI, LULC, etc. have been discovered to be frequently employed in evaluating the sand mining operations in the river. Use of additional materials, such as M-sand, quarry stone dust, and rock crushing, is another option for situational remediation. Also suggested were topics like e-waste. The study showed that stringent measures must be taken to protect our ecosystem and there is an urgent need to monitor sand mining activities. To evaluate and track the sand mining activities, including remote sensing data and GIS, a comprehensive field study is needed. Practical research to acquire information and awareness campaigns will have better results in involving concerns people.

**Acknowledgments** The authors acknowledge Department of Civil and Environmental Engineering, Birla institute of Technology for giving all the kind of support in drafting this chapter.

## References

Abidin, M. Z., Kutty, A. A., Lihan, T., & Zakaria, N. A. (2018). Hydrological change effects on Sungai Langat water quality. *Sains Malaysiana, 47*(7), 1401–1411. https://doi.org/10.17576/jsm-2018-4707-07

Addis, H. K., & Klik, A. (2015). Predicting the spatial distribution of soil erodibility factor using USLE nomograph in an agricultural watershed, Ethiopia. *International Soil and Water Conservation Research, 3*(4), 282–290. https://doi.org/10.1016/j.iswcr.2015.11.002

Ahamad, A., Raju, N. J., & Madhav, S. (2020). Trace elements contamination in groundwater and associated human health risk in the industrial region of southern Sonbhadra, Uttar Pradesh, India. *Environmental Geochemistry and Health, 42*(10), 3373–3391. https://doi.org/10.1007/s10653-020-00582-7

Al Kafy, A., Rahman, M. S., Al Faisal, A., Hasan, M. M., & Islam, M. (2020). Modelling future land use land cover changes and their impacts on land surface temperatures in Rajshahi, Bangladesh. *Remote Sensing Applications: Society and Environment, 18*(April), 100314. https://doi.org/10.1016/j.rsase.2020.100314

Ali, M. I. (2019). Status of water quality in watersheds due to mining industry activities. *International Journal of Scientific and Technology Research, 8*(12), 1799–1805.

Aminuddin, N. M., Desa, S. M., Awang, S., Yahaya, N. K. E. M., Hashim, N., San, L. Y., Abdullah, S. N. F., & Hanapi, N. H. M. (2021). An assessment of the potential, suitability and sustainability of the sand mining site in the Kemaman River basin, Terengganu using acoustic Doppler current profiler. *Malaysian Journal of Applied Sciences, 6*(2), 48–60. https://doi.org/10.37231/myjas.2021.6.2.308

Angillieri, M. Y. E. (2012). Morphometric characterization of the Carrizal basin applied to the evaluation of flash floods hazard, San Juan, Argentina. *Quaternary International, 253*, 74–79. https://doi.org/10.1016/j.quaint.2011.05.011

Arabameri, A., Rezaei, K., Pourghasemi, H. R., Lee, S., & Yamani, M. (2018). GIS-based gully erosion susceptibility mapping: A comparison among three data-driven models and AHP knowledge-based technique. *Environmental Earth Sciences, 77*(17). https://doi.org/10.1007/s12665-018-7808-5

Arsyad, A., Rukmana, D., Salman, D., & Alimuddin, I. (2020). Impact of sand mining on the changes of morphological and physical dynamics in Sa'dang River, Pinrang District, Indonesia. *Journal of Degraded and Mining Lands Management, 8*(1), 2451–2460. https://doi.org/10.15243/jdmlm

Arulbalaji, P., & Padmalal, D. (2020). Sub-watershed prioritization based on drainage morphometric analysis: A case study of Cauvery River basin in South India. *Journal of the Geological Society of India, 95*(1), 25–35. https://doi.org/10.1007/s12594-020-1383-6

Ashraf, M. A., Maah, M. J., Yusoff, I., Wajid, A., & Mahmood, K. (2011). Sand mining effects, causes and concerns: A case study from bestari jaya, Selangor, Peninsular Malaysia. *Scientific Research and Essays, 6*(6), 1216–1231. https://doi.org/10.5897/SRE10.690

Atejioye, A. A., & Odeyemi, C. A. (2018). Analysing impact of sand mining in Ekiti State, Nigeria using GIS for sustainable development. *World Journal of Research and Review, 6*(2), 26–31.

Aydin, H., Ustaoğlu, F., Tepe, Y., & Soylu, E. N. (2021). Assessment of water quality of streams in Northeast Turkey by water quality index and multiple statistical methods. *Environmental Forensics, 22*(1–2), 270–287. https://doi.org/10.1080/15275922.2020.1836074

Bagwan, W. A., & Gavali, R. S. (2021). Dam-triggered land use land cover change detection and comparison (transition matrix method) of Urmodi River watershed of Maharashtra, India: A remote sensing and GIS approach. *Geology, Ecology, and Landscapes*, 1–9. https://doi.org/10.1080/24749508.2021.1952762

Balogun, A. L., Yekeen, S. T., Pradhan, B., & Althuwaynee, O. F. (2020). Spatio-temporal analysis of oil spill impact and recovery pattern of coastal vegetation and wetland using multispectral satellite Landsat 8-OLI imagery and machine learning models. *Remote Sensing, 12*(7). https://doi.org/10.3390/rs12071225

Ben Ameur, M., Masmoudi, S., Abichou, A., Medhioub, M., & Yaich, C. (2019). Use of the magnetic, geochemical, and sedimentary records in establishing paleoclimate change in the environment of Sebkha: Case of the Sebkha Mhabeul in southeastern Tunisia. *Comptes Rendus – Geoscience, 351*(7), 487–497. https://doi.org/10.1016/j.crte.2019.10.003

Ben Othman, R., El Euch Khay, S., Loulizi, A., & Neji, J. (2019). Laboratory evaluation of an ecological pavement construction material: Sand concrete reinforced with polypropylene fibres. *European Journal of Environmental and Civil Engineering, 23*(3), 287–299. https://doi.org/10.1080/19648189.2016.1277372

Benchaa, S., Gheriani, R., Achouri, A., Bouguettaia, H., & Mechri, M. L. (2021). Structural characterizations of dune sand and construction sand of Sidi Slimane and Zaouia El Abidia areas in the Touggourt region in Southeast Algeria. *Arabian Journal of Geosciences, 14*(22). https://doi.org/10.1007/s12517-021-08303-9

Bhattacharya, R. K., Das Chatterjee, N., & Dolui, G. (2019). Consequences of sand mining on water quality and instream biota in alluvial stream: A case-specific study in South Bengal River, India. *Sustainable Water Resources Management, 5*(4), 1815–1832. https://doi.org/10.1007/s40899-019-00345-y

Bibak, M., Sattari, M., Tahmasebi, S., Agharokh, A., & Namin, J. I. (2020). Marine macro-algae as a bio-indicator of heavy metal pollution in the marine environments, Persian Gulf. *Indian Journal of Geo Marine Sciences, 49*(March), 357–363.

Cavaleri, L., Borg, R. P., La Mantia, F. P., Prakash, K. S., Ch, D., & Rao, H. (2017). Strength characteristics of quarry dust in replacement of sand. *IOP Conference Series: Materials Science and Engineering, 225*(1), 012074. https://doi.org/10.1088/1757-899X/225/1/012074

Chakrabarti, T. (2019). Assessment of seasonal variations in physico-chemical parameters in Panchet reservoir, Dhanbad district, Jharkhand. *Annals of Plant and Soil Research, 21*(4), 390–394.

Chandra, P., Patel, P. L., Porey, P. D., & Gupta, I. D. (2014). Estimation of sediment yield using SWAT model for Upper Tapi basin. *ISH Journal of Hydraulic Engineering, 20*(3), 291–300. https://doi.org/10.1080/09715010.2014.902170

Chandrasekaran, A., Senthil Kumar, C. K., Sathish, V., Manigandan, S., & Tamilarasi, A. (2021). Effect of minerals and heavy metals in sand samples of Ponnai river, Tamil Nadu, India. *Scientific Reports, 11*(1), 23199. https://doi.org/10.1038/s41598-021-02717-x

Chauhan, S. S. (2010). Mining, development and environment: A case study of Bijolia mining area in Rajasthan, India. *Journal of Human Ecology, 31*(1), 65–72. https://doi.org/10.1080/09709274.2010.11906299

Chen, W., He, B., Nover, D., Duan, W., Luo, C., Zhao, K., & Chen, W. (2018). Spatiotemporal patterns and source attribution of nitrogen pollution in a typical headwater agricultural watershed in southeastern China. *Environmental Science and Pollution Research, 25*(3), 2756–2773. https://doi.org/10.1007/s11356-017-0685-8

Damodhara Reddy, B., Aruna Jyothy, S., Kiran Kumar, N., & Hemanth Kumar, K. (2020). An experimental investigation on concrete by partial replacement of cement by fly ash and fine aggregate by quarry dust. *IOP Conference Series: Materials Science and Engineering, 1006*(1). https://doi.org/10.1088/1757-899X/1006/1/012033

Darmajati, Y., Samodra, G., & Purwanto, T. (2021, November). *Slope stability analysis based on change in slope geometry using slope stability analysis based on change in slope geometry using multitemporal UAV image*.

Das, A., Santra, P. K., & Bandyopadhyay, S. (2021). The 2016 flood of Bihar, India: An analysis of its causes. *Natural Hazards, 107*(1), 751–769. https://doi.org/10.1007/s11069-021-04604-0

Datta, R., & Litt, T. B. D. (2020). Water quality of the Ganges in West-Bengal during covid-19 lockdown and unlock period shows the betterment of bod level: An analytical study water quality of the Ganges in West-Bengal during covid-19 lockdown and unlock period shows the betterment of bod. *International Journal of Environmental and Ecology Research, 2*(1), 29–34

Deb, S., & Sahu, S. S. (2010). Study of mineralogy and weathering of two soil profiles of undulating plateau area of Jumar subwatershed, Jharkhand, India. *International Journal of Agriculture, Environment and Biotechnology, 3*(September), 295–301.

Delang, C. O. (2018). Causes and distribution of soil pollution in China. *Environmental & Socio-Economic Studies, 5*(4), 1–17. https://doi.org/10.1515/environ-2017-0016

Deng, M., Yang, X., Dai, X., Zhang, Q., Malik, A., & Sadeghpour, A. (2020). Heavy metal pollution risk assessments and their transportation in sediment and overlay water for the typical Chinese reservoirs. *Ecological Indicators, 112*(September 2019), 106166. https://doi.org/10.1016/j.ecolind.2020.106166

Diago, M., Iniesta, A. C., Soum-Glaude, A., & Calvet, N. (2018). Characterization of desert sand to be used as a high-temperature thermal energy storage medium in particle solar receiver technology. *Applied Energy, 216*(October 2017), 402–413. https://doi.org/10.1016/j.apenergy.2018.02.106

Dimri, D., Daverey, A., Kumar, A., & Sharma, A. (2021). Monitoring water quality of river ganga using multivariate techniques and WQI (Water Quality Index) in Western Himalayan region of Uttarakhand, India. *Environmental Nanotechnology, Monitoring and Management, 15*, 100375. https://doi.org/10.1016/j.enmm.2020.100375

Doloksaribu, D. C. N., Barus, T. A., & Sebayang, K. (2020). The impact of marine sand mining on sea water quality in Pantai Labu, Deli Serdang Regency, Indonesia. *IOP Conference Series: Earth and Environmental Science, 454*(1). https://doi.org/10.1088/1755-1315/454/1/012086

Donovan, M., & Monaghan, R. (2021). Impacts of grazing on ground cover, soil physical properties and soil loss via surface erosion: A novel geospatial modelling approach. *Journal of Environmental Management, 287*(March), 112206. https://doi.org/10.1016/j.jenvman.2021.112206

Duan, H., Cao, Z., Shen, M., Liu, D., & Xiao, Q. (2019). Detection of illicit sand mining and the associated environmental effects in China's fourth largest freshwater lake using daytime and nighttime satellite images. *Science of the Total Environment, 647*, 606–618. https://doi.org/10.1016/j.scitotenv.2018.07.359

Duncan, A. E., & De Vries, N. (2018). Assessment of heavy metal pollution in the sediments of the river pra and its tributaries. *Water, Air, & Soil Pollution, 229*, 272.

Elmayel, I., Higueras, P. L., Bouzid, J., Noguero, E. M. G., & Elouaer, Z. (2019). *Recent advances in geo-environmental engineering, geomechanics and geotechnics, and geohazards* (Vol. 49, Issue January). Springer. https://doi.org/10.1007/978-3-030-01665-4

Eslamian, F., Qi, Z., Tate, M. J., & Romaniuk, N. (2020). Lime application to reduce phosphorus release in different textured intact and small repacked soil columns. *Journal of Soils and Sediments, 20*(4), 2053–2066. https://doi.org/10.1007/s11368-020-02564-9

Evans, B. R., Brooks, H., Chirol, C., Kirkham, M. K., Möller, I., Royse, K., Spencer, K., & Spencer, T. (2022). Vegetation interactions with geotechnical properties and erodibility of salt marsh sediments. *Estuarine, Coastal and Shelf Science, 265*, 107713. https://doi.org/10.1016/J.ECSS.2021.107713

Filho, W. L., Hunt, J., Lingos, A., Platje, J., Vieira, L. W., Will, M., & Gavriletea, M. D. (2021). The unsustainable use of sand: Reporting on a global problem. *Sustainability (Switzerland), 13*(6), 1–16. https://doi.org/10.3390/su13063356

Fitzpatrick, R. W., & Chittleborough, D. J. (2018). Titanium and zirconium minerals. *Soil Mineralogy with Environmental Applications, 7*(January), 667–690. https://doi.org/10.2136/sssabookser7.c22

Gallo, A., Zannoni, D., Valotto, G., Nadimi-Goki, M., & Bini, C. (2018). Concentrations of potentially toxic elements and soil environmental quality evaluation of a typical Prosecco vineyard of the Veneto region (NE Italy). *Journal of Soils and Sediments, 18*(11), 3280–3289. https://doi.org/10.1007/s11368-018-1999-y

Gencel, O., Gholampour, A., Tokay, H., & Ozbakkaloglu, T. (2021). Replacement of natural sand with expanded vermiculite in fly ash-based geopolymer mortars. *Applied Sciences (Switzerland), 11*(4), 1–18. https://doi.org/10.3390/app11041917

Ghosh, P. K., & Jana, N. C. (2021). Study of river sensitivity for sustainable management of sand quarrying activities in Damodar river, West Bengal, India. *Current Science, 121*(6), 810–822. https://doi.org/10.18520/cs/v121/i6/810-822

Goh, K. (2019). Urban waterscapes: The hydro-politics of flooding in a Sinking City. *International Journal of Urban and Regional Research, 43*(2), 250–272. https://doi.org/10.1111/1468-2427.12756

Gutiérrez, J. P., van Halem, D., Uijttewaal, W. S. J., del Risco, E., & Rietveld, L. C. (2018). Natural recovery of infiltration capacity in simulated bank filtration of highly turbid waters. *Water Research, 147*, 299–310. https://doi.org/10.1016/j.watres.2018.10.009

Hackney, C. R., Darby, S. E., Parsons, D. R., Leyland, J., Best, J. L., Aalto, R., Nicholas, A. P., & Houseago, R. C. (2020). River bank instability from unsustainable sand mining in the lower Mekong River. *Nature Sustainability, 3*(3), 217–225. https://doi.org/10.1038/s41893-019-0455-3

Hackney, C. R., Vasilopoulos, G., Heng, S., Darbari, V., Walker, S., & Parsons, D. R. (2021). Sand mining far outpaces natural supply in a large alluvial river. *Earth Surface Dynamics, 9*(5), 1323–1334. https://doi.org/10.5194/esurf-9-1323-2021

Halder, B., Bandyopadhyay, J., & Banik, P. (2021). Monitoring the effect of urban development on urban heat Island based on remote sensing and geo-spatial approach in Kolkata and adjacent areas, India. *Sustainable Cities and Society, 74*(July), 103186. https://doi.org/10.1016/j.scs.2021.103186

Hamzah, M. L., Amir, A. A., Maulud, K. N. A., Sharma, S., Mohd, F. A., Selamat, S. N., Karim, O., Ariffin, E. H., & Begum, R. A. (2020). Assessment of the mangrove forest changes along the Pahang coast using remote sensing and GIS technology. *Journal of Sustainability Science and Management, 15*(5), 43–58. https://doi.org/10.46754/JSSM.2020.07.006

Huo, J., Min, X., & Wang, Y. (2021). Zirconium-modified natural clays for phosphate removal: Effect of clay minerals. *Environmental Research, 194*(December 2020), 110685. https://doi.org/10.1016/j.envres.2020.110685

Hussain, S. T., & Ali, S. A. K. (2021). Removal lead Pb (II) from wastewater using kaolin clay. *IOP Conference Series: Materials Science and Engineering, 1058*(1), 012069. https://doi.org/10.1088/1757-899x/1058/1/012069

Indriasari, N., Kusratmoko, E., Indra, T. L., & Julzarika, A. (2018). Identification of ex-sand mining area using optical and SAR imagery. In *IOP Conference Series: Earth and Environmental Science, 149*(1), 012041. IOP Publishing. https://doi.org/10.1088/1755-1315/149/1/012041

Jaiswal, D., & Pandey, J. (2019). Anthropogenically enhanced sediment oxygen demand creates mosaic of oxygen deficient zones in the Ganga River: Implications for river health. *Ecotoxicology and Environmental Safety, 171*(December 2018), 709–720. https://doi.org/10.1016/j.ecoenv.2019.01.039

Jiang, L., Liu, Y., Wu, S., & Yang, C. (2021). Analyzing ecological environment change and associated driving factors in China based on NDVI time series data. *Ecological Indicators, 129*. https://doi.org/10.1016/j.ecolind.2021.107933

Juen, L., & De Marco, P. (2011). Odonate biodiversity in terra-firme forest streamlets in Central Amazonia: On the relative effects of neutral and niche drivers at small geographical extents. *Insect Conservation and Diversity, 4*(4), 265–274. https://doi.org/10.1111/j.1752-4598.2010.00130.x

Kamaraj, M., & Rangarajan, S. (2021). Predicting the future land use and land cover changes for Bhavani Basin, Tamil Nadu, India using QGIS MOLUSCE plugin. *Environmental Science and Pollution Research, 29*, 86337–86348.

Kaufmann, J. (2020). Evaluation of the combination of desert sand and calcium sulfoaluminate cement for the production of concrete. *Construction and Building Materials, 243*, 118281. https://doi.org/10.1016/j.conbuildmat.2020.118281

Khadija, D., Hicham, A., Rida, A., Hicham, E., Nordine, N., & Najlaa, F. (2021). Surface water quality assessment in the semi-arid area by a combination of heavy metal pollution indices and statistical approaches for sustainable management. *Environmental Challenges, 5*(July), 100230. https://doi.org/10.1016/j.envc.2021.100230

Koehnken, L., Rintoul, M. S., Goichot, M., Tickner, D., Loftus, A. C., & Acreman, M. C. (2020). Impacts of riverine sand mining on freshwater ecosystems: A review of the scientific evidence and guidance for future research. *River Research and Applications, 36*(3), 362–370. https://doi.org/10.1002/rra.3586

Kondolf, M. G. (1994). Geomorphic and environmental effects of instream gravel mining. *Landscape and Urban Planning, 28*(2–3), 225–243. https://doi.org/10.1016/0169-2046(94)90010-8

Kumar, V., & Acharya, A. K. (2021). Analysis the amounts of heavy metals and trace elements in water of different sources of Ranchi city by using ICP-OES technique. *International Research Journal of Engineering and Technology, 8*(11), 1606–1611. www.irjet.net

Kumar, V., Bharti, P. K., Talwar, M., Tyagi, A. K., & Kumar, P. (2017). Studies on high iron content in water resources of Moradabad district (UP), India. *Water Science, 31*(1), 44–51. https://doi.org/10.1016/j.wsj.2017.02.003

Kumar, P. S., Gayathri, R., & Rathi, B. S. (2021). A review on adsorptive separation of toxic metals from aquatic system using biochar produced from agro-waste. *Chemosphere, 285*(June), 131438. https://doi.org/10.1016/j.chemosphere.2021.131438

Leventeli, Y., & Yalcin, F. (2021). Data analysis of heavy metal content in riverwater: Multivariate statistical analysis and inequality expressions. *Journal of Inequalities and Applications, 2021*(1). https://doi.org/10.1186/s13660-021-02549-3

Li, Z. W., Zhang, G. H., Geng, R., & Wang, H. (2015). Rill erodibility as influenced by soil and land use in a small watershed of the Loess Plateau, China. *Biosystems Engineering, 129*, 248–257. https://doi.org/10.1016/j.biosystemseng.2014.11.002

Liang, K., Jiang, Y., Qi, J., Fuller, K., Nyiraneza, J., & Meng, F. R. (2020). Characterizing the impacts of land use on nitrate load and water yield in an agricultural watershed in Atlantic Canada. *Science of the Total Environment, 729*, 138793. https://doi.org/10.1016/j.scitotenv.2020.138793

Ma, Z., Li, X., Peng, T., Zhang, J., Dou, L., Yu, H., Liu, J., Ye, X., Feng, Z., Li, M., Guo, B., Song, C., Zhao, Z., & Li, J. (2020). Landscape evolution of the Dabanshan planation surface: Implications for the uplift of the eastern tip of the Qilian Mountains since the Late Miocene. *Geomorphology, 356*. https://doi.org/10.1016/j.geomorph.2020.107091

Madhav, S., Ahamad, A., Kumar, A., Kushawaha, J., & Mishra, P. K. (2018). Geochemical assessment of groundwater quality for its suitability for drinking and irrigation purpose in rural areas of Sant Ravidas Nagar (Bhadohi), Uttar Pradesh. *Geology, Ecology, and Landscapes, 9508*, 1–10. https://doi.org/10.1080/24749508.2018.1452485

Mahadevan, P (2019). Sand Mafias in India, Disorganized crime in a growing economy. *Global Initiative Against Transnational Organized Crime*. https://globalinitiative.net/wp-content/uploads/2019/07/Sand-Mining-in-India-Report-17Jul1045-Web.pdf

Mane, K. M., Nadgouda, P. A., & Joshi, A. M. (2020). An experimental study on properties of concrete produced with M-sand and E-sand. *Materials Today: Proceedings, 38*(5), 2590–2595. https://doi.org/10.1016/j.matpr.2020.08.086

Marco, H., Scarr, S., & Daigle, K. (2021). *The messy business of sand mining explained*. Reuters Graphics. https://graphics.reuters.com/GLOBAL-ENVIRONMENT/SAND/ygdpzekyavw/

Masindi, V., Foteinis, S., Tekere, M., & Ramakokovhu, M. M. (2021). Facile synthesis of halloysite-bentonite clay/magnesite nanocomposite and its application for the removal of chromium ions: Adsorption and precipitation process. *Materials Today: Proceedings, 38*, 1088–1101. https://doi.org/10.1016/j.matpr.2020.06.084

McCarroll, R. J., Masselink, G., Valiente, N. G., Wiggins, M., Scott, T., Conley, D. C., & King, E. V. (2020). Impact of a headland-associated sandbank on shoreline dynamics. *Geomorphology, 355*, 107065. https://doi.org/10.1016/J.GEOMORPH.2020.107065

Meng, X., Cooper, K. M., Liu, Z., Li, Z., Chen, J., Jiang, X., Ge, Y., & Xie, Z. (2021). Integration of α, β and γ components of macroinvertebrate taxonomic and functional diversity to measure of impacts of commercial sand dredging. *Environmental Pollution, 269*, 116059. https://doi.org/10.1016/j.envpol.2020.116059

Miheretu, B. A., & Yimer, A. A. (2018). Spatial variability of selected soil properties in relation to land use and slope position in Gelana sub-watershed, Northern highlands of Ethiopia. *Physical Geography, 39*(3), 230–245. https://doi.org/10.1080/02723646.2017.1380972

Mishra, S., Kumar, A., & Shukla, P. (2021). Estimation of heavy metal contamination in the Hindon River, India: An environmetric approach. *Applied Water Science, 11*(1), 1–9. https://doi.org/10.1007/s13201-020-01331-y

Nazneen, S., & Raju, N. J. (2017). Distribution and sources of carbon, nitrogen, phosphorus and biogenic silica in the sediments of Chilika lagoon. *Journal of Earth System Science, 126*, 1–13. https://doi.org/10.1007/s12040-016-0785-8

Nazneen, S., Singh, S., & Raju, N. J. (2018, May). Heavy metal fractionation in core sediments and potential biological risk assessment from Chilika lagoon, Odisha state, India. *Quaternary International*. https://doi.org/10.1016/j.quaint.2018.05.011

Nazneen, S., Raju, N. J., Madhav, S., & Ahamad, A. (2019). Spatial and temporal dynamics of dissolved nutrients and factors affecting water quality of Chilika lagoon.

Ndimele, P. E., Owodeinde, F. G., Giwa-Ajeniya, A. O., Moronkola, B. A., Adaramoye, O. R., Ewenla, L. O., & Kushoro, H. Y. (2021). Multi-metric ecosystem health assessment of three inland water bodies in south-west, Nigeria, with varying levels of sand mining activities and heavy metal pollution. *Biological Trace Element Research*. https://doi.org/10.1007/s12011-021-02907-8

Ng, W. X., & Park, E. (2021). Shrinking Tonlé Sap and the recent intensification of sand mining in the Cambodian Mekong River. *Science of the Total Environment, 777*. https://doi.org/10.1016/j.scitotenv.2021.146180

Nguyen, T. M., Lin, T. H., & Chan, H. P. (2019). The environmental effects of urban development in Hanoi, Vietnam from satellite and meteorological observations from 1999–2016. *Sustainability (Switzerland), 11*(6). https://doi.org/10.3390/su11061768

Nodefarahani, M., Aradpour, S., Noori, R., Tang, Q., Partani, S., & Klöve, B. (2020). Metal pollution assessment in surface sediments of Namak Lake, Iran. *Environmental Science and Pollution Research, 27*(36), 45639–45649. https://doi.org/10.1007/s11356-020-10298-x

Nowak, M. M., Dziób, K., & Bogawski, P. (2019). Unmanned aerial vehicles (UAVs) in environmental biology: A review. *European Journal of Ecology, 4*(2), 56–74. https://doi.org/10.2478/eje-2018-0012

Nurhasan, U., & Saputra, P. Y. (2018). Analysis of sand mining areas in lumajang using WEBGIS, *59*(Iceml), 350–355. https://doi.org/10.2991/iceml-18.2018.77

Okeke, C., Abbey, S., Oti, J., Eyo, E., Johnson, A., Ngambi, S., Abam, T., & Ujile, M. (2021). Appropriate use of lime in the study of the physicochemical behaviour of stabilised lateritic soil under continuous water ingress. *Sustainability (Switzerland), 13*(1), 1–26. https://doi.org/10.3390/su13010257

Okur, H., & Erturaç, M. K. (2021). Temporal monitoring of vast sand mining in NW Turkey: Implications on environmental/social impacts. https://doi.org/10.31223/X5HK5T.

Omar, N., Abdullah, E. C., Petrus, A. A., Mubarak, N. M., Khalid, M., Agudosi, E. S., Numan, A., & Aid, S. R. (2021). Single-route synthesis of binary metal oxide loaded coconut shell and watermelon rind biochar: Characterizations and cyclic voltammetry analysis. *Biomass Conversion and Biorefinery*. https://doi.org/10.1007/s13399-021-01367-3

Otvos, E. G. (2020). Coastal barriers – Fresh look at origins, nomenclature and classification issues. *Geomorphology, 355*. https://doi.org/10.1016/j.geomorph.2019.107000

Ouma, Y. O., Okuku, C. O., & Njau, E. N. (2020). Use of artificial neural networks and multiple linear regression model for the prediction of dissolved oxygen in rivers: Case study of hydrographic basin of River Nyando, Kenya. *Complexity, 2020*. https://doi.org/10.1155/2020/9570789

Padmalal, D., Maya, K., Sreebha, S., & Sreeja, R. (2008). Environmental effects of river sand mining: A case from the river catchments of Vembanad lake, Southwest coast of India. *Environmental Geology, 54*(4), 879–889. https://doi.org/10.1007/s00254-007-0870-z

Padmalal, D., Sreelash, K., Raj, V. T., & Sajan, K. (2018). River discharge, major ion chemistry and sediment transport of the Bharathapuzha River, Southwest India: Implications on catchment erosion. *Journal of the Geological Society of India, 92*(5), 568–578. https://doi.org/10.1007/s12594-018-1069-5

Pal, S., & Debanshi, S. (2018). Influences of soil erosion susceptibility toward overloading vulnerability of the gully head bundhs in Mayurakshi River basin of eastern Chottanagpur Plateau. *Environment, Development and Sustainability, 20*(4), 1739–1775. https://doi.org/10.1007/s10668-017-9963-3

Pandey, S., Kumari, N., & Priya, S. (2021). Soil quality and pollution assessment around Jumar watershed of Jharkhand, India. *Arabian Journal of Geosciences, 14*(24), 2748. https://doi.org/10.1007/s12517-021-09091-y

Park, E., Loc, H. H., Van Binh, D., & Kantoush, S. (2021). The worst 2020 saline water intrusion disaster of the past century in the Mekong Delta: Impacts, causes, and management implications. *Ambio*. https://doi.org/10.1007/s13280-021-01577-z

Pathak, D., Whitehead, P. G., Futter, M. N., & Sinha, R. (2018). Water quality assessment and catchment-scale nutrient flux modeling in the Ramganga River basin in North India: An application of INCA model. *Science of the Total Environment, 631–632*, 201–215. https://doi.org/10.1016/j.scitotenv.2018.03.022

Pavlidis, G., & Tsihrintzis, V. A. (2018). Environmental benefits and control of pollution to surface water and groundwater by agroforestry systems: A review. *Water Resources Management, 32*(1), 1–29. https://doi.org/10.1007/s11269-017-1805-4

Peduzzi, P. (2014). Sand, rarer and one thinks. *UNEP Global Environmental Alert Service, 2012*(March), 1–15.

Piyadasa, R. U. K. (2011). River sand mining and associated environmental problems in Sri Lanka. *IAHS-AISH Publication, 349*(December 2004), 148–153.

Purushothaman, P., & Chakrapani, G. J. (2007). Heavy metals fractionation in ganga river sediments, India. *Environmental Monitoring and Assessment, 132*(1–3), 475–489. https://doi.org/10.1007/s10661-006-9550-9

Ramya, R., & Kumari, M. N. (2020). *Sand mining detection – Using IOT*. 2020 7th international conference on smart structures and systems, ICSSS 2020, pp. 29–32. https://doi.org/10.1109/ICSSS49621.2020.9202088.

Ranjith, S., Shivapur, A. V., Shiva Keshava Kumar, P., Hiremath, C. G., & Dhungana, S. (2019). Water quality evaluation in term of WQI river Tungabhadra, Karnataka, India. *International Journal of Innovative Technology and Exploring Engineering, 8*(9 Special Issue 2), 247–253. https://doi.org/10.35940/ijitee.I1051.0789S219

Reddy, B. M., Guddeti, S. S. A. I., & Nagamani, K. (2020). Mapping of sand mining areas using remote sensing and GIS: A case study in parts of Swarnamukhi River bed, Chittoor District, Andhra Pradesh. *The Bioscan, 15*(1), 1–4.

Rezaei, K., Guest, B., Friedrich, A., Fayazi, F., Nakhaei, M., Aghda, S. M. F., & Beitollahi, A. (2009). Soil and sediment quality and composition as factors in the distribution of damage at the December 26, 2003, bam area earthquake in SE Iran (M s∈=∈6.6). *Journal of Soils and Sediments, 9*(1), 23–32. https://doi.org/10.1007/s11368-008-0046-9

Safiur Rahman, M., Shafiuddin Ahmed, A. S., Rahman, M. M., Omar Faruque Babu, S. M., Sultana, S., Sarker, S. I., Awual, R., Rahman, M. M., & Rahman, M. (2021). Temporal assessment of heavy metal concentration and surface water quality representing the public health evaluation from the Meghna River estuary, Bangladesh. *Applied Water Science, 11*(7), 1–16. https://doi.org/10.1007/s13201-021-01455-9

Saha, A., Ramya, V. L., Jesna, P. K., Mol, S. S., Panikkar, P., Vijaykumar, M. E., Sarkar, U. K., & Das, B. K. (2021). Evaluation of spatio-temporal changes in surface water quality and their suitability for designated uses, Mettur Reservoir, India. *Natural Resources Research, 30*(2), 1367–1394. https://doi.org/10.1007/s11053-020-09790-5

Sahoo, S., Dhar, A., Debsarkar, A., & Kar, A. (2018). Impact of water demand on hydrological regime under climate and LULC change scenarios. *Environmental Earth Sciences, 77*(9), 1–19. https://doi.org/10.1007/s12665-018-7531-2

Sahoo, A., Samantaray, S., & Ghose, D. K. (2021). Prediction of flood in Barak River using hybrid machine learning approaches: A case study. *Journal of the Geological Society of India, 97*(2), 186–198. https://doi.org/10.1007/s12594-021-1650-1

Sarath, N. G., & Puthur, J. T. (2021). Heavy metal pollution assessment in a mangrove ecosystem scheduled as a community reserve. *Wetlands Ecology and Management, 29*(5), 719–730. https://doi.org/10.1007/s11273-020-09764-7

Sathya, A., Thampi, S. G., & Chithra, N. R. (2021). Development of a framework for sand auditing of the Chaliyar River basin, Kerala, India using HEC-HMS and HEC-RAS model coupling. *International Journal of River Basin Management*, 1–14. https://doi.org/10.1080/15715124.2021.1909604

Sengani, F., & Zvarivadza, T. (2019). *Proceedings of the 18th symposium on environmental issues and waste management in energy and mineral production*. Springer. https://doi.org/10.1007/978-3-319-99903-6

Serrano, J., Shahidian, S., & da Silva, J. M. (2019). Evaluation of normalized difference water index as a tool for monitoring pasture seasonal and inter-annual variability in a Mediterranean agro-silvo-pastoral system. *Water (Switzerland), 11*(1). https://doi.org/10.3390/w11010062

Shalini Tirkey, A., Pandey, A. C., & Nathawat, M. S. (2013). Use of satellite data, GIS and RUSLE for estimation of average annual soil loss in Daltonganj watershed of Jharkhand (India). *Journal of Remote Sensing Technology, 1*(May), 20–30. https://doi.org/10.18005/jrst0101004

Shrestha, S., Miranda, I., Kumar, A., Pardo, M. L. E., Dahal, S., Rashid, T., Remillard, C., & Mishra, D. R. (2019). Identifying and forecasting potential biophysical risk areas within a tropical mangrove ecosystem using multi-sensor data. *International Journal of Applied Earth Observation and Geoinformation, 74*(September 2018), 281–294. https://doi.org/10.1016/j.jag.2018.09.017

Singh, M., Müller, G., & Singh, I. B. (2002). Heavy metals in freshly deposited stream sediments of rivers associated with urbanization of the Ganga Plain, India. *Water, Air, and Soil Pollution, 141*, 35–54.

Singh, R. K., Singha, M., Singh, S. K., Pal, D., Tripathi, N., & Singh, R. S. (2018). Land use/land cover change detection analysis using remote sensing and GIS of Dhanbad District, India. *Eurasian Journal of Forest Science, 6*(2), 1–12. https://doi.org/10.31195/ejejfs.428381

Soutsos, M. N., Tang, K., & Millard, S. G. (2011). Concrete building blocks made with recycled demolition aggregate. *Construction and Building Materials, 25*(2), 726–735. https://doi.org/10.1016/j.conbuildmat.2010.07.014

Sreebha, S., & Padmalal, D. (2011). Environmental impact assessment of sand mining from the small catchment rivers in the southwestern coast of India: A case study. *Environmental Management, 47*(1), 130–140. https://doi.org/10.1007/s00267-010-9571-6

Stajkowski, S., Zeynoddin, M., Farghaly, H., Gharabaghi, B., & Bonakdari, H. (2020). A methodology for forecasting dissolved oxygen in urban streams. *Water (Switzerland), 12*(9). https://doi.org/10.3390/W12092568

Subha Dharani, S., Gayathri, B., & Sanjeevi, S. (2010). Predicting possible landcover changes in the coral islands of Gulf Mannar due to climate change induced sea-level rise – A remote sensing based study. In *Proceedings of the international conference on "recent advances in space technology services and climate change – 2010", RSTS and CC-2010, 2004* (pp. 344–349). https://doi.org/10.1109/RSTSCC.2010.5712866

Sun, L., Gao, F., Xie, D., Anderson, M., Chen, R., Yang, Y., Yang, Y., & Chen, Z. (2021). Reconstructing daily 30 m NDVI over complex agricultural landscapes using a crop reference curve approach. *Remote Sensing of Environment, 253*(October), 112156. https://doi.org/10.1016/j.rse.2020.112156

Surendar, M., Beulah Gnana Ananthi, G., Sharaniya, M., Deepak, M. S., & Soundarya, T. V. (2021). Mechanical properties of concrete with recycled aggregate and M-sand. *Materials Today: Proceedings, 44*, 1723–1730. https://doi.org/10.1016/j.matpr.2020.11.896

Tamura, T., Nguyen, V. L., Ta, T. K. O., Bateman, M. D., Gugliotta, M., Anthony, E. J., Nakashima, R., & Saito, Y. (2020). Long-term sediment decline causes ongoing shrinkage of the Mekong megadelta, Vietnam. *Scientific Reports, 10*(1), 4–10. https://doi.org/10.1038/s41598-020-64630-z

Teng, J., Xia, S., Liu, Y., Yu, X., Duan, H., Xiao, H., & Zhao, C. (2021). Assessing habitat suitability for wintering geese by using Normalized Difference Water Index (NDWI) in a large floodplain wetland, China. *Ecological Indicators, 122*(August 2020), 107260. https://doi.org/10.1016/j.ecolind.2020.107260

Teo, F. Y., Chun Kiat, C., Ab Ghani, A., & Zakaria, N. A. (2017, August). River sand mining capacity in Malaysia. *Proceedings 37th IAHR world congress*.

Tetsopgang, S., Bongsiysi, B. B., Dinayen, L. S., & Nkenglefac, T. F. D. (2020). Geotechnical assessment of sand for civil engineering in western Cameroon. *Extractive Industries and Society, 7*(2), 497–504. https://doi.org/10.1016/j.exis.2019.05.005

Thakur, S., Maity, D., Mondal, I., Basumatary, G., Ghosh, P. B., Das, P., & De, T. K. (2020). Assessment of changes in land use, land cover, and land surface temperature in the mangrove forest of Sundarbans, northeast coast of India. *Environment, Development and Sustainability, 23*(2), 1917–1943. https://doi.org/10.1007/s10668-020-00656-7

Tsymbarovich, P., Kust, G., Kumani, M., Golosov, V., & Andreeva, O. (2020). Soil erosion: An important indicator for the assessment of land degradation neutrality in Russia. *International Soil and Water Conservation Research, 8*(4), 418–429. https://doi.org/10.1016/j.iswcr.2020.06.002

UNEP-GEAS. (2014). *Sand, rarer than one thinks*. United Nations Environment Program (UNEP). Global Environmental Alert Service (GEAS), 2012(March), pp. 1–15. https://wedocs.unep.org/bitstream/handle/20.500.11822/8665/GEAS_Mar2014_Sand_Mining.pdf?sequence=3&isAllowed=y

Uniyal, B., Jha, M. K., Verma, A. K., & Anebagilu, P. K. (2020). Identification of critical areas and evaluation of best management practices using SWAT for sustainable watershed management. *Science of the Total Environment, 744*, 140737. https://doi.org/10.1016/j.scitotenv.2020.140737

Upgupta, S., & Singh, P. K. (2020). Quantifying the dynamics and drivers of landscape change in an opencast coal mining area of Central India (East Bokaro, Jharkhand). *Proceedings of the National Academy of Sciences India Section A – Physical Sciences, 90*(3), 565–577. https://doi.org/10.1007/s40010-018-0589-0

Usman, U. A., Yusoff, I., Raoov, M., Alias, Y., Hodgkinson, J., Abdullah, N., & Hussin, N. H. (2021). Natural sources of iron and manganese in groundwater of the lower Kelantan River basin, north-eastern coast of Peninsula Malaysia: Water quality assessment and an adsorption-based method for remediation. *Environmental Earth Sciences, 80*(12), 1–17. https://doi.org/10.1007/s12665-021-09717-0

Vandana, M., John, S. E., Maya, K., Sunny, S., & Padmalal, D. (2020). Environmental impact assessment (EIA) of hard rock quarrying in a tropical river basin—Study from the SW India. *Environmental Monitoring and Assessment, 192*(9). https://doi.org/10.1007/s10661-020-08485-x

Varekar, V., Yadav, V., & Karmakar, S. (2021). Rationalization of water quality monitoring locations under spatiotemporal heterogeneity of diffuse pollution using seasonal export coefficient. *Journal of Environmental Management, 277*(December 2019), 111342. https://doi.org/10.1016/j.jenvman.2020.111342

Wang, Z. F., Ding, J. Y., & Yang, G. S. (2012). Risk analysis of slope instability of levees under river sand mining conditions. *Water Science and Engineering, 5*(3), 340–349. https://doi.org/10.3882/j.issn.1674-2370.2012.03.009

Wang, P., Zhang, X., & Qi, S. (2019). Was the trend of the net sediment flux in Poyang Lake, China, altered by the Three Gorges Dam or by sand mining? *Environmental Earth Sciences, 78*(3), 1–12. https://doi.org/10.1007/s12665-019-8063-0

WWF. (2018). Living planet report – 2018: Aiming higher. In *Environmental conservation* (Vol. 26, Issue 4). https://www.wwf.eu/campaigns/living_planet_report_2018/

Xie, R., Xiao, H., & Ashraf, M. A. (2020). Application of GIS/RS for monitoring of the ecological environment in a coastal zone. *Arabian Journal of Geosciences, 13*(6). https://doi.org/10.1007/s12517-020-5114-5

Xu, X., Shrestha, S., Gilani, H., Gumma, M. K., Siddiqui, B. N., & Jain, A. K. (2020). Dynamics and drivers of land use and land cover changes in Bangladesh. *Regional Environmental Change, 20*(2). https://doi.org/10.1007/s10113-020-01650-5

Yoobanpot, N., Jamsawang, P., Poorahong, H., Jongpradist, P., & Likitlersuang, S. (2020). Multiscale laboratory investigation of the mechanical and microstructural properties of dredged sediments stabilized with cement and fly ash. *Engineering Geology, 267*(December 2019), 105491. https://doi.org/10.1016/j.enggeo.2020.105491

Yue, H., Liu, Y., Li, Y., & Lu, Y. (2019). Eco-environmental quality assessment in China's 35 major cities based on remote sensing ecological index. *IEEE Access, 7*, 51295–51311. https://doi.org/10.1109/ACCESS.2019.2911627

Zhang, S., Fan, W., Li, Y., & Yi, Y. (2017). The influence of changes in land use and landscape patterns on soil erosion in a watershed. *Science of the Total Environment, 574*, 34–45. https://doi.org/10.1016/j.scitotenv.2016.09.024

Zhang, C., Shan, B., Zhao, Y., Song, Z., & Tang, W. (2018). Spatial distribution, fractionation, toxicity and risk assessment of surface sediments from the Baiyangdian Lake in northern China. *Ecological Indicators, 90*(December 2017), 633–642. https://doi.org/10.1016/j.ecolind.2018.03.078

Zhao, Y., Duan, X., Han, J., Yang, K., & Xue, Y. (2018). The main influencing factors of soil mechanical characteristics of the gravity erosion environment in the dry-hot valley of Jinsha river. *Open Chemistry, 16*(1), 796–809. https://doi.org/10.1515/chem-2018-0086

Zheng, S., Cheng, H., Tang, M., Xu, W., Liu, E., & Gao, S. (2022). Sand mining impact on Poyang Lake: A case study based on high-resolution bathymetry and sub-bottom data. *Journal of Oceanology and Limnology, 40*, 1404–1416.

# Comprehensive River Health Assessment System for Indian Rivers: A Case Study of Central Indian River Narmada


**Parul Gurjar and Vipin Vyas**

## Abbreviations

| | |
|---|---|
| DO | Dissolved Oxygen |
| GIS | Geographical Information System |
| IBI | Index of Biological Integrity |
| IUCN | International Union for Conservation of Nature |
| LC | Land Cover |
| LU | Land Use |
| PHA | Physical Habitat Assessment |
| PHI | Physical Habitat Index |
| RBP | Rapid Bio assessment Protocol |
| RHI | River Health Index |
| RIVPACS | River Invertebrate Prediction Classification System |
| SWI | Stream Water Index |
| USEPA | United States Environmental Protection Agency |

## 1 Introduction

The landforms and river channels manage the fluvial flow among the hierarchical network of the watershed. For a better ecological assessment, the holistic approach of evaluation should be taken into account. The ecological assessment of a riverine ecosystem includes water quality (physicochemical parameters), biotic diversity (fish, invertebrates, plants and microorganisms), hydrology (precipitation, flow, and runoff), geomorphology (sediment load, instability, drainage network), and habitat

P. Gurjar (✉)
Department of Environmental Science and Limnology, Barkatullah University, Bhopal, India

V. Vyas
Department of Bioscience, Barkatullah University, Bhopal, India
e-mail: vipin.vyas@bubhopal.ac.in



S. Kanhaiya et al. (eds.), *Rivers of India*,
https://doi.org/10.1007/978-3-031-49163-4_7

structure (spatial and temporal variability) (Maddock, 1999). This chapter deals with ecosystem health of rivers, its measuring tools, challenges, and future prospects with reference to a case study on River Narmada.

## 2 River Health: An Integrative Approach

For societal benefits, humans have immeasurably degraded rivers that threatened their existence. For the protection of rivers, scientists throughout the world have commonly agreed to call the condition of river as river health. Despite several scientific arguments for accurate river health, it still seems indefinable. River health, a term which describes the condition of the river, is used commonly for public address. By recognizing the adverse effects of human-induced activities, several river monitoring and restoration programs have started including predictive model approach like RIVPACS in Europe (Wright, 1995), AUSRIVAS in Australia, and multimetric approach in the United States (Karr, 1981; Smith et al., 1999; Karr & Chu, 2000; Yoder & Kulik, 2003; Nguyen et al., 2014; Petesse et al., 2016) (Fig. 1).

The concept of river health was initiated in the nineteenth century in Europe as RIVPACS (River Invertebrate Prediction Classification System) where the river biomonitoring was based on macroinvertebrate assessment species (Clarke et al., 2003). Later, multimetric approach of monitoring river health by using comprehensive physical, chemical, and biological components is incorporated by many scientists (Cuffney et al., 2000; An et al., 2002; Wei et al., 2009; Kim & An, 2015; Wang et al., 2019; Atique et al., 2019).

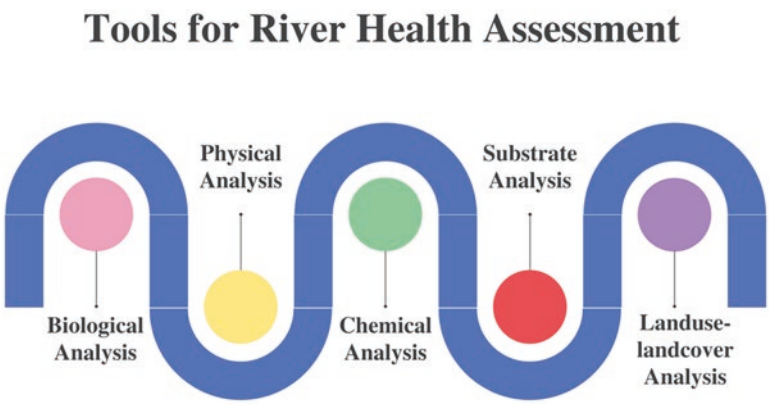


**Fig. 1** Tools for the assessment of river health

## 3 Assessment Methods

The river health assessment of central region of Narmada river basin based on the following methods is as follows:

1. *Land Use and Land Cover Pattern*: The land use-land cover changes are accelerated by agricultural-runoff, sediment load, urbanization, point-source pollution, and commercialization, which are often the major cause of pollution retention in the aquatic ecosystem. The study on water quality deterioration of wheeler lake basin of Northern Alabama reported that land use-land cover changes temporarily affected the environment and public health (ADEM, 1998). The land management practices are primarily responsible for the surface run-off along with the agricultural nutrient load transported and mixed with the streams (Waters, 1995). This agricultural run-off in the stream water through rapid farming practice is responsible for the land use-land cover changes (Changnon & Demise, 1996; Kroening & Fallon, 1996; Raloff, 2004). The agricultural surface runoff of Mississippi River carries huge tons of sediment deposited through water flow into the Gulf of Mexico (Ferber et al., 2004). Several studies have investigated that land use-land cover dynamically affects the physical habitat and biological communities (Troelstrup & Perry, 1989; Richards & Host, 1994; Wang et al., 2019). The effect of agricultural runoff, domestic waste, and urban disposal has significantly affected the diversity and richness of aquatic organisms (Bis et al., 2000). The increasing urbanization and rapid landscape deterioration are affecting the catchment of the rivers in the present study. Landscape dynamics and vegetation of River Sharavathi in the Indian Western Ghats in relation to fish diversity resulted that the streams with dense tree species were also rich in fish diversity (Sreekantha et al., 2007). This study reveals that the biotic communities strongly correlate with the landscape along with the in-stream habitat and substrate. Agricultural practices also show faunal composition changes that indicate disruption of the river continuum due to anthropogenic stress (Nautiyal & Mishra, 2012).
2. *Substrate Analysis*: Minshall (1984) profoundly explained the relation of substrate in the aquatic ecology. He stated that "substratum act as a stage for aquatic organisms where they perform." The aquatic substrate provides habitat for the organisms to rest, lay eggs, hatch, root, and seek refuge from predators. It comprises a variety of organic and inorganic materials where organic material acts as a food in the form of algae, detritus course and fine particles, etc. The inorganic material such as cobble, gravel, pebble, silt, sand, clay, bedrock, and boulders plays an important role in habitat formation and is resulted from the hilly erosion and strong water current (Wentworth, 1922). Water current is responsible for the movement of particles. The stronger water current carries the larger particle size. The downstream effect of different size of particles in the river stretch forms a pattern of the heterogeneous substrate. This heterogeneous structure is important for the survival of diverse forms of life underwater. Plenty of organisms depend on different substrate particles and habitat preferences for their life cycle stages

and reproduction (Culp et al., 1983; Giller & Malmqvist, 2001; Beauger et al., 2006). The heterogeneous habitat plays a vital role in shaping rich and diverse taxa. Trans-Himalayan region of India was studied by using species richness, distribution pattern, and habitat use of ichthyofauna (Sivakumar, 2008). Their observation indicates that species richness was higher in the substrate having pebble, gravel, and sand substrate. This habitat heterogeneity and variable substrate support rich biodiversity of freshwater fishes (Wikramanayake, 1990).

3. *Physical Habitat*: Physical habitat is the surrounding area which interacts with the in-stream fauna and influences its structure and composition (Gorman & Karr, 1978; Schlosser, 1982; Schlosser, 1987; Frissell et al., 1986; Angermeier, 1987; Cummins, 1988; Osborne & Wiley, 1992; Richards et al., 1993; Richards & Host, 1994; Poff & Allan, 1995). The physical habitat plays an essential role for the in-stream biological potential and supports spatially and temporally within the selected region (Vyas et al., 2013; Sharma et al., 2018). Habitat is affected by both in-stream and surrounding topographical features and is a major determinant of aquatic community potential (Aadland, 1993). Physical habitat can be defined in the classical sense as a place to live, specifically the small-scale area that constitutes an organism's daily environment. It can be considered within a stream with unique characteristics of substrate, depth, and velocity. Physical habitat is an important factor that can affect both the structure and composition of resident biological communities (Hynes, 1968; Ward & Stanford, 1979; Meffe & Sheldon, 1988; Calow & Petts, 1994).

   The term habitat implies some biological significance, and that it is not just an identifiable physical feature. The importance of physical habitat in determining the condition of river ecosystem is implicit in its definition that the productivity of any stream system is likely to be determined by four key factors, i.e., water quality, the energy budget, the physical structure of the channel, and the flow regime. Based on these factors, a combination of the last two produces the physical habitat for living biota. Physical habitat is the living space determined by the interaction of the structural features of the channel and the hydrological regime. The hydrologic regime has also been recognized as playing an important role in deciding the biotic composition, structure, and function of aquatic ecosystems.

   Physical habitat is a useful element for evaluating river health as it provides the natural link between the physical environment and its inhabitants. It acts as a fundamental unit on which river conservation recommendations are based (Maddock, 1999). Barbour et al. (1999) proposed a Visual Based Habitat Assessment method in which Rapid Bioassessment Protocol (RBP) was used to assess various habitat parameters. Rapid Bioassessment Protocols are based on the integrated approach to evaluate the river health by incorporating physical habitat, biotic community, and water quality.

   Biotic communities and habitat are closely linked because the habitat is one of the major factors that directly influence the aquatic ecosystems' biological condition. Hynes (1975) divided the river catchment spatially into five chronological orders (stream, segment, reach, pool-riffle, and microhabitat), and each scale exerts a particular form of action (Frissell et al., 1986). Microhabitat units

in a stream support number of native and rare biological taxa, and a slight habitat disturbance can decrease their number. As these species are sensitive to habitat degradation, it becomes mandatory to assess habitat as a part of the bioassessment approach.

4. *Chemical Condition*: The excellent quality of water certainly has an adequate range of physical, chemical, and biological characteristics. Various factors like temperature, turbidity, nutrients, hardness, alkalinity, and dissolved oxygen play a vital role in plants and animals' growth. In a natural aquatic ecosystem, various chemical parameters occur in optimum concentration. This concentration increased due to eutrophication, rapid growth of population, increased industrial activities, urbanization, exploitation of natural resources, extension of irrigation, and lack of environmental regulations and local awareness (Mehedi et al., 1999). The impact of human activities is not only on the quality of water but also on the aquatic biodiversity.

   A healthy aquatic ecosystem is dependent on its physicochemical properties of water and biological diversity. Nutrient supply and healthy ecosystem is the prime requirement of aquatic organisms for their growth. Physicochemical characteristics play an essential role in the healthy balance of the aquatic ecosystem. Their maintenance of optimum level in the aquatic ecosystem is necessary for consistent growth and natural dynamics. Therefore, evaluating water quality is required for the ecosystem productivity (Hute, 1986).

   Riverine water is highly variable, which occurs not only with regard to the spatial distribution but also over time. Temporal variations in precipitation, surface runoff, interflow, groundwater flow, and pumped in and outflows have a strong effect on river discharge and subsequently on the concentration of pollutants in river water (Vega et al., 1998). For effective maintenance of water quality through appropriate control measures, continuous monitoring of water quality parameters is essential to maintain the biodiversity and ecological importance of rivers (Ward & Stanford, 1979).

   In any aquatic ecosystem, physicochemical parameters affect the survival, reproductive growth, and production of fishes either positively or negatively depending on their source. Excessive concentration of physicochemical parameters can cause a long- or short-term effect on the abundance, richness, and composition of species. An increase in the amount of nutrient, organic matter, or contaminant concentrations in surface waters, sediments, or food sources observed low species diversity, with an increase in the abundance of stress-tolerant species (Sarkar et al., 2002). Physicochemical analysis was used to characterize point source pollution. not meant to address habitat degradation. These physicochemical analyses are considered too time-consuming and expensive rather than biological-based assessments (Karr et al., 1986). Previous studies indicated the shortcomings of water quality monitoring, and hence biological monitoring tools should also be included as a part of water quality management (Bere & Nyamupingidza, 2014). So, a drastic change was shifted to the biological assessments, and in the recent times, the use of biological indicators has

rapidly increased, and methods of biological monitoring tools were developed in many countries like the United States, Europe, Africa, Australia, Japan, China, etc.

5. *Biological Condition*: Biological indicators can cover a wide array of pressure and multiple stressors for a longer period of time and space. They are helpful in determining the pollution level at regional scale and can represent overall health status of river ecosystem. To assess the biotic health, an Index of Biological Integrity (IBI) is considered as a useful tool and a widely applicable system to evaluate riverine condition. Karr (1981) studied IBI for the first time and proposed an assessment system by using a series of fish community attributes related to species composition, trophic guild, and habitat structure and fish health to evaluate the quality of an aquatic biota. Karr et al. (1986) assessed the biological integrity of lotic waters. They discussed widely about the different perspectives of IBI with that of Jordan Creek, Illinois.

   IBI has been a widely applicable and effective tool for using fish assemblage data to assess the environmental quality of aquatic habitats (Simon & Lyons, 1995). The original version of IBI has been modified in numerous ways for application in many different regions and habitat types, and IBI is now best contemplated as a family of related indices rather than a single index. The multimetric index was used to evaluate the biotic integrity based on fish assemblage at Maryland Biological Stream Survey (Roth et al., 2000). They quantitatively evaluated the ability of various attributes of the fish assemblage structure to discriminate between the reference sites and the sites known to be degraded, using statistical tests and classification efficiency.

   The fish diversity of undisturbed streams increases from upstream to downstream (Vila-Gispert et al., 2002). The streams passing through human settlements generally receive pollutants from point sources (industrial and municipal sewage) and non-point sources including agricultural and urban runoff and atmospheric deposition (Walton et al., 2007). An aggregate of seven metrics (NAT, DMS, INT, SL, %INSCT, %TOL, %FHW), six each for headwater and wade able streams, have been tested and served as an effective model for stream biomonitoring using fish as the biological indicator and defined as Kentucky Index of Biotic Integrity (Compton et al., 2003). A fish-based IBI including 28 biological variables was studied for upstream brooks of Flanders (Belgium) where nine metrics were studied. Here trisection method (5, 3, and 1) was applied by following the European Water Framework (Breine et al., 2004; Goffaux et al., 2001). The water bodies of Flanders reported poor health status in many rivers due to the dense population, intensively developed agricultural and industrial activities (Belpeire et al., 2000).

   The IBI of northern mid-Atlantic slope drainages including Hudson, Delaware, and Susquehanna River drainage was examined where metrics appeared sensitive to environmental degradation in all the three river basins based on the fish species composition, and none of the site among 27 stations proved excellent (Daniels et al., 2002). The evaluation of IBI at Sorocaba River

by using fish assemblage indicates that on many sampling stations, the sensitive species were substituted by tolerant species which response in stress situation of environmental disturbance (Marciano et al., 2004). The quantitative basis for using fish indicators to assess river health in eastern Australia states that the spatial variation in these attributes of fish assemblages could be predicted by observing slight environmental disturbance, but the accuracy of predictions varied with the method used (Kennard et al., 2005).

The assessment of fish-based IBI in a heavily impacted segment of a tropical river in Brazil reported that IBI was comparatively low, due to most exposed areas, decreasing habitat condition and increasing effects of organic and industrial pollutants due to lower water flow (Pinto & Araujo, 2007). Here, IBI was positively correlated with tributary and riparian condition but shown negative correlation with urban conditions. Another, fish-based IBI of central Alberta Rivers was assessed where relative abundance of carnivores in a fish catch was high when concentrations of nitrogen and road densities in basins were low, whereas high proportion of omnivores occurred in river sections having high densities of roads in basins (Stevens and Council, 2008; Stevens et al., 2006). The effect of environmental quality and mesohabitat structure on a biotic integrity index based on fish assemblages of cerrado streams of rio cuiaba basin, Brazil, indicated low biotic integrity which can be associated with the existence of water barriers instead of land use pattern (Machado et al., 2011).

The development and evaluation of a fish-based index of Mediterranean streams has been proved as an effective tool even on species poor streams (Aparicio et al., 2011). The study of multimetric index based on fish fauna for assessing streams at a mesohabitat scale emphasizes the importance of considering the structural and biological variability of aquatic environment to capture the significance of integrity loss due to human influence (Casatti & Teresa 2013). Similarly, the rivers and streams of Minnesota concluded that the less anthropogenically disturbed sites presented stable biological community and minimal temporal variation response rather than unnatural sites. The natural habitat reflects more diverse and stable biological community that supports sustenance of better ecological condition (Dolph et al., 2010) (Fig. 2).

IBI was framed by using a range of fish attributes assemblages (Karr, 1981). Its 12 attributes, or metrics, fall into three broad categories: species composition, trophic composition, and fish abundance and condition (Karr et al., 1986; Fausch & Bramblett, 1991). Karr (1981) proposed IBI which could be adopted as a standard method for monitoring river health (Saylor & Scott, 1987). The index has a value of its capacity to assess the relative environmental quality of rivers within and among regions (Harris & Silveira, 1999). Trisection method or traditional scoring method was adapted from Karr (1981) and developed by Goffaux et al. (2001). This index was applied to streams (Karr et al., 1986; Allan & Flecker 1993), rivers (Plafkin et al., 1989; Bremblett & Fausch, 1991; Ganasan & Hughes, 1998), estuaries (Thompson & Fitzhugh, 1986), and lakes (Dionne & Karr, 1992; Minns et al., 1994) of temperate and tropical countries.

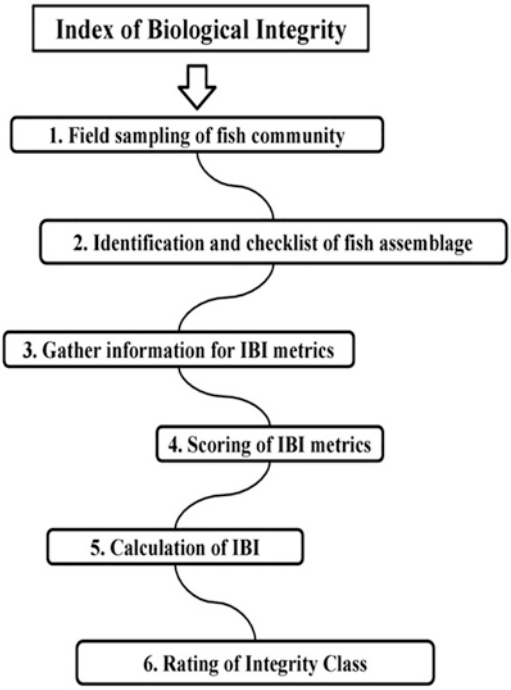


**Fig. 2** Key steps in developing fish-based Index of Biological Integrity (IBI) for river ecosystem. (Modified from Karr et al., 1986)

## 4 Towards Protection and Conservation of Fish Biodiversity

The biological analysis plays a vital role in ecological functioning, used to assess the biotic communities occurring on a particular reach or site (Noss & Harris, 1986). Several authors and researchers gave various definitions of biodiversity. According to Soule 1985, the preservation of biological diversity is important which was mentioned in the goals of conservation biology. The study of fish diversity is important in order to evaluate the aquatic health and its suitability for the fishes. A healthy habitat with minimal anthropogenic disturbance shall attract large number of fish individuals which increases the assemblage (Karr, 1981). Study of fish assemblage variation could be useful in conservation of stream fishes (Li et al., 2018).

There is a wide availability of literature pertaining to the freshwater fishes of India, but most of them are concerned with taxonomy (Menon & Devi, 1992; Jayaram, 1999). Extensive amount of work has been done regarding fish assemblage structure by Kar et al. (2003) in North-East and Arun (1998) in Kerala. In spite of lacking with the knowledge of fish assemblage studies and their habitat in the Indian rivers, researchers across the country have initiated in south India (Arunachalam et al., 1997), Himalayas (Johal et al., 2002; Negi et al., 2007), Ganga basin (Lakra et al., 2010a, b), Central Western Ghats (Bhat, 2003), and Vyas et al. (2006, 2010) in Madhya Pradesh. In Madhya Pradesh, River Narmada is the largest river providing freshwater and livelihood to the locals. The fisheries of River

Narmada have been the focal point of interest for many researchers Hora and Nair (1941); Karamchandani et al. (1967); Anon (1971); Indian Ministry of Agriculture and Irrigation, New Delhi (1976); Dubey (1984); and Rao et al. (1991).

## 5 The Narmada Case Study

Narmada is the largest Central Indian River which flows from east to west. It originates from Maikal ranges near Amarkantak, Annuppur district at an elevation of 1057 m (3467.8 ft.) with 22°40′ N latitude and 81°35′ E longitude. It is considered as a sacred river and known as the lifeline of Central Indian state: Madhya Pradesh. It travels in states of Madhya Pradesh, Maharashtra, and Gujarat. Flowing through kakrana in Alirajpur district, it travels to Maharashtra and then Gujarat to meet Arabian Sea at Gulf of Cambay (Gulf of Khambhat). The river eventually forms common boundaries between states of Maharashtra and Madhya Pradesh and Maharashtra and Gujarat of about 35 and 39 km, respectively. It completes a long journey of 1312 km approx. Before draining into Gulf of Cambay. It receives 41 principal tributaries where 22 tributaries meet at left bank and 19 tributaries at right bank (Fig. 3).

Several authors have worked on River Narmada, and the survey of pertinent literature indicates the presence of a total of 122 species of fishes. Hora and Nair (1941) were the pioneers to provide information of the ichthyofaunal assemblage of river Narmada and recorded 40 species from the hill streams that join the river in Satpura ranges at Hoshangabad district. At that point of time, no barrier was

**Fig. 3** Showing River Narmada near Hoshangabad district

constructed on the tributaries of Narmada River, and therefore, these species may easily reach at the downstream of Narmada River (Dubey, 1984).

During the past few decades, some surveys on fish fauna of Narmada River have been conducted. The first detailed survey conducted by Karamchandani et al. (1967) recorded 77 fish species belonging to 41 genera, 19 families, and 7 orders inclusive of 11 species recorded by Hora and Nair (1941) by confining their survey to Hoshangabad area during the period of 1959–1964. Another study was executed by the Department of Fisheries, Govt. of MP in the year 1967–1971 (Anon, 1971) which covers the stretch from Jabalpur to Khalghat reporting 46 species belonging to 27 genera, 14 families, and 7 orders in the stretch. Rao et al. (1991) have undertaken pre-impoundment survey at Punasa, Omkareshwar, Mandleswar, Maheshwar, and Barwani and have enlisted 84 fish species.

Another rapid survey of fish fauna on River Narmada was carried out by CIFRI (Central Inland of Fisheries Research Institute) from January 2010 to March 2013 (Das et al., 2013). Many researchers studied ichthyofaunal diversity and composition of central region of river Narmada and its tributaries (Hora & Nair, 1941; Vyas et al., 2006; Bakawale & Kanhere, 2006; Vyas et al., 2007; Khedkar et al., 2014; Vishwakarma & Vyas, 2016; Kumar et al., 2017; Shukla & Bhat, 2017; Gurjar et al., 2020). The previous studies reveal that Narmada River has diverse fish fauna and the central region is potentially important for the survival of several aquatic species. Narmada characterizes high biodiversity with variable geomorphology and substrate cover. It shows different mesohabitat types such as pool, riffle, run, and fall (Vyas et al., 2009).

This paper addresses the central zone of river Narmada and its tributaries Sip and Dudhi situated in the state of Madhya Pradesh, India. This study encompasses different assessing tools based on biological, chemical, and physical conditions (Table 1).

**Table 1** River health assessment tools assessed for the central Narmada River

| S. No. | Module | Assessing tool/Index | Attributes assessed | Condition Category |
|---|---|---|---|---|
| 1. | Biological condition | Index of Biological Integrity (IBI) | 1. Taxonomic richness<br>2. Habitat composition<br>3. Trophic composition<br>4. Fish health and abundance | Acceptable<br>Moderately Acceptable<br>Impaired |
| 2. | Physical condition | Physical Habitat ndex (PHI) | 1. Epifaunal substrate<br>2. Pool substrate characterization<br>3. Pool variability<br>4. Sediment deposition<br>5. Channel flow status<br>6. Channel alteration<br>7. Channel sinuosity | Optimal<br>Sub-optimal<br>Marginal<br>Poor |
| 3. | Chemical condition | Stream Water Index (SWI) | 1. Dissolved oxygen<br>2. Conductivity<br>3. pH<br>4. Turbidity | Good<br>Fair<br>Poor |

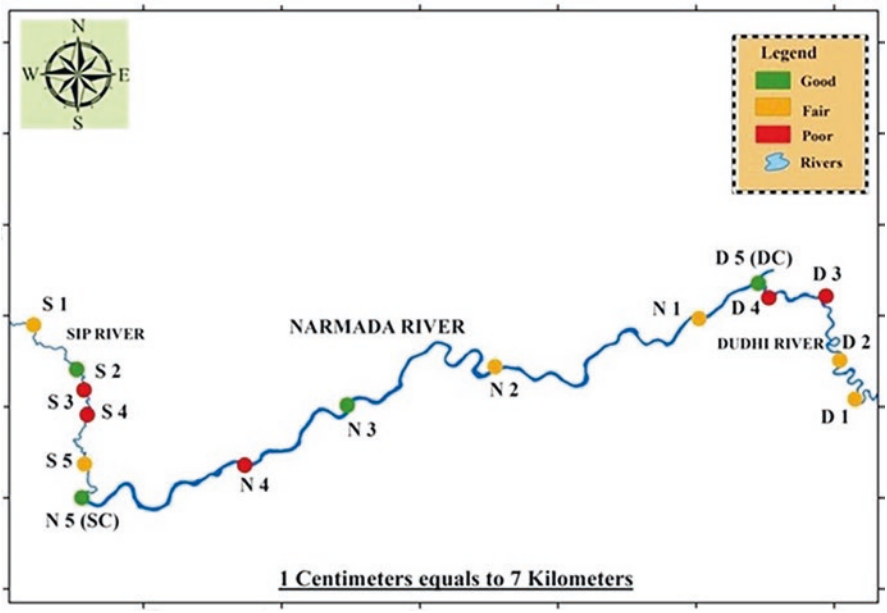


**Fig. 4** River health status of central Narmada riverscape based on physical, chemical, and biological conditions using GIS software

For easy understanding of these attributes, a discrete set of condition category was developed based on the quality of each attribute found at selected sampling stations of river Narmada. The results of the sampling sites are categorized into three classes: good, fair, and poor based on the occurrence of attribute value (Fig. 4).

The observation of this study reveals that land use-land cover has shown strong relation with IBI scoring. The sites that exhibit natural land use especially forested in the riverine catchment showed optimum PHA, IBI, and SWI ranges. Sampling sites showing rapid channel deterioration with dominance of human-induced activities also resulted in lower ranges of IBI, PHA, and SWI scores. The use of multimetric methods reflects the degree of disturbance and is helpful in taking effective measures to combat river health issues. So, it could be concluded that the health status of River Narmada and its tributaries Dudhi and Sip is moderate, and the main cause for their deterioration is anthropogenic disturbance.

## 6 Results and Recommendations

The land use-land cover alteration converting natural habitat into agricultural and waste dumping areas due to extensive anthropogenic disturbance. The destruction of riparian zone areas for agricultural practices resulted in increased soil erosion, nutrient load, and degraded water quality. Excessive water abstraction for agricultural

practices, potable water supply, and industrial purposes are increasing on an alarming rate. This increased water drawl practice is declining water availability and leading to loss of fish diversity. Some parts of the study area are subjected to excessive fishing which is showing negative impacts on the assemblage structure. Practice of illegal sand mining, point and non-point discharge in the river system by local residents along with industrial waste, is deteriorating water quality, reducing dissolved oxygen, increasing eutrophication, and making tough survival for the biological communities. Recommendations based on the present study are suggested here, and their implementation in the study area could improve the river health condition.

- Long-term monitoring assessment programs including application of integrity indices should be encapsulated because they can provide useful information about the condition of river health. Use of locally adaptable attributes of ecological integrity could improve assessment index system at regional scale.
- The modification in physical habitat and land use-land cover pattern for the purpose of damming, irrigation, water abstraction, sand mining, etc. should be avoided, and guidelines for local residents and visitors should be prepared for appropriate maintenance of physical habitat. Plantation and river restoration programs should be executed on the eroded and denuded riparian areas to develop healthy riparian zone of River Narmada and its tributaries.
- For the conservation and management of aquatic biodiversity, regulatory measures must be taken to avoid overexploited, destructive fishing, and risk of extinction. The species like *Tor tor* (Mahseer, state fish of Madhya Pradesh) and other threatened species should be conserved through captive breeding with the help of government authorities and local fishermen.
- The involvement of NGOs could be prolific to restore and manage river catchment through awareness of local residents. There are some instructions to fishermen folks that they need to know while fishing:
  - Fisherman community should be provided the knowledge of conservation status of different fishes that comes under their catch, so that they do not collect naturally rare and poorly conserved fishes.
  - They should restrict themselves from fishing during the monsoon period, so that the breeding process in fishes can occur.
  - They should not use the net of very small mesh size, because this could include fries and fingerlings of fishes and catching them will lead to decrease in the biodiversity.
  - They should not leave their torn and unused nets in the river as this could be harmful for the organisms residing in the river.
  - They should not use explosives like dynamite for convenient fishing because it could damage the ecology and habitat of the organisms.
  - Overfishing should not be practiced.
  - They should sell only the fully mature and adult fish into the market.
  - They should encourage healthy fishing and should not exploit the aquatic ecosystem.
  - Participatory management method should be used among the fishermen community for better management of aquatic resources.

## 7 Concluding Remarks Concerning Rivers of India

Water resources are rapidly degraded by the activities of human society. The major river systems and their tributaries worldwide are facing severe human-induced degradation. Indian Rivers are now undergoing serious issue of existence (Nandi et al., 2016) due to watershed disturbance, unplanned land use pattern, sediment properties (Maya & Seralathan, 2005), and increasing urbanization (Kovacs et al., 2002; Meyer, 1997). In India, the studies on aquatic ecology have been conducted on several rivers such as River Ganga (Dwivedi et al., 2018; Chaudhary et al., 2017; Bhutiani et al., 2016), River Narmada (Kumar & Vyas, 2014; Vyas et al., 2012), Yamuna (Sharma & Kansal, 2011; Misra, 2010), Godavari (Akkaraboyina & Raju, 2012; Ghorade et al., 2014), Gomti (Singh et al., 2005), Betwa (Patel & Datar, 2014), and Hindon (Suthar et al., 2009). All these studies are based on single assessment approach, which is limited to either physicochemical or biodiversity analysis and could not evaluate the ecological integrity of the riverine ecosystem. Thus, it is necessary to imply an integrated assessment method based on multimetric indices; not just a single health assessment method so that overall health status could be reflected (Carlisle et al., 2008; Zhang et al., 2018; Zhu & Chang, 2008). The methods for assessing enormous anthropogenic disturbance led by humans are essential for measuring aquatic health (Young et al., 2004, 2005). The application of combined biological, chemical, and physical aspects reflects the river health assessment method more effectively and feasibly, which helps to imply appropriate measures for restoration and preservation of aquatic ecosystems.

## References

Aadland, L. P. (1993). Stream habitat types: Their fish assemblages and relationship to flow. *North American Journal of Fisheries Management, 13*, 790–806.

ADEM (Alabama Department of Environmental Management). (1998). *ADEM's strategy for sampling environmental indicators surface water quality status*. Alabama Department of Environmental Management.

Akkaraboyina, M. K., & Raju, B. S. N. (2012). A comparative study of water quality indices of river Godavari. *International Journal of Engineering Research and Development, 2*(3), 29–34.

Allan, J. D., & Flecker, A. S. (1993). Biodiversity conservation in running waters. *Bioscience, 43*(1), 32–43.

An, K. G., Park, S. S., & Shin, J. Y. (2002). An evaluation of a river health using the index of biological integrity along with relations to chemical and habitat conditions. *Environment International, 28*(5), 411–420.

Angermeier, P. L. (1987). *Spatiotemporal variation in habitat selection by fishes in small Illinois streams. Community and evolutionary ecology of North American stream fishes* (pp. 52–60). University of Oklahoma Press.

Anon. (1971). Fisheries department, M.P. Fisheries survey in Narmada River, 1967–1971.

Aparicio, E., Catot, G., Moyle, P. B., & Bethou, E. (2011). Development and evaluation of a fish-based index to assess biological integrity of Mediterranean streams. *Aquatic Conservation: Marine and Freshwater Ecosystems, 21*, 324–337.

Arun, L. K. (1998). Status and distribution of fishes in Periyar Lake-stream system of Southern-western Ghats. In *Fish genetics. Biodiversity conservation* (Vol. 5, pp. 77–87). Natcon Publishing.

Arunachalam, M., Johnson, J. A., & Sankarnarayanan, A. (1997). Fish diversity in rivers of Northern Karnataka. *International Journal of Ecology and Environmental Sciences, 23*, 327–333.

Atique, U., Lim, B., Yoon, J., & An, K. G. (2019). Biological health assessments of lotic waters by biotic integrity indices and their relations to water chemistry. *Water, 11*(3), 436.

Bakawale, S., & Kanhere, R. R. (2006). Study on the fish species diversity of the river Narmada in Western zone. *Research Journal of Animal, Veterinary and Fishery Sciences, 1*(6), 18–20.

Barbour, M. T., Grritsen, J., Snyder, B. D., & Stribling, J. B. (1999). *Rapid Bioassessment protocols for use in streams and wadeable rivers: Periphyton, Benthic macro invertebrate and fish second edition*. EPA 841-B-99-002. U.S. Environmental protection Agency/Office of Water.

Beauger, A., Lair, N., Reyes-Marchant, P., & Peiry, J. L. (2006). The distribution of macro invertebrate assemblages in a reach of the river Allier (France), in relation to riverbed characteristics. *Hydrobiologia, 571*, 63–76. https://doi.org/10.1007/sI0750-006-0217-x

Belpeire, C., Smolders, R., Auweele, I. V., Ercken, D., Breine, J., Thuyne, G. V., & Ollevir, F. (2000). An index of biotic integrity characterizing fish populations. *Hydrobiologia, 424*, 17–34.

Bere, T., & Nyamupingidza, B. B. (2014). Use of biological monitoring tools beyond their country of origin: A case study of the south African scoring system version 5 (SASS5). *Hydrobiologia, 722*(1), 223–232.

Bhat, A. (2003). Diversity and composition of freshwater fishes in river systems of Central Western Ghats, India. *Environmental Biology of Fishes, 68*, 25–38.

Bhutiani, R., Khanna, D. R., Kulkarni, D. B., & Ruhela, M. (2016). Assessment of Ganga river ecosystem at Haridwar, Uttarakhand, India with reference to water quality indices. *Applied Water Science, 6*(2), 107–113.

Bis, B., Zdanowicz, A., & Zalewski, M. (2000). Effect of catchment properties on hydrochemistry, habitat complexity and invertebrate community structure in a lowland river. *Hydrobiologia, 422*(423), 369–387.

Bramblett, R. G., & Fausch, K. D. (1991). Variable fish communities and the index of biotic integrity in a western Great Plains river. *Transactions of the American Fisheries Society, 120*(6), 752–769.

Breine, J., Simoen, I., Goethals, P., Quataert, P., Ercken, D., Liefferinghe, C. V., & Belpaire, C. (2004). A fish based index of biotic integrity for upstream brooks in flanders (Belgium). *Hydrobiologia, 522*(1), 133–148.

Calow, P., & Petts, G. E. (Eds.). (1994). *The rivers handbook* (Vol. 2). Blackwell Scientific.

Carlisle, D. M., Hawkins, C. P., Meador, M. R., Potapova, M., & Falcone, J. (2008). Biological assessments of Appalachian streams based on predictive models for fish, macroinvertebrate, and diatom assemblages. *Journal of the North American Benthological Society, 27*(1), 16–37.

Casatti, L., & Teresa, F. B. (2013). A multimetric index based on fish fauna for the evaluation of the biotic integrity of streams at a mesohabitat scale. *Acta Limnologica Brasiliensia, 623*, 12.

Changnon, S. A., & Demissie, M. (1996). Detection of changes in streamflow and floods resulting from climate fluctuations and land use drainage changes. *Climatic Change, 32*, 411–421.

Chaudhary, M., Mishra, S., & Kumar, A. (2017). Estimation of water pollution and probability of health risk due to imbalanced nutrients in River Ganga, India. *International Journal of River Basin Management, 15*(1), 53–60.

Clarke, R. T., Wright, J. F., & Furse, M. T. (2003). RIVPACS models for predicting the expected macroinvertebrate fauna and assessing the ecological quality of rivers. *Ecological Modelling, 160*(3), 219–233.

Compton, M. C., Pond, G. J., & Brumley, J. F. (2003). *Development and application of Kentucky Index of Biotic Integrity (KIBI)*. Kentucky Department for Environmental Protection, Division of Water, Water Quality Branch.

Cuffney, T. F., Meador, M. R., Porter, S. D., & Gurtz, M. E. (2000). Responses of physical, chemical, and biological indicators of water quality to a gradient of agricultural land use in the Yakima River Basin, Washington. *Environmental Monitoring and Assessment, 64*, 259–270.

Culp, J. M., Walde, S. J., & Davies, R. W. (1983). Relative importance of substrate particle size and detritus to stream benthic macroinvertebrate microdistribution. *Canadian Journal of Fisheries and Aquatic Sciences, 40*, 1568–1574.

Cummins, K. W. (1988). The study of stream ecosystems: A functional view. In L. R. Pomeroy & J. J. Alberts (Eds.), *Concepts of ecosystem ecology* (Ecological studies (analysis and synthesis)) (p. 67). Springer. https://doi.org/10.1007/978-1-4612-3842-3_12

Daniels, R. A., Murray, K., Halliwell, D. B., Miller, D. L., & Bilger, D. M. (2002). An index of biological integrity for northern mid-Atlantic slope drainages. *American Fisheries Society, 131*, 1044–1060.

Das, A. K., Sharma, P. K., Jha, B. C., & Biswas, B. K. (2013). *Fishes of Madhya Pradesh* (p. 144). Central Inland Fish Research Institute.

Dionne, M., & Karr, J. R. (1992). Ecological monitoring of fish assemblages in Tennessee River reservoirs. (Eds. D.H. McKenzie, D.E. Hyatt, and V. J. McDonald). *Ecological Indicators, 1*, 259–281.

Dolph, C. L., Sheshukov, A. Y., Chizinski, C. J., Vondracek, B., & Wilson, B. (2010). The index of biological integrity and the bootstrap: Can random sampling error affect stream impairment decisions? *Ecological Indicators, 10*(2), 527–537.

Dubey, G. P. (1984). *Narmada basin water development plan. Development of fisheries, part I and II*. Narmada Planning Agency, Government of Madhya Pradesh.

Dwivedi, S., Mishra, S., & Tripathi, R. D. (2018). Ganga water pollution: A potential health threat to inhabitants of Ganga basin. *Environment International, 117*, 327–338.

Fausch, K. D., & Bramblett, R. G. (1991). Disturbance and fish communities I intermittent tributaries of a western Great Plains river. *Transactions of the American Fisheries Society, 120*, 752–769.

Ferber, D., Herring, H., & Mlot, C. (2004). New life on the Mississippi. *Nature Conservation, 54*, 24–33.

Frissell, C. A., Liss, W. J., Warren, C. E., & Hurley, M. D. (1986). A hierarchical framework for stream habitat classification: Viewing streams in a watershed context. *Environmental Management, 10*(2), 199–214.

Ganasan, V., & Hughes, R. M. (1998). Application of an index of biological integrity (IBI) to fish assemblages of the rivers Khan and Kshipra (Madhya Pradesh), India. *Freshwater Biology, 40*(2), 367–383.

Ghorade, I. B., Lamture, S. V., & Patil, S. S. (2014). Assessment of heavy metal content in Godavari river water. *International Journal of Research in Applied, Natural and Social Sciences, 2*(6), 23–26.

Giller, P. S., & Malmqvist, B. (2001). *The biology of streams and rivers* (pp. 1–296). Oxford University Press.

Goffaux, D., Roset, N., Breine, J. J., Oberdorff, T., & Kestemont, P. (2001). *A biotic index of fish integrity (IBIP) to evaluate the ecological quality of lotic ecosystems – Application to the Meuse River Basin*. Final report: Life97/ENV/B/000419, p. 171.

Gorman, O. T., & Karr, J. R. (1978). Habitat structure and fish communities. *Ecology, 59*, 507–515.

Gurjar, P., Lakhera, K., & Vyas, V. (2020). Ecological health assessment of river sip, a tributary of Central Indian River Narmada by using habitat assessment. *Indian Journal of Applied and Pure Biology, 35*(1), 17–23.

Harris, J. H., & Silveira, R. (1999). Large-scale assessments of river health using an index of biotic integrity with low-diversity fish communities. *Freshwater Biology, 41*, 235–252.

Hora, S. L., & Nair, K. K. (1941). Fishes of the Satpura range, Hoshangabad district, central provinces. *Records of the Indian Museum, 43*(3), 361–373.

Hute, M. (1986). *Textbook of fish culture* (2nd ed.). Fish News Book.

Hynes, H. B. N. (1968). Further studies on the invertebrate fauna of a Welsh mountain stream. *Archives Hydrobiologia, 65*, 360–379.

Hynes, H. B. N. (1975). The stream and its valley. *Verhandlungin Internationale Vereingung fur Theoretische und Angewandte Limnologie, 19*, 15.

Indian Ministry of Agriculture and Irrigation. (1976). Report on the National Commission of Agriculture, Indian Ministry of Agriculture and Irrigation, New Delhi. part VIII. Fisheries. 270pp.

Jayaram, K. C. (1999). *The freshwater fishes of the Indian region* (551pp.). Narendra Publishing House.

Johal, M. S., Tandon, K. K., Tyor, A. K., & Rawal, Y. K. (2002). Fish diversity in different habitats in the streams of lower, middle Western Himalayas. *Polish Journal of Ecology, 50*(1), 45–56.

Kar, D., Kumar, A., Bohra, C, & Singh, L.K. (2003). Fishes of Barak drainage, Mizoram and Tripura. In: *Environment, pollution and management* (604pp.). APH Publishing.

Karamchandani, S. J., Desai, V. R., Pisolkar, M. D., & Bhatnagar, G. K. (1967). Biological investigation on the fish and fisheries of Narmada River (1958-66). *Bulletin Central Inland Fisheries Institute, Barrackpore, 10*, 1–39.

Karr, J. R. (1981). Assessment of biotic integrity using fish communities. *Fisheries, 6*(6), 21–27.

Karr, J. R., & Chu, E. W. (2000). Sustaining living rivers. *Hydrobiologia, 422*(423), 1–14.

Karr, J. R., Fausch, K. D., Angermeir, P. L., Yant, P. R., & Scholosser, I. J. (1986). *Assessing biological integrity in running waters: A method and its rationale*. Illinois Natural History Survey Special Publication 5, 28pp.

Kennard, M. J., Arthington, A. H., Pusey, B. J., & Harch, B. D. (2005). Are alien fish a reliable indicator of river health? *Freshwater Biology, 50*, 174–193.

Khedkar, G. D., Jamdade, R., Naik, S., David, L., & Haymer, D. (2014). DNA barcodes for the fishes of the Narmada, one of India's longest rivers. *PLoS One, 9*(7), e101460.

Kim, J. Y., & An, K. G. (2015). Integrated ecological river health assessments, based on water chemistry, physical habitat quality and biological integrity. *Water, 7*(11), 6378–6403.

Kovacs, T. G., Martel, P. H., & Voss, R. H. (2002). Assessing the biological status of fish in a river receiving pulp and paper mill effluents. *Environmental Pollution, 118*(1), 123–140.

Kroening, S. E., & Fallon, J. D. (1996, May 20–21). *Sources and sinks for nitrogen and phosphorus in part of the Upper Mississippi River Basin, Minnesota and Wisconsin, 1991–1993* [Abstract]. In Minnesota Water '96–changing patterns of power and responsibility: Implications for water policy, fifth Biennial conference onwater resources in Minnesota, University of Minnesota, Water Resources Research Center, p. 96.

Kumar, A., & Vyas, V. (2014). Diversity of macrozoobenthos in the selected reach of River Narmada (central zone), India. *International Journal of Research in Biological Sciences, 4*(3), 60–68.

Kumar, A., Sharma, R., & Vyas, V. (2017). Diversity of Macrozoobenthos in Dudhi River-A tributary of river Narmada in the central zone, India. *International Journal of Pure & Applied Biosciences, 5*(4), 1998–2007.

Lakra, W., Sarkar, U., Gopalakrishnan, A., & Kathirvelpandian, A. (2010a). *Threatened freshwater fishes of India* (p. 20). NBFGR. ISBN: 978-81-905540-5-3.

Lakra, W. S., Sarkar, U. K., Kumar, R. S., Pandey, A., Dubey, V. K., & Gusain, O. P. (2010b). Fish diversity, habitat ecology and their conservation and management issues of a tropical river in Ganga basin, India. *The Environmentalist, 30*(4), 306–319. https://doi.org/10.1007/s10669-010-9277-6

Li, T., Huang, X., Jiang, X., & Wang, X. (2018). Assessment of ecosystem health of the Yellow River with fish index of biotic integrity. *Hydrobiologia, 814*(1), 31–43.

Machado, N. Venticinque, E. M., & Penha, J. (2011). Effect of environmental quality and mesohabitat structure on a Biotic Integrity Index based on fish assemblages of cerrado streams from Rio Cuiabá basin, Brazil. *Brazilian Journal of Biology, 71*(3), 577–586.

Maddock, I. (1999). The importance of physical habitat assessment for evaluating river health. *Freshwater Biology, 41*, 373–391.

Marciano, F. T., Chaudhry, F. H., & Ribeiro, M. C. (2004). Evaluation of the index of biotic integrity in the Sorocaba River Basin (Brazil, SP) based on fish communities. *Acta Limnologica Brasiliensia, 16*(3), 225–237.

Maya, K., & Seralathan, P. (2005). *Studies on the nature and chemistry of sediments and water of Periyar and Chalakudy rivers, Kerala, India* (Doctoral dissertation, Department of Marine Geology and Geophysics, Faculty of Science).

Meffe, G. K., & Sheldon, A. L. (1988). The influence of habitat structure on fish assemblage composition in southeastern Blackwater streams. *American Midland Naturalist, 120*, 225–240.

Mehedi, M. Y., Kamal, D., Azam, K., & Khan, Y. S. A. (1999). Trace metals in coastal water along the ship breaking area, Chittagong, Bangladesh. *Khulna University Studies, 1*, 289–293.

Menon, A. K., & Devi, R. (1992). Puntius sharmai, a new cyprinid fish from Madras. *Journal of the Bombay Natural History Society, 89*(3), 353–354.

Meyer, J. L. (1997). Stream health: Incorporating the human dimension to advance stream ecology. *Journal of the North American Benthological Society, 16*(2), 439–447.

Minns, C. K., Randall, R. G., Cairns, V. W., & Moore, J. E. (1994). An index of biotic integrity (IBI) for fish assemblage in the littoral zones of Great Lakes' areas of concern. *Canadian Journal of Fisheries and Aquatic Sciences, 51*, 1804–1822.

Minshall, G. W. (1984). Aquatic insects-substratum relationships. In V. H. Resh & D. M. Rosenberg (Eds.), *The ecology of aquatic insects* (pp. 358–400). Praeger.

Misra, A. K. (2010). A river about to die: Yamuna. *Journal of Water Resource and Protection, 2*(5), 489.

Nandi, I., Tewari, A., & Shah, K. (2016). Evolving human dimensions and the need for continuous health assessment of Indian rivers. *Current Science, 111*(2), 263–271.

Nautiyal, P., & Mishra, A. S. (2012). Longitudinal distribution of benthic macroinvertebrate fauna in a Vindhyan River, India. *International Journal of Environmental Sciences, 1*(3), 150–158. ISSN: 2277-1948.

Negi, R. K., Joshi, B. D., Negi, T., & Chand, P. A. (2007). *Study on stream morphology of some selected streams hill streams of district Nainital with spatial reference to its biotic communities*. In Proceedings of National Seminar on Limnology, Jaipur, pp. 288–295.

Nguyen, H. H., Everaert, G., Gabriels, W., Hoang, T. H., & Goethals, P. L. (2014). A multimetric macroinvertebrate index for assessing the water quality of the Cau river basin in Vietnam. *Limnologica, 45*, 16–23.

Noss, R. F., & Harris, L. D. (1986). Nodes, networks, and MUMs: Pre- serving diversity at all scales. *Environmental Management, 10*, 299–309.

Osborne, L. L., & Wiley, M. J. (1992). Influence of tributary spatial position on the structure of warmwater fish communities. *Canadian Journal of Fisheries and Aquatic Science, 49*(4), 671–681.

Patel, A., & Datar, M. (2014). Seasonal variations of physico-chemical characteristics of River Betwa in Vidisha District. *International journal of Environmental Science and Technology, 3*, 2205–2214.

Petesse, M. L., Siqueira-Souza, F. K., de Carvalho, F. C. E., & Petrere, M. (2016). Selection of reference lakes and adaptation of a fish multimetric index of biotic integrity to six amazon floodplain lakes. *Ecological Engineering, 97*, 535–544.

Pinto, B. C. T., & Araujo, F. G. (2007). Assessing of biotic integrity of the fish community in a heavily impacted segment of a tropical river in Brazil. *Brazilian Archives and Technology an International Journal, 50*(3), 489–502.

Plafkin, J. L., Barbour, M. T., Porter, K. D., Gross, S. K., & Hughes, R. M. (1989). *Rapid bioassessment protocol for the use in streams and rivers: Benthic macroinvertebrate and fish*. Environmental Protection Agency EPA/440/4-89/001.

Poff, N. L., & Allan, J. D. (1995). Functional organization of stream fish assemblages in relation to hydrological variability. *Ecology, 76*(2), 606–627.

Raloff, J. (2004). Dead waters. *Science News, 165*, 360–362.

Rao, K. S., Chatterjee, S. N., & Singh, A. K. (1991). Studies on pre impoundment fishery potential of Narmada basin (western region) in the context of Indira sagar, Maheshwar, Omkareshwar and Sardar Sarovar reservoirs. *Journal of Inland Fisheries Society of India, 23*(1), 34–41.

Richard, C., Johnson, L.B. and Host, G.E. (1996). Landscape-scale influences on stream habitats and biota .*Canadian* Journal of Fisheries and Aquatic Science, 53: 295–311.

Richards, C., & Host, G. (1994). Examine land use influences on stream habitats and macroinvertebrates: A GIS approach. *Water Resources Bulletin, 30*(4), 729–738.

Richards, C., Host, G. E., & Arthur, J. W. (1993). Identification of predominant environmental factors structuring stream macroinvertebrate communities within a large agricultural catchment. *Freshwater Biology, 29*, 285–294.

Roth, N. E., Southerland, M. T., Chaillou, J. C., Kazyak, P. F., & Stranko, S. A. (2000). *Refinement and validation of a fish index of biotic integrity for Maryland streams*. Maryland Development of Natural Resources.

Sarkar, S. K., Bhattacharya, B., Debnath, S., Bandopathaya, G., & Giri, S. (2002). Heavy metals in biota from Sundarban wetland ecosystem, India: Implications to monitoring and environmental assessment. *Aquatic Ecosystem Health & Management, 5*(4), 467–472.

Saylor, C., & Scott, E. M. (1987). *Application of the index of biotic integrity to existing TVA data*. Tennessee Valley authority, Division of Air and Water Resources, TVA/ONRED/AWR 87/32, Norris, Tennessee, 25 pp.

Schlosser, I. J. (1982). Fish community structure and function along two habitat gradients in a headwater stream. *Ecological Monographs, 52*, 395–414.

Schlosser, I. J. (1987). A conceptual framework for fish communities in small warmwater streams. In *Community and evolutionary ecology of North American stream fishes*. University of Oklahoma Press.

Sharma, D., & Kansal, A. (2011). Water quality analysis of River Yamuna using water quality index in the national capital territory, India (2000–2009). *Applied Water Science, 1*(3–4), 147–157.

Sharma, R., Kumar, A., & Vyas, V. (2018). Physical habitat assessment of the Ganjal and Morand River using GIS techniques. *Journal of the Indian Society of Remote Sensing, 46*(3), 443–450.

Shukla, R., & Bhat, A. (2017). Environmental drivers of α-diversity patterns in monsoonal tropical stream fish assemblages: A case study from tributaries of Narmada basin, India. *Environmental Biology of Fishes, 100*(7), 749–761.

Simon, T. P., & Lyons, J. (1995). Application of the index of biotic integrity to evaluate water resource integrity in freshwater ecosystems. In W. S. Davis & T. P. Simon (Eds.), *Biological assessment and criteria: Tools for water resource planning and decision making* (pp. 245–262). Lewis Publishers.

Singh, K. P., Malik, A., & Sinha, S. (2005). Water quality assessment and apportionment of pollution sources of Gomti river (India) using multivariate statistical techniques – A case study. *Analytica Chimica Acta, 538*, 355–374.

Sivakumar, K. (2008). Species richness, distribution pattern and habitat use of fishes in the trans-Himalayas, India. *Electronic Journal of Ichthyology, 1*, 31–42.

Smith, M. J., Kay, W. R., Edward, D. H. D., Papas, P. J., Richardson, K. S. J., Simpson, J. C., Pinder, A. M., Cale, D. J., Horwitz, P. H. J., Davis, J. A., Yung, F. H., Norris, R. H., & Halse, S. A. (1999). AusRivAS: Using macroinvertebrates to assess ecological condition of rivers in Western Australia. *Freshwater Biology, 41*, 269–282.

Sreekantha, M. D., Chandran, S., Mesta, D. K., Rao, G. R., Gururaja, K. V., & Ramachandra, T. V. (2007). Fish diversity in relation to landscape and vegetation in central western ghats, India. *Current Science, 92*(11), 1592–1603.

Stevens, C., & Council, T. (2008). *A fish based index of biological integrity for assessing river condition in Central Alberta*. Technical Report, T-2008-001, Produced by the Alberta Conservation Sherwood Park and Lethbridge, Alberta, Canada. 29 pp.

Stevens, C., Scrimgeour, Tonn, W., Paszkowski, C., Sullian, M., & Millar, S. (2006). *Developing and testing of a fish based index of biological integrity to quantify the health of grassland streams in Alberta*. Technical report (T-2006-001). Produced By Alberta Conservation Association, 50 pp.

Suthar, S., Nema, A. K., Chabukdhara, M., & Gupta, S. K. (2009). Assessment of metals in water and sediments of Hindon River, India: Impact of industrial and urban discharges. *Journal of Hazardous Materials, 171*(1–3), 1088–1095.

Thompson, B. A., & Fitzhugh, G. R. (1986). *A use attainability study: An evaluation of fish and macroinvertebrate assemblages of the lower Calcasieu River* (pp. 1–143). Louisiana Center for Wetlands Resources, Coastal Fisheries Institute, Lousiana State University. Baton Rouge, LSU-CFI-29.

Troelstrup, N. H., & Perry, J. A. (1989). Water quality in southeastern Minnesota streams: Observations along a gradient of land use and geology. *Journal of the Minnesota Academy of Science, 55*, 6–31.

Vega, M., Pardo, R., Barrado, E., & Deban, L. (1998). Assessment of seasonal and polluting effects on the quality of seasonal and polluting effects on the quality of river water by exploratory data analysis. *Water Research, 32*, 3581–3592.

Vila-Gispert, A., Garcia-Berthou, E., & Moreno-Amich, R. (2002). Fish zonation in a Mediterranean stream: Effects of human disturbances. *Aquatic Sciences, 6*, 163–170.

Vishwakarma, K. S., & Vyas, V. (2016). Comparative study of ichthyofaunal diversity of Sip and Jamner Rivers: A tributary of river Narmada (Central India). *International Journal of Fisheries and Aquatic Studies, 4*(3), 604–610.

Vyas, V., Bara, S., Parashar, V., Damde, D., & Tuli, R. P. (2006). Temporal variation in fish biodiversity of River Narmada in Hoshangabad Region. *Fishing Chimes, 27*, 49–53.

Vyas, V., Parashar, V., Bara, S., & Damde, D. (2007). Fish catch composition of River Narmada with reference to common fishing gears in Hoshangabad area. *National Bulletin of Life Sciences, 4*(1), 1–6.

Vyas, V., Parashar, V., & Damde, D. (2009). Fish biodiversity and preferential habitats of fishes in selected stretch of Narmada River. *Nature Environment and Pollution Technology, 8*, 81–89.

Vyas, V., Parashar, V, & Damde, D. (2010). *Documentation of aquatic biodiversity in rivers and ponds of M.P.* Report submitted to M.P. State Biodiversity Board.

Vyas, V., Kumar, A., Wani, S. G., & Parashar, V. (2012). Status of riparian buffer zone and floodplain areas of River Narmada, India. *International Journal of Environmental Sciences, 3*(1), 659–674.

Vyas, V., Kumar, A., Parashar, V., & Tomar, S. (2013). Physical habitat assessment of River Denwa using GIS techniques. *Journal of the Indian Society of Remote Sensing, 41*(1), 127–139.

Walton, B. M., Salling, M., Wyles, J., & Wolin, J. (2007). Biological integrity in urban streams: Toward resolving multiple dimensions of urbanization. *Landscape and Urban Planning, 79*, 110–123.

Wang, S., Zhang, Q., Yang, T., Zhang, L., Li, X., & Chen, J. (2019). River health assessment: Proposing a comprehensive model based on physical habitat, chemical condition and biotic structure. *Ecological Indicators, 103*, 446–460.

Ward, J. V., & Stanford, J. A. (Eds.). (1979). *The ecology of regulated streams*. Plenum Press.

Waters, T. F. (1995). *Sediment in streams* (American Fisheries Society Monograph 7, 251 pp.). American Fisheries Society.

Wei, M., Zhang, N., Zhang, Y., & Zheng, B. (2009). Integrated assessment of river health based on water quality, aquatic life and physical habitat. *Journal of Environmental Sciences, 21*(8), 1017–1027.

Wentworth, C. K. (1922). A scale of grade and class terms for clastic sediments. *Journal of Geology, 30*, 377–392.

Wikramanayake, E. D. (1990). Ecomorphology and biogeography of a tropical stream fish assemblage: Evolution of assemblage structure. *Ecology, 71*(5), 1756–1764.

Wright, J. F. (1995). Development and use of a system for predicting the macroinvertebrate fauna in flowing waters. *Australian Journal of Ecology, 20*(1), 181–197.

Yoder, C. O., & Kulik, B. H. (2003). The development and application of multimetric indices for the assessment of impacts to fish assemblages in large rivers: A review of current science and applications. *Canadian Water Resources Journal, 28*(2), 301–328.

Young, R., Townsend, C., & Matthaei, C. (2004). *Functional indicators of river ecosystem health – An Interim Guide for Use in New Zealand* (Report no. 870). Ministry for the Environment – Sustainable Management Fund Contract 2208.

Young, T. P., Petersen, D. A., & Clary, J. J. (2005). The ecology of restoration: Historical links, emerging issues and unexplored realms. *Ecology Letters, 8*(6), 662–673.

Zhang, X., Meng, Y., Xia, J., Wu, B., & She, D. (2018). A combined model for river health evaluation based upon the physical, chemical, and biological elements. *Ecological Indicators, 84*, 416–424.

Zhu, D., & Chang, J. (2008). Annual variations of biotic integrity in the upper Yangtze River using an adapted index of biotic integrity (IBI). *Ecological Indicators, 8*, 564–572.

# Assessment of Seasonal Variation in Water Quality of Gomti River, Jaunpur City, India


**Dipak Prasad, Jyoti Kumar, Praveen K. Rai, Brototi Biswas, Ashutosh Singh, and Mukesh Ranjan**

## 1 Introduction

Natural and human influences are two major causative factors of ecology which are affecting the water resources rapidly. Human conscious are having high awareness about the outcomes, but feeble will power, which are being overlooked the severe issues. Deteriorating water quality status has become a worldwide problem of concern as population growth, industrial and agricultural conducts expand, and changing climate intimidates to cause major alterations to the hydrological cycle.

Today, the most prevalent issue on water quality is eutrophication; it results in high nutrient loads mainly phosphorus and nitrogen, which considerably harm beneficial uses of water. Major sources of nutrients include agricultural runoff, domestic sewage (also a source of microbial pollution), industrial effluents, and atmospheric inputs from fossil fuel burning and bush fires (UNDESA, 2015). River is having a role in carrying off the urban and industrial waste and surface runoff through various sources as agricultural land in their huge drainage basins.

D. Prasad
Department of Geography, DDU Gorakhpur University, Gorakhpur, India

J. Kumar
Department of Geography, Allahabad University, Allahabad, India

P. K. Rai
Department of Geography, K.M.C. Language University, Lucknow, India

B. Biswas
Department of Geography &RM, Mizoram University, Aizawl, India

A. Singh (✉)
Department of Geography, Mizoram University, Aizawl, India

M. Ranjan
Department of Statistics, Mizoram University, Aizawl, India



S. Kanhaiya et al. (eds.), *Rivers of India*,
https://doi.org/10.1007/978-3-031-49163-4_8

The massive pressure to the integrity of the world's great rivers has endangered the basis of world economies and the sources of drinking water. River water dilutes and degrades water pollutants faster than stable water, but the world figure shows that water bodies like river in the world are insensitively polluted and in inferior condition. Industries, agriculture, and population concentrated along the river are the major sources for pollution (CWC, 2018). The main areas that are subject to water quality threats are largely correlated to population densities and areas of economic growth, with the future scenarios determined largely by the same factors. In about all of the contents, water quality of almost all the rivers is in worse condition since the 1990s (UNEP, 2016).

There are lots of primary threats faced by the major river basins of the world. Deterioration of water quality is one of the major considerable threats among the primary threats (Wong et al., 2007). The world population residing in Iran, Pakistan, Bhutan, Afghanistan, Maldives, India, Nepal, Bangladesh, and Sri Lanka are only one-fourth of the total, but these regions have 4.5% (1945 billion $m^3$) of the world's annual water resources which are renewable (43,659 billion $m^3$). India by far largest in terms of population and area, in South Asia, is home to one-sixth of the world's population, while only endowed with 1/25th of the world's available water resources (UNEP, 2008). Further, lack of water resources and increasing population pressure are major causes of water pollution. Water bodies in India are polluted with organics and other bacteria due to regular discharge of untreated water through industrial and domestic sector.

Rivers in India are polluted severely and have worsening condition due to pollution from multiple sources such as domestic, industrial, and other economic sectors. Union government, in 2017, said that out of 445 river stretches, 275 rivers of India are heavily polluted. So the river water in these sources is unfit for consumption and was heavily laden with bacteria and pollutants like zinc and lead. There are several efforts for water quality assessment which has been taken into consideration as by Sisodia and Moundiotya (2006), Ziauddin and Siddiqui (2007), Dhakad et al. (2008), Samantray et al. (2009), Kumar and Dua (2009), Razak et al. (2009), Parmar and Parmar (2010), Singh and Pandey (2010), Singh and Singh (2010, 2014a, b), Bharti and Katyal (2011), Chauhan and Thakor (2012), Singh (2014), Babel and Wahid (2008), Bhardawaj et al. (2010), Carle et al. (2005), Singh (2002), Nickson (2004), Subramanian (2004), Singha et al. (2005), Phiri et al. (2005), Swedish Water House Report 21 (2007), UNEP Report (2007), Kumar et al. (2008), WHO (2009), Lurent et al. (2010), Bhardawaj et al. (2010), CPCB Report (2010), Central Water Commission Report (2011), Dutta et al. (2011), Susilo and Febrina (2011), UN Water Members and Partners (2011), Singh et al. (2016), Madhav et al. (2018), Abida and Harikrishna (2008), Dutta et al. (2015), Horton (1965), UNEP (2010), United Nation Department of Economic and Social Affairs (2015), and WHO (2013a, b) had worked on assessment of water quality by water quality index (WQI).

The region is located in the Ganga plain and in the basin of Gomti River. The river enters from the western part of the city and flows towards the east, and further it meets river Ganga near Ghazipur. It covers a total distance of about 941 km and drains into the river Ganga at Kaithi near Varanasi. This river basin covers 14

districts partially or fully, flowing through both rural and urban areas. Lucknow, Sultanpur, and Jaunpur are the three major urban settlements on the banks of the river. Kathna, Sarayan, Reth, Luni, Kalyani, and Sai are the major tributaries of the river Gomti. Jaunpur is an ancient city situated on the bank of the river Gomti which bisects the municipal area of Jaunpur city (located between 25°44′ to 25°46′ North latitude and 82°40′ to 82°43′ East longitude) in the north and south directions. The river flows 5.5 km of its course in Jaunpur city. The study tries to evaluate the status of water quality of river Gomti stretch in Jaunpur city. It also set targets to determine the level of variables to assess an integrated result which will depict the precise quality status in order to manage the various site points for planning and prospects.

## 2 Sample Station

Water samples were collected for two periods, pre-monsoon and post-monsoon seasons, from eight (8) cites selected stations in Jaunpur city drained by the Gomti River. The eight sample stations were taken from Nadiapar to Miyanpur Ghat. All of them are located at the entire stretch of 5.5 km along the course of the Gomti River in Jaunpur city. The first station (Nadiapar Ghat) is situated at the upstream (Before 2 km entering the city) course of the river. Further downstream, Tarapur Ghat sample station is located 1 kilometer from Nadiapar Ghat. The third station at Gular Ghat is located 2.4 km downstream from Nadiapar Ghat just before the Shahi Bridge. Hanuman Ghat (fourth station) is located on the left bank of Gomti River east of Shahi Bridge. The other sample stations along the downstream are Balua Ghat sample station, Miyanpur Ghat in the right bank, and Chachakpur Ghat sample station which is located at the margin of the city (Fig. 1). The sampling stations listed are located on a stable space, with little deviation in the geographic location. All the samples were collected physically from a depth of 8 to 10 cm below from the surface of the river water.

## 3 Analytical Methods

Some of the parameters, e.g., pH, dissolved oxygen, electrical conductivity, and total dissolved solids were analyzed directly at each of the station instantly using portable water analysis kit. Methods of Eaton et al. (1998), Trivedy and Goel (1986), and Tandon (1995) were used to analyze the other parameters, e.g., alkalinity, total hardness, calcium, and magnesium ions. Water quality index was calculated to evaluate the seasonal variation of water quality.

Water quality index (WQI) was calculated for each month for assessing the suitability of water for biotic communities and also drinking purposes. Eleven important physicochemical properties were taken under consideration using the WHO standards. WQI for each station has been calculated through pH, BOD, dissolved

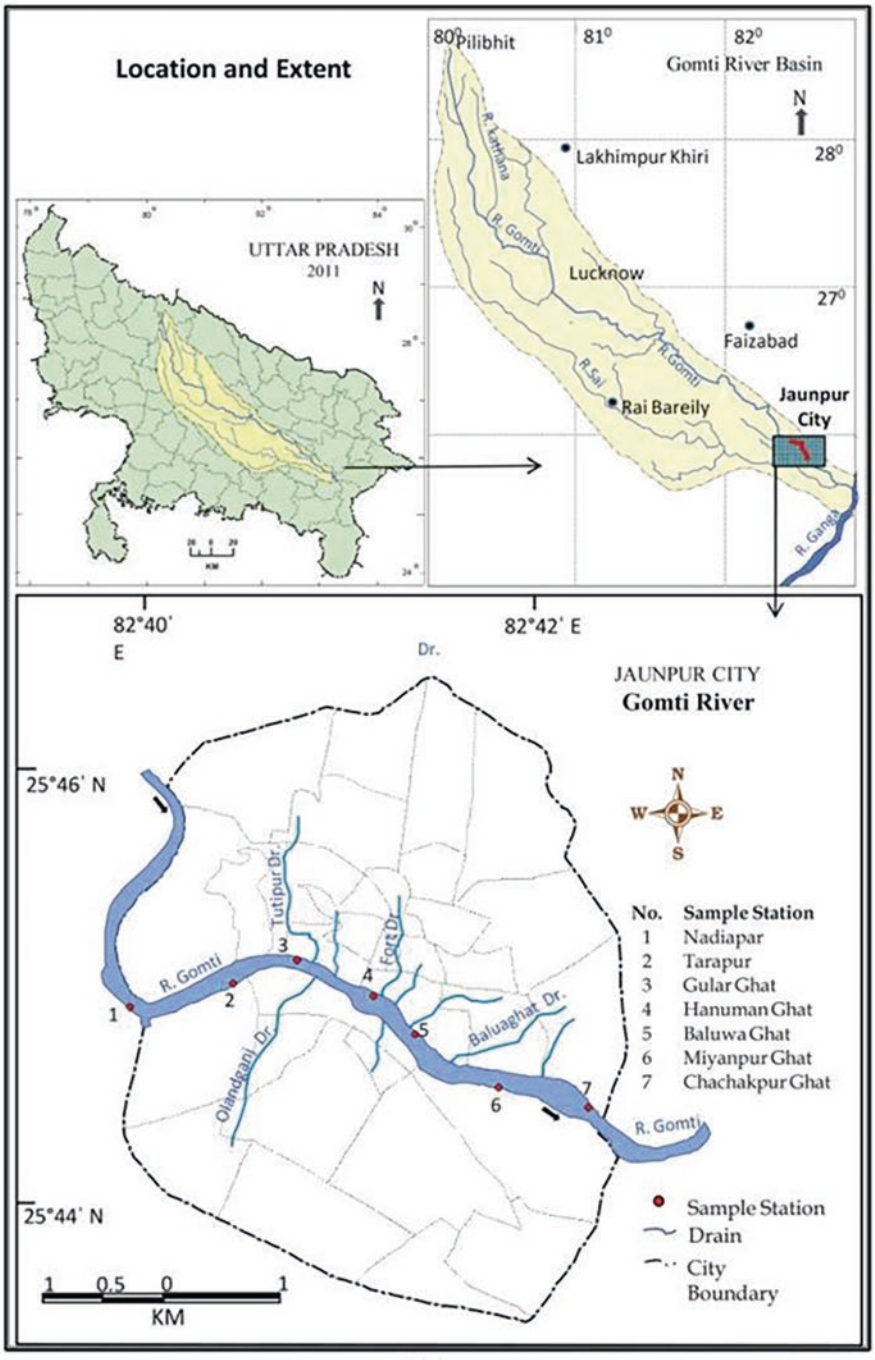


**Fig. 1** Map showing the Gomati River Basin (after Jigyasu et al., 2014) and sampling locations

oxygen (DO), total dissolved solids (TDS), electrical conductivity (EC), total hardness, calcium (Ca) ions, magnesium (Mg) ions, chloride, alkalinity, COD, and total alkalinity.

## 4 Result and Discussion

### *4.1 Level of Water Parameter in Gomti River, Pre-monsoon, Jaunpur City*

The study of various water parameters was made to acquire their level during different seasons. Studies show that the pH during the pre-monsoon period is high due to the huge influx of sewage and wastewater discharged from drains into the Gomti River. In general, the pH level declines from Nadiapar Ghat to Chachakpur sample stations due to an increasing number of drains and sewage (Table 1). During the post-monsoon period, the pH level declines due to a huge discharge of freshwater at an average of 7.68. The BOD is found high at all the sample stations. It varies from 6.5 mg/L (Nadiapar Ghat) to 8.4 mg/L (Chachakpur) with an average of 7.45 mg/L during pre-monsoon period. BOD level during pre-monsoon is higher than post-monsoon period at Nadiapar to Miyanpur Ghat due to discharge of sewage water from various drains. It shows that the BOD level remains higher than the standard given by the WHO guidelines. The DO (dissolved oxygen) is significant in

**Table 1** Water quality during pre-monsoon, Gomti River, Jaunpur city, 2016

| Sl. no. | Parameter | Nadiapar Ghat | Tarapur | Gular Ghat | Hanuman Ghat | Balua Ghat | Miyanpur Ghat | Chachakpur | WHO standard |
|---|---|---|---|---|---|---|---|---|---|
| 1 | pH | 8 | 8.0 | 8 | 7.8 | 7.7 | 7.6 | 7.6 | 8.5 |
| 2 | BOD (mg/L) | 6.5 | 7.1 | 7.5 | 7.9 | 8.9 | 8.9 | 8.4 | 6 |
| 3 | DO (mg/L) | 3.9 | 3.7 | 3.6 | 2.1 | 2.6 | 2.5 | 2.9 | 5 |
| 4 | Conductivity µ mohos/cm | 430.7 | 437.0 | 443.2 | 459.8 | 460.3 | 465.7 | 466.5 | 300 |
| 5 | Total hardness (mg/L $CaCO_3$) | 202 | 209.3 | 212.5 | 223.5 | 225 | 249.5 | 258.5 | 500 |
| 6 | Calcium (mg/L $Ca^{++}$) | 36 | 36.1 | 36.2 | 39.6 | 41.4 | 45 | 45.2 | 75 |
| 7 | Magnesium (mg/L $mg^{++}$) | 21.7 | 22.2 | 24.7 | 25.3 | 26 | 26.4 | 26.2 | 50 |
| 8 | Chloride (mg/L) | 24.8 | 25.7 | 25.8 | 27.8 | 28.5 | 32.8 | 31.4 | 250 |
| 9 | Alkalinity (mg/L CaCO3) | 211.5 | 225.3 | 239 | 241 | 250.5 | 260 | 269 | 200 |
| 10 | COD (mg/L) | 9.5 | 14.4 | 15.7 | 19.9 | 19.3 | 20.9 | 20.7 | 10 |
| 11 | T.D.S. (mg/L) | 218.5 | 220.0 | 225.5 | 233.5 | 252 | 256 | 254 | 500 |

Source: Field survey, 2016

determining the water quality criteria of water. Temperature plays an important function in determining DO in an aquatic body. DO levels observed during the pre-monsoon ranged between 3.9 mg/L (Nadiapar Ghat) and 2.9 mg/L (Chachakpur), with an average of 3.4 mg/L. During the early part of pre-monsoon period, there is a gradual decline in DO level. For the rest of the summer season, it remains comparatively low when the temperature of the river water increases and leads to increase in the rate of respiration and organic decomposition, whereas during the post-monsoon season, the DO level remains high at all the sample stations, ranging between 4.5 mg/L (Nadiapar Ghat) to 3.9 mg/L (Chachakpur) with an average of 4.17 mg/L due to huge influx of freshwater.

Conductivity ranges between 430.7μ mohos/cm (Nadiapar Ghat) to 466.5μ mohos/cm (Chachakpur) with an average of 451.9μ mohos/cm which is much extremely high than the WHO standard (300μ mohos/cm), but during the post-monsoon season, it ranges from 344.9μ mohos/cm (Nadiapar Ghat) to 411.9μ mohos/cm (Chachakpur) with an average of 377.2μ mohos/cm, due to the flux of rain water in the river (Table 2). The total hardness (TH) during the pre-monsoon ranges between 202 mg/L (Nadiapar Ghat) and 258.5 mg/L (Chachakpur) with an average of 225.7 mg/L, much below the standard limit of 300 μ mohos/cm, whereas during the post-monsoon period, TH ranges between 182 mg/L (Nadiapar Ghat) to 203.0 mg/L (Chachakpur) with an average of 194.0 mg/L. COD is a useful indicator of organic pollution in surface water (Nagwenya, 2006). Its level is lower than the

**Table 2** Water quality during post-monsoon, Gomti River, Jaunpur city, 2016

| Sl. no. | Parameter | Nadiapar Ghat | Tarapur | Gular Ghat | Hanuman Ghat | Balua Ghat | Miyanpur Ghat | Chachakpur | WHO standard |
|---|---|---|---|---|---|---|---|---|---|
| 1 | pH | 7.9 | 7.8 | 7.8 | 7.7 | 7.6 | 7.5 | 7.5 | 8.5 |
| 2 | BOD (mg/L) | 6.1 | 7.3 | 7.7 | 8.2 | 8.5 | 8.8 | 8.7 | 6 |
| 3 | DO (mg/L) | 4.5 | 4.4 | 4.4 | 4.1 | 4.0 | 3.9 | 3.9 | 5 |
| 4 | Conductivity μ mohos/cm | 344.9 | 348 | 355.1 | 377.2 | 394.9 | 408.4 | 411.9 | 300 |
| 5 | Total hardness (mg/L CaCO3) | 182 | 183 | 188.5 | 198.5 | 201 | 202.5 | 203 | 500 |
| 6 | Calcium (mg/L $Ca^{++}$) | 27 | 28.6 | 35.6 | 39.2 | 41.2 | 42.4 | 42.6 | 75 |
| 7 | Magnesium (mg/L $Mg^{++}$) | 18.1 | 18.6 | 19.2 | 20.1 | 21.7 | 22.6 | 22.7 | 50 |
| 8 | Chloride (mg/L) | 22.5 | 23.1 | 24.3 | 26.5 | 29.3 | 26.2 | 25.1 | 250 |
| 9 | Alkalinity (mg/L $CaCO_3$) | 203.2 | 208.3 | 213.5 | 217 | 225.5 | 232 | 235.5 | 200 |
| 10 | COD (mg/L) | 11.55 | 16.01 | 17.7 | 20.42 | 20.1 | 21.7 | 18.3 | 10 |
| 11 | T.D.S. (mg/L) | 192 | 202.5 | 219 | 222.5 | 227.5 | 238.5 | 239.5 | 500 |

Source: Field survey, 2016

permissible limit at Nadiapar sample station both during the pre- and post-monsoon periods because it is located in the outer fringe of the city with no drains. However, other sample stations show high concentrations of COD levels during the pre-monsoon ranging from 14.4 mg/L (Tarapur) to 20.7 mg/L (Chachakpur).

## 5 Calculation Water Quality Index (WQI)

The water quality index embodies a specific number (as grade) that represents the basic water quality at a definite location. Ziauddin and Siddiqui (2007) have defined it as a score showing the compound weight of various water quality parameters on the overall quality of water. Selection of many parameters might expand the water quality index, so different water parameters should be used as to the intended use of water (Sisodia & Moundiotya, 2006). Weighted Arithmetic Index method has been used for the calculation of the WQI present study (Chauhan & Thakor, 2012). The present analysis starts with the quality rating of each parameter; thus a quality rating ($Q_i$) was calculated (Table 3) as given below.

$$\text{Quality rating}\left(Q_i\right) = 100\left[\frac{\left(V_n - V_i\right)}{\left(S_n - V_i\right)}\right] \tag{1}$$

Where

$V_n$ = Estimated value of the $n$th parameter at a given sampling.
$V_i$ = Ideal value of $n$th parameter in pure water.
$S_n$ = Standard permissible value of $n$th parameter.

Each of the ideal values ($V_i$) are used as zero for drinking water except for pH = 7.0 and dissolved oxygen = 14.6 mg/L.

Calculation of relative weight ($W_i$) was done by a value inversely proportional to the recommended standard ($S_i$) of the corresponding parameters:

**Table 3** WQI of Gomti River, pre- and post-monsoon, Jaunpur, 2018

| Sample St. no. | Sample points | Pre-monsoon WQI | Post-monsoon WQI |
|---|---|---|---|
| I. | Nadiapar Ghat | 95.29 | 92.87 |
| II. | Tarapur | 106.42 | 104.36 |
| III. | Gular Ghat | 110.78 | 109.06 |
| IV. | Hanuman Ghat | 115.31 | 115.79 |
| V. | Balua Ghat | 122.50 | 115.91 |
| VI. | Miyanpur Ghat | 124.32 | 119.00 |
| VII. | Chachakpur | 120.53 | 114.02 |

Source: Field Survey, 2018

$$\text{Relative weight}\left(W_i\right) = \frac{1}{S_\text{i}} \tag{2}$$

Generally, WQI is discussed for a specific and intended use of water. In this study, the WQI for drinking water is considered. The overall WQI was calculated by using the following equation:

$$\text{Water Quality Index}\left(WQI\right) = \frac{\sum W_i Q_i}{\sum W_i} \tag{3}$$

$$WQI = \frac{\sum W_i Q_i}{\sum W_i} = \frac{44.29}{0.63} = \mathbf{69.86}$$

On the basis of different parameters for pre- and post-monsoon period, WQI is classified as good (below 100), moderately good (100–110), moderately poor (110–120), and poor (120 and above) (Table 4).

The data acquired from sampling stations shows that the parameters at downstream and the WQI are ranging from good to severe. The water quality is comparatively good in relation to the other six stations being located upstream of river Gomti in Jaunpur city. As per the observed data, these stations have good quality water for the purpose of drinking with conventional treatment. The sample station, particularly the second station which is located at Tarapur, has reasonably poor quality during the pre-monsoon season due to heavy influx load (solid waste) and wastewater discharged before the monsoon. However, during the monsoon season, the quality of water changes for the better due to commingle of freshwater caused by rainfall and surface runoff (Fig. 2).

Station III (Gular Ghat) has moderately good quality of water ranging from 109.06 to 110.78, respectively, for the post- and pre-monsoon periods due to the heavy discharges from Tutipur drain from the northern part and Olandganj drain from the southern part of the city. The northern region of this point is a highly dense populated area, and domestic discharges as wastewater and solid waste generation are very high and result in form of river water pollution. The fourth station, named Hanuman Ghat, is situated near the middle of the city and has a very large population density. The region around this point is the older part of the city; thus the region is developed as a residential cum commercial area. Several small and huge

**Table 4** Water quality classification based on WQI value

| Sl. no. | WQI value range | Water quality |
|---|---|---|
| 1 | Below 100 | Good |
| 2 | 100–110 | Moderately poor |
| 3 | 110–120 | Poor |
| 4 | Above 120 | Severe |

***Source***: Field Survey, 2018

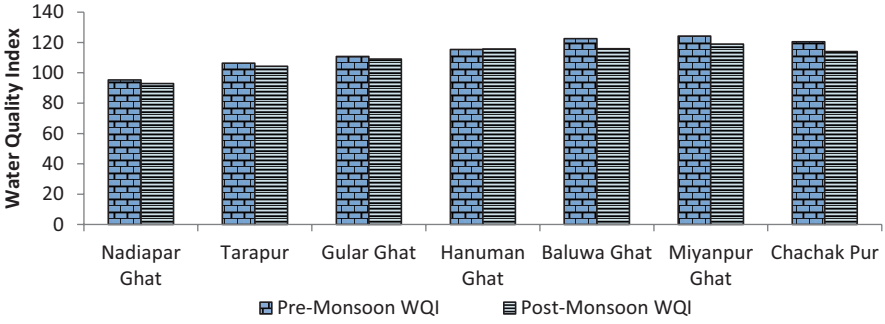


**Fig. 2** WQI of Gomti River, pre- and post-monsoon, Jaunpur, 2018

wastewater drains discharge huge amounts of polluted water into the river without any treatment procedure. Fort drain is one of the major drains which join the river from the northern part of the region. Thus, this station has a comparatively higher load of pollution, and WQI ranges from 115.31 to 115.89 from pre-monsoon to post-monsoon, respectively. The fifth station is also a highly polluted station, as several drains join the point from Machharhatta, Rasmandal, Pyarali, Tadtala, and Urdubazar wards in the northern region and from Olandganj, Umarpur, Jahangirabad, and Hussainabad ward in southern part of the city, which results to higher pollution load at Balua Ghat ranging between 120.83 and 122.50 WQI from post- to pre-monsoon period, respectively. The sixth sample station, Miyanpur Ghat, has very high WQI from the rest of the point as it ranges between 123.27 and 124.32 from pre-monsoon to post-monsoon periods, respectively. The region around this point is also a highly populated region of the city. Several drains discharge wastewater from Miyanpur, Hussainabad, Rashmand, and Machharhatta ward from both sides of the river. There is a decreasing trend in pollution that can be seen in the last station (Chachakpur), which is located at almost the end of the stretch in the city area. The population density around this sample station is comparatively lower than the other stations located upstream. This station has WQI ranging between 119.60 and 120.53 from the post-monsoon to pre-monsoon periods, respectively.

## 6 Conclusion

It is reflected through the study that the river water is found severely polluted due to huge discharge of domestic, municipal, as well as industrial waste through various drains from both sides of the river. The increase in value of alkalinity and total hardness were observed higher due to domestic and municipal waste discharges. Domestic waste, municipal waste, and industrial effluent are very high from Tarapur to Miyanpur Ghat. WQI values at various sampling stations represent that there is progressive amplification in WQI values along the downstream specifies that an increase in pollution is due to effluent discharge. The severe water quality (WQI) at

sampling station VI is due to human economic activities and unplanned development. The DO, BOD, TDS, COD, and other parameters at some of the stations have been observed beyond the permissible limit; water samples are polluted and are not appropriate for beneficial uses without any conventional handling. The regular increase in water quality index values along the downstream indicates an increase in the level of pollutants due to the heavy discharge by domestic and various industries along the stretch. The dreadful WQI values at all the sampling stations are due to various anthropogenic activities, which should be immediately healed to save the surface water quality of the region.

## References

Abida, B., & Harikrishna. (2008). Study on the quality of water in some streams of Cauvery River. *Journal of Chemistry, 5*(2), 377–384.

Babel, M. S., & Wahid, S. M. (2008). *Fresh water under threat, South Asia* (pp. 1–29). United Nation Environmental Programme.

Bhardawaj, V., Singh, D. S., & Singh, A. K. (2010). Water quality of the Chhoti Gandak River using principal component analysis, Ganga Plain, India. *Journal of Earth System Science, 119*(1), 117–127.

Bharti, N., & Katyal, D. (2011). Water quality indices used for surface water vulnerability assessment. *International Journal of Environmental Sciences, 2*(1), 154–173.

Carle, M. V., Halpin, P. N., & Stow, C. A. (2005). Patterns of watershed urbanization and impacts on water quality. *Journal of the American Water Resources Association, 41*(3), 693–708.

Central Water Commission Report. (2011). *Water quality hot spots in river of India*. Central Water Commission.

Chauhan, N. B., & Thakor, F. J. (2012). A study of Water Quality Index (WQI) of Heranj Lake, Dist. Kheda-Gujarat. *Asian Journal of Biological Sciences, 3*(3), 582–588.

CPCB Report. (2010). *Status of water quality in India-2009, Delhi*. Central Pollution Control Board.

CWC. (2018). *River water quality monitoring*. http://www.india-wris.nrsc.gov.in/wrpinfo/index.php?title=River_Water_Quality_Monitoring#River_Water_Pollution

Dhakad, N. K., Shinde, D., & Choudhary, P. (2008). Water quality index of ground water (GWQI) of Jhabua town, M.P. (India). *Journal of Environmental Research and Development, 2*(3), 443–446.

Dutta, V., Srivastava, R. K., Yunus, M., Ahmed, S., Pathak, V. V., Rai, A., & Prasad, N. (2011). Restoration plan of Gomti River with designated best use classification of surface water quality based on river expedition. *Monitoring and Quality Assessment, 4*(III), 80–104.

Dutta, V., Sharma, U., & Kumar, R. (2015). Assessment of river ecosystems and human-induced stress on hydrological regime – A case study of Gomti River Basin, India. In: *E-proceedings of the 36th IAHR world congress*.

Eaton, A. D., Clesceri, L. S., Greenberg, A. E., & Franson, M. A. H. (1998). *Standard methods for the examination of water and wastewater*. American Public Health Association, Washington, DC.

Horton, R. K. (1965). An index number system for rating water quality. *Journal of the Water Pollution Control Federation, 3*, 300–305.

Jigyasu, D. K., Kuvar, R., Shahina, Singh, P., Singh, S., Singh, I. B., & Singh, M. (2014). Chemical weathering of biotite in the Ganga Alluvial Plain. *Current Science, 106*(11), 1484–1486.

Kumar, A., & Dua, A. (2009). Water quality index for assessment of water quality of river ravi at Madhopur (India). *Global Journal of Environmental Sciences, 8*(1), 49–57.

Kumar, S. K., Rammohan, V., Sahayan, J. D., & Jeevanandam, M. (2008). Assessment of groundwater quality and hydro-geochemistry of Manimuktha River basin, Tamil Nadu, India. *Environmental Monitoring and Assessment, 159*(1–4), 341–351.

Lurent, M., Francois, A., & Marie, M. J. (2010). Assessment of groundwater quality during dry season in South-Eastern Brazzaville, Congo. *International Journal of Applied Biology and Pharmaceutical Technology, I*(3), 762–769.

Madhav, S., Ahamad, A., Kumar, A., Kushawaha, J., Singh, P., & Mishra, P. K. (2018). Geochemical assessment of groundwater quality for its suitability for drinking and irrigation purpose in rural areas of Sant Ravidas Nagar (Bhadohi), Uttar Pradesh. *Geology, Ecology, and Landscapes, 2*(2), 127–136.

Nagwenya, F. (2006) *Water quality trends in the Eerste River, Western Cape, 1990–2005*. A mini thesis submitted in partial fulfillment of the requirements for the degree of Magister Scientiae: Integrated Water Resources Management in the Faculty of Natural Science, University of Western Cape, p. 41.

Nickson, R. T. (2004). Arsenic and other drinking water quality issues, Muzaffargarh District, Pakistan. *Applied Geochemistry, 20*, 1–14.

Parmar, K., & Parmar, V. (2010). Evaluation of water quality index for drinking purposes of river Subarnarekha in Singhbhum District. *International Journal of Environmental Sciences, 1*(1), 77–81.

Phiri, O., Mumba, P., Moyo, B. H. Z., & Kadewa, W. (2005). Assessment of the impact of industrial effluents on water quality of receiving rivers in urban areas of Malawi. *International Journal of Environmental Science and Technology, 2*(3), 237–244.

Razak, A., Asiedu, A. B., EntsuaM, R. E. M., & Graft-Johnson, K. A. A. (2009). Assessment of the water Quality of the Oti River in Ghana. *West African Journal of Applied Ecology, 15*. https://doi.org/10.4314/wajae.v15i1.49427

Samantray, P., Mishra, B. K., Panda, C. R., & Rout, S. P. (2009). Assessment of Water Quality Index in Mahanadi and Atharabanki Rivers and Taladanda Canal in Paradip area, India. *Journal of Human Ecology, 26*(3), 153–161.

Singh, R. B. (2002). *Environmental problems and management; a geographical study of Lucknow city*. Unpublished thesis: Department of Geography, BHU, Varanasi, pp. 48–58.

Singh, M. (2014). Exploration for eco reforms strategies and management of urban landscape of Jaunpur City. *Indian Journal of Life Sciences, 4*(1), 89–93.

Singh, N. B., & Pandey, S. (2010). Heay metal content in Gomti River water, sediment and hydrobiota in Jaunpur. *Asian Journal of Environmental Science, 5*(1), 53–57.

Singh, M., & Singh, R. N. (2010). Pollution status of Gomati River at Kerakat, Jaunpur, U.P. *Indian Journal of Scientific Research, 1*(2), 101–102.

Singh, P. K., & Singh, A. K. (2014a). Assessment of the microbiological quality of the river Gomati at Jaunpur (U.P.) India. *International Journal of Life Science & Pharma Research, 4*(4), 11–16.

Singh, P. K., & Singh, A. K. (2014b). Water quality assessment of river Gomati at Jaunpur (U.P.) India. *International Journal of Pharma and Bio Sciences, 5*(4), 520–526.

Singh, V. P., Raghuvanshi Singh, A. K., Singh, P., Singh, S. K., & Singh, A. K. (2016). Assessment of water quality in the river Gomati at Jaunpur (U.P.). *Annals of Plant Science, 5*(3), 1312–1317.

Singha, K. P., Malik, A., Mohan, D., Sinha, S., & Singh, V. K. (2005). Chemometric data analysis of pollutants in wastes water-a case study. *Analytica Chimica Acta, 532*, 15–25.

Sisodia, R., & Moundiotya, C. (2006). Assessment of the water quality index of wetland Kalakho Lake, Rajasthan, India. *Journal of Environmental Hydrology, 14*, 1–23.

Subramanian, V. (2004). Water quality in South Asia. *Asian Journal of Water, Environment and Pollution, 1*(1, 2), 41–54.

Susilo, G. E., & Febrina, R. (2011). The simplification of DOE Water Quality Index calculation procedures using graphical analysis. *Australian Journal of Basic and Applied Sciences, 5*(2), 207–214.

Swedish Water House Report 21. (2007). *Planning for drinking water and sanitation in peri-urban areas*. Britt-Louise Andersson: Stockholm International Water Institute, SIWI.

Trivedy, R. K., & Goel, P. K. (1986). Chemical and Biological method for water pollution studies. *Environmental publication* (Karad, India), *6*, 10–12.

Tandon, H. L. S. (1995). *Methods of analysis of soil, plants, water and fertilizers*. Fertilizer Development and Consultation Organization. New Delhi.

UNDESA (United Nation Department of Economic and Social Affairs) (2015). *International decade for action 'Water for life' (2005–2015). Water quality.* Available at https://www.un.org/waterforlifedecade/quality.shtml

UN Water Members and Partners. (2011). *Water quality*. UN-Water Partners. www.unwater.org

UNEP. (2010). *Clearing the waters: A focus on water quality solutions*. Pacific Institute.

UNEP. (2016). *A snapshot of the world's water quality: Towards a global assessment, Nairobi, Kenya*. Available at uneplive.unep.org/media/docs/assessments/unep_wwqa_report_web

UNEP Report. (2007). *Global drinking Water Quality Index development and sensitivity analysis report* (p. 3). UNEP.

United Nations Environment Programme. (2008). *Water Quality for Ecosystem and Human Health* (2nd ed.). UNEP.

WHO. (2009). *Calcium and magnesium in drinking-water public health significance* (pp. 2–50). WHO.

WHO. (2013a). *World health statistics 2013*. World Health Organisation.

WHO. (2013b). *Fast fact progress on sanitation and drinking water, 2013*. World Health Organization. http://www.who.int/water_sanitation_health/en/index.html

Wong, C. M., Williams, C. E., Pittock, J., Collier, U., & Schelle, P. (2007). *World's top 10 rivers at risk*. WWF HSBC Yangtze Programme.

Ziauddin, A., & Siddiqui, N. A. (2007). Ground water quality of a coastal area – A case study. *Ecology, Environment and Conservation, 13*(3), 645–648.

# Geomorphology of the Son River Basin, India Based on Remotely Sense Data: A Review


**S. Kanhaiya, S. Singh, S. K. Yadav, and S. D. Pasi**

## 1 Introduction

The development of remote sensing and GIS technology has tremendously helped the study of the Earth's surface, shape, and landscapes in recent decades. Morphometric analysis involves taking measurements and studying the Earth's surface and landforms mathematically (Clarke, 1966). Based on remotely sensed data, the main morphometric parameters of a river basin can be estimated with ease. Morphometric analysis can be used to determine a river basin's fundamental properties, including its area, height, form, size, slope, and profiles (Kanhaiya et al., 2018).

The tracking of the neotectonic fingerprints that control the dynamics of the entire basin is also greatly aided by the morphometric parameters (Thomas et al., 2010). Organizing the various streams, measuring the area and perimeter of catchments, calculating the length of drainage channels, stream frequency, bifurcation ratio, texture, circulatory ratio, and channel maintenance constant are all made simpler by the assessment of the morphometric parameters (Nag and Chakraborty, 2003). Different morphometric parameters can be used to investigate a river basin's topography, surface water hydrology, sediment yield, structural controls, geomorphological past, drainage patterns and evaluation history (Strahler, 1957). The use of morphometric analysis and results is necessary to apply appropriate catchment management approaches (Senadeera et al., 2001; Kanhaiya et al., 2018).

S. Kanhaiya (✉) · S. K. Yadav · S. D. Pasi
Department Earth and Planetary Sciences, Prof. Rajendra Singh (Rajju Bhaiya) Institute of Physical Sciences for Study and Research, VBS Purvanchal University, Jaunpur, Uttar Pradesh, India

S. Singh
Department of Geology, Institute of Earth and Environmental Sciences, DR. Rammanohar Lohia Avadh University, Ayodhya, Uttar Pradesh, India



S. Kanhaiya et al. (eds.), *Rivers of India*,
https://doi.org/10.1007/978-3-031-49163-4_9

Since the last 10 years, numerous researchers in India have embraced morphometric analysis as a powerful tool for river basin management and assessing geotechnical control (Singh & Kanhaiya, 2015; Prakash et al., 2016, 2017; Kanhaiya et al., 2018). The objective of this research is to characterize the morphometric parameters of the Son River Basin, to ascertain how the underlying geology affects those parameters, and to produce a substantial body of knowledge about the relationships between surface morphometry and subsurface lithology for integrated basin management.

## 2 Study Area

The various morphometric parameters of the Son River and its major tributaries (i.e., Ghaghghar River, Kanhar River, Dongar River and Rihand River) were compiled and interpreted in the current paper. One of the major rivers in Central India, the Son River flows through the Vindhyan hills and is located between 22°43′48″N and 25°42′21″N and 82°03′31″E and 84°51′44″E (Rao, 1975). Of its total length of 784 km, 500 km are in Madhya Pradesh, 82 km are in Uttar Pradesh, and 202 km are in Jharkhand and Bihar. The Ganga River and the river's 71,259 km$^2$ catchment area meet in the Patna district of Bihar after rising in Amarkantak, Madhya Pradesh (Rao, 1975).

The Ghaghghar River, which runs from the village of Soma between latitudes of 24°32′58.02″N and 24°31′43.14″N and 83°23′19.02″E and 83°02′47.42″E, forms a significant barrier between the Bijaigarh shale and the Scarp sandstone. The river rapidly alters its course and begins following a N-S trend before interring in the Rohtas limestone and then in glauconitic sandstone before confluence with River Son at Patwdh village in Sonbhadra district of Uttar Pradesh. This is due to the Markundi Fault striking in an ENE-WSW direction.

With a length of 400 km and a basin area of 5654 km$^2$, the Kanhar River (23°12′N to 24°27.2′N and 83° 2′E to 84°1′E) is a significant tributary of the Son River that flows through the Indian states of Chhattisgarh, Jharkhand and Uttar Pradesh. The Kanhar River rises in Gidha-Dhodha on the Khudia plateau in the Chhattisgarh district of Jashpur, where it merges with the Son River northeast of the village of Kota in the Uttar Pradesh district of Sonbhadra.

The Son-Narmada North Fault is where the Dongar River originates from the Mahakoshal Group of Rock (24°32′24.51″N to 24°36′3.01″N and 82°47′38.56″E to 82°48′43.71″E). The Dongar River then begins to flow in the lower Vindhyan before coming together with the Son River close to Newari Village of Sonbhadra District, Uttar Pradesh. It is a little river with a length of 12 km and a drainage area of 35.17 km$^2$ in total (Fig. 1). The river flows first in a westward direction before turning northward and flowing into lower Vindhyan.

A tributary of the Son River, the Rihand River runs through the Indian states of Madhya Pradesh, Uttar Pradesh and Chhattisgarh. Geographic latitudes 22°30′N to 24°30′N and longitudes 82°00′E to 83°45′E are where the Rihand River is located (Fig. 1). About 2100 m above mean sea level, in the area southwest of the Mainpat plateau, the Matiranga hills are the source of the Rihand River. For around 160 km,

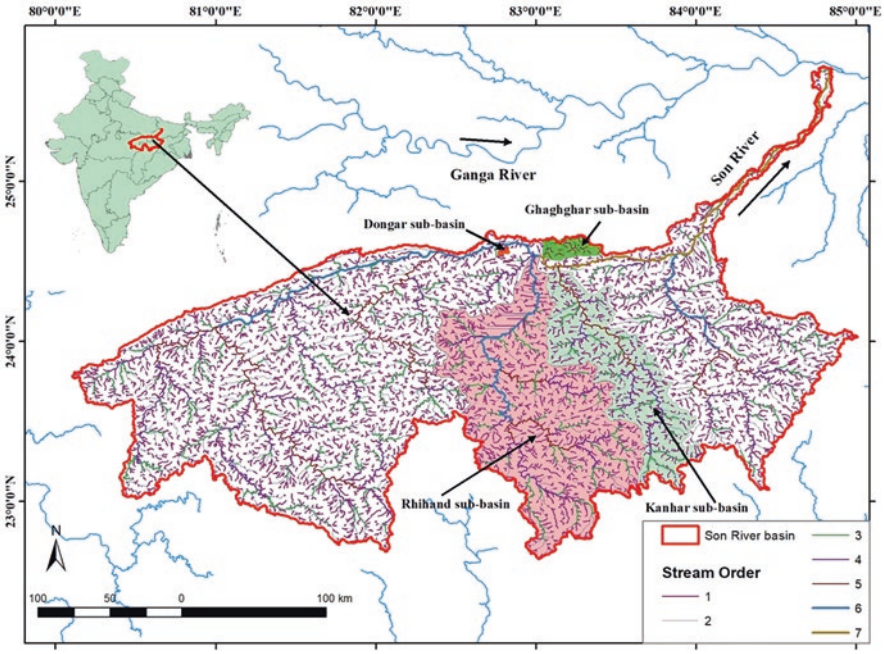


**Fig. 1** Map of the study area showing Son River Basin

the river flows north through the center of the Surguja district. After that, it travels through the Singrauli district of Madhya Pradesh into the Sonbhadra district of Uttar Pradesh, where it is known as Rihand, and merges with the Son River.

## 3 Result and Discussion

Morphometric information from past studies has been compiled for a comparison analysis of the Son River and its tributaries, the Ghaghghar River, Kanhar River, Dongar River, and Rihand River. Dongar River has a fourth-order stream, Son River has a sixth-order stream, Kanhar River has a seventh-order drainage stream, Ghaggar River has a third-order stream network and Rihand River has a third-order stream network (Table 1).

This suggests that Son, Dongar, Ghaghghar, and Rihand River follow Kanhar River in the stream order of importance. Dendritic drainage patterns are typical of Son River and its tributaries, with trellis drainage patterns in some of the basins. The tributaries of Son River, Ghaghghar River, Rihand River, Dongar River and Kanhar River all have average stream length ratios of 0.66, 0.79, 1.56, 0.83 and 0.51 respectively. The slope and local topography affect the ratios of different river stream lengths, which in turn affect the flow and erosional activity of the watershed.

**Table 1** Showing the stream order (Nu) of the Son River and its tributaries (values are taken from the Rai et al., 2014, 2017; Kanhaiya et al., 2018; Kumar et al., 2018; Singh et al., 2019)

| River/stream order (Nu) | I | II | III | IV | V | VI | VII |
|---|---|---|---|---|---|---|---|
| Son River | 4789 | 1991 | 205 | 22 | 07 | 01 | |
| Kanhar River | 9541 | 3337 | 856 | 204 | 39 | 9 | 1 |
| Ghaghghar River | 26 | 5 | 1 | | | | |
| Dongar River | 19 | 12 | 3 | 1 | | | |
| Rihand River | 4113 | 2240 | 1699 | | | | |

The bifurcation ratio is defined as the ratio of the number of stream segments in one order to those in the next higher level (Schumm, 1956). Horton (1945) interpreted the bifurcation ratio as a gauge of relief and dissections. It also exerts a large amount of control over the runoff's infirmity and acts as a gauge for the drainage network's degree of ramification (Mesa, 2006). With the exception of regions where geology is dominant, Strahler (1957) found that the bifurcation ratio changes only slightly between geographic regions or environmental settings.

The Son River Basin's bifurcation ratio is 4.70 (mean; range: 2.41–7.0), while the Rihand River Basin's is 1.57 (mean; range: 1.31–1.83). Bifurcation ratios in the Dongar River Basin range from 1.58 to 4.0, with a mean of 2.86. It is 1.583.0 for the first to second orders, indicating that the basin is formed in an inhomogeneous terrain, but it is 4.0 for the second to third orders and 3.0 for the third to fourth orders, indicating that the topography is variable. The variance in stream network and morphology is also reflected in the change in bifurcation ratio. The bifurcation ratio in the Kanhar river basin ranges from 2.86 to 9, with a mean value of 4.0.

Higher values indicate that there is a strong structural control and a risk of floods in this zone, while lower values indicate that the subbasin is less affected by structural disturbances. There is virtually little structural control in the Ghaghghar River Basin, as evidenced by the mean bifurcation ratio of 5.1 and the bifurcation ratios of 5.0 and 5.2, respectively. The Son River Basin has a drainage density rating of 0.26 km/km$^2$, which denotes a rough drainage texture, a permeable subsurface and dense vegetation cover.

The drainage density for the Rihand River Basin is 0.06 km/km$^2$, indicating that the region has a coarse drainage texture, little runoff, less risk of erosion and close-packed channel spacing. The low drainage density estimates point to the Rihand River Basin area's low relief and extremely resistant permeable material. A basin area with a dense canopy of vegetation, a moderate drainage density and porous subsoil are revealed by the Dongar River, which shows drainage density of 1.21 km/km$^2$. The Ghaghghar River Basin has a drainage density value of 0.36 km/km$^2$, which indicates a rough drainage texture, a permeable subsurface and dense vegetation cover.

The Kanhar River Basin reveals a permeable subsurface with an intermediate drainage density and low to moderate relief with a drainage density of 1.72 km/km$^2$. The combination between the geology of the basin region and climate is what causes fluctuations in drainage density. The distance between drainage ways is referred to as drainage density because, according to Horton (1932), there is a strong correlation

between drainage density, precipitation, and evaporation. A higher drainage density indicates that the channels are closer together.

Both the Son River Basin and the Rihand River have relief ratios of 2.23 and 1.33, respectively, indicating low to moderate relief and slope. The Kanhar River Basin has a relief ratio of 0.09, which implies very little relief. The Ghaghghar River Basin has a larger relief ratio (4.67) than the Kanhar River Basin, indicating a steeper slope. Again, the Dongar River Basin has an extraordinarily low relief ratio, 0.03 (less than 1.0), indicating low relief, which reveals the basement rocks as minute ridges and mounds.

The Ghaghghar River has the highest relief ratio of all the rivers, and the Dongar River has the lowest relief ratio, showing variances in drainage and basin slope steepness. This illustrates how the channel gradient and relief of several watersheds connect to one another. Relief ratio is a gauge of the general steepness of a drainage basin as well as the rate of erosional processes occurring on the slope of the basin (Schumm, 1956; Rai et al., 2017). The ratio of a circle's diameter to its greatest length in relation to the same area as the drainage basin is known as the elongation ratio, according to Schumm (1956).

The geology and aerial climate have a significant impact on this determination of the river basin's form. To determine whether a basin is circular, elongated or oval in shape, it is essential to use the morphometric statistic known as the elongation ratio. Circular shapes have an elongation ratio value larger than 0.9, oval shapes between 0.9 and 0.8, less than 0.7 and basin shapes with an elongation ratio extremely close to 0.

While the Dongar River's elongation ratio of 0.86 indicates that the basin is oval-shaped and has moderate-to-high surface runoff, the Son River's elongation ratio of 0.55 indicates that the basin is more or less elongated. The Ghaghghar River's elongation ratio of 0.64 indicates that the basin is less elongated and has low to moderate surface runoff. The Rihand River's elongation ratio value of 0.25 indicates a relatively modest amount of surface runoff and an extended basin. The Kanhar River's elongation ratio value of 0.48 indicates little surface runoff, high infiltration rates, and a somewhat elongated shape for the basin.

With a circulation ratio of 0.11 for the Rihand River Basin and 0.60 for the Ghaggar River Basin, the Son River Basin circulatory ratio is 0.13, the Kanhar River Basin circulation ratio is 0.15 and the Dongar River Bas circulation ratio is 0.13. The circulation ratio values discovered for several basins are similar to the elongation ratio of the basins. The circulatory ratio is usually influenced by the length and frequency of the streams, slope, geological features and local weather circumstances. It also acts as a signpost for the young, old and mature phases of any given watershed's development. The stream frequency is calculated as the sum of all stream segments for each unit area (Horton, 1932).

The stream frequency of the Son River Basin is 0.26 km/km$^2$, that of the Rihand River Basin is 0.60 km/km$^2$, that of the Dongar River Basin is 1.02 km/km$^2$, that of the Ghaghghar River Basin is 0.07 km/km$^2$ and that of the Kanhar River Basin is 2.45 km/km$^2$. Overall, the stream frequency measurements showed that all of the river basins under study had low topography and permeable subsurface material (Table 2).

**Table 2** Showing the different morphometric parameters of Son River and its tributaries (values are taken from the Rai et al., 2014, 2017; Kumar et al., 2018; Singh et al., 2019)

| River/morphometric parameters | Son River | Kanhar River | Dongar River | Rihand River | Ghaghghar River |
|---|---|---|---|---|---|
| Stream order | 6 | 7 | 4 | 3 | 3 |
| Total stream length (km) | 17820.69 | 9798.71 | 92.67 | 815.34 | 162.57 |
| Mean stream length ratio (RL) | 0.66 | 0.53 | 0.84 | 1.56 | 0.79 |
| Mean bifurcation ratio (Rb) | 4.70 | 1.57 | 2.86 | 5.7 | 5.1 |
| Form factor (F) | 0.25 | 0.18 | 0.46 | 0.3 | 0.32 |
| Circulatory ratio (Rc) | 0.13 | 0.15 | 0.13 | 0.11 | 0.60 |
| Drainage density (Dd) | 0.26 | 1.72 | 1.21 | 0.06 | 0.36 |
| Stream frequency (Fs) | 0.26 | 2.45 | 1.02 | 0.6 | 0.07 |
| Elongation ratio (Re) | 0.55 | 0.48 | 0.86 | 0.25 | 0.64 |

## 4 Summary and Conclusion

Kanhar is the seventh-order stream basin, followed by the Dongar River (fourth order), Rihand and Ghaghghar according to thorough morphometric studies of the Son River and its tributaries. Stream orders 1 through 6 (third order) are present in the Son River. The drainage patterns of all the examined rivers, which range from dendritic to sub-dendritic, point to a more or less consistent lithology in the basin region. According to the stream length ratio and circulation ratio, the Son, Rihand, Kanhar, and Dongar River Basins appear to be in a young stage of geomorphic evolution, but the Ghaghghar River is in a young to mature stage. The Son and Ghaghghar River Basins feature substantial relief compared to the Kanhar, Dongar, and Rihand River Basins has modest relief. The Son, Ghaghghar, Rihand and Kanhar River basins are elongated according to the elongation ratio, while the Dongar Basin has an oval shape. Lower values of the elongation ratio imply limited infiltration capacity and are very vulnerable to erosion and sediment load, whereas higher values reflect good infiltration ability. The bifurcation ratio of the Son, Ghaghghar and Kanhar Rivers suggests some tectonic influences on the basins; however, the Dongar and Rihand Rivers are not affected by any tectonic activity. The Son, Ghaghghar and Kanhar Basin's structural variety, trellis drainage pattern, and lithological variation all indicate tectonic control. Son River and all of its tributaries have coarse drainage densities, with the exception of Dongar River, which has a moderate drainage texture. Overall, the comprehensive comparative morphometric assessments of the Son River and its tributaries are very helpful for future infrastructure development as well as for managing watersheds, managing groundwater, and preventing floods.

**Acknowledgments** SK is thankful to the University Grant Commission, New Delhi, for providing UGC-BSR-Startup-Grant (Letter No. F. 30-517/2020). SDP is grateful to the CSIR, New Delhi, for providing financial assistance in the form of Junior Research Fellowship (JRF). We also gratified to the editors of the book for inviting us to write the chapter.

## References


Clarke, C. (1966). *Morphometry from maps* (Essay in geomorphology) (pp. 235–274). Elsevier publication company.

Horton, R. E. (1932). Drainage basin characteristics. *Transactions American Geophysical Union Publications, 13*, 350–361.

Horton, R. E. (1945). Erosional development of streams and their drainage basins: Hydrophysical approach to quantitative morphology. *Geological Society of America Bulletin, 56*, 275–370.

Kanhaiya, S., Singh, B. P., Singh, S., Mittal, P., & Srivastava, V. K. (2018). Morphometric analysis, bed-load sediments and weathering intensity in the Khurar River Basin, Central India. *Geological Journal*. https://doi.org/10.1002/gj.3194

Kumar, B., Venkatesh, M., & Tripathi, A. (2018). A GIS-based approach in drainage morphometric analysis of Rihand River Basin, Central India. *Sustainable Water Resource Management, 4*, 45–54. https://doi.org/10.1007/s40899-017-0118-3

Mesa, L. M. (2006). Morphometric analysis of a subtropical Andean basin (Tucuman, Argentina). *Environmental Geology, 50*, 1235–1242.

Nag, S. K., & Chakraborty, S. (2003). Influence of rock type and structure in the development of drainage network in hard rock area. *Journal of Indian Society of Remote Sensing, 31*(1), 625–635.

Prakash, K., Singh, S., & Shukla, U. K. (2016). Morphometric changes of the Varuna river basin, Varanasi district, Uttar Pradesh. *Journal of Geomatics, 10*, 48–54.

Prakash, K., Mohanty, T., Pati, J. K., Singh, S., & Chaubey, K. (2017). Morpho-tectonics of the Jamini River basin, Bundelkhand Craton, Central India; using remote sensing and GIS technique. *Applied Water Science, 7*, 3767–3782.

Rai, P. K., Mohan, K., Mishra, S., Ahmad, A., & Mishra, V. N. (2014). A GIS-based approach in drainage morphometric analysis of Kanhar River Basin, India. *Applied Water Science, 7*(1), 217–223.

Rai, P. K., Mishra, V. N., & Mohan, K. (2017). A study of morphometric evolution of the Son basin, India using geospatial approach. *Remote Sensing Applications: Society and Environment, 7*, 9–20.

Rao, K. L. (1975). *India's water wealth* (255 p). Orient Longman.

Schumm, S. A. (1956). Evolution of drainage system and slopes in badlands at Perth Amboy, NEW Jessey. *Geological Society of America Bulletin, 67*, 597–646.

Senadeera, K. P. G. W., Piyasiri, S., & Nandalal, K. D. W. (2001). The evolution of morphometric characteristics of Kotmale reservoir catchment using GIS as a tool, Sri Lanka. *The International Archives of Photogrammetry, Remote Sensing and Spatial Information Sciences, 34*(3), 1–3.

Singh, S., & Kanhaiya, S. (2015). Morphometry of the Barakar river basin, India: A remote sensing and GIS approach. *International Journal of Current Research, 7*(7), 17948–17955.

Singh, S., Kanhaiya, S., Singh, A., & Chaubey, K. (2019). Drainage network characteristics of the Ghaggar River Basin (GRB), Son Valley, India. *Geology, Ecology, and Landscapes, 3*(3), 159–167.

Strahler, A. (1957). Quantitative analysis of watershed geomorphology. *Transactions American Geophysical Union Publications, 38*, 913–920.

Thomas, J., Joseph, S., & Thrivikramaji, K. P. (2010). Morphometric aspects of a small tropical mountain river system, the southern Western Ghats, India. *International Journal of Digital Earth, 3*, 135–156.

# Role of Rivers in the Carbon Cycle and the Impact of Anthropogenic Activities


**Deepika Sharma**

## Abbreviations

| | |
|---|---|
| C | Carbon |
| $CH_4$ | Methane |
| $CO_2$ | Carbon dioxide |
| DIC | Dissolved Inorganic Carbon |
| DOC | Dissolved Organic Carbon |
| DOM | Dissolved Organic Matter |
| GHG | Greenhouse Gas |
| $HCO_3$ | Bicarbonate |
| NASA | National Aeronautics and Space Administration |
| OM | Organic Matter |
| POC | Particulate Organic Matter |
| SGD | Submarine Groundwater Discharge |

## 1 Introduction

The water that runs across rivers supports the flora and animals together with the inhabitants of its banks. Rivers are described as "the gutters down which flow the ruins of continents" in Leopold et al. (1964). The statement refers to how rivers affect the geomorphology of continents, which digests the majority of images of the global carbon cycle. The global carbon cycle controls the amount of atmospheric $CO_2$, which in turn controls the temperature and habitability of our planet. By dispersing silt and organic matter across the landscape, rivers play a significant role in the carbon cycle. Around the world, rivers have undergone extensive man-made modification, which has an impact on important biogeochemical cycles. In the coastal regions of the world, rivers transport and transform enormous amounts of carbon. For instance, the breakdown of vascular plant-derived OM to $CO_2$ is boosted

D. Sharma (✉)
School of Environmental Sciences, Jawaharlal Nehru University, New Delhi, India
e-mail: deepik99_ses@jnu.ac.in



S. Kanhaiya et al. (eds.), *Rivers of India*,
https://doi.org/10.1007/978-3-031-49163-4_10

by up to six times in the Amazon River when algae-rich tributaries mix with the silt and terrestrially generated OM-rich main channel (Ward et al., 2017). Globally, a sizable amount of carbon is transported and changed in the coastal regions. This transformation and transfer of carbon, which is caused by mechanisms such as altering hydrology, water temperature, and in-stream metabolic rates, clearly demonstrates the effects of urbanization and climate change. Changes in sources and exports have an impact on ecosystem activity, food webs, and greenhouse gas emissions (Smith & Kaushal, 2015). By connecting the oceans and mountain rocks while traversing the floodplains, they become the Earth's circulatory system. Major rivers' banks served as the starting point for the development of major civilizations. Rivers have supported a variety of other activities, while the chronicles eventually contributed their essence through the location, history, and cultural heritage. Some of them are agriculture, aquaculture, transportation, industrial development, and entertainment (Borthakur & Singh, 2016). Although there are numerous nutrients that are part of the living processes, one important ingredient that is transported by river waters is carbon, which is a necessary component of all life on Earth. The human population that is concerned about climate change develops strategies to sequester surplus atmospheric carbon dioxide in the Earth. The rivers are among the most comprehensible sources of carbon export from the boundaries of continents. They produce a significant flow, which may be calculated from estimations of water output and aqueous carbon concentrations. Considering the recent increases in $CO_2$ concentrations in the atmosphere, it is essential to comprehend the carbon cycle and $CO_2$ exchange among the environment's many reservoirs. The movement of carbon from the land to the oceans and atmosphere is facilitated by rivers and estuaries. Numerous estuarine processes have a significant influence on these fluxes because carbon participates in a variety of organic and inorganic processes, including "biological productivity, oxidation/degradation of organic carbon, dissolution and precipitation of calcite, and $CO_2$ exchange with the atmosphere."

Recent studies, for instance, show that there is a significant "outgassing of riverine carbon to the atmosphere" due to the "high $pCO_2$ of river waters" in comparison to the atmosphere. In a study on the three main Himalayan rivers—the Ganga, Brahmaputra, and Meghna Rivers—the carbonate systems, the direct release of carbon dioxide from river water into the atmosphere has been examined. They discovered pCO2 levels higher than the atmospheric pCO2 level in the lower reaches of these rivers, where deep soils have developed and high air temperatures drive active soil respiration, despite the fact that the upper portions of these rivers are known to have low pCO2 levels due to active chemical weathering. An easy mixing calculation shows that subsurface water fluxes control seasonal fluctuations in these river water carbonate systems. During the rainy season, the majority of the lowlands are submerged, increasing the input of subsurface flow to river water carbonate systems and raising pCO2 concentrations (Manaka et al., 2015).

## 2 River and Biogeochemical Linkages

A complex interaction of "physical, chemical, and biological processes" taking place on the land, in the riparian zone along the banks, in the surface waters upstream, and in the channel sediments, results in the chemical composition of the water collected from the river at any point along its course. Element cycles can be significantly impacted by biogeochemical processes, particularly for elements that are present in trace levels yet are essential for biosynthesis. Therefore, "biogeochemistry" refers to the changes in element cycles that involve interactions between the biota and the geochemical features of the watersheds. The atmospheric $CO_2$ is changed into dissolved bicarbonate ions ($HCO_3^-$) in water, which is then transported by rivers to the oceans via weathering of both carbonates and silicates caused by the interaction of terrestrial rocks with water. Normal conditions result in 21% oxygen and 0.03% carbon dioxide by volume in the dry atmosphere at sea level; however, these percentages may vary in soil due to OM decomposition.

$$\{CH_2O\} + O_2 \rightarrow CO_2 + H_2O \tag{1}$$

As a result, the oxygen concentration of the soil's air may drop as low as 15%, and its carbon dioxide content may increase by a few percentage points as a result of this process, which also produces carbon dioxide while consuming oxygen (Manahan, 2001). The groundwater's dissolved $CO_2$ levels significantly rise as a result of this OM degradation, which lowers pH and speeds up the weathering of carbonate minerals, particularly $CaCO_3$. Rivers' biogeochemistry depends on energy storage from photosynthesis or the decomposition of organic materials to support biosynthesis and respiration. The biogeochemical cycling of carbon between its two main pools, land and ocean, depends on rivers entering the ocean. Physiologically inert metal complexed humic compounds, polyphenols, and polysaccharides, as well as more unstable chemicals including polypeptides, fatty acids, and carbohydrates that disintegrate quickly in the riverine environment, may be found as carbon molecules in these pools (Gupta et al., 1997). The total amount of organic carbon estimated to have been transferred annually from the rivers to the oceans ranges from $0.03 \times 10^{15}$ g $Ca^{-1}$ to $1.0 \times 10^{15}$ g $Ca^{-1}$ with the global average being around $0.5 \times 10^{15}$ g $Ca^{-1}$ organic carbon. The distribution of the river load's dissolved and particle fractions defines this transfer. Other ions like calcium and magnesium, minerals from organic matter, and particles from the land are also transported by rivers to the oceans, enhancing biological production and consuming $CO_2$, especially in coastal areas.

## 2.1 Carbon as the Element

One of the most plentiful elements in the universe, carbon is responsible for the structure of our entire biological system, encompassing both water and land. Biological things are mostly composed of carbon in its organic form. The atmosphere, lithosphere, and hydrosphere are the three components of the biosphere where carbon can be found. By converting, outgassing, and storing more than half of the C they take in from terrestrial ecosystems before transferring it to the seas, inland rivers make a large contribution to the global carbon cycle. Terrestrial carbon imports into freshwaters are frequently comparable to the net output of terrestrial ecosystems (Hotchkiss et al., 2015). Large rivers' carbon and nutrient fluxes are assumed to reflect the processes occurring in their tributaries, floodplains, and watersheds. Due to their physical size and logistical issues, large rivers make it difficult to determine carbon dynamics. Over the past 20 years, researchers have looked into a number of prominent rivers in temperate and tropical nations, including "the Amazon; major North American, Russian Arctic, and Siberian rivers; the Parana and Orinoco; and major African rivers." Long-term investigations of the world's major rivers are lacking, nevertheless, and are necessary to comprehend their nature as non-steady-state systems characterized by episodic events.

## 2.2 Biogeochemical Processes of Carbon

Carbon is everywhere, making it difficult to comprehend how it moves above and below, or how it is emitted or stored by the Earth system. It is said that the carbon cycle is a complicated process wherein carbon is converted from organic to inorganic and vice versa. A process of recycling, almost through the process of respiration, which involves the breakdown and release of energy from complex carbon-containing compounds, both living things—animals and plants—release $CO_2$ into the atmosphere. Getting a Handle on Carbon Dioxide–Climate Change: Vital Signs of the Planet (nasa.gov)) report that the atmospheric concentration of carbon dioxide ($CO_2$) is approximately 412 parts per million as of the year 2021. This is the most fundamental process of carbon uptake, in which plants and specific microbes absorb water and $CO_2$ to produce sugars and starch. Photosynthesis is a process that is fueled by sunlight and enzymes. As a waste product, oxygen is emitted here.

$$6CO_2 + 12H_2O \Leftrightarrow C_6H_{12}O_6 + 6H_2O + 6O_{2...} \tag{2}$$

Every ecosystem, including river systems, maintains the biogeochemical link between the elements C and O through photosynthesis, aerobic respiration, and breakdown. The process of turning inorganic carbon into light-dependent organic matter is known as photosynthesis. Because the process is reversible, biosynthesis

takes place on the right while respiration and breakdown take place on the left. Fast oxidation of stored organic matter by industry, agriculture, forest fires, and internal combustion engines may have a significant impact on the global climate because photosynthesis is so pervasive that it affects the composition of oxygen in the atmosphere. Because of this, organic material that has been stored by industry, agriculture, forest fires, and internal combustion engines is oxidizing at a startling rate, which could have a huge impact on the climate. In respiration (aerobic respiration), organic matter is oxidized in the presence of molecular $O_2$.

$$\{CH_2O\} + O_2(g) \rightarrow CO_2 + H_2O\ldots \tag{3}$$

Use of oxidants other than $O_2$ during anaerobic respiration, such as $NO_3^-$ and $SO_4^{2-}$, is considered. As part of the process of exchanges of matter and energy in the form of food from organism to organism, animals can access organic carbon by consuming plants or other animals. The decomposers, which break down dead plants and animals during the decomposition process, accompany further processing. Some features of chemical reactions are controlled by the significant contribution of microbes to the carbon cycle. As a result of algae, which are carbon-fixing organisms in water, consuming $CO_2$, the pH of the water rises, resulting in the precipitation of $CaCO_3$ and $CaCO_3.MgCO_3$. By reducing organic C, N, S, and P to simple organic forms that plants may use, the biomass breakdown by bacteria and fungi prevents the buildup of excessive water residue.

This process, together with the residual humus residue, is crucial to the biogeochemical cycling of the elements and is necessary for maintaining the soil's ideal physical condition. Another factor is methane formation, which is the last stage of anaerobic breakdown of organic matter. Methane-forming bacteria, including *Methanobacterium*, are found in anoxic (oxygen-free) sediments, and they play a significant role in local and global carbon cycles. About 80% of the methane that reaches the atmosphere comes from this source. Higher hydrocarbons are oxidized under aerobic circumstances by Micrococcus, Pseudomonas, Mycobacterium, and Nocardia, which is an important environmental mechanism for removing petroleum waste from soil and water. The treatment of municipal wastewater includes another process known as

$$\{CH_2O\} + O_2(g) \rightarrow CO_2 + H_2O + \text{biomass}\ldots \tag{4}$$

Burning biomass releases carbon back into the atmosphere as well. Thus, this carbon is also stored in living things, particularly in plants with longer life spans, like trees. Another illustration is the fossilization of plants and animals, which results in the storage of carbon in the rock itself and, under the appropriate circumstances, the formation of fossil fuels. Moreover, the carbon that is present in non-living things, such as rocks, shells, the atmosphere, and the oceans, is known as inorganic carbon. Its trip downstream begins with the natural acid rain droplets, dissolving the minerals in the rocks. The acid is further neutralized, changing into carbon dioxide and

subsequently bicarbonate, which flow into the water and eventually into rivers. While carbon dissolved into rivers is transported to the oceans, where it is then stored in the deep-sea sediments for millions of years, this process helps to remove carbon dioxide from the atmosphere on a large scale. While several activities have an impact on the carbon that flows down the river or is discharged back into the atmosphere, we must measure the quantity of carbon that enters the water in order to lessen its effect on the climate. The drainage basin where the total amount of carbon received in the water consists of the mixture of all the components from diverse sources is where the biogeochemical activities of major rivers can be combined. Different amounts of rainfall and runoff affect hydrology, which in turn affects the biogeochemistry of carbon. Rivers start to play a more active role in the basins' overall carbon balance (Richey et al., 2009).

## *2.3 Forms of Riverine Carbon*

As shown in Fig. 1, the major three types of carbon in river waters—DIC, POC, and DOC—come from various natural inputs. River eutrophication is a crucial cause for algal POC that adds to near-anoxic conditions when it comes to the coastal zonation, along with the expanding anthropogenic components. Dissolved inorganic carbon, often known as DIC (carbonate + bicarbonate + $CO_2$), is the main form of carbon released into many rivers and streams around the world. Numerous physical and chemical factors, including "pH, temperature, alkalinity, dissolved oxygen, etc., and biological activities occurring inside the river's watershed," determine the chemical composition of the river. For instance, during the dry season, the Godavari river's upper reaches witness fresh and autochonous Particulate Organic Matter (POM), whereas the lower reaches see deteriorated content and a rise in inorganic suspended matter. Heavy rainfall causes a flushing of humus across the entire basin, which favors allochthonous, degraded POM. It is crucial to interpret the biotic processes because they influence water quality, fish production, and the global carbon budget. They also provide a detailed, "integrated record of natural and anthropogenic activities within the drainage basin" (Balakrishna & Probst, 2005) (Fig. 2).

Since they not only transfer carbon from terrestrial sources to the marine environment but also encourage a variety of in situ activities that can significantly affect the carbon content, fluvial systems are exceptional in their contribution to monitoring the biosphere's global carbon budget. Changes in carbon concentrations and forms can happen naturally as a result of processes like atmospheric gas exchange (particularly carbon dioxide degassing), storage in sediments at the bottom of rivers (via organic matter microbe decomposition), and an increase in plankton production, which is primarily brought on by human activities like increased nutrient input from agricultural land, sewage, and industrial activities. According to a study published in the journal *Nature*, dissolved organic carbon (DOC), which is mostly created by plant decomposition, is a "very dynamic and reactive component" of the Earth's overall carbon cycle in freshwater river systems. Contrarily, DIC is created

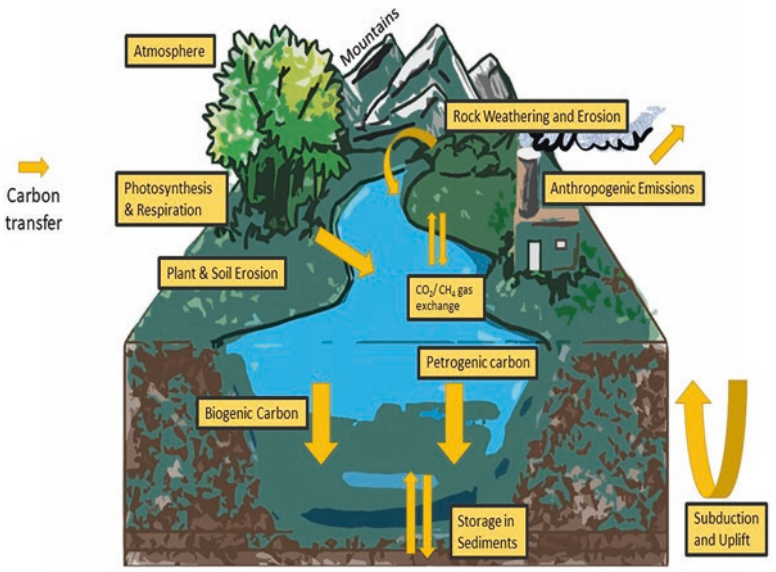


**Fig. 1** The Carbon Cycle: The sequence of processes through which carbon compounds are interconverted in the environment, involving the incorporation of carbon dioxide into living tissue via photosynthesis and its return to the atmosphere through respiration, the decomposition of dead organisms, and the combustion of fossil fuels. Transportation of carbon from rivers to the sea. Some part of it settles on the seafloor and is buried and disconnected from the atmosphere for millions of years which eventually makes its way back to the surface in the form of rocks. Simultaneously, the river also erodes the carbon-containing rocks into the particles which are carried downstream. This process exposes the carbon to the air that oxidizes the previously locked-up carbon into carbon dioxide that can leak back out to the atmosphere (https://www.whoi.edu/press-room/news-release/river-carbon/)

from atmospheric $CO_2$ through the weathering of silicates, the creation of carbonate from rock, the consumption of SOM, and other processes. A comprehensive understanding of the carbon cycle can be developed by measuring the amount of carbon dioxide absorbed from the atmosphere during the weathering of rocks and by learning more about biogeochemistry and carbon cycling to identify the sources of inorganic carbon in river water. Assessing C isotope in DIC is one of the most accurate methods to determine the different sources of DIC in rivers because aspects of fractionations of different carbonate species and gaseous $CO_2$ in dissolved river water are well documented. The weathering of minerals, soil and root respiration, mineralization of in-stream DOC, and other activities that function as carbon sinks on land all contribute to the creation of DIC in streams and rivers. The $CO_2$ dissolved from terrestrial respiration, which includes soil and roots, contributes to the DIC pool in the stream via groundwater or shallow soil flow channels. Bicarbonate is produced when carbonate rocks dissolve in the presence of carbonic acid or any other acid, and it is also a result of the reaction between carbonic acid and silicate rocks. Depending on a specific region of land's temperature, vegetation, and

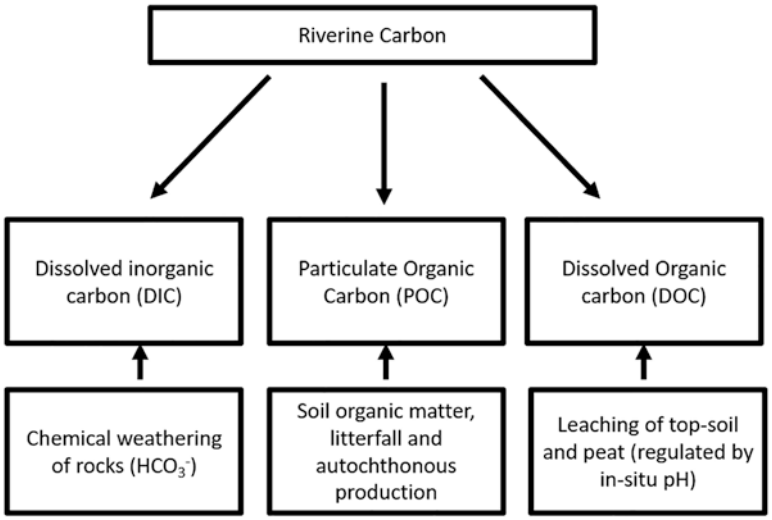


**Fig. 2** Flow chart showing different forms of riverine carbon

underlying geology, a variety of terrestrial processes take place at varying rates. The amount of dissolved inorganic carbon (including carbon dioxide) produced by "ecosystem respiration (ER = heterotrophic + autotrophic respiration)" in streams varies significantly and is mainly regulated by "temperature, organic carbon intake, stream biota," and "nutrients." "The amount of POC that is transported ranges from 0.19 to $0.23 \times 10^{15}$ $gCa^{-1}$, of which 35% is made up of labile POC. Due to $CO_2$ inputs from terrestrial sources, in situ aquatic mineralization of terrestrial organic carbon (hence referred to as "internal production"), as well as abiotic $CO_2$ creation, inland waterways are commonly oversaturated with $CO_2$. As a result, changes in land cover, temperature, terrestrial ecosystem processes, the relationship between land and water, and internal $CO_2$ generation will cause changes in $CO_2$ concentrations and emissions from flowing waters. Over the past 10 years, our conceptual understanding of how freshwater ecosystems fit into larger carbon budgets has undergone tremendous change, yet the ratio of internal production to $CO_2$ emissions from flowing waters is still not well constrained. Most freshwater budgets evaluate carbon sequestration, emissions, and export before using these fluxes to determine the terrestrial inputs to inland rivers. Although this method has been useful for integrating land-water carbon budgets, it restricts our understanding of the functional contributions of streams and rivers to carbon budgets. According to Hotchkiss et al. (2015), it is unknown to what extent freshwater ecosystems act as passive conduits (or "chimneys") for terrestrially generated $CO_2$ as opposed to actively metabolizing terrestrial OC to $CO_2$. River intake makes up just 7.5% of primary output, but due to its stability, it may have a considerable impact on the total amount of carbon buried in coastal regions. Because riverine carbon fluxes make up less than 10% of annual anthropogenic carbon emissions, more research into them is not necessary in terms of global

carbon cycle modeling. However, studies of river carbon flow, which are directly influenced by river mass movement, may offer crucial insight into the biogeochemical cycle operating in coastal ecosystems at the regional level. In addition to directly ingesting POM, rivers also provide nutrients to the estuary that help phytoplankton grow. Extreme weather and hydrologic conditions have the power to significantly modify how rivers travel in large quantities (Degens & Ittekkot, 1985; Spitzy & Ittekkot, 1991).

## 3 Quantification of Carbon Transport by Rivers

Although the carbon fluxes across rivers are minor on a global scale, they frequently play significant roles in the creation of regional carbon budgets (coastal zones and deltas), underlining the lack of C sinks. This can also be applied to changes in land use and cover caused by anthropogenic activity. Whether the carbon cycle is global or regional, the inland freshwater ecosystem, including rivers, plays a significant quantitative role (Cole et al., 2007). In comparison to any other biotic pathway, the increase in $CO_2$ partial pressure has caused the surface ocean solution to dissolve more $CO_2$ into the solution, creating a significant abiotic pathway for atmospheric C sequestration into the ocean. In terms of atmospheric $CO_2$, rivers are net contributors. The majority of the $HCO_3$ transportation in the flowing waters is represented as carbon dioxide, which is changed due to the fluctuating conditions of weathering of corresponding rocks like aluminosilicate or carbonate rocks. Excess carbon dioxide is derived from groundwater contributions of organic C that is respired in either soil systems or within the stream or river. The export of DIC by riverine export, which results from the fixation of carbon from the atmosphere, is estimated to be between 0.21 and 0.3 Pg C $year^{-1}$ by Cole et al. (2007). On a global scale, around 50% of the bicarbonate carried by rivers comes from the weathering of silicate, while the remaining 50% comes from the bicarbonate that is released from $CO_2$ sequestration. The other half of the bicarbonate that is carried results from carbonate weathering, whereas the other half originates from the sequestration of carbon dioxide. Groundwater has npt been given much consideration in the global carbon budgets yet. Although it "comprises 97% of the world's liquid freshwater" and includes sizable amounts of both organic and inorganic carbon, the estimation of SGD (Submarine Groundwater Discharge) indicates that it contributes just "1.4–12% of river influx, with the most accepted range between 5 and 10%." The amount of carbon being oxidized and stored within the basin, an estimate of the organic carbon flux from rivers to the ocean, and changes in flux or storage over time are all significant elements for assessing river carbon. Even though tropical river systems provide more than 60% of all water discharge and 34% of all suspended load to the world's oceans, they have received less attention than their temperate counterparts. The vast bulk of information about tropical river systems is restricted to a few of large river systems. Due to this, leaving inland rivers out of landscape carbon budgets could lead to an overestimation of terrestrial $CO_2$ absorption and storage. Rushing rivers

are hotspots for $CO_2$ emissions, outgassing at a much faster rate than lake and terrestrial ecosystems despite their little area coverage. Understanding the rates and factors that contribute to C cycling in flowing waterways is crucial given their significant impact on C transformations, movement, and emissions in the environment.

A sizable river called the Ganges traverses the southern slopes of the Himalayas. The transboundary river runs through Bangladesh and India. The migration of current organic C from the Himalayan riverine area is responsible for 10–20% of the global flow into the oceans, according to research. The "movement of organic C in the Ganga River's headwaters" has not previously been the subject of any research (Panwar et al., 2017). The rate of continental erosion, the capacity of rivers, the amount of leaching, mineralization, and sediment deposition are just a few examples of "extrinsic and intrinsic fluvial processes" that have a significant impact on the evaluation of fluvial organic carbon flow. The Ganga-Brahmaputra River system has deposited organic carbon (OC) in the Bay of Bengal over the last 15 million years, making up 10–20% of the entire world burial flux. A total of more than 65% of sediments are transported by the Ganga River, which is formed by the "Higher Himalayan Crystalline." The "Higher Himalayan Crystalline," which creates the Ganga River, transports a total of more than 65% of the sediments. The "Alaknanda River" is a Ganges tributary that travels through the Western Himalayas of India. A study was conducted to ascertain the effects of seasonal erosivity on the dissolved organic carbon concentration and physiography of the basin, which serves as an important control parameter for the movement, oxidation, and residence time of the OM. Alaknanda provides 66% of the total DOC flow carried by the Ganga River at Devprayag. The comparison with previously published data shows that the Ganga River transfers organic carbon largely as POC downstream in the Himalayan foothills and mostly as a dissolved load upstream due to changes in physiography and chemical weathering rate. The Hooghly estuary, one of its deltaic tributaries, was the subject of research. A high-suspended sediment load is seen during the monsoon. The Sundarban mangrove forest, which becomes the main source of inorganic fertilizers, is traversed by the estuary. Typically, it is seen that the estuarine transfer of nutrients associated with litter and sediment has a significant impact on the DIC fluxes of the Hooghly river's coastal zone, which are determined by using biogeochemical modeling. The calculated annual fluxes are $2.76 \times 10^6$ t or $230 \times 10^9$mol (Mukhopadhyay et al., 2006). The goal of this research was to analyze the role of upland tributaries in the transportation mechanisms impacting the Godavari's lateral carbon and nitrogen flows. The study was conducted on the Godavari river in India. In the river basin, dissolved inorganic carbon (DIC) is by far the most significant method of carbon transfer. Up to 75% of the total carbon burden is attributable to it.

According to Sarin et al. (2002), DOC and POC fluxes account for 21% and 4% of total fluxes, respectively. Because of extensive human activity in the upper basin, DOC fluxes outpace POC fluxes. In contrast, the POC and DOC fluxes in streams in the middle basin are comparable. However, due to silt entrainment in river channels and dam sites, downstream particulate organic carbon export is 35% lower than upstream and tributary imports. We propose that for severely damaged watersheds in tropical climates, long-term monitoring of sediment and carbon flow downstream

is required. The main stem and tributaries of the large tropical river Godavari (India), according to a case study of its biogeochemistry, contain an abundance of total carbon varying from 13.8 to 50.7 mg C $L^{-1}$. In a different study of the Godavari river system, it was found that during the high season, the soil in the lower basin of the river is the main source of organic matter (OM; C/N ratios range from 8.1 to 14), while during the other seasons, river-derived (in situ) phytoplankton serves as the main source (C/N ratios range from 4 to 8). The intermediate "C/N ratios (between 4 and 8)" show that phytoplankton and soil organic matter are cautiously combined. Larger net outputs of organic carbon are caused by deforestation, agricultural activities, intense rainfall, and considerable erosion. Due to inflow from the watershed and flood plains, OM concentrations in river channels are higher during monsoons. One percent or less of the DIC fluxes from all rivers in the globe are exported to the seas through the Godavari river. Two tropical river basins' diverse hydrological sections' water sources are revealed by the analysis of oxygen stable isotope ratios (18O) and hydrogen stable isotope ratios (2H). This is related to "the increased vapor recycling process occurring in these basins and the continental wind pattern dictating the north-east winter monsoon."

The bicarbonate is the major anion at the Alaknanda River, which is primarily owing to the rock weathering influencing the water chemistry, as seen in Table 1's representation of the bicarbonate and DOC data of several Indian rivers. As a result, the Alaknanda River and its tributaries have an alkaline pH. According to Singh and Hasnain (1998), silicate weathering and carbonate weathering both have a role in the basin's overall regulation. Similar to this, weathering regulates the slightly acidic to slightly alkaline waters of the rivers Narmada and Tapti (Sharma & Subramanian, 2008). The anthropogenic sources of bicarbonate along the river

**Table 1** Bicarbonate and DOC estimates of different Indian rivers

| River | Bicarbonate (mg/L) | DOC (mg/L) |
|---|---|---|
| Arkavathy | 616 (Gogeredoddi; Max) 227 (Koggedoddi; Min) | – |
| Pennar | 237.7 (pre-monsoon)<br>171.8 (monsoon)<br>141.5 (post monsoon) | – |
| Ponnaiyar | 289.1 (pre-monsoon)<br>215.2 (monsoon)<br>317.7 (post monsoon) | – |
| Pazhayar | 51 | – |
| Periyar | 12 to 25 | – |
| Ganga (Buxar) | 124.44 | – |
| Ulhas River | 59.6 | – |
| Alaknanda (Devprayag) | 68.3 | 0.60–1.29 |
| Bhagirathi | 42.1 | 0.68–1.13 |
| Ganga (Rishikesh) | 4.9–34.2 | 1–1.19 |
| Yamuna | 102.3 | 0.98–4.7 (Sharma et al. 2017) |
| Gomti | 54.9 | – |
| Narmada | 20.5–179 | 1.70–33.9 |
| Tapti | 130–334 | 3.60–13.9 |

Arkavathy include limestone, which is used to raise the pH of the soil or to buffered lakes to treat acidification. As wastewater from industry and home usage contains bicarbonate from cleaning chemicals and food leftovers, human interventions like effluent from wastewater treatment plants can also increase alkalinity to a stream. According to CWC data on river water quality scenario, Department of Water Resources, River Development, and Ganga Rejuvenation, similar perturbations are seen for rivers Pennar and Ponnaiyar.

When elucidating the biogeochemical cycling of carbon during the low water-flow season, the carbon isotopic composition (13C value) of both organic and inorganic river carbon in the Swarna and Nethravati Rivers clearly demonstrates the discrete dominance of carbon from autochthonous and allochthonoussources (Muguli et al., 2013). Because there is less organic carbon in these basins, atmospheric/soil $CO_2$ regulates river carbon mostly through the weathering of rock. The "relative difference in the typical carbon isotopic compositions of these two rivers, with the Nethravati water mirroring the average $\delta^{13}C_{DIC}$ composition of carbon fluid containing Charnockite" serves as additional evidence for this finding.

## *3.1 Integrating the Rivers into the Carbon Budget*

The design of two boxes—one for the ocean and one for the terrestrial realm—illustrates a streamlined picture of the carbon cycle. Additionally, the gas interacts with the third box, which stands in for the atmosphere. The underlying gaps in the global budget's imbalances were revealed by this approach, according to earlier studies on the carbon budget (Cole et al., 2007). More small compartments and the accompanying processes have been added to models as they have evolved in order to consider a more in-depth version of their interactions. The models that represent the aquatic habitats that exist on land are rarely explicit. Numerous studies conducted throughout the 1970s and 1980s have demonstrated that considerable amounts of terrestrial organic and inorganic carbon C are transported from the land to the sea. It is really intriguing that it has been described as "the pipe" that moves carbon from the land to the ocean. "A straightforward mass balance equation was developed, according to one study, to follow the fate of organic and inorganic carbon in a integrated freshwater and terrestrial C budget," where the amount of carbon imported into the aquatic system can be calculated as the net carbon gas balance of the aquatic system with the atmosphere, plus storage and export in drainage waters and rivers (along with the direct groundwater discharge) to the sea. Any export of volatile organics to the air is also taken into account here. According to reports, the amount of organic carbon exported from the river to the sea ranges between 0.38 to 0.53 Pg $C^{-1}$. The availability of various elements from rivers, including carbon from primarily terrestrial sources, is necessary for the "steady-state chemistry of the oceans." Although estimates of riverine organic and inorganic carbon fluxes continue to be improved by new geospatial tools and scaling and modeling approaches, these fluxes are not notably different from earlier estimates. Today, yearly carbon

flows to all significant ocean basins and seas are accessible. Fluxes are often closely related to river discharge, with a few exceptions where characteristics like extensive peat and carbonate coverage as well as high rates of erosion in watersheds limit carbon inputs (Bauer et al., 2013). In comparison to their benthic NPP, mangroves are known to export enormous volumes of POC and DOC into the ocean. "Global mangroves export 86 Tg C $yr^{-1}$ of dissolved inorganic carbon (DIC) to adjacent coastal waters, which appeared to be significantly more than the estimated total export of POC, DOC, and CO2 emission from the mangrove ecosystem's submerged flood plains." Recent research has demonstrated that mangroves contribute significantly to the global exchangeable DOC (EDOC, volatile and semi-volatile OC) flow from the ocean to the atmosphere, accounting for around 60% of the total global EDOC flow. These assessments of the organic and inorganic carbon derived from mangroves, however, are based on a scant amount of research. Uncertainty is introduced and accepted due to data upscaling because unstudied portions of mangroves are still included in global budgets (Ray et al., 2018).

Natural and human-made factors are altering the amount of water that is imported from the River C into the coastal ocean. Watershed carbon stocks and fluxes, fluctuations in the water balance (precipitation and evapotranspiration), and all of these factors might affect inputs. The management of evapotranspiration through temperature regulation and the effects of climate change on the amount and frequency of rainfall events are examples of hydrological alterations. Additionally, it is required to take land management measures like plant removal and irrigation that affect evapotranspiration rates. Recent research has demonstrated that a range of practices have been found to modify carbon stocks (biogeochemical response) and flows at the drainage-network level, including the use of sulfuric acid, agricultural practices, peatland disturbance, permafrost melting, wetland loss, and reservoir construction. The amount of water that has been discharged (precipitation less evapotranspiration) is calculated by multiplying the carbon content (hydrological and biogeochemical reaction) by the amount of water. Numerous significant activities have an impact on the sources and fluxes of carbon in estuaries. Estuaries contain a mix of "organic and inorganic carbon sources obtained from terrestrial materials carried by fresh river water (with a salinity of zero), marine sources carried by shelf seawater (with a salinity of greater than or equal to 30), and materials that are peculiar to estuaries." Salinity-induced flocculation, sedimentation, microbial respiration, and photooxidation all result in the loss of organic carbon. Whether an estuary is a net carbon source or a net carbon sink may affect how much carbon is sent to the shelf.

Physical and biogeochemical processes regulate organic carbon's origin, movement, and final location. Carbon is transferred at the point where the plume and shelf waters converge by sorption and desorption. Movable and fluidized mud layers, bioturbation, and physical resuspension all aid in transporting organic carbon to the open ocean. The benthic nepheloid layer contains substantial amounts of suspended sediment that can be deposited at and resuspended from depocenters. While upwelling zones in outer shelf waters may improve primary output, high sediment loads in plumes may limit primary production in the inner shelf waters. The abbreviations DOC, POC, and DIC stand for dissolved organic carbon, particulate organic carbon, and dissolved inorganic carbon, respectively.

## 4 Impact of Human Activities

There are still many gaps in our knowledge of the natural, untouched carbon cycle of the coastal ocean. It can be challenging to distinguish between natural and artificial factors that are causing changes in the coastal carbon cycle due to land use changes, river impoundments, fertilizer inputs, wetland degradation, and climate change. Despite the fact that several anthropogenic sources have been identified as perturbing river and estuarine carbon fluxes, quantitative evaluations of their impact on these fluxes are still lacking. Around 2.7 Pg of carbon are moved from terrestrial to aquatic ecosystems globally. Although 1.2 Pg of carbon is respired as $CO_2$ and 0.6 Pg is retained in sediments, only 0.9 Pg of carbon is deposited in the ocean. The movement of carbon from the land to the sea has been greatly accelerated by human activities such as agricultural liming, increasing soil erosion, chemical weathering, and urban wastewater inputs. Furthermore, removing riparian vegetation and fertilizer from urban and agricultural areas may boost the output of native carbon. The decomposition of organic carbon in river and estuarine sediments may be accelerated by warming caused by urban heat islands and climate change. Although river engineering modifications like flood-control levees affect how carbon is cycled through rivers, it is challenging to quantify and notice these changes. The atmospheric $CO_2$ is absorbed when this organic carbon is buried in ocean sediment. Organic carbon that has accumulated in floodplains may oxidize and emit $CO_2$ into the atmosphere (Fig. 3).

It was shown in this issue of AGU Advances that engineered river bank stabilization can increase the amount of organic carbon transported to the seas while decreasing the amount of organic carbon oxidized in floodplains. This shows that solutions for bank stabilization may allow for more efficient $CO_2$ removal from the environment. The way nutrients, particularly organic carbon, are cycled through rivers has been impacted by human activities and channel engineering. Floodplains' ability to store carbon is reduced as a result of agriculture and development draining the soil's carbon content. Dams reduce the quantity of organic carbon discharged into the seas by holding silt in reservoirs. By preventing rivers from overflowing, artificial levees and other bank stabilization techniques reduce the amount of silt and organic carbon that is deposited on the floodplain. Bank stabilization has the ability to reduce riverine $CO_2$ emissions to the atmosphere while increasing the quantity of organic carbon buried in the oceans because organic carbon deposited in floodplains may be converted to $CO_2$. In order to determine the global terrestrial $CO_2$ sink, which is defined as the flux remaining after accounting for all other components of the anthropogenic carbon budget, as well as for determining both the coastal and global carbon budgets, it is not only necessary to understand the precise direction and magnitude of various human impacts on individual fluxes. At least some of the anthropogenic carbon dioxide absorbed by terrestrial ecosystems is thought to be carried to the coastal ocean, according to researchers looking at riverine organic carbon export. The shift in terrestrial carbon storage predicted by the IPCC4 and others may be overestimated given that a sizeable portion of the displaced carbon is

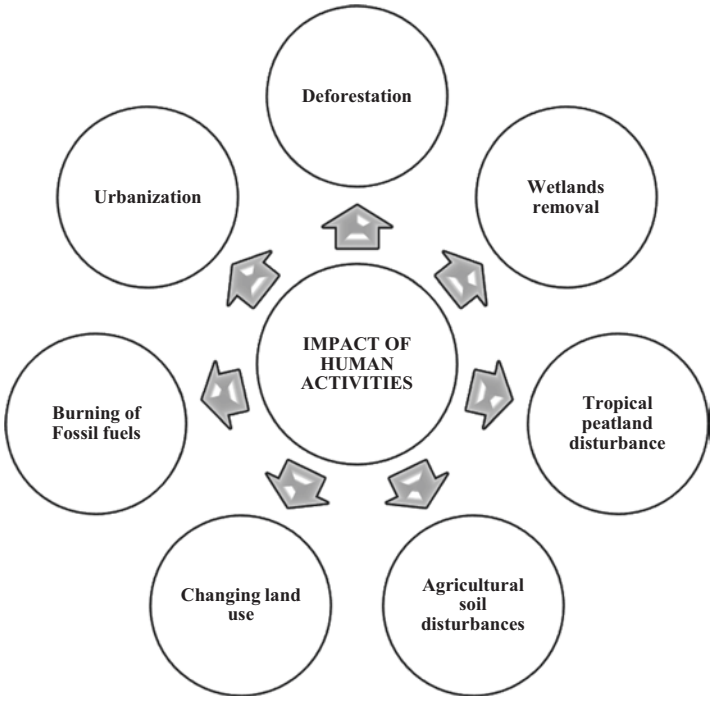


**Fig. 3** Flow chart showing anthropogenic factors impacting riverine carbon

stored in coastal waters and sediments. Earth system models must include coastal carbon processes in order to support the necessary regulations and mitigation programs. It is vital to quantify the time evolution of coastal carbon transfers and fluxes and to include them in Earth system models.

## *4.1 Deforestation*

Because deforestation lowers evapotranspiration on the land surface and increases runoff, river discharge, erosion, and sediment fluxes from the land surface, deforestation alters the hydrological, geomorphological, and biochemical states of streams. A study was carried out in the world's biggest continuous tropical forest and savannah habitat, which is located in Tanzania. This river discharge accounts for approximately 25% of total world river discharge. According to the findings of the research, almost two-thirds of the reported 25% increase in discharge has happened in the previous 50 years, which is a result of the deforestation that has occurred during that time period, was discovered. While there have been significant international attempts to conserve the Amazon rainforest, the vast majority of deforestation has taken place and continues to occur. As a result of deforestation, about 55% of the natural

vegetation has been lost, and the hydrological and morphological elements of an 82,632 $km^2$ watershed of the Araguaia River in east-central Brazil have been significantly altered (Coe et al., 2011).

## *4.2 Urbanization*

The Terai region of northern West Bengal (India) has experienced rapid infrastructure development as a result of economic policies put in place in 1991. This has resulted in the perceptible fragmentation of river channels, excessive in-channel sediment mining, and widespread land-use alteration of the floodplains. This study used an integrated methodology framework of remote sensing and field survey to conduct its research with the aim of examining the effects of anthropogenic interventions on the fluvial regime of the lower reaches of the Balason and Mahananda Rivers in the sub-Himalayan region over the past 30 years. In the majority of the places investigated, it was discovered that naturally vegetated zones had been transformed into built-up areas after being transformed into agricultural land and grassland, tea plantation, or barren ground. Unrestricted sediment mining and river channel embanking, which were directly linked to channel narrowing, were shown to have contributed to a considerable amount of channel narrowing between 1987 and 2017, according to research.

Cross-profiles and observed multitemporal channel width were compared, and the findings showed that the bed was significantly lowered (3.15 m) and that the channel was narrowing at an astounding rate (18.8 m/year). It has been found that rivers are beginning to show signs of losing their current equilibrium condition, which, if it happens, will cause the groundwater table to sink, flood frequency to decrease, existing river infrastructure to become unstable, and the ecology of rivers to be destroyed. Numerous recommendations have also been made with the aim of encouraging the judicious use of riverine resources by local communities and policymakers in order to restore the socio-hydrological as well as the eco-hydrological amenities of these rivers (Mitra et al., 2020). Riverine ecosystems must be preserved because they are also an essential natural habitat. A range of pressures, including as a changing water regime, increasing human intervention and biological invasion, climate change, land development, and other site-specific problems like eutrophication and urbanization, have an impact on these systems. As a result of urbanization, riparian vegetation is being replaced by impermeable and less permeable surfaces. As a result, flooding is happening more frequently, there is more surface runoff overall, and it takes less time for runoff to form. When there has been a substantial amount of rain, the entire city may have flooded. In this study, Olokeogun and Kumar (2020) used a variety of indicators generated from remote sensing data to analyze the vulnerability of riparian zones in the Indian city of Dehradun as a result of urbanization.

### 4.3 Burning of Fossil Fuels

The productivity of marine life may be impacted by manmade sources of nutrients to the oceans, such as rivers and air dust, but these effects are rarely investigated. Changes in marine nutrient inventories, and consequently changes in export production and ocean carbon storage, may occur if the delivery of the major physiologically limiting nutrients (nitrogen, phosphorus, ferrous, and silicon) from riverine, atmospheric, or sedimentary sources is altered, or if removal rates (such as denitrification) change. When compared to P, which is insufficient in relation to the nutrient needs of phytoplankton, the upward fluxes of significant nutrients are relatively insufficient in N on a global scale. The geographical partitioning of $CO_2$ uptake may be altered by a few tenths of a PgC/year since the atmospheric concentration gradients also reflect the natural fluxes brought on by weathering, the transfer of carbon by rivers, and the subsequent outgassing from the ocean. It is common to underestimate the effects of atmospheric emissions of carbon dioxide ($CO_2$) and methane ($CH_4$), particularly those resulting from incomplete fossil fuel combustion, burning of tropical biomass, and methane from tropical wetlands. As a result of their inclusion in the inversion, the latitudinal partitioning of the atmosphere is revised by up to 0.1 PgC/year (Prentice et al., 2001).

### 4.4 Changing Land Use

Land management is now commonly acknowledged to have a significant impact on lowering riverine carbon emissions to the coastal ocean. The release of silt and POC from the soil has increased dramatically as a result of agricultural activity. Higher carbon fluxes to the coastal ocean are not usually the result, though, as the vast majority of the terrestrial material is either redeposited on land or kept in artificial reservoirs and agricultural impoundments. According to estimates by Bauer et al. (2013), current POC flows in reservoirs, for instance, have been decreased to roughly 90% of pre-anthropogenic values. Carbon fluxes in river basins are anticipated to increase in the future, both as sources and sinks, as a result of widespread human-induced changes in land use and land cover (Sarin et al., 2002). As a result of being fertilized by river-borne inorganic fertilizers, there may be an increase in the quantity of carbon carried to and stored in marine sediments, which might represent a sizable net sink for anthropogenic $CO_2$. The humid tropics of South Asia are particularly susceptible to lateral C transfer due to heavy precipitation and fast land use and cover change. According to the National Institute of Environmental Health Sciences, urbanization increases the amount of organic matter in streams and soils from both natural (such as soil, leaves, and algae) and anthropogenic (such as sewage, grass clippings) sources. When flooding happens frequently, the inputs of natural particulate organic matter from riparian vegetation and soil erosion, which support the downstream DOM pool through leaching and decomposition, can rise.

By increasing food availability and reducing canopy cover (which increases accessible light), it is possible to boost autochthonous output. This biomass adds to the autochthonous DOM pool as it breaks down over time, whether on a daily or seasonal basis. Diverse point and nonpoint sources, including sewage pipe leaks and septic systems, can let dissolved organic matter (DOM) and nutrients from wastewater reach waterways. The rate at which DOM is leached from soils and benthic sediments may also be impacted by increasing stream temperatures and salinization levels.

## *4.5 Agricultural Soil Disturbances*

The biogeochemistry of surface waters has been significantly changed as a result of human-induced increases in carbon and fertilizer inputs. Along with terrestrial sources, atmospheric deposition (AD) is a major source of carbon and nutrients for estuaries, oceans, coastal regions, and freshwaters. Numerous variables, like as light, temperature, metabolic activity occurring inside the system, and fertilizer input from the airshed and watershed, have an impact on the carbon cycle in surface streams. Surface waters are extremely vulnerable to nutrient deposition from the atmosphere. In the open ocean zone, nutrient deposition from the atmosphere promotes primary production and phytoplankton growth. It has been discovered that atmospheric deposition has a significant impact on the quality of surface water due to the increase in the autochthonous carbon pool and the increase in the allochthonous carbon input from the watershed. Overall, the effects of these actions include eutrophication and a change in the regional carbon budget. Surface water bodies that are remote from emission sources may be affected by nutrients that are delivered by the air. The availability of nutrients in the atmosphere will therefore continue to promote autotrophy throughout a greater variety of geographical areas, despite major efforts to prevent eutrophication (Singh & Pandey, 2019).

## *4.6 Tropical Peatland Disturbances*

With a total carbon content of over 89,000 teragrams1 (one teragram is equal to one billion kilos), tropical peatlands hold one of the greatest stocks of terrestrial organic carbon in the entire planet. Peatlands provide enormous carbon reserves that may be held for hundreds of years because of their high water tables and low breakdown rates. The results of a study indicate that it is possible to quantify the annual export of fluvial organic carbon from peat swamp forests that are both intact and that have previously experienced human disturbance. The overall fluvial organic carbon flow from disturbed peat swamp forests was found to be almost 50% higher than the overall fluvial organic carbon flow from intact peat swamp forests in this study. The leaching of dissolved organic carbon from intact peat swamp forests is primarily

derived from recent primary production (plant growth), rather than from older primary production (plant decay), according to carbon-14 dating of dissolved organic carbon (which accounts for more than 91% of total organic carbon). On the other hand, the majority of the dissolved organic carbon from disturbed peat swamp forest is made up of considerably older (hundreds to thousands of years) carbon that was generated from deep within the peat column. According to the study, the estimate of total carbon lost from disturbed peatlands is increased by 22% when the generally ignored river carbon loss component of the peatland carbon budget is taken into account. More accurate calculations reveal that wetland disturbance has increased river organic carbon flux from Southeast Asia by 32% since 1990. This increase accounted for more than half of the total yearly fluvial organic carbon flux from all European peatlands during that time. These results highlighted the requirement for improved analyses of the impact of drainage and deforestation on tropical peatland carbon balances, as well as the requirement for measuring river carbon losses (Moore et al., 2013).

## *4.7 Wetland Removal*

Wetlands rank among the most significant ecosystems in the climate change response plan in terms of carbon sequestration (CS), and they are the most important ecosystems overall. Despite this, human interference is reducing their current CS capability, and further reductions are anticipated under scenarios of global population expansion and climate change, among other things. In order to boost wetlands' capacity to store carbon, numerous strategies have been proposed in the literature (Were et al., 2019). This will help to ensure that wetlands continue to be important for maintaining the global carbon (C) balance and reducing climate change. Wetlands can enhance water quality by removing contaminants from surface streams. Because they offer three different types of pollution treatment—sediment trapping, nutrient removal, and chemical detoxification—wetland pollution removal techniques are especially important. A bog is formed when water from a stream channel or surface runoff enters a wetland and grows in volume while passing through dense vegetation. Water suspended particles may settle on the marsh surface and become stranded there because the flow velocity has reduced. After being deposited, sediments can be held together by the roots of marsh plants. It is possible that up to 90% of the sediments present in runoff or stream flow will be removed from the system as the water passes through wetlands in the case of runoff or stream flow. Additionally, because soil particles are linked to contaminants like heavy metals, the settling of sediment in wetlands contributes to an improvement in the water quality. Pet waste, wastewater treatment and disposal systems, agricultural and lawn fertilizers, and a number of other sources of nitrogen and phosphorus can act as plant fertilizers in natural water bodies, leading to an overabundance of algae, cyanobacteria, and other species. Such growth might cause the extinction of nearby plant and animal species as well as the release of hazardous substances into

the environment. Before entering a water body, runoff and stream flow may pass through wetlands where plants may take up the nutrients and deposit them in less dangerous chemical forms, lowering the risk of contamination. The natural equilibrium of the wetland habitat is restored when marsh plants rot and release nutrients into the environment. Due to wetland areas' ability to effectively remove excess nutrients from the water, many towns have created wetland areas specifically for the purpose of treating effluent from secondary sewage treatment facilities. It is not advised to use naturally occurring wetlands for this purpose since there is a maximum amount of additional material that can be put to a wetland before the natural plant and chemical processes become overburdened and cease to function properly. Along with the settling soil particles, some of the toxic substances that runoff brings into a wetland are also retained. Some of these toxins may be buried in the sediments as a result of biological activity and constant exposure to sunlight, while others may be changed by the action of microbes or by sunlight exposure into less hazardous chemical forms. The likelihood is that the plants will take in more pollution.

## 5 Balance for Climate

The main sources of atmospheric nutrient supply are chemical emissions from industry and agricultural practices, and changes in these sources are largely responsible for the regional trend in AD inputs. Throughout the Ganga River Basin, there has been a steady increase in the amount of nutrients deposited in the atmosphere. According to the results of this study, the 37-kilometer part of the river grid under consideration receives "32.65 tonnes of organic carbon per year from atmospheric sources." The sub-watershed, which includes surface water, is thought to have an annual AD-OC concentration that varies between 84.94 and 270.30 tons. Surface water data on carbon sources, sinks, and their connections to air- and watershed features are essential inputs for "regional climate modeling and river management methods." Finding out whether seasonality and human activities/processes have an effect on the spatiotemporal variability of carbon and nutrient intake to the river was one of the study's key objectives. River DOC saw significant oscillations over time, and these variations cannot be entirely attributed to phytoplankton-associated DOC. In addition to DOC's allochthonous and autonomous contributions to rivers and other water bodies, increased availability of nutrients from the atmosphere also benefits these bodies of water. The fact that DOC increases noticeably during the rainy season and that there is a significant correlation between runoff DOC and AD-nutrients raises the possibility that changes in the air-watershed interaction brought on by people will significantly increase DOC in the Ganga. The terrestrial decomposition of organic matter (DOC) (DOC) alters the productivity of

watersheds, community structure, and ecosystem metabolism. It has a detrimental effect on both the accessibility of dissolved nutrients and metals in the water and the carbon cycle. Over the past 10 years, DOC levels have increased significantly throughout much of the northern hemisphere, especially in the Arctic. The quantity and quality of runoff, changes in land use, and the chemistry of atmospheric deposition are only a few of the variables that have an impact on the concentrations of DOC in surface waters. The transfer of river carbon to the coastal ocean is known to be impacted by climate. Due to the significance of transport restrictions, watersheds with high precipitation have higher river discharge rates, and several studies have long shown that discharge is the primary factor controlling the dynamics of carbon fluctuation. Temperature has an impact on both abiotic and biotic mechanisms that alter "water throughput, flow patterns, dissolution rates, and watershed carbon stocks." As a result, the overall impact of temperature on carbon fluxes differs depending on the region and whether the carbon is biological or inorganic. It is now clear that hydrologic "events," such as heavy rainfall from tropical storms, play a significant influence in the disproportionate transport of riverine organic carbon in addition to annual precipitation and temperature. The erosive power of violent storms, especially in mountainous locations, is responsible for the majority of POC transfer from watersheds to the coastal ocean. Increases in riverine dissolved organic carbon (DOC) concentrations and, consequently, yearly riverine DOC export to coastal systems are possible outcomes of these events. For instance, a single tropical storm may be responsible for more than 40% of a typical annual river DOC export. On a decadal time scale, a single large flood event can export between 80% and 90% of POC from mountainous areas. The most intense storms would probably become more frequent, influencing DOC and POC of the river transfer to coastal waters, even if the change in storm frequency is difficult to anticipate. Now, it is possible to predict the riverine transport of terrestrial carbon to the coastal ocean with moderate to high precision. On the other hand, future river carbon dynamics and related uncertainty are anticipated to be significantly impacted by climate change. Today, a number of studies point to precipitation—rather than, instance, temperature—as having the greatest influence on these fluxes in the next decades. In addition, under "future climate change scenarios, swift river transportation time is associated with large hydrological events that will contribute to the sidestepping of terrestrial C processing in rivers, as well as episodic disruption of carbon budgets of coasts, and a modification in the timing of delivery of terrestrial carbon to the coastal ocean." It is challenging to estimate the magnitude of these changes because the current generation of Earth system models does not simulate oscillations in river carbon.

## 6 Conclusion

River networks have a large amount of control over key carbon cycle activities. They become essential for evaluating carbon emissions created by humans and for furthering the impact of the atmosphere. Changes are made to the timing, character,

and size of carbon flows. The results paint a clear picture of the crucial role played by rivers in the global cycling of carbon, which is accompanied by the release of various greenhouse gases into the atmosphere. Rivers move about 200 million tons of carbon annually. Terrigenous OM for the ocean primarily comes from this source. The majority of the carbon dioxide released by rocks and plants is absorbed by rivers. The remainder is broken down and released back into the atmosphere, while a portion is carried downstream to the open waters. River-based land-based transfer is the origin of DOC. When it enters the ocean, it is stored in the deep water for millions of years. Because of their variability, the systems that control GHG emissions from river networks are not fully understood by our current study. We can better understand the changing climate and land use with further research.

This overview talks about the many carbon inputs that help rivers create their elemental cycles. We must investigate how much carbon enters the ocean and the processes it undergoes in rivers in order to fight the effects of a changing climate. This could lead to the creation of a significant method for modifying the climate. The process by which rivers transmit carbon may be significantly impacted by chemical changes and river route variations. Residential sewage flow, in particular, seasonal fluctuations brought on by flood plains and river catchment soils, might intensify the anthropogenic impact on DOC concentrations.

## References

Balakrishna, K., & Probst, J. L. (2005). Organic carbon transport and C/N ratio variations in a large tropical river: Godavari as a case study, India. *Biogeochemistry, 73*(3), 457–473. https://doi.org/10.1007/s10533-004-0879-2

Bauer, J. E., Cai, W. J., Raymond, P. A., Bianchi, T. S., Hopkinson, C. S., & Regnier, P. A. G. (2013). The changing carbon cycle of the coastal ocean. *Nature, 504*(7478), 61–70. https://doi.org/10.1038/nature12857

Borthakur, A., & Singh, P. (2016). India's lost rivers and rivulets. *Energy, Ecology and Environment, 1*(5), 310–314. https://doi.org/10.1007/s40974-016-0039-2

Buis, A. (2019). *The atmosphere: Getting a handle on carbon dioxide – Climate change: Vital signs of the planet* (http://nasa.gov)

Coe, M. T., Latrubesse, E. M., Ferreira, M. E., & Amsler, M. L. (2011). The effects of deforestation and climate variability on the stream flow of the Araguaia River, Brazil. *Biogeochemistry, 105*(1–3), 119–131. https://doi.org/10.1007/s10533-011-9582-2

Cole, J. J., Prairie, Y. T., Caraco, N. F., McDowell, W. H., Tranvik, L. J., Striegl, R. G., Duarte, C. M., Kortelainen, P., Downing, J. A., Middelburg, J. J., & Melack, J. (2007). Plumbing the global carbon cycle: Integrating inland waters into the terrestrial carbon budget. *Ecosystems, 10*(1), 172–185. https://doi.org/10.1007/s10021-006-9013-8

CWC reports on water quality scenario of rivers, Department of Water Resources, River Development & Ganga Rejuvenation. http://www.cwc.gov.in/sites/default/files/volume-1.pdf

Degens, E. T., & Ittekkot, V. (1985). Particulate organic carbon – An overview. *Mitt Geol Palaeont Inst Univ Hamburg, SCOPE/UNEP Sonderbd, 58*, 7–27.

Gupta, L. P., Subramanian, V., & Ittekkot, V. (1997). Biogeochemistry of particulate organic matter transported by the Godavari River, India. *Biogeochemistry, 38*, 103–128. https://doi.org/10.1023/A:1005732519216

Hotchkiss, E. R., Hall, R. O., Jr., Sponseller, R. A., Butman, D., Klaminder, J., Laudon, H., Rosvall, M., & Karlsson, J. (2015). Sources of and processes controlling CO2 emissions change with the size of streams and rivers. *Nature Geoscience, 8*(9), 696–699. https://doi.org/10.1038/ngeo2507

Leopold, L. B., Wolman, M. G., & Miller, J. P. (1964). *Fluvial processes in geomorphology*. W.H. Freeman.

Manahan, S. E. (2001). *Fundamentals of environmental chemistry*. CRC Press LLC.

Manaka, T., Ushie, H., Araoka, D., et al. (2015). Spatial and seasonal variation in surface water $pCO_2$ in the Ganges, Brahmaputra, and Meghna Rivers on the Indian subcontinent. *Aquatic Geochemistry, 21*, 437–458. https://doi.org/10.1007/s10498-015-9262-2

Mitra, S., Roy, A. K., & Tamang, L. (2020). Assessing the status of changing channel regimes of Balason and Mahananda River in the Sub-Himalayan West Bengal, India. *Earth Systems and Environment, 4*(2), 409–425. https://doi.org/10.1007/s41748-020-00160-y

Moore, S., Evans, C. D., Page, S. E., Garnett, M. H., Jones, T. G., Freeman, C., Hooijer, A., Wiltshire, A. J., Limin, S. H., & Gauci, V. (2013). Deep instability of deforested tropical peatlands revealed by fluvial organic carbon fluxes. *Nature, 493*(7434), 660–663. https://doi.org/10.1038/nature11818

Muguli, T., Lambs, L., Otto, T., Gurumurthy, G. P., Teisserenc, R., Moussa, I., Balakrishna, K., & Probst, J.-L. (2013). First assessment of water and carbon cycles in two tropical coastal rivers of south-west India: An isotopic approach. *Rapid Communications in Mass Spectrometry: RCM, 27*, 1681–1689. https://doi.org/10.1002/rcm.6616

Mukhopadhyay, S. K., Biswas, H., De, T. K., & Jana, T. K. (2006). Fluxes of nutrients from the tropical River Hooghly at the land–ocean boundary of Sundarbans, NE Coast of Bay of Bengal, India. *Journal of Marine Systems, 62*(1–2), 9–21. https://doi.org/10.1016/j.jmarsys.2006.03.004

Olokeogun, O. S., & Kumar, M. (2020). An indicator based approach for assessing the vulnerability of riparian ecosystem under the influence of urbanization in the Indian Himalayan city, Dehradun. *Ecological Indicators, 119*, 106796. https://doi.org/10.1016/j.ecolind.2020.106796

Panwar, S., Gaur, D., & Chakrapani, G. J. (2017). Total organic carbon transport by the Alaknanda River, Garhwal Himalayas, India. *Arabian Journal of Geosciences, 10*(9), 207. https://doi.org/10.1007/s12517-017-3003-3

Prentice, I. C., Farquhar, G. D., Fasham, M. J. R., Goulden, M. L., Heimann, M., Jaramillo, V. J., Kheshgi, H. S., Le Quéré, C., Scholes, R. J., & Wallace, D. W. R. (2001). The carbon cycle and atmospheric carbon dioxide. In J. T. Houghton, Y. Ding, D. J. Griggs, M. Noguer, P. J. V. D. Linden, X. Dai, K. Maskell, & C. A. Johnson (Eds.), *Climate change 2001: The scientific basis* (pp. 183–237). Cambridge University Press.

Ray, R., Baum, A., Rixen, T., Gleixner, G., & Jana, T. K. (2018). Exportation of dissolved (inorganic and organic) and particulate carbon from mangroves and its implication to the carbon budget in the Indian Sundarbans. *Science of the Total Environment, 621*, 535–547. https://doi.org/10.1016/j.scitotenv.2017.11.225

Richey, J. E., Krusche, A. V., Johnson, M. S., da Cunha, H. B., & Ballester, M. V. (2009). The Role of rivers in the regional carbon balance. In *Amazonia and global change, geophysical monograph series*. AGU. https://doi.org/10.1029/2008GM000734

Sarin, M. M., Sudheer, A. K., & Balakrishna, K. (2002). Significance of riverine carbon transport: A case study of a large tropical river, Godavari (India). *Science in China Series C Life Sciences-English Edition, 45*, 97–108.

Sharma, S. K., & Subramanian, V. (2008). Hydrochemistry of the Narmada and Tapti Rivers, India. *Hydrological Processes, 22*, 3444–3455. https://doi.org/10.1002/hyp.6929

Sharma, S., Jha, P. K., Ranjan, M. R., Singh, U. K., Kumar, M., & Jindal, T. (2017). Nutrient Chemistry of River Yamuna, India. *Asian Journal of Water, Environment and Pollution, 14*(2), 61–70. https://doi.org/10.3233/ajw-170016

Singh, A. K., & Hasnain, S. T. (1998). Major ion chemistry and weathering control in a high altitude basin: Alaknanda River, Garhwal Himalaya, India. *Hydrological Sciences Journal, 43*(6), 825–843. https://doi.org/10.1080/02626669809492181

Singh, R., & Pandey, J. (2019). Non-point source-driven carbon and nutrient loading to Ganga River (India). *Chemistry and Ecology, 35*(4), 344–360. https://doi.org/10.1080/02757540.2018.1554061

Smith, R. M., & Kaushal, S. S. (2015). Carbon cycle of an urban watershed: Exports, sources, and metabolism. *Biogeochemistry, 126*(1–2), 173–195. https://doi.org/10.1007/s10533-015-0151-y

Spitzy, A., & Ittekkot, V. (1991). Dissolved and particulate organic matter in Rivers. In R. F. C. Mantoura, J. M. Martin, & R. Wollast (Eds.), *Ocean margin processes in global change* (pp. 5–17). Wiley.

Ward, N. D., Bianchi, T. S., Medeiros, P. M., Seidel, M., Richey, J. E., Keil, R. G., & Sawakuchi, H. O. (2017). Where carbon goes when water flows: Carbon cycling across the aquatic continuum. *Frontiers in Marine Science, 4*, 7. https://doi.org/10.3389/fmars.2017.00007

Were, D., Kansiime, F., Fetahi, T., Cooper, A., & Jjuuko, C. (2019). Carbon sequestration by wetlands: A critical review of enhancement measures for climate change mitigation. *Earth Systems and Environment, 3*(2), 327–340. https://doi.org/10.1007/s41748-019-00094-0

# Decline of Dholavira Urban Settlement of Harappan Civilization in Kachchh was Associated with Global Climate Change Rather than the Decline of any Major Fluvial System

**Mamata Ngangom and M. G. Thakkar**

## 1 Introduction

It has long been believed that the Indus/Harappan civilization was river-based because two of its most significant towns, Harappa and Mohenjo-Daro, are situated next to sizable perennial Himalayan Rivers (Flam, 1993; Wright et al., 2008). According to reports (Mughal, 1997; Possehl, 2002), the majority of the Harappan villages were located along the current dry beds of the Ghaggar-Hakra Rivers. Numerous studies demonstrate the presence of numerous paleochannels along the current Ghaggar-Hakra channels, which are thought to be the remains of the fabled Saraswati River (Ghose et al., 1979, 1980; Kochar, 2000; Lal, 2002; Oldham, 1893; Pal et al., 1980; Radhakrishna & Merh, 1999; Valdiya, 1996, 2013). The Aryan invasion, floods brought on by hydrological disasters, shifting river courses and sea levels, social unrest, and a decline in trade are just a few of the theories put forth for the decline and abandonment of the Harappan civilization (Lahiri, 2000; McIntosh, 2007; Possehl, 2002; Ratnagar, 2000, 2006). The transformation or decline of the Indus civilization in northwest India occurred around four millennia ago as a result of the Ghaggar-Hakra River drying up due to river reorganization (Gupta, 2001; Kenoyer, 2008; Lal, 2002; Misra et al., 1984; Mughal, 1997; Possehl, 2002; Valdiya, 2002; Wright et al., 2008). The alteration of the Indus urban system was caused by the weakening of the ISM, which also caused a drop in monsoonal rivers (Giosan et al., 2012). However, the reasons for this civilization's demise, such as abrupt climatic change, fluctuating sea levels, or a lack of natural resources, are still a topic of debate among researchers (Das et al., 2017; Dixit et al., 2014, 2018; Galili, 1988;

M. Ngangom (✉)
School of Earth Sciences, Banasthali Vidyapith, Banasthali, Rajasthan, India

M. G. Thakkar
Department of Earth and Environmental Science, KSKV Kachchh University, Bhuj-Kachchh, Gujarat, India



S. Kanhaiya et al. (eds.), *Rivers of India*,
https://doi.org/10.1007/978-3-031-49163-4_11

Giosan et al., 2012; Sarkar et al., 2016; Sengupta et al., 2019; Staubwasser et al., 2003; Wright et al., 2008).

In Gujarat's Kachchh and Saurashtra region, the Harappan civilization also thrived across a significant area (Rao, 1991). Dholavira, a significant Harappan archaeological site on the Tropic of Cancer, is situated at 23°53′10″N and 70°13′0″E, on the western edge of Khadir Island and within the Great Rann of Kachchh in Gujarat, Western India (Fig. 1). Dholavira was recently added to the UNESCO list of world heritage sites during the 44th session of the UNESCO World Heritage Committee, which was held in Fuzhou, China. Locally called as Kotada Timba, the Dholavira archaeological (Harappan) site denotes a sizable fort housing the ruins of a fortified ancient city. It is also one of the five greatest Harappan sites and the most notable Indus civilization archaeological site in India (Sengupta et al., 2019). One of the rocky uplifts of the Island belt uplift in the Kachchh basin, Khadir Island's northern hill range is home to the Mansar and Manhart streams, which are the source of the Dholavira urban community. Bisht (2005) asserts that the Harappans used the most effective technique for directing the flow of such streams in the artificial tanks built within the stream itself, suggesting that even with the highest tide, the seawater might not be reaching Dholavira.

The southwest monsoonal winds that cause maritime storm surges and the ensuing continental fluvial influxes are primarily responsible for flooding the salty playa landscape of the Great Rann of Kachchh (GRK) during the monsoon season (Glennie & Evans, 1976; Gupta, 1975). Despite the fact that there were numerous Harappan sites active between 5000 and 4000 years ago in areas close to the Great Rann of Kachchh, the region is currently uninhabitable due to its harsh climate and lack of freshwater resources (Singh, 1996). It is so intriguing to comprehend why this community exists on the periphery of the Great Rann of Kachchh. According to Pascoe (1964), during the Holocene, the Rann of Kachchh's basin was filled with silt that had been carried there by streams that were draining the nearby fields. The Rann of Kachchh is estimated to be a hotspot of mature and late Harappan habitation, which is thought to have existed between 7000 and 3900 BP and was a riverine and trade-oriented society (Maurya et al., 2013; Sarkar et al., 2020). The Rann of Kachchh is also thought to be a depocenter of Holocene sediments. Merh (2005) further asserted that people from the Indus valley formerly traveled via significant rivers and a shallow sea connecting them to Kachchh and Saurashtra. The Rann sediments may be the key to recreating the Holocene paleoclimate, according to recent studies (Basu et al., 2019; Makwana et al., 2019; Ngangom et al., 2012, 2017; Pillai et al., 2017, 2018; Sarkar et al., 2020; Sengupta et al., 2019).

Currently, only two temporary rivers discharge into the Great Rann of Kachchh: the Luni in the east and the Nara in the west. According to Danino (2010) and Sankaran (1999), the Nara River is thought to be a remnant of the Vedic Saraswati River, which once flowed via connecting tributaries of the now nearly dry Ghaggar-Hakra Rivers further east than they do today (Danino, 2010; Sankaran, 1999). Another theory put up by Bhargava (1964) was that a distributary of the Saraswati delta runs southward, close to Khadir Island, over the Little Rann and the Nal Sarovar, and eventually empties into the Gulf of Cambay. Additionally, in northern

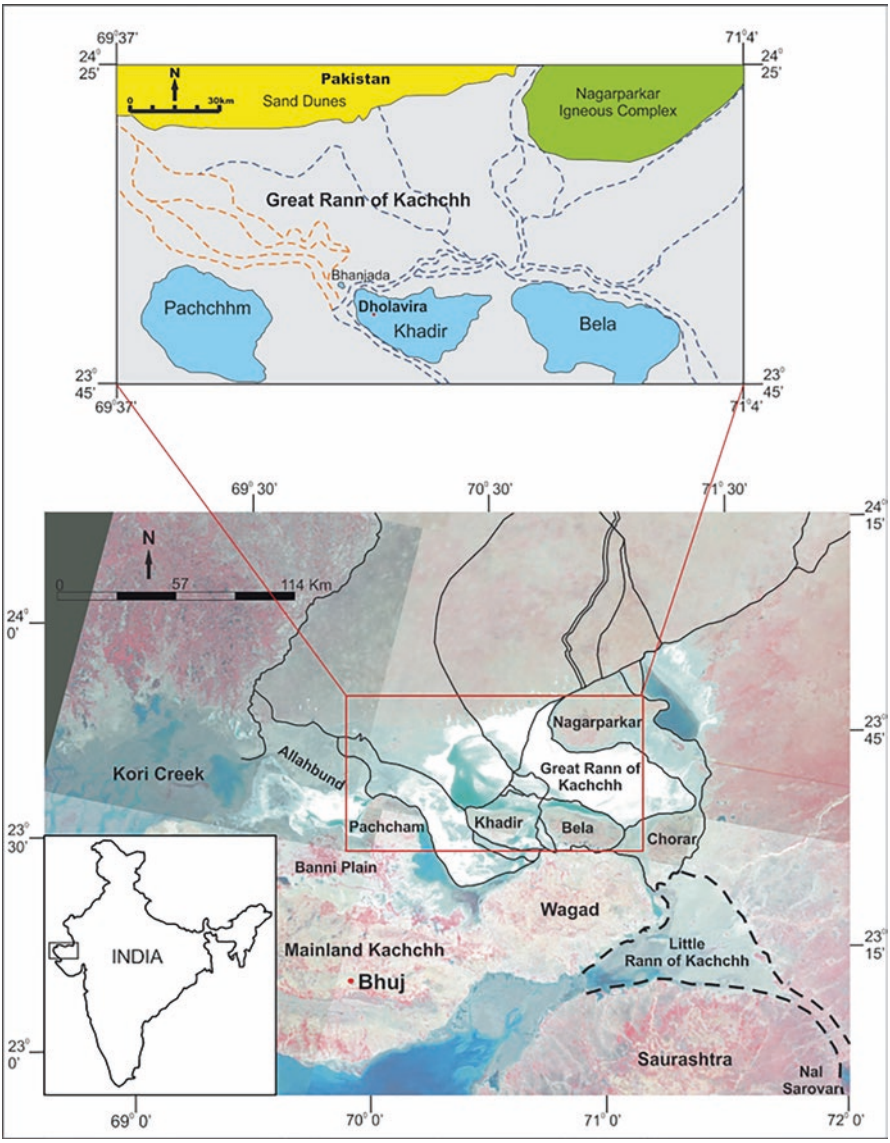


**Fig. 1** Landsat Satellite Imagery of the Kachchh peninsula showing its paleo-drainage courses (after Bhargava, 1964; Malik et al., 1999; Gupta et al., 2011). Marked window shows the paleochannel map of the eastern Great Rann of Kachchh prepared using satellite imagery. Note all the channels drain through the gap between the Khadir Island and sandy bets of Trangadi and Bara-Nana Bhangra Bets

Rann, Drishadvati, Proto-Shatadru (Hakra), and Saraswati Rivers were recognized as three deltaic river mouths (Malik et al., 1999). The current Ghaggar River is a major course of the Saraswati, which once flowed through parts of Jaisalmer

(Rajasthan, India), the surrounding region of Pakistan, and finally discharged sediments in the Rann of Kachchh was reported based on remote sensing data and earlier literature (Gupta et al., 2004). Similar to this, Rajani and Rajawat (2011) mapped palaeochannels in northwest India and Pakistan using multisensor satellite data, indicating the existence of a significant river system (Saraswati) that formerly flowed from the Himalaya through the Rann of Kachchh to the Arabian Sea. According to studies, the Indus and its distributaries were thought to have flowed more east during the mid-Holocene, with its vast delta system being positioned inside the eastern GRK (Giosan et al., 2006; Clift et al., 2012; Khonde et al., 2017). The GRK may have received sub-Himalayan sediments by channels of the Ghaggar, Hakra, and Nara Rivers, which were still running up to 3000 years ago, according to a provenance analysis of bed load sediments along the palaeochannels of the GRK using trace elements and Sr-Nd isotopes (Giosan et al., 2012., Chatterjee & Ray, 2017; Khonde et al., 2017). Additionally, according to archaeological evidence from the eastern Great Rann (Lindstrom, 2013; Rajesh, 2011), urban Harrapan people lived there, especially on the Khadir Island, which is home to one of the most significant urban Harrapan sites on the Indian Subcontinent (Bisht, 2010; Lindstrom, 2013).

The continuation of civilization depends on a consistent supply of fresh river water and efficient exchange of information with the outside world, both of which are influenced by the climate. The objectives of the current study are to ascertain if a fluvial system formerly existed in the Eastern Great Rann of Kachchh (EGRK) and whether the disappearance of the urban settlement of Dholavira is related to changes in the hydrological condition or as a result of global climatic changes. We have therefore made an effort to answer the aforementioned problems using thorough sedimentological and geochemical investigation backed by remote sensing and geochronology.

## 2 Study Area and Quaternary Successions

The research region is located on the northwest side of Khadir Island, a part of the Island Belt Uplift (IBU), which extends from east to west and has formed a steep mountainous topography, in the middle of the low-lying, salt-encrusted Great Rann (Biswas, 1993) (Fig. 1). Khadir Island's greatest elevation according to the digital elevation model (DEM) is 280 m, with northern escarpments rising between 30 and 60 m above sea level and sloping gently southward before merging with the GRK (Fig. 2a). This island comprises mainly Mesozoic as well as Tertiary sediments (Biswas, 1987). Quaternary sediments are discovered to have been deposited on the western edge of the island, where they converge with the Rann sediment to the south (Fig. 2c). Approximately 10 km southwest of the Khadir island is the long, linear Trangadi Bet islet, which is made entirely of fine sand and silt. Bara and Nana Bhangra Bets, the other two islets south of Khadir Island, feature quaternary alluvium deposits that are between 3 and 4 m thick (Fig. 2c).

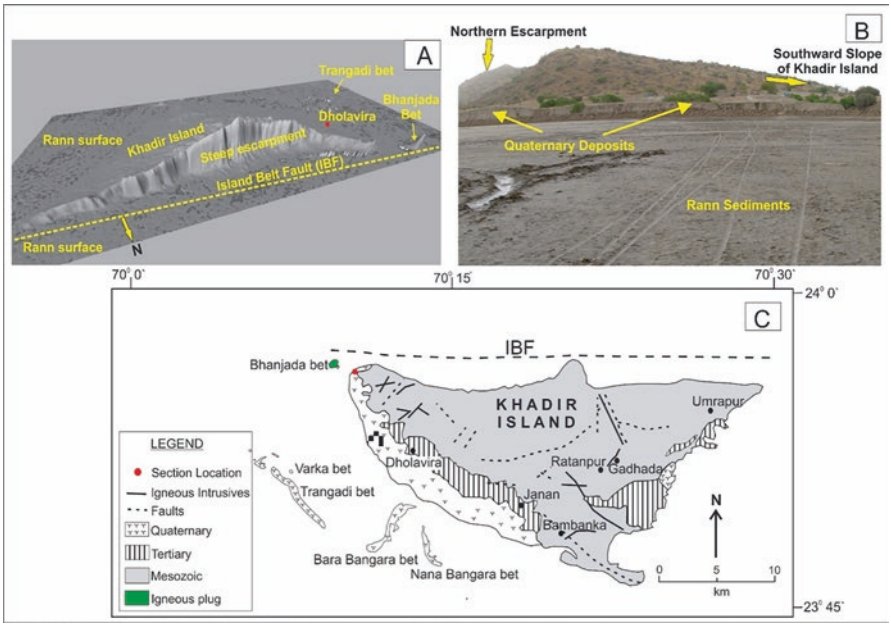


**Fig. 2** (**a**) Digital elevation model (DEM) of the study area depicts steep escarpments of Khadir Island to the north, parallel to the Island Belt Fault. The gentle slope to the south is concurrent with the regional dip of the beds. Note the abruptly rising Bhanjada Bet in the west, Trangadi Bet in the southwest. (**b**) Incised alluvial succession exposed in the northwest of Khadir Island. (**c**) Map of the study area showing major geological units exposed in Khadir Island along with major faults, intrusive bodies, and sampled location of the present study

In this investigation, ~4.5 m thick quaternary alluvium deposits that were exposed on the NW edge of the Khadir island (N 23°56′13.3″ and E 70°10′30.3″) were examined; this is shown in Fig. 2b. On the basis of sediment succession, facies architecture, and textural character, five lithounits have been identified as having been deposited over the Mesozoic rocks during the quaternary (Fig. 3). At the base of the succession, rounded to sub-rounded, imbricated Mesozoic lithoclasts with a maximum size of 4 cm are deposited. Following the gravel, there is a layer of coarse sand with distinct nodular calcretes that is 35 cm thick (KP 6L), followed by a layer of well-stratified medium to fine sand that is 25 cm thick (KP 6U) (Unit I). Unit II is composed of a laminated fine sand layer (KP 4L) that is 30 cm thick on top of a coarse sand horizon (KP 5) that is 75 cm thick. Unit III's bottom horizon (KP 4U) is 35 cm thick with huge coarse sand, while its top horizon (KP 3) is 75 cm thick with fine sand. Unit IV consists of clay intercalation (KP 2L) and alternate layers of fine and coarse sand measuring 65 cm thick. The bottom of the topmost Unit V is made up of coarse sand (KP 2U), and the upper part is made up of weakly weathered fine sand (KP 1).

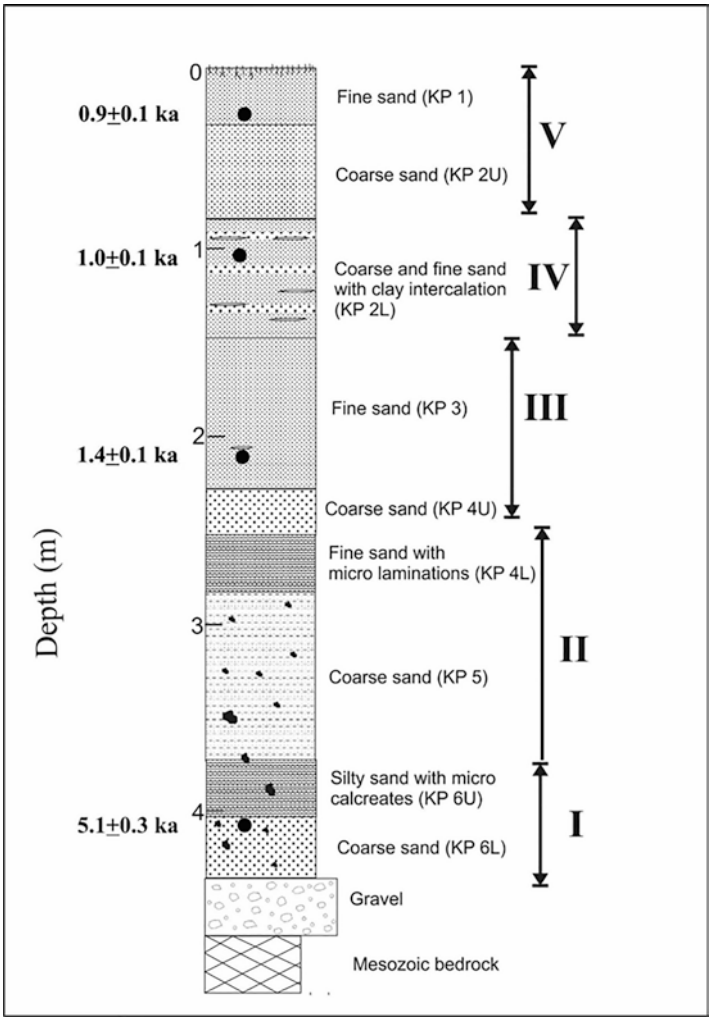


**Fig. 3** Lithostratigraphy of the Khadir Island alluvial succession along with the optical ages

## 3 Grain Size Analysis

The incised quaternary alluvial deposit's fining upward sequences have been identified using grain-size analysis. Table 1 contains sedimentological information on the sediments, and the following brief description of distinguishing characteristics follows:

(a) Graphic median (φ50): Denotes half of the particles by weight are coarser to it and half are fine (Folk, 1974). The obtained values range from 1.67 to 2.75φ, averaging 2.35φ (Table 1). The average value shows the dominance of fine sand-size sediments.

**Table 1** Table showing the sedimentological data used in to ascertain sand, silt, and clay %, graphic median (φ50), mean (Mz), standard deviation ($\sigma_{I}$), skewness ($SK_1$), and kurtosis ($K_G$)

| Sample No. | Sand % | Silt % | Clay % | Φ 95 | Φ 84 | Φ 75 | Φ 50 | Φ 25 | Φ 16 | Φ 5 | Mz | $\sigma_I$ | $SK_1$ | $K_G$ |
|---|---|---|---|---|---|---|---|---|---|---|---|---|---|---|
| KP 1 | 99.53 | 0.42 | 0.04 | 3.50 | 2.95 | 2.85 | **2.25** | 1.80 | 1.40 | 0.50 | **2.20** | **0.842** | **−0.131** | **1.171** |
| KP 2(U) | 94.62 | 3.46 | 1.89 | 4.05 | 3.40 | 3.00 | **2.65** | 2.00 | 1.70 | 0.90 | **2.583** | **0.902** | **−0.114** | **1.291** |
| KP 2(L) | 99.22 | 0.64 | 0.14 | 3.30 | 2.85 | 2.70 | **2.15** | 1.95 | 1.85 | 1.52 | **2.283** | **0.520** | **0.346** | **0.973** |
| KP 3 | 99.35 | 0.55 | 0.1 | 3.50 | 3.00 | 2.90 | **2.65** | 2.10 | 1.87 | 1.27 | **2.507** | **0.620** | **−0.309** | **1.142** |
| KP 4(U) | 91.1 | 3.75 | 5.15 | 4.25 | 3.60 | 3.15 | **2.75** | 2.00 | 1.72 | 1.02 | **2.690** | **0.959** | **−0.084** | **1.151** |
| KP 4(L) | 94.44 | 1.64 | 3.91 | 4.10 | 3.20 | 2.90 | **2.35** | 1.92 | 1.75 | 1.45 | **2.430** | **0.764** | **0.246** | **1.108** |
| KP 5 | 99.89 | 0.1 | 0.02 | 2.92 | 2.25 | 2.05 | **1.67** | 1.35 | 1.22 | 0.92 | **1.713** | **0.560** | **0.1396** | **1.171** |
| KP 6(U) | 97.69 | 1.28 | 1.08 | 3.72 | 3.20 | 2.90 | **2.30** | 1.80 | 1.55 | 1.00 | **2.35** | **0.825** | **0.067** | **1.013** |
| KP 6(L) | 95.31 | 1.15 | 3.54 | 4.00 | 3.00 | 2.85 | **2.37** | 1.82 | 1.55 | 1.05 | **2.31** | **0.8095** | **−0.013** | **1.174** |
| Average | | | | | | | **2.35** | | | | **2.34** | **0.756** | **0.0164** | **1.133** |

(b) Graphic mean (Mz): Measure of central tendency, which is calculated by the formula φ16 + φ 50 + φ 83/3 (Folk, 1974). The calculated values range from 1.713 to 2.69φ with an average value of 2.34φ (Table 1). The average value denotes that the major sediment class is fine sand-size particles (Fig. 4).

(c) Graphic standard deviation ($\sigma_1$): Measure of particle size sorting or uniformity of distribution, and it is calculated by the formula φ 84 – φ 16/4 + φ 95 – φ 5/6.6 (Folk, 1974). The values obtained ranged from 0.52 to 0.959 φ (Table 1). Out of nine samples, three samples are moderately well sorted ranging from 0.52 to 0.62 φ, and the other six samples are moderately sorted ranging from 0.764 to 0.959 φ. Hence, the general tendency is exhibited by the moderate nature of sorting with an average value of 0.756 φ (Fig. 4).

(d) Graphic skewness (Sk1): Determines whether coarse or fine sediments are more or less often distributed or dominant. It is calculated by the formula φ 84 + φ 16–2 φ 50/(φ 84 – φ 16) + φ 95 + φ 5–2 φ 50/(φ 95–2 φ 5). The negative value indicates material that is coarsely skewed, whereas the positive value indicates more material that is finely skewed (Folk, 1974). The skewness value ranges from −0.309 φ (coarse skewed) to +0.346 φ (strongly fine skewed) (Table 1). It is found that one sample is showing strongly fine skewed, two fine skewed, three near symmetrical, two coarse skewed and another one sample is showing strongly coarse skewed. However, the average value of 0.0164 shows a near symmetrical nature (Fig. 4).

(e) Graphic kurtosis ($K_G$): Peakedness of the distribution and quantifies the proportion of sorting in the curve's tails to its center. It is referred to as platykurtic if the tails are better sorted than the central portions and leptokurtic if the central portions are better sorted. Both are sorted similarly if the mesokurtic condition is predominant (Folk, 1974). The values obtained vary from 0.973 φ (mesokurtic) to 1.291 φ (leptokurtic), although there are more leptokurtic sediments (six), ranging from 1.142 φ to 1.291 φ, and fewer mesokurtic sediments (three),

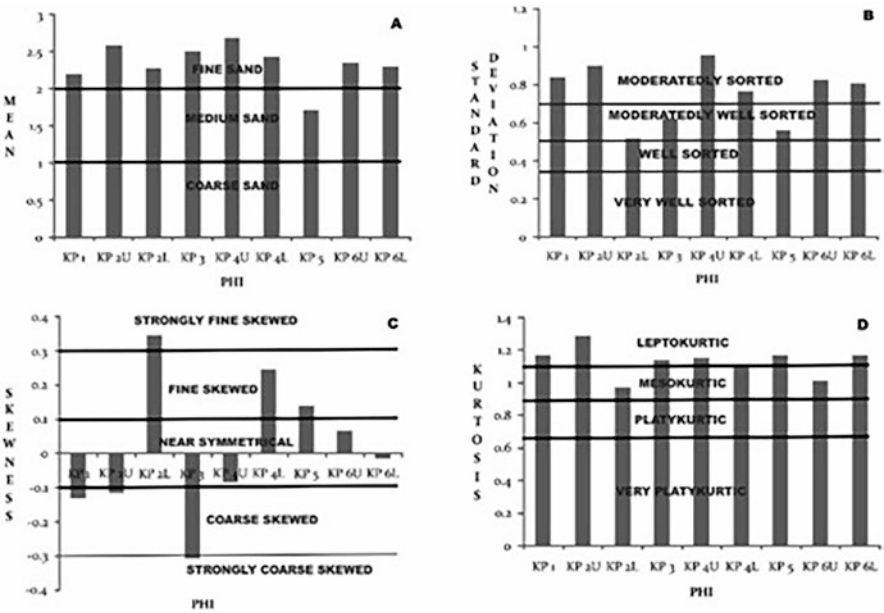


**Fig. 4** Comparative histograms of all samples showing (**a**) mean, (**b**) standard deviation, (**c**) skewness, and (**d**) kurtosis values

ranging from 0.973 φ to 1.108 φ (Table 1). Hence, the average value of 1.133 φ shows leptokurtic nature (Fig. 4).

Hence, the grain size from Khadir Island indicates that the majority of the samples are fine sand, moderately sorted, near-symmetrical, and mostly leptokurtic (Table 1; Fig. 4).

According to Visher (1969), the saltation population size is between 1.75 φ and 2.5 φ, the saltation truncation between suspension and saltation occurs between 2.75 φ and 3.5 φ, and the fluvial sands typically have a suspension population (>20%). Our samples have a saltation population that falls between 1.75 φ and 3φ, a saltation truncation point between 3 φ and 3.5 φ, and a suspension population that is roughly 40%; sliding and rolling populations are almost nonexistent (Fig. 5a). Friedman (1961) asserts that because the dune sands are more meticulously sorted, they may be easily distinguished from river sands. Additionally, to distinguish between coastal dune and river sand as well as the beach sand, bivariate plots between mean diameter and standard deviation (Moiola & Weiser, 1968) and skewness and standard deviation (Friedman, 1961) are utilized. Figure 5b and c shows that the samples from Khadir Island belong in the category of river sand. This strengthens the idea that the alluvium deposits on Khadir Island were formed in a river setting.

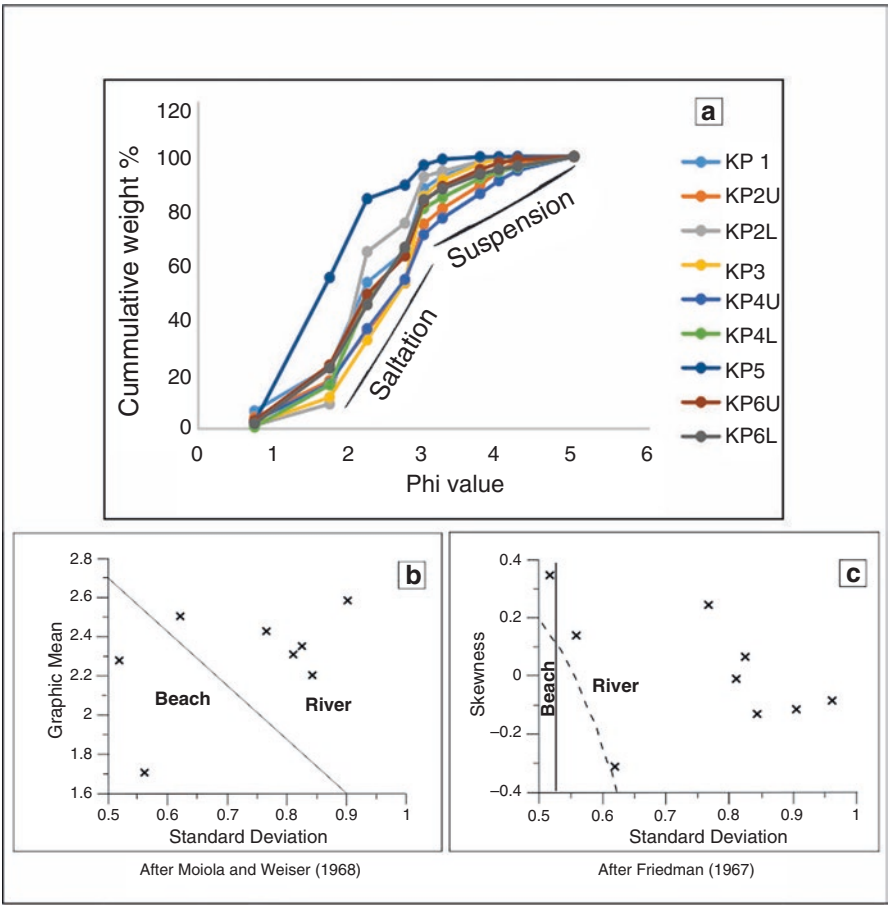


**Fig. 5** (**a**) Cumulative frequency curve showing the depositional trend of all the samples. (**b**) Bivariate plots (Standard Deviations vs. Skewness and Standard Deviation vs. Graphic mean) depict that the sediments of Khadir Island were deposited in a fluvial environment

## 4 Geochemistry and Chronology

Major element geochemistry of 80 samples along with the country rocks was carried out using XRF spectrometry at the National Facility for Planetary Science and Exploration Program (PLANEX), Physical Research Laboratory, Ahmedabad to ascertain the provenance and level of post-depositional changes of the sediments. In accordance with (McLennan's (1993) standards, the Chemical Index of Alteration (CIA) was determined on samples of carbonate-free sediment. Khadir Island is primarily composed of sediments from the Mesozoic and Tertiary periods (Biswas, 1987). The CIA values for the two samples of Mesozoic sandstone and Tertiary limestone are 84 and 40, respectively, while the CIA values for the quaternary

alluvial deposit range from 62 to 90. The Tertiary limestone's low value of 40 is caused by the material's high calcium (Ca) concentration.

Although the principal element composition of the igneous rock is comparable to that of alkaline igneous rocks, Paul et al. (2008) assessed the CIA value of the rock to be 43. To comprehend the provenance of the sediments and the post-depositional weathering trend, the major element oxides of the quaternary alluvial sediments and country rocks are plotted in a triangle diagram with $Al_2O_3$-CaO* + $Na_2O$-$K_2O$ at the tip (Nesbitt & Young, 1982, 1984) (Fig. 6). Due to the fact that the mobile components (CaO + $Na_2O$) are lost preferentially during weathering, the weathering trend is parallel to the $Al_2O_3$-CaO* + $Na_2O$ axis. We contrasted the quaternary alluvial deposits of Khadir Island with the weathering trends of two end components, alkaline igneous rock, Mesozoic, and Tertiary sedimentary rocks (Fig. 6). The quaternary sediments are discovered to have a weathering trend that is parallel to the two-end members, but if the source of the sediment came from outside the study area, its weathering trend would have deviated from the two-end members weathering trend (local lithology), as shown in Fig. 6.

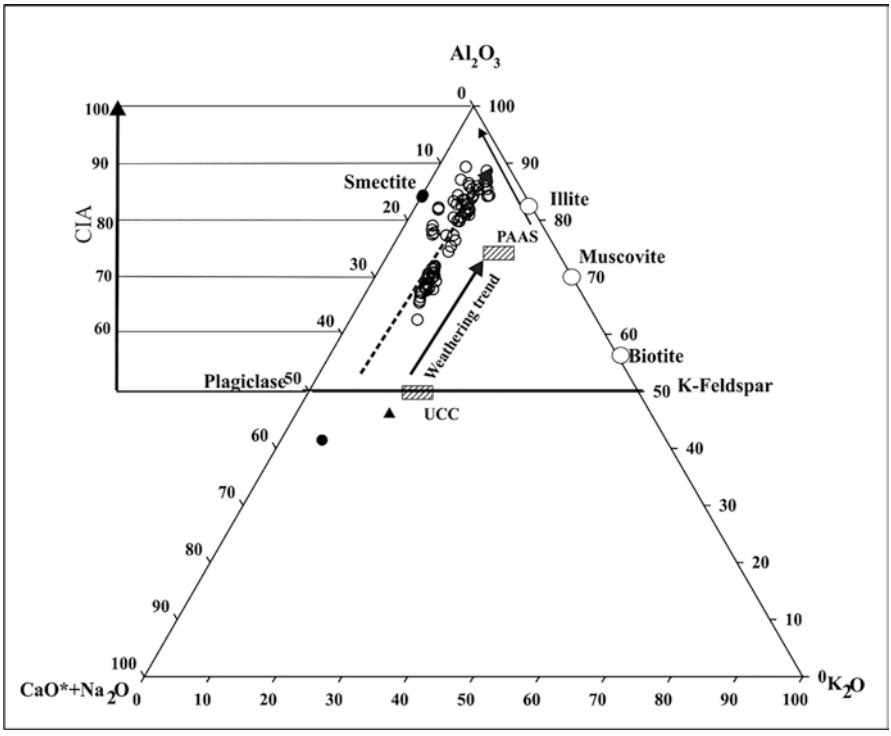


**Fig. 6** A-CN-K plot of the Khadir Island alluvium sediment and the local lithology (Mesozoic sandstone, Tertiary limestone, and igneous rock). The secondary minerals plot above the K-feldspar and Plagioclase, both having a CIA value of 50. Intermediate weathering products like illite and smectite (CIA, 75–85) plot between A corner and feldspar join (CIA = 50). UCC (Upper Continental Crust) and PAAS (Post-Achaean Average Australian Shale)

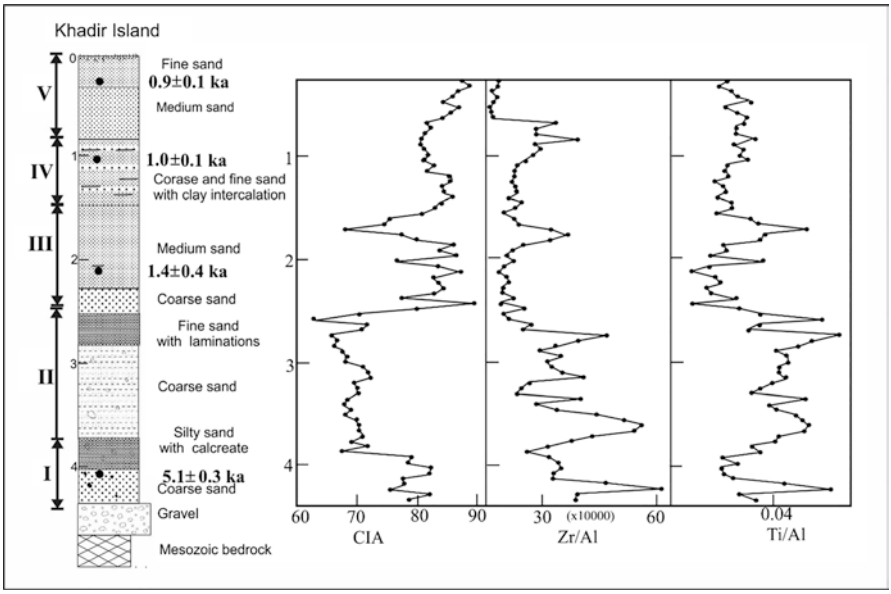


**Fig. 7** Plot of CIA, Zr/Al Ti/Al ratios showing temporal changes in the weathering pattern during the aggradation of different sedimentary units. The gray rectangular boxes shown in the figure correspond well with the periods of enhanced weather (CIA) and show events of relatively strengthening of ISM

To further identify the temporal changes in monsoon intensity throughout the aggradation of various litho units, CIA value, Zr/Al, and Ti/Al are plotted (Fig. 7). In the current situation, monsoon variability influences chemical weathering, which is measured using CIA (Nesbitt & Young, 1982). In order to identify the periods of variance in monsoon occurrences, Zr/Al and Ti/Al ratios are employed as a proxy for aridity because their amounts increase with an increase in aeolian flux (Deplazes et al., 2014; Larrasoaña et al., 2003; Wehausen & Brumsack, 2000). The Physical Research Laboratory in Ahmedabad analyzed OSL samples obtained from recently exposed quaternary alluvial sections of the Khadir Island using the single aliquot regeneration (SAR) methodology developed by Murray and Wintle (2000). Table 2 contains information on radioactivity assays, dosage rate, and SAR ages. Figure 3 shows that Unit I, the first unit in the fining upward sequence, has an age of 5.10.3 ka, Units III and IV have ages that range from 1.40.1 ka to 1.00.1 ka, and Unit V has an age of 0.90.1 ka.

## 5 Discussion

Following the retreat of a shallow marine sea, it is hypothesized that the continental process began to dominate the Eastern Great Rann of Kachchh around 2 ka (Glennie & Evans, 1976; Maurya et al., 2013). The Luni and Nara Rivers, which empty at the

**Table 2** Table showing the details of geochronology

| Sample No. | Latitude/ longitude | U (ppm) | Th (ppm) | K % | De (Gy) | Dose rate (Gy/ ka) | Age (ka) |
|---|---|---|---|---|---|---|---|
| BBN-1 | N 23:56:37.774/E 70:08:24.329 | 3.08 ± 0.06 | 9.72 ± 0.2 | 1.24 ± 0.02 | 2.9 ± 0.2 | 2.5 ± 0.2 | 1.1 ± 0.1 |
| BBN-2 | N 23:56:37.774/E 70:08:24.329 | 2.00 ± 0.04 | 4.87 ± 0.1 | 0.84 ± 0.01 | 2.6 ± 0.2 | 1.6 ± 0.1 | 1.6 ± 0.1 |
| BBN-3 | N 23:56:37.774/E 70:08:24.329 | 2.39 ± 0.05 | 6.88 ± 0.1 | 0.95 ± 0.02 | 3.9 ± 0.3 | 1.9 ± 0.1 | 2.0 ± 0.2 |
| BBN-4 | N 23:56:37.774/E 70:08:24.329 | 3.81 ± 0.07 | 9.70 ± 0.2 | 1.49 ± 0.03 | 6.6 ± 0.3 | 2.9 ± 0.2 | 2.3 ± 0.2 |
| KH – TL1 | N 23:56:12.805/E 70:10:29.177 | 1.3 ± 0.06 | 8.3 ± 0.4 | 1.01 ± 0.0.01 | 1.6 ± 0.2 | 1.8 ± 0.7 | 0.9 ± 0.1 |
| KH – TL3 | N 23:56:12.805/E 70:10:29.177 | 2.72 ± 0.05 | 9.1 ± 0.3 | 1.18 ± 0.01 | 12 ± 0.2 | 2.3 ± 0.1 | 5.1 ± 0.3 |
| KH/ DV/ TL-1 | N 23:56:12.805/E 70:10:29.177 | 3.4 ± 0.02 | 11.3 ± 0.5 | 1.48 ± 0.01 | 4 ± 0.1 | 2.9 ± 0.2 | 1.4 ± 0.1 |
| KH/ DV/ TL-2 | N 23:56:12.805/E 70:10:29.177 | 1.4 ± 0.07 | 4.2 ± 0.2 | 0.62 ± 0.006 | 1.3 ± 0.1 | 1.3 ± 0.1 | 1.0 ± 0.1 |

eastern and western edges of the Rann, respectively, currently supply sediment to the Eastern Great Rann of Kachchh. According to studies based on satellite remote sensing data (Deo et al., 2011; Pokharia et al., 2011; Rajani & Rajawat, 2011), an active river system existed during the Harappan civilization. The Eastern Great Rann of Kachchh may have received sediments from a river system, according to several studies (Clift et al., 2012; Giosan et al., 2006; Gupta et al., 2004; Khonde et al., 2017). The region would have had a rather continuous sediment deposit if it had a big river system; however, the quaternary alluvial deposits are observed to be patchy and near to the Khadir Island (Fig. 2c). According to Khonde et al. (2011), sediments were deposited along the beaches of the rocky island until 500 years ago near Khadir Island. This suggests the existence of a shallow but navigable sea. The studies conducted by Ngangom et al. (2017), on the other hand, show deposition occurs in a river environment along the northern edge of Khadir Island.

The Indian Summer Monsoon is the primary cause of precipitation in western India. As a result, it is possible to infer that the Khadir Island alluvium sediments exhibit multiple fining upwards sequences as a sedimentological expression of the hydroclimatic variability of the mid-Holocene. This conclusion is supported by grain size analysis data, which demonstrate the dominance of fine sand, moderate

sorting, and near-symmetrical and leptokurtic nature of the sediments (Fig. 4). The earliest fluvial deposit (Unit I) on Khadir Island was deposited at about 5 ka, while the periodic younger episodes are dated to be 1.4 ka and 1 ka, according on optical chronology of the sediments and facies architecture (Fig. 3) (Mayewski et al., 2004; Steig, 1999). Makwana et al. (2021) recently found that during the late Harappan era, the Banni Plains of Kachchh gradually strengthened the Indian Summer Monsoon. The Himalayas, Western Saurashtra, Parsons Valley Lake, Tamil Nadu, and the Himalayas have all observed enhanced Indian Summer Monsoon conditions throughout the mid-Holocene (Khathayat et al., 2017; Thakur et al., 2019; Raja et al., 2019). Unit I does a good job of indicating Khadir Island's improved mid-Holocene precipitation status at about 5 ka. The considerable decrease in fluvial processes could be the cause of the absence of younger fluvial sediment succession dating back to 5 and >1 ka. Giosan et al. (2012) claim that the Harappan-dominated terrain saw increased aridity conditions after 5 ka, which resulted in a rather stable fluvial landscape in western India. The urban Harappan civilization thus fell in the already arid Indus valley, while sedentary agriculture emerged in the drying central and southern regions of India (Ponton et al., 2012). It was proposed that the aridity and weakening of the ISM started after 5 ka based on the continental (Dixit et al., 2014; Giosan et al., 2012) and marine (Gupta et al., 2003; Lückge et al., 2001) climate reconstruction records. Based on the analysis of oxygen isotopes found in gastropod shells from a relict lake around the Harappan site in northwest India, Dixit et al. (2014) suggest that the ISM began to diminish generally after about 4 ka. Many ancient civilizations are thought to have developed, declined, and vanished due to changes in climate that occurred during the Holocene epoch (globally correlatable drought episode around about 4200 years). The Harappan civilization's demise, along with the Akkadian Empire, the Old Kingdom of Egypt, and the Early Bronze Age civilization of Greece and Crete, may have been impacted by the larger-scale climatic event that caused cooling, drought, and social collapse at 4200 calyr BP, according to Weiss and Bradley (2001). Similar to how the Yangtze civilization in China came to an end, the 4200 calyr BP climate event is similarly thought to be responsible (Yasuda et al., 2004; Yasuda, 2008). According to Staubwasser et al. (2003), the Harappan civilization perished as a result of the emergence of a centennial-scale (200–800 year) drought cycle around 4200 cal BP. According to Sengupta et al. (2019), the Meghalayan Age, which began between 4300 and 4100 years ago, caused the catastrophic drought that resulted in the downfall of the Harappan settlement at Dholavira, Kachchh, and a change in the humid fluvial landscape.

According to Dixit et al. (2014), the isotopic data in Fig. 3a shows an increase in isotopic value, which implies a mild ISM up to about 2 ka, followed by a modest fall in the isotopic value (rather favorable ISM), which lasted up to around 0.5 ka. Our observation, which demonstrates that late Holocene fluvial activity was noticeably stronger, is consistent with this. Between 2000 and 1500 years ago, according to Lückge et al. (2001), the ISM was strengthened and rejuvenated. During the last 1.5 ka (MWP between 900 and 1300 AD; (Mann, 2002b), centennial-scale climatic changes, particularly the Medieval Warm Period (MWP), have been observed. As

the topmost fining upward sequences in our current study, Unit IV and V have been dated to 1 ka (1015 AD) and 0.9 ka (1115 AD), respectively; corresponding to the MWP, it is possible that the streams near Khadir Island also responded to the century-scale small-amplitude climatic perturbation. According to Gupta et al. (2003), a significant surge in G. Bulloides off the coast of Oman in the eastern Arabian Sea suggests a brief rise in the ISM during the Medieval Warm Period, which is known as 600–1200 years ago. A warm and humid environment was present during the Medieval Warm Period, according to pollen analyses from the western and central Indian subcontinent (Farooqui et al., 2013) and the Northeast Himalayas (Bhattacharyya et al., 2007). The lack of river sediment younger than 1 ka in the current research area may be due to the aridity condition becoming more severe, which is speculatively linked to the Little Ice Age (Mann, 2002a; Sinha et al., 2007).

The general tendency of aridity that causes the ISM to decline and was observed elsewhere on the Indian subcontinent during the Little Ice Age (Kale et al., 2000; Nigam & Khare, 1994) also aligns well with our research. The high-resolution weathering (CIA) and aridity (Zr/Al and Ti/Al) data are seen to provide strong support for the sedimentological properties of the Khadir Island alluvium series (Fig. 7). The mature Harappan civilization period's significantly elevated ISM corresponds nicely with the high CIA estimate of 5 ka. The low ratios of Zr/Al and Ti/Al also indicate this increased precipitation state. The Indian Summer Monsoon then begins to weaken, as shown by a general decline in CIA value and an increase in the Zr/Al and Ti/Al ratios. Without an absolute geochronology, we can only speculate that this time period coincides with the waning of the Indian Summer Monsoon, which lasted for around 4–3 ka (Dixit et al., 2014; Ponton et al., 2012; Staubwasser et al., 2003). According to Bhattacharyya et al. (2007), Farooqui et al. (2013), and Gupta et al. (2003), the significantly enhanced Indian Summer Monsoon associated with the Medieval Warm Period is consistent with persistently high CIA values and low ratios of Zr/Al and Ti/Al until roughly 0.9 ka. The alluvium samples weathering pattern shows a strong correlation with the local lithology of Khadir Island (Fig. 6). This indicates that the fluvial deposits visible along Khadir Island's northwest coast were formed locally, with little to no exogenous input from the main river system. This disproves the idea that a sizable fluvial system was active around 5 ka and is consistent with the conclusions (Tyagi et al., 2012) reached by studying the western Great Rann of Kachchh (WGRK). Since the Great Rann may have had a marginally high sea until around 2 ka (Maurya et al., 2013; Tyagi et al., 2012), we hypothesize that the influence of relatively finer sediments from the Khadir Island region may have resulted from the salt-induced commutation of the sedimentary rocks. When there were periods of somewhat enhanced ISM, the sediments were occasionally mobilized into the lowland areas during extreme hydrological events, which may have assisted the Harappans in maintaining their economy on Khadir Island throughout the mid-Holocene. Thus, the present study supports the earlier hypothesis that the downfall of the Harappan civilization was not related to the presence of a significant fluvial system (Clift et al., 2012; Giosan et al., 2012; Tyagi et al., 2012), instead

a gradual weakening in the Indian Summer Monsoon after 5 ka (onset of the Meghalayan Age ~4.2 ka) and before the Medieval Warm Period could be the main cause for the fall of the Harappan civilization in EGRK (Dholavira, Khadir Island).

## 6 Conclusion

Following are some major conclusions drawn from the sedimentological, geochemistry, and chronology of the current study conducted at the Khadir Island:

1. Over the past five thousand years, the Indian Summer Monsoon's fluctuating intensity has an effect on the EGRK's desert region.
2. The existence of fining upward sequences suggests extremely harsh hydrological circumstances related to times of enhanced Indian Summer Monsoon.
3. The majority of the samples are fine sand, fairly sorted, nearly symmetrical, and leptokurtic, according to grain size analyses. The fluvial depositional trend is illustrated by cumulative frequency graphs. The dominance of river sand is also demonstrated by bivariate plots between the mean diameter and standard deviation and the skewness and standard deviation.
4. Quaternary sediment geochemical research shows that they exhibit Mesozoic and Tertiary geochemical fingerprints, disproving the idea that a significant fluvial system was extant in the EGRK during the mid-Holocene.
5. The current study adds support to the earlier hypothesis that the decline of the Harappan civilization at Dholavira in the EGRK was not due to the presence of a significant fluvial system, but rather may have been caused by a gradual weakening of the Indian Summer Monsoon after 5 ka (the beginning of the Meghalayan Age was 4.2 ka) and prior to the Medieval Warm Period.

**Acknowledgments** The authors acknowledge the Department of Science and Technology (DST). Government of India for financial support (SR/S4/ES-TG/023/2008 and SR/FTP/ES-49/2013). Mamata Ngangom appreciates the Vice-Chancellor, Banasthali Vidyapith for administrative support. The authors are grateful to Physical Research Laboratory, Ahmedabad, and the scientists, NavinJuyal and Anil Shukla, for their support in geochronological and geochemical analysis and fruitful discussions. The anonymous reviewers are acknowledged for giving their time to improve this MS.

## References

Basu, S., Prasanta, S., Pillai, A. S., & Ambili, A. (2019). Response of grassland ecosystem to monsoonal precipitation variability during the mid-late Holocene: Inferences based on molecular isotopic records from Banni Grassland, western India. *PLOS ONE, 14*(4), 0212743. https://doi.org/10.1371/journal.pone.0212743

Bhargava, M. L. (1964). *The geography of Rigvedic India* (1st ed.) Lucknow.

Bhattacharyya, A., Sharma, J., Shah, S. K., & Chaudhury, V. (2007). Climatic changes last 1800 years BP from Paradise Lake, Sela Pass, Arunachal Pradesh, Northeast Himalaya. *Current Science, 93*, 983–987.

Bisht, R. S. (2005). The water structures and engineering of the Harappan at Dholavira (India). In C. Jarrige & V. Lefevre (Eds.), *South Asian archaeology 2001* (Vol. 1, pp. 11–25). Editions Research sur les Civilisations.

Bisht, R. S. (2010). Does Dholavira Sheds new light on the antiquity of the Buddhist Stupa architecture? In I. A. Khan, R. Barret, & R. Trivedi (Eds.), *International seminar on Buddhist heritage, Gujarat* (pp. 75–76). The Maharaja Sayajirao University of Baroda and Government of Gujarat.

Biswas, S. K. (1987). Regional tectonic framework, structure and evolution of the western marginal basins of India. *Tectonophysics, 135*, 307–327.

Biswas, S. K. (1993). *Geology of Kachchh* (p. 450). K.D.M. Institute of Petroleum Exploration.

Chatterjee, A., & Ray, J. S. (2017). Sources and depositional pathways of mid-Holocene sediments in the Great Rann of Kachchh, India: Implications for fluvial scenario during the Harappan culture. *Quaternary International, 443*, 177–187. https://doi.org/10.1016/j.quaint.2017.06.008

Clift, P. D., Carter, A., Giosan, L., Durcan, J., Duller, G. A. T., Macklin, M. G., Alizai, A., Tabrez, A. R., Danish, M., VanLaningham, S., & Fuller, D. Q. (2012). U-Pb zircon dating evidence for a Pleistocene Sarasvati river and capture of the Yamuna river. *Geology, 40*, 211–214.

Danino, M. (2010). *The lost river: On the trail of the Sarasvatī*. Penguin.

Das, A., Prizomwala, S., Makwana, N., & Thakkar, M. (2017). Late Pleistocene-Holocene climate and sea level changes inferred based on the tidal terrace sequence, Kachchh, western India. *Palaeogeography Palaeoclimatology Palaeoecology, 473*, 82–93. https://doi.org/10.1016/j.palaeo.2017.02.026

Deo, S. G., Ghate, S., & Rajaguru, S. N. (2011). Holocene environmental changes and cultural patterns in coastal western India: A geoarchaeological perspective. *Quaternary International, 229*, 132–139.

Deplazes, G., Lückge, A., Stuut, J., Pätzold, J., Kuhlmann, H., Husson, D., Fant, M., & Haug, G. H. (2014). Weakening and strengthening of the Indian monsoon during Heinrich events and Dansgaard-Oeschger oscillations. *Paleoceanography, 29*, 99–114.

Dixit, Y., Hodell, D. A., Sinha, R., & Petrie, C. A. (2014). Abrupt weakening of the Indian summer monsoon at 8.2 Kyr B.P. *Earth and Planetary Science Letters, 391*, 16–23. https://doi.org/10.1130/G35236.1

Dixit, Y., Hodell, D. A., Giesche, A., Tandon, S. K., Gázquez, F., Saini, H. S., et al. (2018). Intensified summer monsoon and the urbanization of Indus civilization in Northwest India. *Scientific Reports, 8*, 4225. https://doi.org/10.1038/s41598-018-22504-5

Farooqui, A., Gaur, A. S., & Prasad, V. (2013). Climate, vegetation and ecology during Harappan period: Excavations at Kanjetar and Kaj, mid-Saurashtra coast, Gujarat. *Journal of Archaeological Science, 40*, 2631–2647.

Flam, L. (1993). *Himalaya to the sea* (J. F. Shroder, Ed.) (pp. 265–287). Routledge.

Folk, R. L. (1974). *Petrology of sedimentary rocks* (182 pp). Hemphill.

Friedman, G. M. (1961). Distinction between dune, beach and river sands from their textural characteristics. *Journal of Sedimentary Petrology, 31*, 514–529.

Galili, E., Weinstein-Evron, M., & Ronen, A. (1988). Holocene sea-level changes based on submerged archaeological sites off the northern Carmel Coast in Israel. *Quaternary Research, 29*, 36–42. https://doi.org/10.1016/0033-5894(88)90069-5

Ghose, B., Zar, A., & Hussain, Z. (1979). The lost courses of the Sarasvati river in the great indian desert: New evidence from LANDSAT imagery. *The Geographical Journal, 145*(3), 446–451.

Ghose, B., Zar, A., & Hussain, Z. (1980). Comparative role of Aravalli and Himalayan river systems in the fluvial sedimentation of Rajasthan desert. *Man and Environment, 4*, 8–12.

Giosan, L., Constantinescu, S., Clift, P. D., et al. (2006). Recent morphodynamics of the Indus Delta shore and shelf. *Continental Shelf Research, 26*, 1668–1684.

Giosan, L., Clift, P. D., Macklin, M. G., Fuller, D. Q., Constantinescu, S., Durcan, J. A., et al. (2012). Fluvial landscape of the Harappan civilization. *Proceedings of the National Academy of Sciences, 109*(26), 1688–1694. https://doi.org/10.1073/pnas.1112743109

Glennie, K. W., & Evans, G. (1976). A reconnaissance of the recent sediments of Ranns of Kutch, India. *Sedimentology, 23*, 625–647.

Gupta, S. K. (1975). Silting of the Rann of the Kutch during the Holocene. *Indian Journal of Earth Sciences, 2*, 163–175.

Gupta, S. P. (2001). River Sarawati in history, archaeology and geology. *Puratattva, 13–14*, 51–54.

Gupta, A. K., Anderson, D. M., & Overpeck, J. T. (2003). Abrupt changes in the Asian southwest monsoon during the Holocene and their links to the North Atlantic Ocean. *Nature, 421*, 354–357.

Gupta, A. K., Sharma, J. R., Sreenivasan, G., & Srivastava, K. S. (2004). New findings on the course of river Sarasvati. *Photonirvachak, 32*, 1–24.

Gupta, A. K., Sharma, J. R., & Sreenivasan, G. (2011). Using satellite imagery to reveal thecourse of an extinct river below the Thar Desert in the Indo-Pak region. *International Journal of Remote Sensing, 32*, 5197e5216.

Kale, V. S., Singhvi, A. K., Mishra, P. K., & Banerjee, D. (2000). Sedimentary records and luminescence chronology of Late Holocene palaeofloods in the Luni River, Thar Desert, Northwest India. *Catena, 40*, 337–358.

Kenoyer, J. M. (2008). *Encyclopedia of archaeology* (pp. 715–733). Elsevier.

Khatayat, G., Cheng, H., Sinha, A., Yi, L., Xianglei, L., Zhang, H., et al. (2017). The Indian monsoon variability and civilization changes in the Indian subcontinent. *Science Advances, 3*(12), e1701296. https://doi.org/10.1126/sciadv.1701296

Khonde, N., Maurya, D. M., Singh, A. D., Chowksey, V., & Chamyal, L. S. (2011). Environmental significance of raised ran sediments along the margins of Khadir, Bhanjada and Kuar Bet islands in Great Rann of Kachchh, western India. *Current Science, 101*, 1429–1434.

Khonde, N. N., Maurya, D. M., & Chamyal, L. S. (2017). Late Pleistocene–Holocene clay mineral record from the Great Rann of Kachchh basin, western India: implications for palaeoenvironments and sediment sources. *Quaternary International, 443*, 86–98.

Kochar, R. (2000). *Vedic people: Their history and geography*. Orient Longman.

Lahiri, N. (2000). *Decline and fall of the Indus civilization*. Permanent Black.

Lal, B. B. (2002). *The Sarasvati flows on: The continuity of Indian culture*. Aryan Books International.

Larrasoaña, J. C., Roberts, A. P., Rohling, E. J., Winklhofer, M., & Wehausen, R. (2003). Three million years of monsoon variability over the northern Sahara. *Climate Dynamics, 21*, 689–698.

Lindstrom, K. E. (2013). *Pottery preferences and community dynamics in the Indus civilization borderlands* [Unpublished Ph.D. Thesis]. University of Wisconsin-Madison.

Lückge, A., Doose-Rolinski, H., Khan, A. A., Schulz, H., & von Rad, U. (2001). Monsoonal variability in the northeastern Arabian Sea during the past 5000 years: Geochemical evidence from laminated sediments. *Palaeogeography, Palaeoclimatology, Palaeoecology, 167*, 273–286.

Makwana, N. M., Prizomwala, S. P., Chauhan, G., Phartiyal, B., & Thakkar, M. G. (2019). Late Holocene Palaeo-environmental change in the Banni Plains, Kachchh, western India. *Quaternary International, 507*, 197–205. https://doi.org/10.1016/j.quaint.2018.11.028

Makwana, N. M., Prizomwala, S. P., Das, A., Phartiyal, B., Sodhi, A., & Vedpathak, C. (2021). Reconstructing the climate variability during the last 5000 years from the Banni Plains, Kachchh, western India. *Frontiers in Earth Science, 9*. https://doi.org/10.3389/feart.2021.679689

Malik, J. N., Merh, S. S., & Sridhar, V. (1999). Palaeo-delta complex of vedic Sarasvati and other ancient rivers of Northwestern India. In B. P. Radhakrishna & S. S. Merh (Eds.), *Vedic Saraswati* (Vol. 42, pp. 163–174). Geological Society of India Memoir.

Mann, M. E. (2002a). Little ice age. In M. C. MacCracken & J. S. Perry (Eds.), *Encyclopedia of global environmental change* (pp. 504–509). Wiley.

Mann, M. E. (2002b). Large-scale climate variability and connections with the Middle East in past centuries. *Climatic Change, 55*, 287–314.

Maurya, D., Khonde, N., Das, A., Chowksey, V., & Chamyal, L. (2013). Subsurface sediment characteristics of the Great Rann of Kachchh, western India based on preliminary evaluation of textural analysis of two continuous sediment cores. *Current Science, 104*(8), 1071–1077.

Mayewski, P. A., Rohling, E. E., Stager, J. C., Karlen, W., Maasch, K. A., Meekar, L. D., Meyerson, E. A., Gasse, F., Kreveld, S. V., Holmgren, K., Lee-Thorp, J., Rosqvist, G., Rack, F., Staubwasser, M., Schneider, R. R., & Steig, E. J. (2004). Holocene climate variability. *Quaternary Research, 62*, 243–255.

McIntosh, J. (2007). *The ancient Indus Valley: New perspectives*. ABC-CLIO.

McLennan, S. M. (1993). Weathering and global denudation. *The Journal of Geology, 3*, 295–303.

Merh, S. S. (2005). The Great Rann of Kachchh: Perception of a field geologist. *Journal of the Geological Society of India, 65*, 9–25.

Misra, V. N., Lal, B. B., & Gupta, S. P. (1984). Climate, a factor in the rise and fall of the Indus civilization: Evidence from Rajasthan and beyond. In *Environmental issues in India: A reader* (pp. 461–490). Dorling Kindersley (India) Pvt, Ltd.

Moiola, R. J., & Weiser, D. (1968). Textural parameters: An evaluation. *Journal of Sedimentary Petrology, 38*(1), 45–53.

Mughal, M. R. (1997). *Ancient Cholistan: Archaeology and architecture*. Ferozsons.

Murray, A. S., & Wintle, A. G. (2000). Luminescence dating of quartz using an improved single-aliquot regenerative-dose protocol. *Radiation Measurements, 32*, 57–73.

Nesbitt, H. W., & Young, G. M. (1982). Early Proterozoic climates and plate motions inferred from major element chemistry of lutites. *Nature, 199*, 715–717.

Nesbitt, H. W., & Young, G. M. (1984). Prediction of some weathering trends of plutonic and volcanic rocks based on thermodynamic and kinetic considerations. *Geochimica et Cosmochimica Acta, 48*, 1523–1534.

Ngangom, M., Thakkar, M. G., Bhushan, R., & Navin, J. (2012). Continental-marine interaction in the vicinity of the Nara River during the last 1400 years, Great Rann of Kachchh, western India. *Current Science, 103*(11), 1339–1342.

Ngangom, M., Bhandari, S., Thakkar, M. G., Shukla, A. D., & Juyal, N. (2017). Mid-Holocene extreme hydrological events in the eastern Great Rann of Kachchh, western India. *Quaternary International, 443*, 188–199. https://doi.org/10.1016/j.quaint.2016.10.017

Nigam, R., & Khare, N. (1994). Effect of river discharge of the morphology of benthonic foraminifera test. *Journal of Geological Society of India, 43*, 457–463.

Oldham, C. F. (1893). The Saraswati and the lost river of the Indian desert. *Journal of the Royal Asiatic Society, 34*, 49–76.

Pal, Y., Sahai, B., Sood, R. K., & Agarwal, D. P. (1980). Remote sensing of the "lost" Saraswati river. *Proceeding Indian National Science Academy (Earth and planetary sciences), 89*, 317–331.

Pascoe, E. H. (1964). *A manual of geology of India and Burma* (Vol. III, pp. 1878–1959). Govt. of India Press.

Paul, D. K., Ray, A., Das, B., Patil, S. K., & Biswas, S. K. (2008). Petrology, geochemistry and paleomagnetism of the earliest magmatic rocks of Deccan Volcanic Province, Kutch, Northwest India. *Lithos, 102*, 237–259.

Pillai, A. S., Ambili, A., Sankaran, M., Prasanta, S., Jha, D., & Ratnam, J. (2017). Mid-late Holocene vegetation response to climatic drivers and biotic disturbances in the Banni grasslands of western India. *Palaeogeography Palaeoclimatology Palaeoecology, 485*, 869–878. https://doi.org/10.1016/j.palaeo.2017.07.036

Pillai, A. S., Ambili, A., Prasad, V., Manoj, M. C., Varghese, S., Prasanta, S., et al. (2018). Multi-proxy evidence for an arid shift in the climate and vegetation of the Banni grasslands of western India during the mid to late Holocene. *The Holocene, 28*(7), 1057–1070. https://doi.org/10.1177/0959683618761540

Pokharia, A. K., Kharakwal, J. S., Rawat, R. S., Osada, T., Nautiyal, C. M., & Srivastava, A. (2011). Archaeobotany and archaeology at Kanmer, a Harappan site in Kachchh, Gujarat: Evidence for adaptation in response to climatic variability. *Current Science, 100*, 1833–1846.

Ponton, C., Giosan, L., Eglinton, T. I., Fuller, D. Q., Johnson, J. E., Kumar, P., & Collett, T. S. (2012). Holocene aridification of India. *Geophysical Research Letters, 39*, L03704. https://doi.org/10.1029/2011GL050722

Possehl, G. (2002). *The Indus civilization: A contemporary perspective*. Altamira Press.

Radhakrishna, B. P., & Merh, S. S. (1999). *Vedic Saraswati, memoir* (Vol. 42). Geological Society of India.

Raja, P., Achyuthan, H., Farooqui, A., Ramesh, R., Kumar, P., & Chopra, S. (2019). Tropical rainforest dynamics and Palaeoclimate implications since the late Pleistocene, Nilgiris, India. *Quaternary Research, 91*(1), 367–382. https://doi.org/10.1017/qua.2018.58

Rajani, M. B., & Rajawat, A. S. (2011). Potential of satellite based sensors for studying distribution of archaeological sites along palaeo channels: Harappan sites a case study. *Journal of Archaeological Science, 38*(9), 2010–2016.

Rajesh, S. V. (2011). *A comprehensive study of the regional chalcolithic cultures of Gujarat* [Unpublished Ph.D. thesis]. Department of Archaeology and Ancient History. The Maharaja Sayajirao University of Baroda, Vadodara, India.

Rao, S. R. (1991). *Dawn and Devolution of Indus civilization*. Aditya Prakashan.

Ratnagar, S. (2000). *The end of the great Harappan tradition*. Manohar Publishers.

Ratnagar, S. (2006). *Understanding Harappa: Civilization in the Greater Indus Valley*. Tulika Books.

Sankaran, A. V. (1999). Saraswati–the ancient river lost in the desert. *Current Science, 77*, 1054–1060.

Sarkar, A., Mukherjee, A. D., Bera, M. K., et al. (2016). Oxygen isotope in archaeological bioapatites from India: Implications to climate change and decline of Bronze Age Harappan civilization. *Scientific Reports, 6*, 26555. https://doi.org/10.1038/srep26555

Sarkar, A., Mukherjee, A. D., Sharma, S., Sengupta, T., Ram, F., Bera, M. K., et al. (2020). New evidence of early Iron Age to Medieval settlements from the southern fringe of Thar Desert (Western Great Rann of Kachchh), India: Implications to climate-culture co-evolution. *Archaeological Research in Asia, 21*, 2352–2267. https://doi.org/10.1016/j.ara.2019.100163

Sengupta, T., Mukherjee, A. D., Bhusan, R., Ram, F., Bera, M. K., Raj, H., et al. (2019). Did the Harappan settlement of Dholavira (India) collapse during the onset of Meghalayan stage drought? *Journal of Quaternary Science, 35*(3), 382–395. https://doi.org/10.1002/jqs.3178

Singh, B. P. (1996). *Indian archaeology 1991–92 – A review*. Archaeological Survey of India.

Sinha, A., Cannariato, K. G., Stott, L. D., Cheng, H., Edwards, R. L., Yadava, M. G., Ramesh, R., & Singh, I. B. (2007). A 900-year 600 to 1500 AD record of the Indian summer monsoon precipitation from the core monsoon zone of India. *Geophysical Research Letters, 34*, L16707. https://doi.org/10.1029/2007GL030431

Staubwasser, M., Sirocko, F., Grootes, P. M., & Segl, M. (2003). Climate change at the 4.2 Ka BP termination of the Indus valley civilization and Holocene South Asian monsoon variability. *Geophysical Research Letters, 30*(8), 14–25. https://doi.org/10.1029/2002GL016822

Steig, E. J. (1999). Mid-Holocene climate change. *Science, 286*, 1485–1487.

Thakur, B., Seth, P., Sharma, A., Pokharia, A. K., Spate, M., & Farooqui, S. (2019). Linking past cultural developments to Palaeoenvironmental changes from 5000 BP to present: A climate-culture reconstruction from Harshad estuary, Saurashtra, Gujarat, India. *Quaternary International, 507*, 188–196. https://doi.org/10.1016/j.quaint.2019.01.019

Tyagi, A. K., Shukla, A. D., Bhushan, R., Thakker, P. S., Thakkar, M. G., & Juyal, N. (2012). Mid-Holocene sedimentation and landscape evolution in the western Great Rann of Kachchh, India. *Geomorphology, 151–152*, 89–98. https://doi.org/10.1016/j.geomorph.2012.01.018

Valdiya, K. S. (1996). Saraswati that disappeared. *Resonance, 1*, 19–28.

Valdiya, K. S. (2002). *Saraswati: The river that disappeared*. Universities.

Valdiya, K. S. (2013). The river Saraswati was a Himalayan-born river. *Current Science, 104*, 42–54.

Visher, G. S. (1969). Grain size distributions and depositional processes. *Journal Sedimentary Petrology, 39*, 1074–1106.

Wehausen, R., & Brumsack, H. J. (2000). Chemical cycles in Pliocene sapropel-bearing and sapropel-barren eastern Mediterranean sediments. *Palaeogeography, Palaeoclimatology, Palaeoecology, 158*, 325–352.

Weiss, H., & Bradley, R. S. (2001). Archaeology: What drives societal collapse? *Science, 291*, 609–610.

Wright, R. P., Bryson, R. A., & Schuldenrein, J. (2008). Water supply and history: Harappa and the Beas regional survey. *Antiquity, 82*, 37–48.

Yasuda, Y. (2008). Climate change and the origin and development of rice cultivation in the Yangtez river basin, China. *AMBIO: A Journal of the Human Environment, 37*, 502–506.

Yasuda, Y., Fujiki, T., Nasu, H., Kato, M., Morita, Y., Mori, Y., Kanehara, M., Toyama, S., Yano, A., Okuno, M., He, J., Ishihara, S., Kitagawa, H., Fukusawa, H., & Naruse, T. (2004). Environmental archaeology at the Chengtoushan site, Hunan province, China and implications for environmental change and the rise and fall of the Yangtze River civilization. *Quaternary International, 123–125*, 149–158.

# Ghaghara River: A Case Study of Flood in Uttar Pradesh by GIS-Based Technique

**Ajay Pratap Singh**

## 1 Introduction

The Ghaghara River, one of the main tributaries of the Ganga River, rises near Mansarovar Lake (4800 m) on the Tibetan Plateau. It is perennial in nature and is the second-longest tributary after the Yamuna in terms of length. After arriving from the Himalaya, it merges with the Sarda River in India to form the left bank of the Ganga tributary. It is 507 km long in Nepal and 1080 km long in India before it meets the Ganga River (Mohan, 2018; Singh et al., 2020; Arya et al., 2020). Figure 1 depicts the Ghaghara River's entire drainage basin.

In Nepal, the Ghaghara River is also referred to as Manchu, Kauriala, or Karnali. It has its source in the Tibetan Mountains, close to Mansarovar Lake. The Sanskrit term "gharghara," which means rattling or laughter, is where the name Ghaghara comes from. Shisha Pani is where the Kauriala River pierces the Himalaya, and shortly after, it branches off into the Girwa River to the east, bringing down the main discharge. Ghaghara, which enters the Ganga Plain close to Bichha town, is formed when the Kauriala and Girwa rivers combine (Mohan, 2018).

## 2 Ghaghara River Valley in Uttar Pradesh

The Ghaghara River valley is significantly wider than the Ganga River valley at the middle of its course, when it is about 60 km wide. The incorporation of the three major river basins, the axial river Ghaghara and the Sarda and Sarju rivers on its western and eastern sides, gives the present-day Ghaghara River valley its tremendous width. In Tanakpur, the Sarda River enters into the Ganga Plain after cutting

A. P. Singh (✉)
Department of Geology, University of Lucknow, Lucknow, Uttar Pradesh, India



S. Kanhaiya et al. (eds.), *Rivers of India*,
https://doi.org/10.1007/978-3-031-49163-4_12

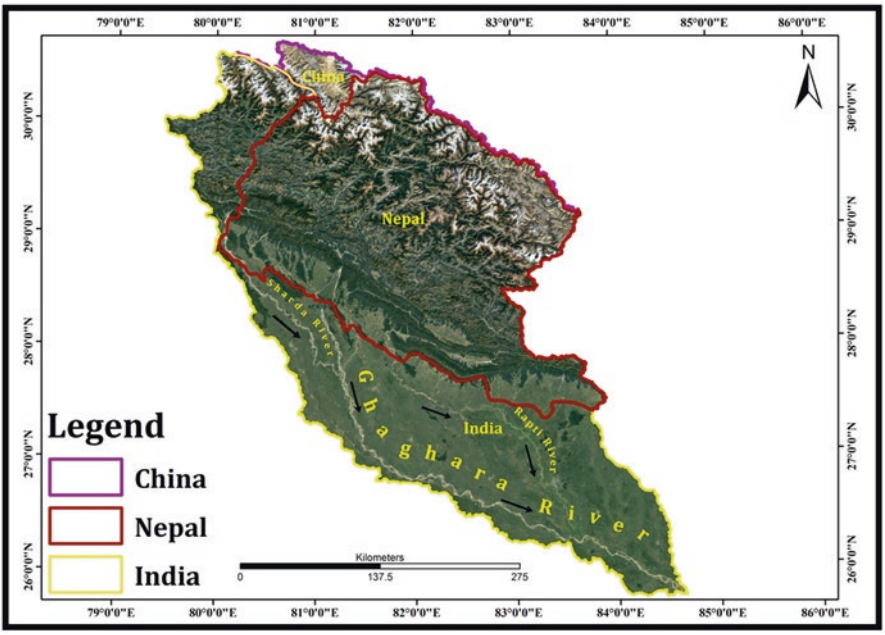


**Fig. 1** Ghaghara catchment with their adjacent countries overlay at the Google Earth image of the 04 – Jan, 2019

through the Siwalik Hills (Mitra et al., 2005). Babai Nala, also known as the Sarju River, rises from the Siwalik Hills. In Nepal's Kumbher district, it reaches the alluvial plain close to the Bargadaha village.

On the basis of valley breadth, valley direction, and active channel characteristics, the Ghaghara River valley in India has been separated into three sectors. The following is a description of the key characteristics of each sector:

## *2.1 Sector A*

It starts when the Sarda, Ghaghara, and Sarju rivers emerge from the plains and go all the way to where they separate into their own valleys (Fig. 2). The Ghaghara, Sarda, and Sarju rivers have a low sinuosity braided channel pattern as they leave the Hills. They have separate valleys and are cut into the Piedmont region. The Ghaghara, Sarda, and Sarju rivers initially have a north-south channel orientation. However, all three rivers thereafter turn eastward and westward at an angle following a line that denotes linear control. Then, all of the rivers begin to flow from northwest to southeast. The Ghaghara River valley is 5–20 km wide, the Sarda River valley is 5–15 km wide, and the Sarju valley is 5–8 km wide. In comparison to the Sarda and Ghaghara River valleys, the width of the Sarju River valley is narrower.

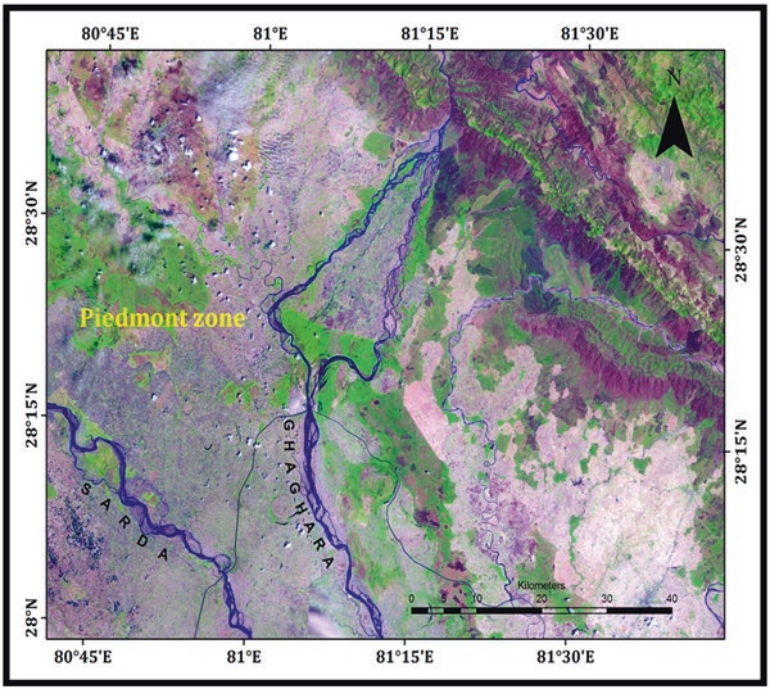


**Fig. 2** Image shows Sector A region of Ghaghara River

Other small tributaries of the Ghaghara River that meet it on its right (western) side include the Suheli and Jauraha rivers in addition to the Sarju and Sarda rivers. The Siwalik Hills serve as the catchment area for Suheli River, and the spring line of the Piedmont Zone is where Jauraha Nadi begins. With straight stretches in between and rapid shifts in stream orientation, the currently active Suheli and Jauraha rivers have low sinuosity meandering channel patterns. The channel features and channel width of the current channel do not match the meander scars next to the Suheli and Jauraha rivers (Mohan, 2018).

## *2.2 Sector B*

It stretches from the spot where the valleys of the Sarda, Ghaghara, and Sarju rivers converge to form an extraordinarily large valley up to Faizabad town, where the width of the valley abruptly decreases (Fig. 3). The Ghaghara River valley is 25–60 km wide. The Ghaghara River valley has significantly uneven right and left valley edges. The majority of the Ghaghara River's channel length in this section displays a northwest southeast inclination, with an east-west orientation beginning a few kilometers upstream of Faizabad. In this section, Sarda River initially exhibits

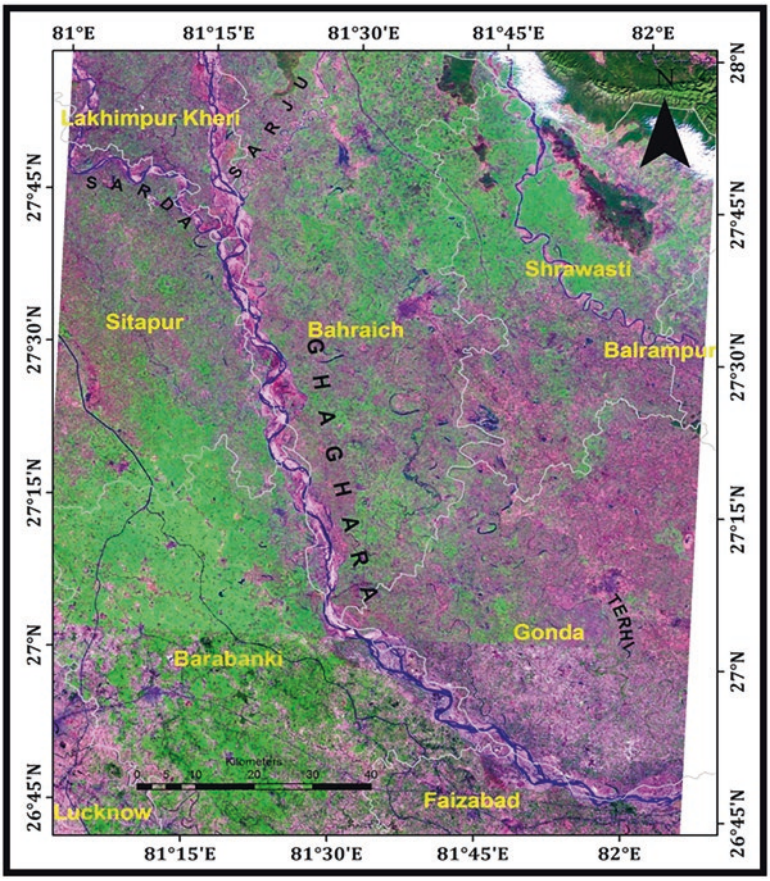


**Fig. 3** Image shows Sector B region of Ghaghara River

a northwest-southeast trend before switching to an east-west inclination. The Sarju River can be either north-south or northeast-southwest oriented.

The Sarda River is located on the western bank of the Ghaghara River, and the Chauka River has a series of meander scars on its western and southern bank that are not related to the river's channel characteristics. The Sarju River, which has a valley wall and displays the presence of multiple ponds, is located on the eastern bank of the Ghaghara River.

The terraces are uniformly formed on either side of the Ghaghara River in the proximal and central portions of sector B of the Ghaghara River basin. The terraces on the right bank of the Ghaghara River (to the south and southwest) abruptly narrow at the distal end, while those on the left side (the northern side) of the river gradually do so.

## 2.3 Sector C

Around 7 km (km) upstream of Barhaj, it stretches from Faizabad town to the junction of the Ghaghara and Rapti rivers in Madhubani (Fig. 4). The Ghaghara River has straight stretches in between its low-intensity braided channel pattern. The valleys range in width from 15 to 25 km. The Ghaghara River has a range of trends, from WNW-ESE to EW-WW.

On the southern side, the T1 terrace is either nonexistent or extremely small. The townships of Faizabad and Ayodhya are situated 15 m above the active river flood plain on topographically higher ground. The T1 terrace, located on the left side (northern side) of the Ghaghara River where a number of meander scars are found, is roughly 12 km broad between Tanda and Belghat. Since the Kuwana River crosses these meander scars, it is possible that the Kuwana River was not in this location when the meander scars were formed.

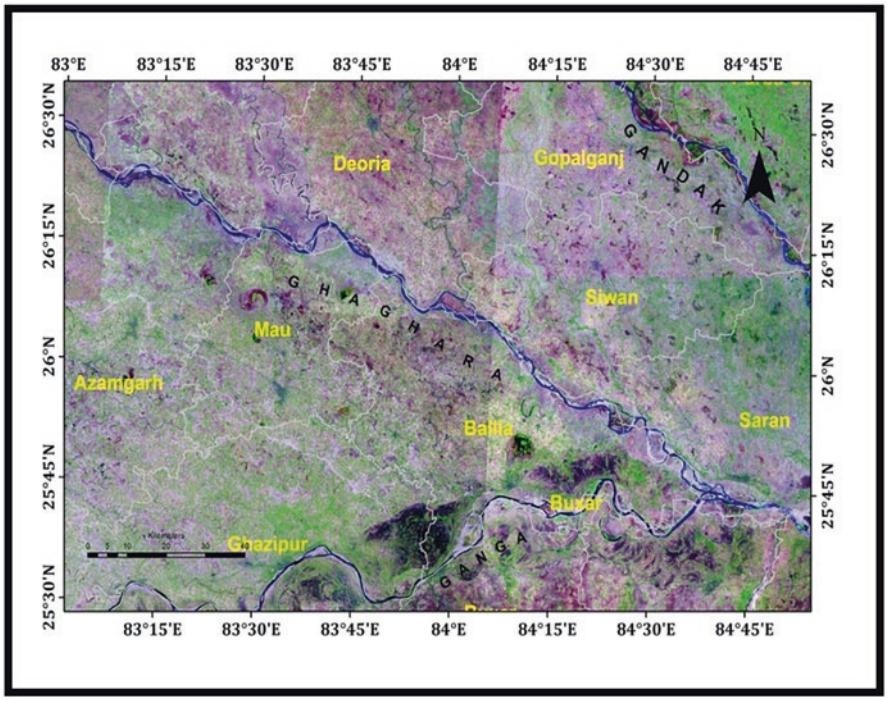


**Fig. 4** Image shows Sector C region of Ghaghara River

## 3 Ghaghara Basin in Uttar Pradesh

In its whole, the Ghaghara River travels through 21 districts in Uttar Pradesh before reaching the confluence. The districts are Pilibhit, Shahjahanpur, Lakhimpur Kheri, Sitapur, Bahraich, Saraswati, Barabanki, Faizabad, Gonda, Balrampur, Siddharthnagar, Basti, Ambedkar Nagar, Sant Kabir Nagar, Maharajganj, Gorakhpur, Azamgarh, Mau, Deoria, Kushinagar, and Ballia (Fig. 5).

The Ghaghara basin is a region in Uttar Pradesh that is roughly 47,082 km$^2$ in size and situated between latitudes 26°–29° N and longitudes 80°–85° E. The Ghaghara (620 km), Rapti (555 km), Kuwano (333 km), Sarda (25 km), Burhi Rapti (201 km), Saryu (229 km), Ami (229 km), and Rohini (154 km) are the principal rivers in the Ghaghara basin in India (Arya & Singh, 2021).

The tropical monsoon that dominates the basin has three distinct seasons: summer, winter, and monsoon. The annual precipitation varies from 900 to 1400 mm, and the mean temperature ranges from 44.4° to 44.8 °C (Mohan, 2018; Arya & Singh, 2021).

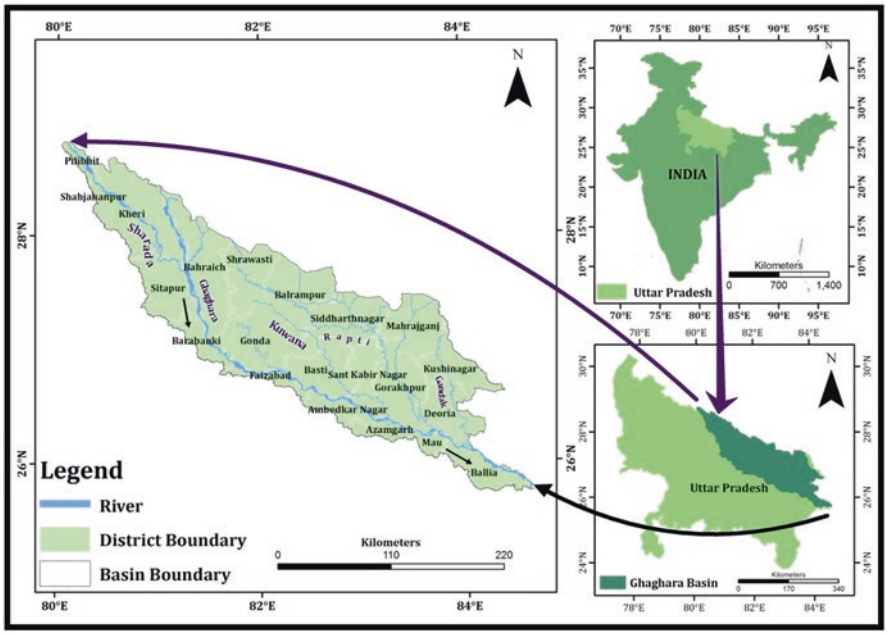


**Fig. 5** Location map of Ghaghara basin in Uttar Pradesh, India

## 4 Flooding in Ghaghara Basin (Uttar Pradesh)

Every year during the monsoon season, the Ghaghara River and its tributaries in the Ghaghara megafan, which are largely supplied by snow, cause floods (Singh, 2020). However, a few days of heavy rain that last for many hours become the main cause of floods in recent years despite human action also playing a role (Singh et al., 2020).

The primary causes that increase a location's risk of flooding are ongoing encroachment along the stream, the restoration of wetlands and water bodies, changes in land use and land cover, deforestation in the upper watershed, and the expansion of dense roadway network. This flooding frequently brings about both monetary injustice and personal sorrow. In order to choose the ideal place for the controlled spread of human civilization in flood-prone areas, flood hazard mapping is therefore essential (Singh et al., 2015).

## 5 Remote Sensing Satellite and GIS-Based Approaches

In the current global context, high-resolution spectral bands from remote sensing (RS) satellite data have developed a workable method for understanding the hydrological conduct and water resource from a board view (Lin et al., 1997; Horritt et al., 2001; Sinha et al., 2008). The MCA technique is also used to build flood risk assessment methodologies utilizing geographic information systems (GIS) (Warner, 2001; Sanjay & Goel, 2002; Gupta & Srivastava, 2010; Patel & Srivastava, 2013; Arya & Singh, 2021).

As we know the Ghaghara basin is susceptible to flooding and has flooded annually for decades as a result of heavy rainfall during the monsoon season, the district-level approach of this basin is the first study that is useful in identifying the hazard risk zone in small areas and can be mitigated at the district administration level.

The current study aims to use the AHP (Ranking) method and weightage overlay analysis (WA) with raster data of rainfall dispersion, slope, drainage density, land use-land cover (LULC), micro watershed size, and soil texture (loamy, sandy, and clayey) to create a flood risk hazard map of the Ghaghara basin in Uttar Pradesh. The management of micro-watersheds in the area will benefit from this method, and it will also give residents of the Ghaghara basin useful information about natural disasters like floods.

### *5.1 Rainfall Distribution*

Daily precipitation data is not readily available, so yearly precipitation averages from 2000 to 2019 have been used instead. Significant rainfall is more likely to result in an overpowering flood than low rainfall, and higher rank was given to significant rainfall while low rank was given to little rainfall (Ajin et al., 2013). Rainfall measurements ranged from 820 to 1250 mm throughout the time frame (Fig. 6a).

## 5.2 Slope Analysis

The slope of the terrain through which the water travels through the drainage channels is a major determinant of the water flow. However, compared to the lowest slope or flat terrain, the steepest slope has a bigger effect on runoff and peak discharge (Singh et al., 2020). The slope angle of the basin varies from 1° to 22° (Fig. 6b). Higher values were given a lower rank because of the comparatively large runoff, while lower values were given a higher rank because of the nearly flat terrain. The majority of the riverside zones, which are significant flood inundation sites, are within 1° to 2° of one another.

## 5.3 Drainage Density (Dd)

Drainage density is a significant feature that makes it difficult for water to go from source to sink. It shows how closely spaced the streams are from one another. Drainage density is a measure of the capacity for infiltration; the higher it is, the less intrusion there will be and the less likely there would be an overflow. Conversely, the lower it is, the more infiltration there will be and the more susceptible there will be to floods (Rai & Mohan, 2014).

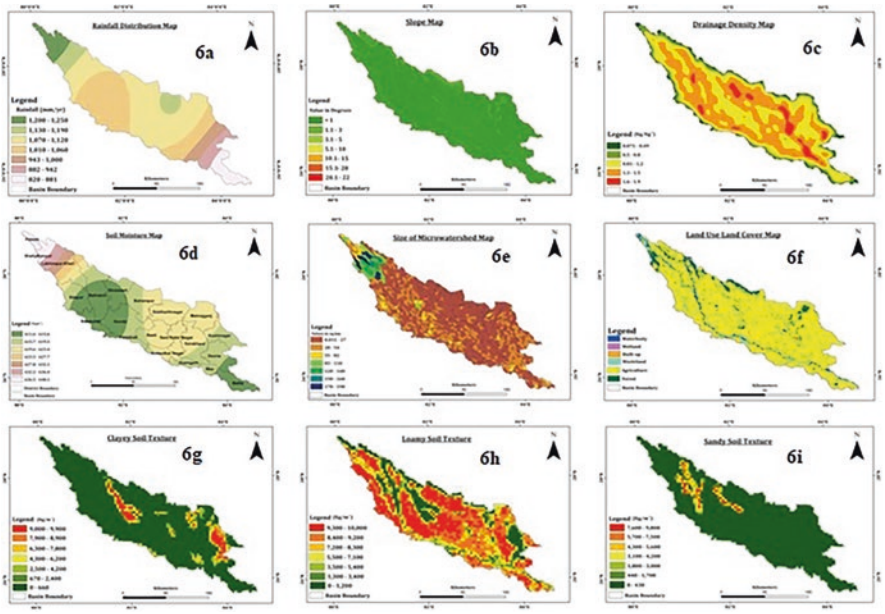


**Fig. 6** Showing (**a**) interpolated rainfall distribution map, (**b**) slope map, (**c**) drainage density map, (**d**) soil moisture map, (**e**) size of micro-watershed map, (**f**) land use-land cover map, (**g**) clayey soil texture, (**h**) loamy soil texture, and (**i**) sandy soil texture

Figure 6c shows the Ghaghara basin's low to moderate drainage density, which ranges between 0.07 and 1.9 kg/kg$^2$. Zones with inadequate drainage density are given larger weights, and zones with acceptable drainage are given lower weights.

### *5.4 Soil Moisture*

The porosity and permeability of the lithology type in a certain area play a major role in determining the variability of soil moisture. According to Arya et al. (2020), alluvial deposition with a highly proportionate fluctuation of sand, silt, and clay resulted in the formation of the Ghaghara basin. The more porous the soil, the more moisture it can hold before flooding since less moisture means there is less direct flow (lower runoff), but greater moisture means there is more direct flow and fewer chances of flooding. Figure 6d shows the interpolated soil moisture distribution rank, which spans from 611.6 to 640 kgm$^1$. Lower values have been given a higher rank, and higher values have been given the lowest rank.

### *5.5 Area of Micro-watershed*

Smaller micro-watersheds are more prone to flooding because longer runoff periods are needed in micro-watersheds with greater drainage regions for a significant rise in water level to constitute a flood (Ajin et al., 2013).

Micro-watersheds can range in size from 0.031 to 190 km$^2$. Figure 6e shows the completed map, where smaller micro-watersheds are ranked higher and bigger micro-watersheds are ranked lower.

### *5.6 Land Use-Land Cover (LULC) Analysis*

Wetland, wasteland, water body, forest, agricultural, and built-up areas are included in the land use-land cover (Fig. 6f). Since there is more precipitation available than in built-up, wasteland, farmland, and forest region, water bodies are more susceptible to floods.

### *5.7 Soil Texture*

Sand is substantially more porous and permeable than clayey soil and loamy soil. Because of this, sandy and loamy soil is more flood-resistant than clayey soil. Figure 6g, h, and i demonstrates the produced map and assigns higher locations to higher estimations of sandy, loamy, and clayey soil surface, while lower values are

ranked lower. The rank of the soil surface information that was downloaded depends on pixel estimates**.**

## *5.8 Multicriteria Analysis (MCA)*

The flood hazard index was calculated using a multicriteria analysis (MCA), which took into account the nine flood conditioning factors of rainfall distribution, slope, drainage density, soil moisture, area of micro-watershed, land use/cover, and clayey, sandy, and loamy soil texture. The themed maps were produced using ArcGIS, and rank values were given to each class for the nine variables. A pairwise comparison matrix was built using the nine-point scale developed to evaluate the impact on floods. A consistence value (CR) of 0.1 was generated when each factor's estimated relative weight was compared using a paired matrix, proving the consistency of the pairwise matrix and the dependability of the factor weights. The FHI value, which ranges from 1 to 9, indicates how susceptible a location is to floods. Using this equation (Eq. 1), the flood hazard index (FHI) is then calculated by the GIS environment and displayed as a digital map.

$$\begin{aligned} \mathrm{FHI} &= 0.26^{*}\ \text{rainfall} + 0.16^{*}\ \text{slope} + 0.15^{*}\ \text{drainage density} + 0.08^{*}\ \text{soil moisture} \\ &+0.10^{*}\ \text{size of micro watershed} + 0.05^{*}\ \text{land use} \\ &-\text{land cover} + 0.06^{*}\ \text{clayey} + 0.06^{*}\ \text{loamy} + 0.04^{*}\ \text{sandy} \end{aligned} \tag{1}$$

## *5.9 Flood Hazard Risk Zone*

In the GIS environment, raster calculators were utilized to obtain the processes for organizing the contributing variables, overlay activity, and hazard area evaluation. The produced map of the flood risk zone is shown in Figs. 7a and 7b, respectively, based on the contributing elements and weightages.

On the flood risk zonation map, the Ghaghara basin in Uttar Pradesh is split into five classes: very low hazard risk zones (4%), low hazard risk zones (8.5%), moderate hazard risk zones (23.6%), high hazard risk zones (42%), and very high hazard risk zones (21.9%). Due to the nearly flat topography, the Ghaghara River and its confluence point with its tributaries, the Tirhi, Kuwana, Rapti, and Gandak River, present a very high danger zone, although the nearby piedmont or foothill region in the Ghaghara basin presents a very low risk zone. There are 27,490 villages in the Ghaghara basin study area, of which 7553 are in a zone with a very high flood risk, 12,705 are in a zone with a high flood risk, 6080 are in a zone with a moderate flood impacting 327 settlements in the Ghaghara waterway, 117 towns along the Rapti waterway, and 6 communities in the Sharda canal. Some in-field flood evidence from the Ghaghara basin is shown in Fig. 8.

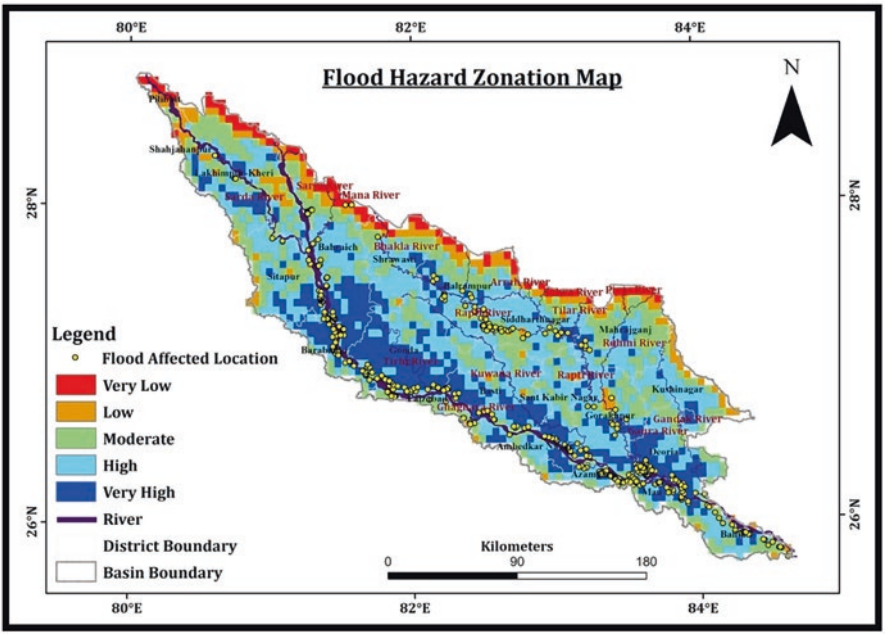


**Fig. 7a** Flood hazard risk zonation map of Ghaghara basin

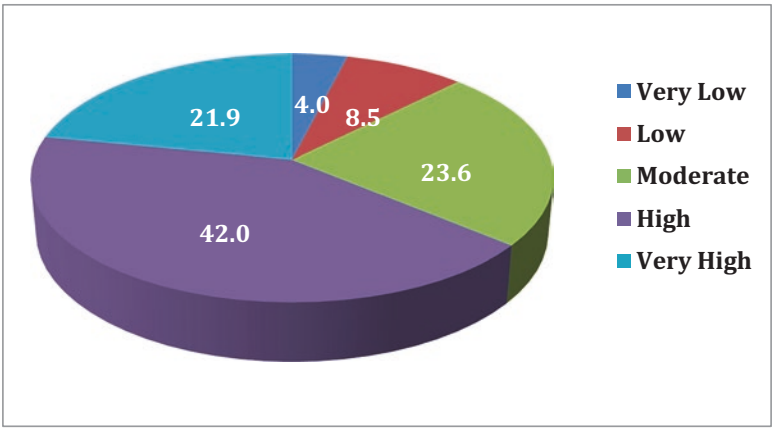


**Fig. 7b** Percentage area pie chart of flood hazard risk zones of Ghaghara basin

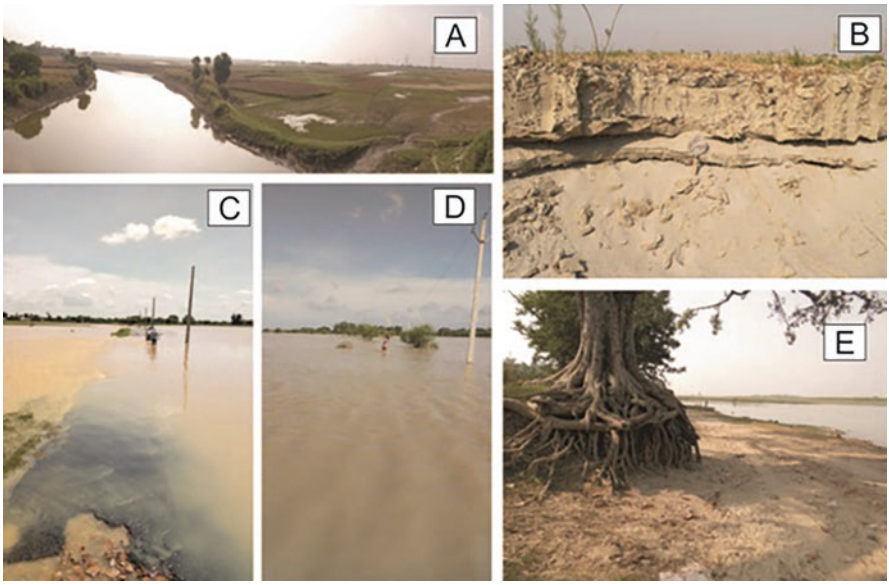


**Fig. 8** Some glimpses of flood in Uttar Pradesh. (**a**) waterlogged areas in Sant Kabir Nagar district (**b**) Near Barabanki's Durjanpur Ghat, lamination in the soil developed as a result of an increase in water level during the flood; (**c**) flood near Pittha village (Balrampur district); (**d**) flood in Panditpurwa village (Balrampur district)

## 6 Discussions

Due to the Ghaghara River's considerable flow fluctuations (very high discharge during the monsoon and extremely low discharge during the dry season), high sediment load, and channel instability, the river is highly susceptible to flooding (Singh et al., 2020). Where the Terhi and Rapti rivers meet the Ghaghara, in the Gonda and Gorakhpur districts, it causes destruction during floods. At their confluence in Bihar, the Ghaghara and Ganga rivers have a higher flow, making them more prone to floods. The flood hazard zonation generated by this study can aid decision-makers or planners in assessing the study region and thinking about effective mitigation strategies for prospective flood disasters. According to Chen et al. (2015), land-use planning and the protection of the surface environment both benefit from this research. The Ghaghara basin has been classified into five zones: very low, low, moderate, high, and very high based on the estimated flood susceptibility.

### *6.1 Very Low and Low Flood Hazard Zone*

The base low and very low flood hazard zones in the Ghaghara basin only cover 8.5% and 4% of the total area, respectively (Fig. 8b). These regions, where especially substantial water flows during the monsoon season are brought on by slope differences, can be found on the north side of the Ghaghara basin, in the foothills of the Himalayas, or in the piedmont zone of the Ganga Plain (Fig. 8a). In the piedmont-siwalik contact zone, the Siwalik rocks have a 70°–90° dip, which increases water gradients and velocity in the piedmont zone during river discharge or rainfall. Due to the smaller distribution of drainage density, rainfall distribution, micro watershed, clayey and loamy soil, dense forest with higher soil moisture content, and sandy soil, these places are less susceptible to flooding dangers.

### *6.2 Moderate Flood Hazard Zone*

A moderate flood zone in the area occupies 23.6% of the total land area (Fig. 8b). The north eastern, north, and western portions of the Ghaghara basin contain the moderate flood zone close to the piedmont zone. The main river and its tributaries are some distance from the moderate flood zone. The zone includes the middle rank of soil types, including clayey, loamy, and sandy soils, as well as rainfall distribution, drainage density, micro watershed size, slope, and land use-land cover (primarily built-up land and agricultural land). This zone's rate of water infiltration is higher than that of the high and very high flood zones but lower than that of the very low and low flood zones.

### *6.3 High Flood Hazard Zone*

The main zone of the study is high flood zones, which accounts for 42% of the catchment area overall (Fig. 8b). Due to a significant water release during the monsoon season, the snow-fed Himalayan Rivers (Rapti, Rohini, ChhotiGandak, Mana, Terhi, and Kuwana) overflow (Srivastava et al., 2016). The old and active flood plains of these rivers are almost entirely covered by the flood surface due to the silt filling the river channel. Rivers in this region are least likely to erode the soil's surface because they are quite sinuous and run in specific straight patterns although channel erosion occurs less frequently than sheet erosion. The region has good sandy soil and a lot of potential for groundwater (Singh et al., 2020). The area's high fertility and water potential, which also adds to the region's high drainage density, high rainfall dispersion, and small micro watershed size, benefit agriculture fields and developed land. This region frequently floods because of the low topography close to the river channels. These areas have a substantial quantity of older $T_0$ surface, which contributes to the flooding being more noticeable there.

### *6.4 Very High Flood Hazard Zone*

The total Ghaghara basin 21.9% is comprised of the higher potential flood zone (Fig. 8b). The research area's center or south-east has the greatest danger of flooding. The zone includes the majority of the Ghaghara River's active flood plain in Gonda, the Rapti in the Gorakhpur district, and the meeting point of the Ghaghara and Chhoti Gandak rivers in Deoria. These regions stand out due to their lowland topography, high drainage density, and high rainfall distribution. Flooding happens in nearby places when flow surpasses the canal's capacity, which can be disastrous. Levee failure brought on by an increase in water level in the river channel and logging and spreading of water brought on by heavy rains are the two elements that cause it. Turtipar, a gauge site between Barhaj and Gothani, experienced flooding 56 times between 1983, 1988, and 1996 as a result of heavy rainfall in the watershed. This is due to the low rate of infiltration in these areas as well.

## 7 Conclusions

The Ghaghara basin is situated in a high-risk area for natural disasters, according to the map of flood risk. Estimates of the flood risk zone place more than 7000 communities in areas of extremely high risk, necessitating comprehensive planning to reduce risk in the Ghaghara basin. Climate-related factors, particularly precipitation and slope fluctuations in and near the Ghaghara River, are reported to play a significant impact in causing natural disasters like floods. Flooding is made worse by the Ghaghara River's and its tributaries, including the Tirhi, Kuwana, Rapti, and Budhi Gandak rivers' transition from foothills to alluvial plain.

## References

Ajin, R. S., Krishnamurthy, R. R., Jayaprakash, M., & Vinod, P. G. (2013). Flood hazard assessment of Vamanapuram River Basin, Kerala, India: An approach using remote sensing & GIS techniques. *Advances in Applied Science Research, 4*(3), 263–274.

Arya, A. K., & Singh, A. P. (2021). Multi criteria analysis for flood hazard mapping using GIS techniques: A case study of Ghaghara River basin in Uttar Pradesh, India. *Arabian Journal of Geosciences, 14*(8), 1–12.

Arya, A. K., Singh, A. P., & Agarwal, K. K. (2020). A multi criteria approach for morpho-tectonic evaluation of Sai River Basin in Uttar Pradesh. *Journal of the Geological Society of India, 96*, 171–179.

Chen, H., Ito, Y., Sawamukai, M., & Tokunaga, T. (2015). Flood hazard assessment in the Kujukuri Plain of Chiba Prefecture, Japan, based on GIS and multicriteria decision analysis. *Natural Hazards, 78*(1), 105–120.

Gupta, M., & Srivastava, P. K. (2010). Integrating GIS and remote sensing for identification of groundwater potential zones in the hilly terrain of Pavagadh, Gujarat, India. *Water International, 35*(2), 233–245.

Horritt, M. S., Mason, D. C., & Luckman, A. J. (2001). Flood boundary delineation from synthetic aperture radar imagery using a statistical active contour model. *International Journal of Remote Sensing, 22*(13), 2489–2507.

Lin, H., Wan, Q., Li, X., Chen, J., & Kong, Y. (1997). GIS based multicriteria evaluation for investment environment. *Environment and Planning B: Planning and Design, 24*, 403–414.

Mitra, D., Tangri, A. K., & Singh, I. B. (2005). Channel avulsions of the Sarda River system, Ganga Plain. *International Journal of Remote Sensing, 26*(5), 929–936.

Mohan, R. (2018). Ghaghara River system—Its current status and value to society. In D. Singh (Ed.), *The Indian Rivers* (Springer Hydrogeology) (pp. 151–164). Springer.

Patel, D. P., & Srivastava, P. K. (2013). Flood hazards mitigation analysis using remote sensing and GIS: Correspondence with town planning scheme. *Water Resources Management, 27*, 2353.

Rai, P. K., & Mohan, K. (2014). Remote sensing data & GIS for flood risk zonation mapping in Varanasi District, India. *Forum Geografic, 13*(1), 25–33.

Sanjay, K., & Goel, M. K. (2002). Assessing the vulnerability to soil erosion of the Ukai dam catchments using remote sensing and GIS. *Hydrological Sciences Journal, 47*(1), 31–40.

Singh, A. P. (2020). The role of channel migration and structural setup in flood hazard of Upper Ghaghara River from Bahraich to Faizabad in Uttar Pradesh, India using Geospatial Approach. *Disaster Advances, 13*(5), 10–32.

Singh, D. S., Prajapati, S. K., Singh, P., Singh, K., & Kumar, D. (2015). Climatically induced levee break and flood risk management of the Gorakhpur region, Rapti River basin, Ganga Plain, India. *Journal of the Geological Society of India, 85*(1), 79–86.

Singh, A. P., Arya, A. K., & Singh, D. S. (2020). Morphometric analysis of Ghaghara River Basin, India, using SRTM data and GIS. *Journal of the Geological Society of India, 95*(2), 169–178.

Sinha, R., Bapalu, G. V., Singh, L. K., & Rath, B. (2008). Flood risk analysis in the Kosi River Basin, North Bihar using multi-parametric approach of AHP. *Indian Journal of Remote Sensing, 36*, 293–307.

Srivastava P., Aruche M., Arya A., Pal D. K., & Singh, L. P. (2016). A micromorphological record of contemporary and relict pedogenic processes in soils of the Indo-Gangetic plains: implications for mineral weathering, provenance and climatic changes. *Earth Surface Processes Landforms, 41*, 771–790.

Warner, M. (2001). Impact of grid size in GIS based flood extent mapping using a 1D flow model. *Physics and Chemistry of the Earth. Part B, Hydrology Oceans and Atmosphere, 26*(7), 517–522.

# Flood Hydrology, Hydraulics and Hydrodynamics of the Tapi River, Western India


**A. D. Patil, U. V. Pawar, G. W. Bramhankar, and P. S. Hire**

## 1 Introduction

Hydrology is the discipline of water and treaties with the source, movement, and dissemination of the waters of the globe (Mutreja, 1995). Flood hydrology, as a subdiscipline of hydrology, has gained appreciation as pragmatic science. The elementary objective of flood hydrology is the quantification of hydrological processes and forecast of floods. The latter is necessary for a diversity of engineering and commercial motives. Although the boundary lithology is an acute factor, the genuine effect of floods depends on the hydraulic physiognomies of flood courses. Consequently, in spite of the complications in the measurement of flood currents, numerous efforts have been made in recent years to compute and model the role of floods in terms flood currents hydraulics and hydrodynamics. It seems that utmost geomorphic work in seasonal tropics is completed by individual flood event. Studies on some large Indian rivers specify that the channel forms and processes are associated to very outsized, but comparatively uncommon flood events (Goswami, 1985; Kale et al., 1994; Gupta, 1995; Kale and Gadgil, 1997; Gupta et al., 1999). The effect of flood flows depends not so much on the volume of water as on the vitality exerted by it. The variations in the width-depth quotient and hydraulic variables by means of discharge have been revealed to very worthwhile notions in assessing the prospective of flood currents to be geomorphologically impactful (Kale et al., 1994; Gupta, 1995). Baker and Costa (1987) recommended that geomorphic efficacy of floods is connected to the stream power defined in terms of channel boundary shear stress and power per unit area of channel bed. Additionally, Baker (1988) and Wohl

A. D. Patil
Department of Geography, RNC Arts, JDB Commerce and NSC Science College, Nashik, Maharashtra, India

U. V. Pawar · G. W. Bramhankar · P. S. Hire (✉)
Department of Geography, HPT Arts and RYK Science College, Nashik, Maharashtra, India



S. Kanhaiya et al. (eds.), *Rivers of India*,
https://doi.org/10.1007/978-3-031-49163-4_13

(1993) noted that the regime conditions of the flood flows and the grade of turbulence also play a role of substantial significance in the erosion and conveyance of coarse sediment. Thus, in the current chapter, an attempt has been made to comprehend flood hydrology, hydraulics, and hydrodynamic characteristics of the Tapi River and its other watercourses, on the foundation of accessible annual peak discharge data and cross-sectional records composed during the field studies.

## *1.1 Geomorphological and Hydrological Characteristics of the Tapi Basin*

The Tapi River is the second largest west flowing river in India which runs for a total length of 724 km and having catchment area of 65,145 km$^2$. The river has its source in the state of Madhya Pradesh (MP) in the Betul District of Central India at an elevation of 730 m ASL (Fig. 1). The river discharges into the Sindhu Sagar (Arabian Sea) near Surat city of the Gujarat state. The geology of the basin consists of Cretaceous-Eocene Deccan Trap basalts and late-Pleistocene alluvium. The middle and lower Tapi and Purna Basins are thickly sheltered by alluvium of the late-Pleistocene period. The basin form is greatly elongated, and interestingly, the major three upper order streams namely Panzara, Purna, and Girna meet the Tapi River from the south (Fig. 1).

The monsoonal climate of the study area is distinguished between distinct wet (June–October) and dry (November–May) seasons. The average per annum

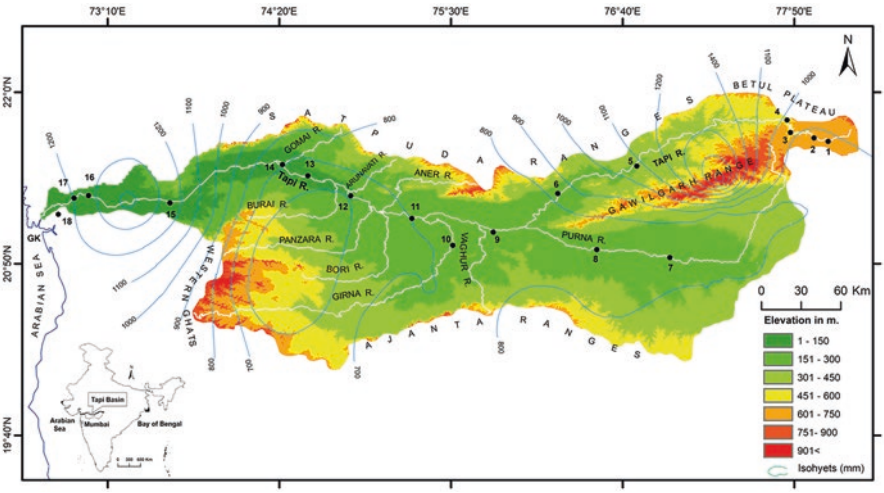


**Fig. 1** Geomorphological setting of the Tapi Basin of western India with Isohyets; 1 = Deodongri; 2 = Dhanora; 3 = Hanuman Ghat; 4 = Teska; 5 = Dedtalai; 6 = Burhanpur; 7 = Gopalkheda; 8 = Yerli; 9 = Bhusawal; 10 = Dapuri; 11 = Savkheda; 12 = Gidhade; 13 = Sarangkheda; 14 = Prakasha; 15 = Ukai; 16 = Ghala; 17 = Kathor; 18 = Surat; GK = Gulf of Khambhat

precipitation of the basin is 814 mm, which is characteristically received between 40 and 50 days (Gunjal, 2016). More than 90% of the per annum rain befalls throughout the rainy summer monsoon season. July is the month that receives utmost rainfall of the basin which contributes about 30% of the total yearly precipitation. Spatially, the per annum rainfall displays a conspicuous dissimilarity within the study area with rainfall between 500 and 1000 mm (Fig. 1). The Tapi Basin falls in the severe rainstorms zone (Dhar & Nandargi, 1995). Consequently, the sporadic heavy precipitations are the effect of incursion of cyclonic storms and depressions initiating above the Bay of Bengal and neighboring land. The rainstorms usually happen for a day or two, and the highest 24-hour heavy rainfall in the basin vary from 157 mm (at Satana on June 27, 1914) to 600.6 mm (at Amalner on July 30, 1992) (Abbi & Jain, 1971; Gunjal, 2016). Yearly hydrographs of the river under review disclose the seasonal rhythm of the summer monsoon precipitation and exhibit a simple regime with merely one distinct peak (Kale & Hire, 2004). The flow in the river increases swiftly in early-mid June with the onset of monsoon over the basin after a long dry period of about 8 months. Over 95% of the flow is recorded in the 4–5 months of summer monsoon, and during the remaining part of the year, the flow dwindles. Hence, 4–5 months of the monsoon season of the year are momentous from the standpoint of the geomorphic efficacy such as erosion and transportation of the sediment.

## 2 Flood Hydrology

Large floods are of prime importance to all the Indian rivers nurtured by monsoon rainfall. Primarily, the geomorphic effectiveness in seasonal tropics is carried out by discrete flood events. Accordingly, an attempt has been made to comprehend amount, variability, and occurrence characteristics of individual flood on the Tapi River and its streams by means of accessible yearly peak discharge data. Before proceeding with the analysis, nonetheless, it is vital to first define the term flood. Broadly, the single highest discharge for each year of gauge record is of significance to hydrologists and geomorphologists. Consequently, Hire (2000) has defined the modest and most appropriate definition of flood for an incised river, either in bedrock or alluvium. It was established on the numerical statistical parameters such as mean and standard deviation of the annual peak discharges. Additionally, in fluvial geomorphology flows with a reappearance interval of 2.33 years to about 5 years are thought to be noteworthy from the point of view of geomorphic effectiveness (Petts & Foster, 1985).

## 2.1 Annual Flood Series Data and Analysis

The hydrologists define the uppermost peak discharge documented for every year for a series of years at a measuring site as annual maximum series (AMS) or annual peak discharge series (Ward, 1978). The measured data (particularly AMS) were acquired from the Central Water Commission (CWC) for four measuring stations on the Tapi River and two stations on its tributary, viz., Purna. Gauge records for the Tapi River are petite and not continuous. The records begin in 1970s for most of the gauging stations. Nevertheless, a site on the lower reaches of the Tapi River namely Ukai has discharge records from early 1940s to late 1970s. The data, therefore, do not deliver very consistent result for forecasting the probability and enormousness of sporadic outsized flood events. Nonetheless, the available measured data (30 to 46 years) have been used to appraise great flows. Primarily, AMS data have been depicted in the form of time series diagrams to get an idea of the interannual deviations in the annual peak floods. Additionally, simple statistical analyses of AMS data have been carried out to diminish and encapsulate the appearances of floods. The numerical parameters that are stated in terms of the moments such as variability, skewness, and coefficient of variation have been computed.

## 2.2 Flood Regime Characteristics

The Tapi River, an important hydrologic system of the India, is considered to be one of the most powerful flood systems in the summer monsoon tropics (Kale et al., 1994). The available measured data specify that the mean flows range between 1433 $m^3s^{-1}$ at Gopalkheda on the Purna River and 14,323 $m^3s^{-1}$ at Ukai on the Tapi River (Table 1). Large flood flows on the Tapi River were recorded in the years 1727, 1776, 1782, 1829, 1837, 1872, 1944, 1959, 1968, and 1970. The utmost ever documented flood on the Tapi River near the mouth at Surat (Fig. 1) is the 1968 catastrophic flood which was 42,450 $m^3s^{-1}$ in magnitude. This flood ranks higher as

**Table 1** Flood flow characteristics of the Tapi River and its tributary

| SN | Site | A $km^2$ | Record Length | Qmin $m^3s^{-1}$ | Qmax $m^3s^{-1}$ | Qm $m^3s^{-1}$ | Flood Range | Qmax/ Qm |
|---|---|---|---|---|---|---|---|---|
| 1 | Burhanpur | 8487 | 46 | 904 | 32,686 | 7203 | 25,745 | 4.71 |
| 2 | Gidhade | 54,750 | 28 | 2541 | 20,898 | 7090 | 14,050 | 3.05 |
| 3 | Sarangkheda | 58,400 | 42 | 600 | 23,044 | 8117 | 15,241 | 2.95 |
| 4 | Ukai | 62,224 | 30 | 3670 | 42,450 | 14,323 | 28,127 | 2.96 |
| 5 | Gopalkheda* | 9500 | 42 | 130 | 4124 | 1433 | 2751 | 3.00 |
| 6 | Yerli* | 16,517 | 46 | 369 | 10,380 | 2576 | 7883 | 4.16 |

Data source: CWC; Qmin = Minimum annual peak discharge; Qmax = Maximum annual peak discharge; Qm = Mean annual peak discharge; A = Catchment area; * = sites on the Purna River; see Fig. 1 for location of sites

compared to some of the large Indian rivers such as Mahanadi, Krishna, and Kaveri. Interestingly, the highest flood of the Tapi Basin, since beginning of the record (1727 onwards) was noted in year 1837. The following section represents the other distinguished features of flood regime of the Tapi River and its major tributary namely Purna.

### 2.2.1 Interannual Variability in Annual Peak Discharges

The temporal patterns of deviation in the annual peak discharges at six gauging sites on the Tapi River and its significant tributary namely the Purna are illustrated in Fig. 2a–f. All the charts reveal high interannual deviations in the annual peak flows. The diagrams also validate the episodic one or two extreme events throughout the data measurement period at all the stations. In general, the array of variation is enormous at a lower reach station, i.e., Ukai (Fig. 2d). The Tapi River at Burhanpur (Fig. 2a) and Sarangkheda (Fig. 2c) also designate great interannual deviations in the amount of yearly peak flows. Copious other workers with Wolman and Miller (1960) have opined that as stream flow becomes more capricious, growing proportion of the sediment load is conveyed by outsized flood flows. Very high year to year deviation in flood flows (Fig. 2a–f), on the Tapi River, and its tributary demonstrates high geomorphic efficiency during the large magnitude floods.

### 2.2.2 Average Magnitude and Variability of Floods

The mean discharge (Qm) and a series of annual peak flows are given in the Table 1. In general, the at-a-station range in flood flow increases with mean discharge. This is to say that at the stations in the lower reaches the flows can fluctuate to a considerable degree. This entails that the flow inconsistency intensified in the lower reaches of the river under review. A cursory look at Table 1 also validates that, as expected, the Qm values at Burhanpur, Gidhade, and Sarangkheda sites are lower than the Qm flow at Ukai gauging station.

According to Kochel (1988), flows that are expected to cause major geomorphic change are those that produce discharges many times beyond the mean flows experienced by a river. This can be merely recognized by assessing the Qmax/Qm ratio. Table 1 designates that for most sites the Qmax/Qm ratio fluctuates between 2 and 5. This stipulates that supreme annual peak flows (Qmax) are 2–5 times greater than average discharges. The more variable the flow is, the more noteworthy the greater discharges become (Wolman & Miller, 1960). The effectiveness of such strong flows on geomorphic activity in channel is likely to be vital.

In addition to the Qmax/Qm ratio, the useful measure of variability in annual peak is the coefficient of variation (Cv). The Cv is the quotient between standard deviation and the mean. It differs between 0.63 and 0.94 (or 63 to 94%) (Table 2) and recommends low to moderate dispersion. Nevertheless, an appraisal with other great Indian Rivers reveals that the variability in peak flows in the Tapi Basin is

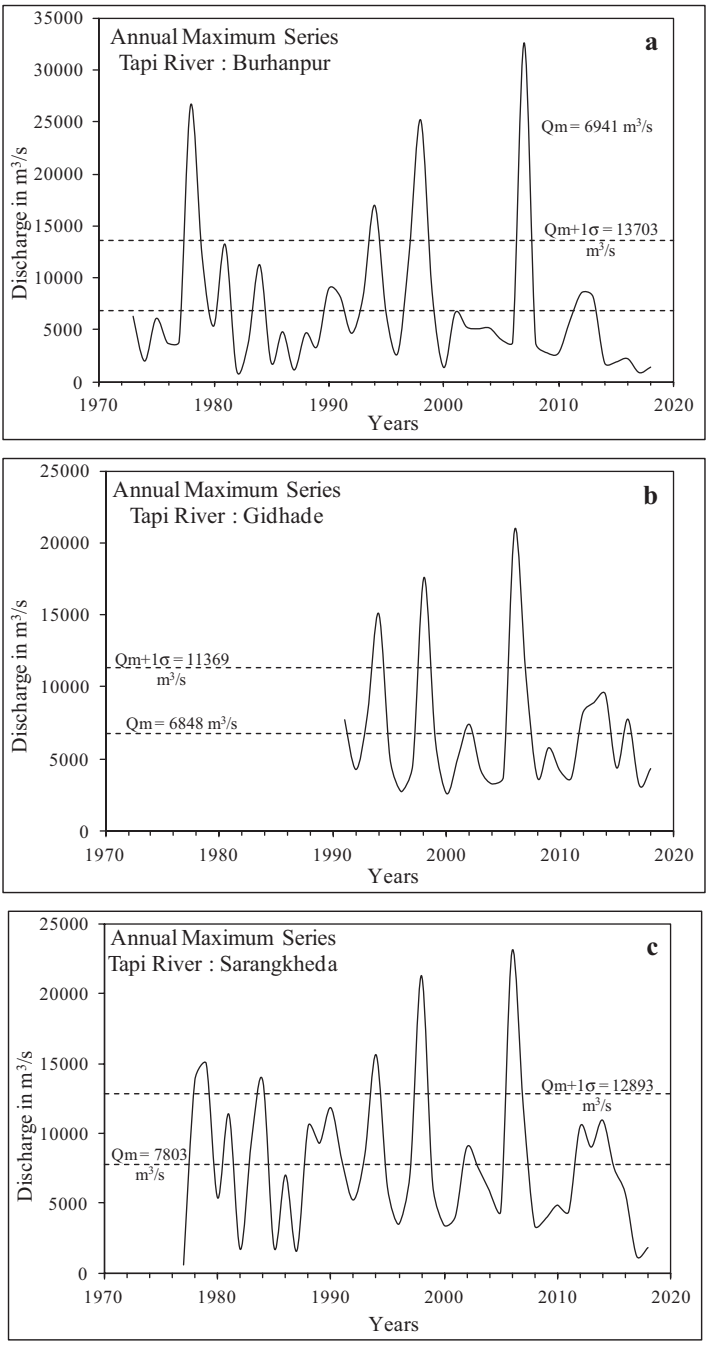


**Fig. 2** Annual maximum series plots (**a**–**f**) of the Tapi and Purna River; Qm = mean annual peak discharge; σ = standard deviation

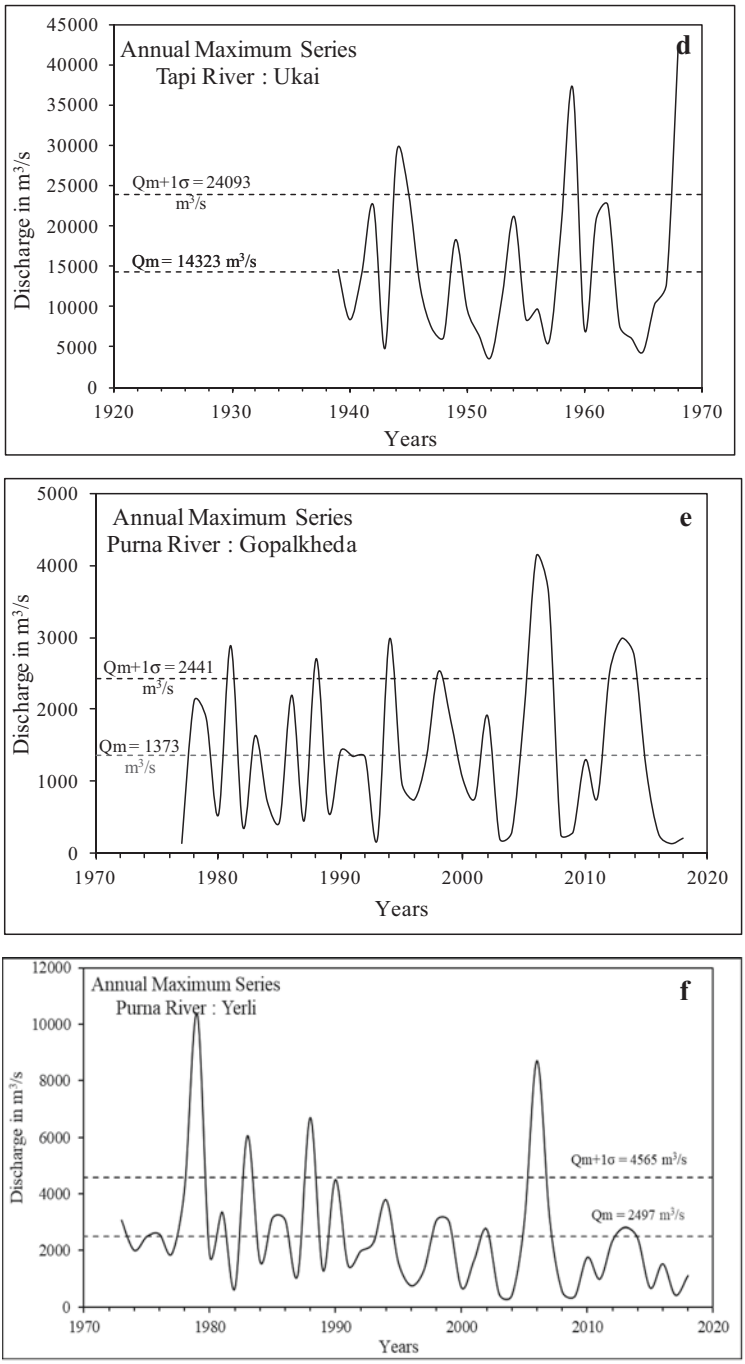


**Fig. 2** (continued)

**Table 2** Discharge characteristics of the Tapi River and its tributary

| SN | Site | Record length | Qmax $m^3s^{-1}$ | Qm $m^3s^{-1}$ | σ | Cv | Cs | Cs/Cv |
|---|---|---|---|---|---|---|---|---|
| 1 | Burhanpur | 46 | 32,686 | 7203 | 6762 | 0.94 | 2.29 | 2.44 |
| 2 | Gidhade | 28 | 20,898 | 7090 | 4520 | 0.64 | 1.81 | 2.84 |
| 3 | Sarangkheda | 42 | 23,044 | 8117 | 5090 | 0.63 | 1.06 | 1.69 |
| 4 | Ukai | 30 | 42,450 | 14,323 | 9770 | 0.68 | 1.33 | 1.95 |
| 5 | Gopalkheda* | 42 | 4124 | 1433 | 1068 | 0.78 | 0.72 | 0.93 |
| 6 | Yerli* | 46 | 10,380 | 2576 | 2067 | 0.80 | 2.05 | 2.55 |

Data source: CWC; Qmax = Maximum annual peak discharge; Qm = Mean annual peak discharge; σ = Standard deviation; Cv = Coefficient of variation; $C_s$ = Coefficient of skewness; * = sites on the Purna River; see Fig. 1 for location of sites

indeed greater than elsewhere (Sakthivadivel & Raghupathy, 1978 and Hire, 2000).In order to further highlight the degree of variability in peak discharges from 1 year to other, deviations from average annual peaks have been illustrated graphically (Fig. 3a–f). The plots substantiate the variable nature of flows in the study area. An astonishing fact indicated by the charts is that the positive deviations are much superior, nonetheless less recurrent. This states that the average value of flow is strongly affected by a few large magnitude discharges.

Several researchers have used the Beard's flash flood magnitude index (FFMI) to appraise the variability of discharge frequency measured as an index of flashiness of flood (Baker, 1977). The FFMI values are computed from the standard deviation of logarithms of AMS. The FFMI of the Tapi River and its tributary range from 0.24 to 0.43 (Table 3). The uppermost FFMI value in the basin is 0.43, which is witnessed in case of the Purna River at Gopalkheda and is attributed to 2006 catastrophic flood persuaded by low pressure system. The average FFMI value of the Tapi Basin is 0.34. This value is superior to the mean FFMI value (0.28) of the World Rivers (McMohan et al., 1992; Erskine & Livingstone, 1999). The moderately superior mean FFMI value of Tapi Basin demonstrates slightly flashy and variable nature of flows on the Tapi River and its tributary Purna, than the average world rivers. The index further designates that the possibility of the river experiencing noteworthy geomorphic work during the large magnitude floods is higher.

### 2.2.3 Skewness

The coefficient of skewness (Cs) is the most extensively used measure of moments in flood hydrological and geomorphological research. Since the AMS data are not normally distributed, it is inevitable to compute the skewness of the data (Table 2). The figures of Cs for all the stations on the Tapi and Purna rivers are positive ranging from 0.72 to 2.29. The skewness values obtained for other large rivers in India (Sakthivadivel & Raghupathy, 1978) are comparable with the skewness values derived for the Tapi and Purna rivers. The positive Cs values propose occasion of one or two (or a few) very outsized floods during the measurement period. Nevertheless, the representation of value of skewness is suspicious when it is

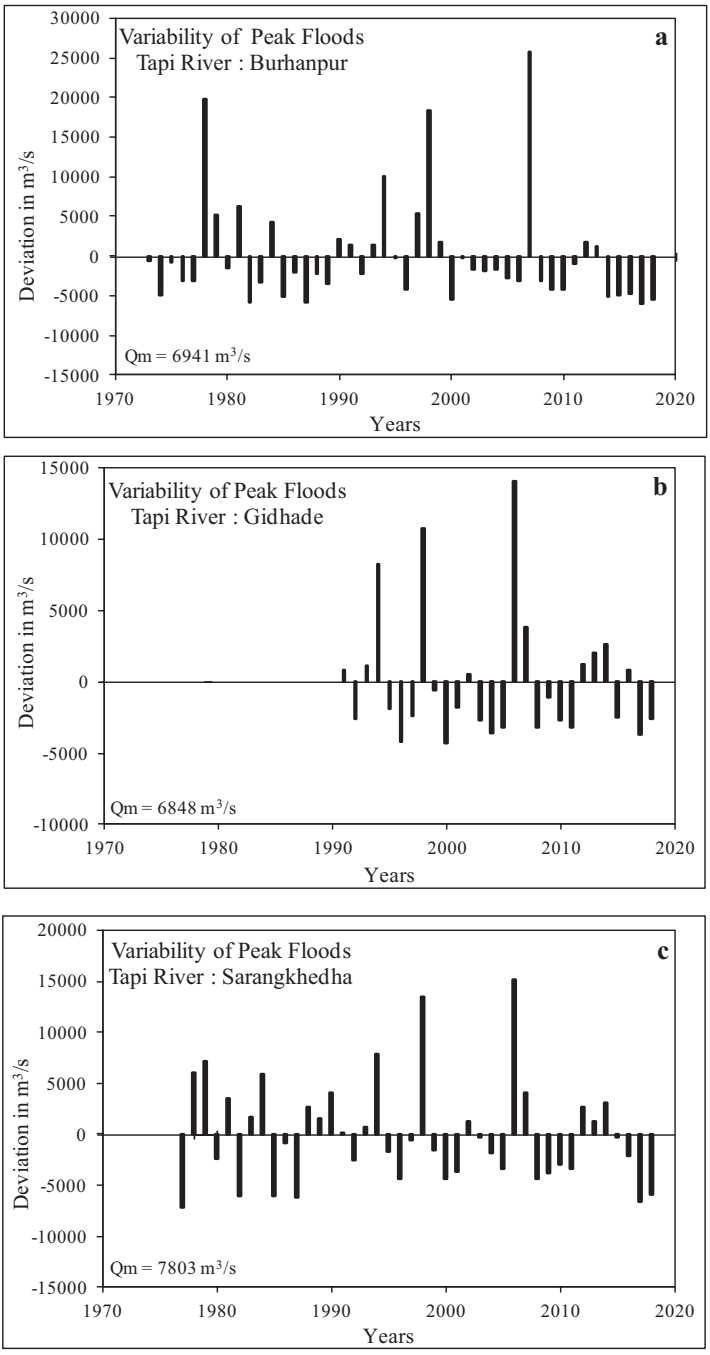


**Fig. 3** Departure from mean annual peak discharge on the Tapi and Purna rivers (**a**–**f**)

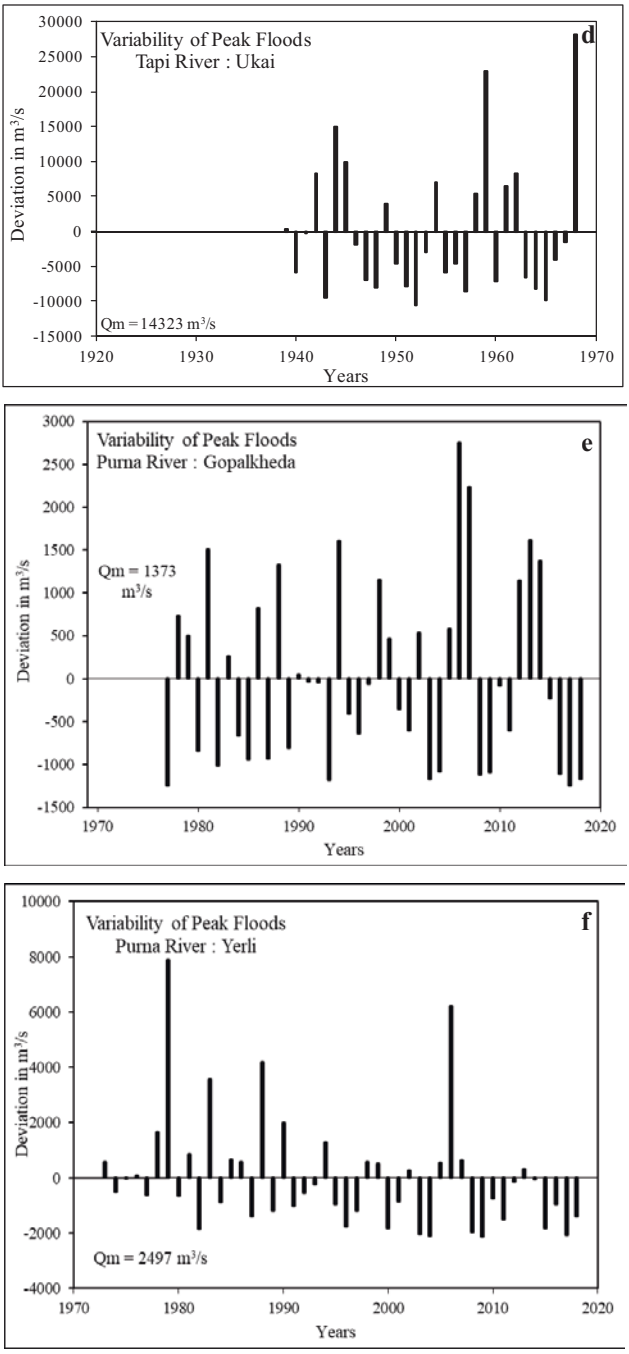


**Fig. 3** (continued)

**Table 3** Flash flood magnitude indices of the Tapi and Purna rivers

| SN | River | Site | Record length (Years) | FFMI |
|---|---|---|---|---|
| 1 | Tapi | Burhanpur | 46 | 0.37 |
| 2 | Tapi | Gidhade | 28 | 0.24 |
| 3 | Tapi | Sarangkheda | 42 | 0.34 |
| 4 | Tapi | Ukai | 30 | 0.28 |
| 5 | Purna | Gopalkheda | 42 | 0.43 |
| 6 | Purna | Yerli | 46 | 0.36 |
| **7** | **Tapi Basin** | **Mean value** | **–** | **0.34** |

Data source: CWC; FFMI = Flash flood magnitude index; see Fig. 1 for location of sites

**Table 4** Unit discharges of the Tapi River and its major tributaries

| SN | River | Site | A $km^2$ | Qmax $m^3s^{-1}$ | Unit discharge $m^3s^{-1}$ $km^{-2}$ |
|---|---|---|---|---|---|
| 1 | Tapi | Kathor | 63,822 | 41,700 | 0.65 |
| 2 | Tapi | Ghala | 63,325 | 17,200 | 0.27 |
| 3 | Tapi | Ukai | 62,224 | 42,450 | 0.68 |
| 4 | Tapi | Sarangkheda | 58,400 | 24,750 | 0.42 |
| 5 | Tapi | Gidhade | 51,517 | 26,665 | 0.52 |
| 6 | Tapi | Savkheda | 48,136 | 24,856 | 0.52 |
| 7 | Tapi | Burhanpur | 8487 | 26,883 | 3.14 |
| 8 | Tapi | Dedtalai | 3860 | 10,150 | 2.63 |
| 9 | Purna | Gopalkheda | 9500 | 4124 | 0.43 |
| 10 | Purna | Yerli | 16,571 | 10,570 | 0.64 |
| 11 | Girna | Dapuri | 8901 | 12,200 | 1.37 |

Data source: CWC and Hire, 2000; A = Catchment area; Qmax = Maximum annual peak discharge; see Fig. 1 for location of sites

derived from less than 50 years of data (Viessman et al., 1989). Subsequently, the quotient between skewness and coefficient of variation (Cs/Cv) has also been applied by some hydrologists to further authenticate the degree of skewness (Shaligram & Lele, 1978). The values of this quotient for diverse discharge measuring sites in the study area range from 0.93 to 2.84 (Table 2). For most large rivers of India, the Cs/Cv ratios are more than 2.0 (Shaligram & Lele, 1978). This, consequently, advocates that the distribution of annual peak discharges is not very skewed.

### 2.2.4 Unit Discharges

Unit discharge is an imperative quantity of the prospective large floods on a river (Gupta, 1988). It is the quotient linking maximum annual peak discharge (Qmax) and the upstream catchment area (A). It is accountable for discharge or water yield per unit drainage area ($m^3s^{-1}$ $km^{-2}$). The calculated unit discharges for each station on the Tapi River and its tributary fluctuate between 0.27 and 3.14 $m^3s^{-1}$ $km^{-2}$

(Table 4). For the Tapi Basin as whole, the unit discharge is 0.65 $m^3s^{-1}$ $km^{-2}$. The values of the unit discharges are less than 1.0. Nevertheless, at a few stations, for instance, Burhanpur, Dedtalai, etc. have much greater unit discharges such as 3.14 and 2.63 $m^3s^{-1}$ $km^{-2}$ correspondingly. The unit discharge of the Tapi Basin (0.65 $m^3s^{-1}$ $km^{-2}$) is greater than other rivers of India with comparable drainage areas. For instance, the unit discharges for the Kaveri River (A = 81,155 $km^2$) and Pennar River (A = 55,213 $km^2$) are 0.16 $m^3s^{-1}$ $km^{-2}$ and 0.24 $m^3s^{-1}$ $km^{-2}$, respectively. Remarkably then, the Tapi Basin, in general, and the upper reaches, in particular, are competent of generating great magnitude floods. Such superior discharges are expected to be effective in terms of geomorphic changes in the channel and valley (Costa & O'Connor, 1995; Kale et al., 1997).

## 3 Flood Hydraulics and Hydrodynamics

Great magnitude flows that are inherently uncommon have capability to yield significant currents into fluvial channels. The geomorphic efficacy coupled with such flows is flexible, in some cases these floods create significant geomorphic changes and in others immaterial (Costa, 1974; Baker, 1977; Gupta, 1983). Scientists are increasingly getting accustomed with the prominence of uncommon great magnitude flows in sculpting the landscape. In order to assess geomorphic efficacy of such flows on the Tapi River and its tributary, parameters of flood hydraulics and hydrodynamics have been investigated.

### *3.1 Change in the Width-Depth Quotient with Flows*

Alluvial as well as bedrock channel reaches of the Tapi River are more or less box-shaped with roughly flat channel bed. Consequently, during the dry season and/or during low flows, the water spreads over the channel beds, and hence the water surface width is more and depth is low. Therefore, the width-depth quotient is more and the river reveals all the physiognomies of a shallow, widespread channel. Occurrence of torrential precipitation can be the source upsurge in channel and flow volume that governs the escalation in the depth of the flood flow. Subsequently, the value of width-depth quotient reduces and the hydraulic competence heightens substantially. Figure 4 illustrates the plot of width-depth quotients for low flows and high magnitude floods for ten fluvial channel cross-sections along the river Tapi. There is a noteworthy fall in the quotients in the middle stretches, as an outcome of very extensive rectangular-shaped channel reaches of the Tapi River (Fig. 4). Profoundly, other rivers of the monsoonal tropical areas have also been found to perform in similar way (Gupta, 1995; Deodhar & Kale, 1999; Kale & Hire, 2004; Hire, 2000).

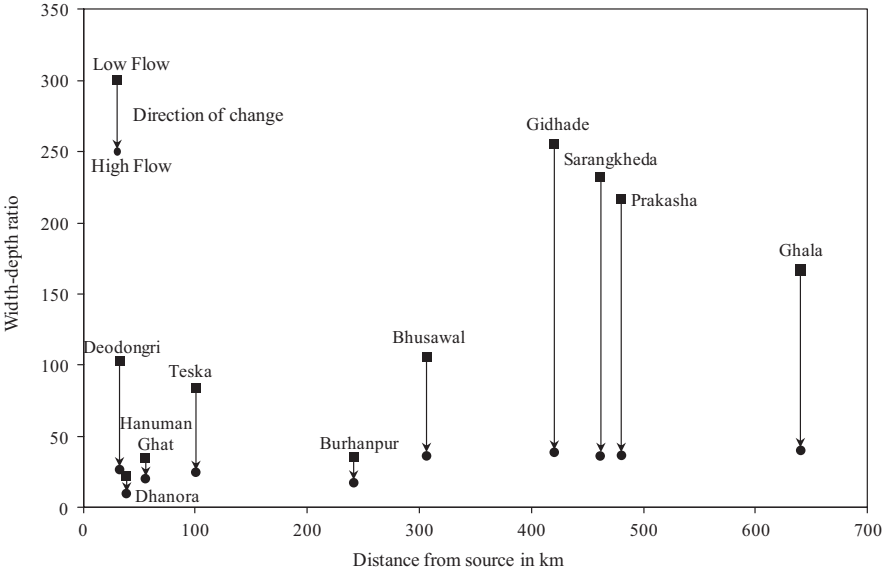


**Fig. 4** Downstream variations in width-depth ratio with discharge; see Fig. 1 for location of sites

In order to assess the association between width-depth quotient and discharge, regression analysis was carried out for five stations in the alluvial channel reaches of the Tapi River, namely, Ghala, Sarangkheda, Gidhade, Savkheda, and Burhanpur (Figs. 1 and 5). The analysis shows that (Fig. 5a–e) the rate of change in width-depth quotient with flows of different magnitude is utmost for the Ghala and Sarangkheda stations where the river reaches, at these localities, are practically rectangular in form. In contrast, at Burhanpur station, the rate of change is lowest as a result of comparatively narrow deep river channel. Irrespective of the channel form, nevertheless, an essential conclusion that immerges is that the large magnitude flood flows become deeper and competent as the flood water rises. This, therefore, recommends that large flood flows are geomorphologically more effectual than low or moderate flows. Other rivers of the Indian tropical monsoonal areas have also been found to behave in the analogous way (Gupta, 1995; Deodhar & Kale, 1999).

## *3.2 Changes in Hydraulic Variables with Increasing Discharge*

The hydraulic variables, for instance, width, depth, and velocity, respond to the fluctuations in flows in the fluvial systems. Changes in these three variables are of utmost importance to hydraulic geometry (HG). HG means the geometric rate of change of hydraulic variables such as width (w), mean depth (d), and mean velocity ($\bar{v}$) as discharge (Q) heightens (Leopold & Maddock, 1953). At-a-station HG

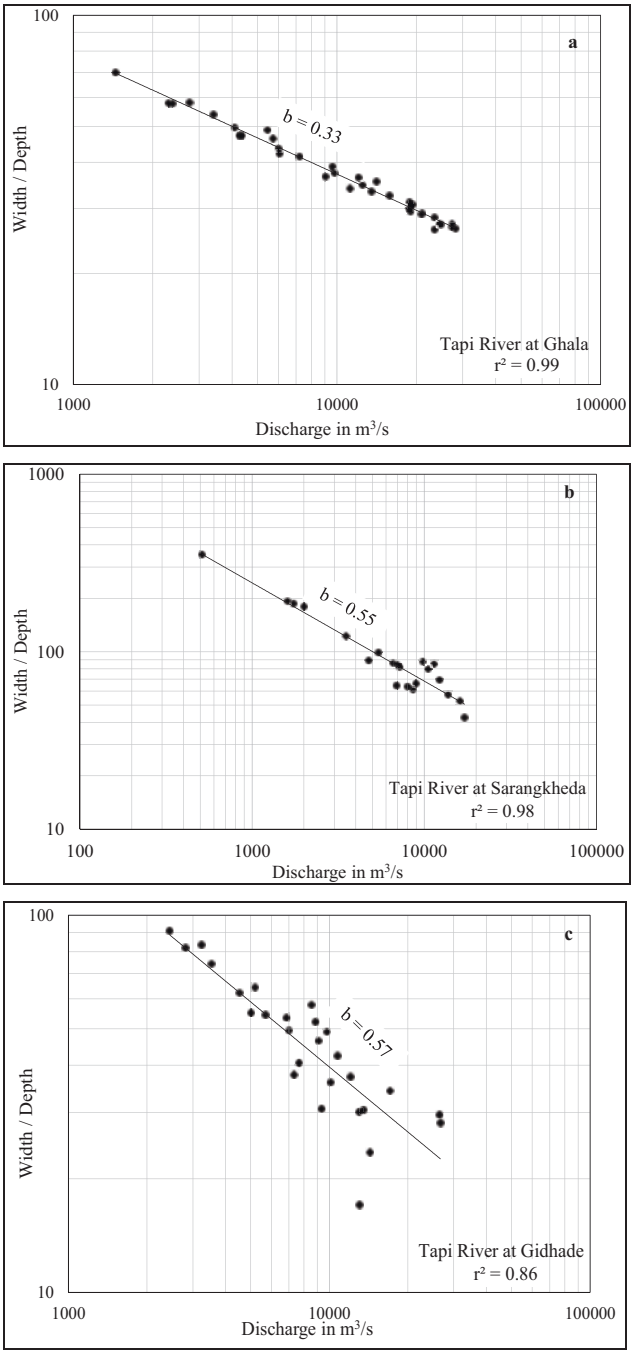


**Fig. 5** Relationship between width-depth quotient and discharge; see Fig. 1 for location of sites

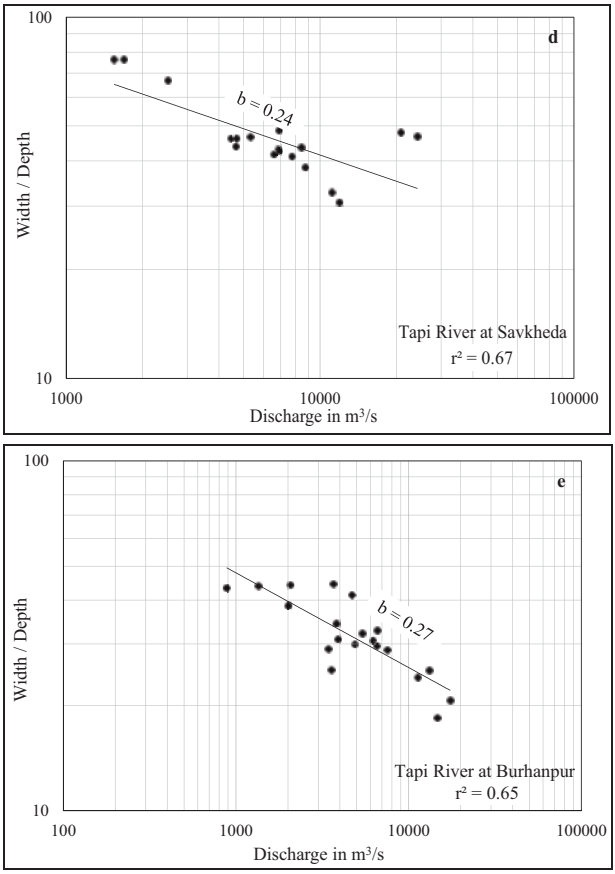


**Fig. 5** (continued)

equations have generated the following relations (Table 5) for the Tapi River (Hire, 2000; Kale & Hire, 2004; Kale & Hire, 2007; Hire & Hire, 2021).

The results of the analysis indicate that the rate of change in width (b) is slower than rate of change in mean depth (f) and mean velocity (m) with escalating discharges for all the stations (Table 5). The Gidhade, Sarangkheda, and Ghala stations on the Tapi River demonstrate much gentler rate of change in width (b) with increasing flow in the channels. This is attributed to near box-shaped nature of river at these stations. The rise in the flood stages, i.e., discharge at these stations, is predominantly adjusted by a remarkable increase in flood flow depth. This has imperative repercussions for competency of the fluvial channel as the energy of flood is directly linked to the flood flow depth (Baker & Costa, 1987). At the sites, viz., Burhanpur and Savkheda, the rate of change in water surface width (b) with discharge is moderate (Table 5) representing more or less semicircular channel form. A compare of exponent values of at-a-station HG of the Mahi and Narmada rivers of western India (Kale et al., 1994; Patil et al., 2018) with the Tapi River (Table 5) demonstrates that both the rivers behave in more or less similar way with increasing flood water

**Table 5** Exponent values of at-a-station HG

| Site | Width (b) | Depth (f) | Velocity (m) |
|---|---|---|---|
| Burhanpur | 0.24 | 0.51 | 0.26 |
| Savkheda | 0.21 | 0.46 | 0.33 |
| Gidhade | 0.03 | 0.60 | 0.36 |
| Sarangkheda | 0.04 | 0.59 | 0.38 |
| Ghala | 0.05 | 0.38 | 0.57 |

Source: Hire, 2000; Kale & Hire, 2004; Kale & Hire, 2007; Hire & Hire, 2021; see Fig. 1 for location of sites

discharge. This alikeness is primarily ascribed to typical box-shaped nature of the fluvial channels of the Mahi, Narmada, and Tapi rivers which are draining into the Sindu Sagar (Arabian Sea). The impressiveness of bedrock as well as alluvial channels of the Tapi River is that even large magnitude discharges that take place at an intermission of a decade are accommodated within the channel, and therefore overbank flooding is meager. Furthermore, since the shape of the Tapi Basin is elongated with high bifurcation quotients, the flood hydrograph peaks are likely to be lower but more sustained flow as compared with rotund basins. However, low pressure systems, such as 1968, passing parallel to the river basin have produced leading ever documented flood with 42,500 $m^3s^{-1}$ discharge in the lower reaches of the Tapi River. The conclusions of HG analysis, thus, prove that the behavior of the alluvial Tapi River is not justly alluvial but quasi-bedrock.

## *3.3 Hydraulic and Hydrodynamic Parameters of Floods*

Geomorphic efficacy of fluvial systems in terms of erosion and transport of coarse sediment is determined by the flood power and the degree of turbulence rather than amount of water and recurrence (Baker, 1988; Baker & Costa, 1987; Wohl, 1993; Baker & Kale, 1998). Accordingly, stream power per unit boundary area, channel boundary shear stress, Froude number, and Reynolds number were computed for discharges of various magnitude (Leopold et al., 1964; Baker & Costa, 1987).

Investigations of flood hydraulic and hydrodynamic parameters of the Tapi River (Table 6) illustrate that the unit stream power and bed shear stress range from 74 to 1518 $Wm^{-2}$ and from 18 to 263 $Nm^{-2}$ correspondingly. The values of unit stream power and bed shear stress are much greater than the values generated by recurrent floods of lesser discharges. Such greater values of flows can erode alluvial channels of the Tapi River and its tributaries and transport boulders as bed load and cobbles and pebbles in suspension (Baker & Costa, 1987; Costa & O'Connor, 1995). The value of peak unit stream power of the alluvial Tapi River at Savkheda is 373 $Wm^{-2}$. This figure is corresponding with other Indian peninsular rivers such as Godavari (310 $Wm^{-2}$) and Narmada (325 $Wm^{-2}$) (Kale, 2007). However, bedrock channels of

**Table 6** Flow dynamics of the Tapi River

| Site/channel type | Q $m^3s^{-1}$ (Qmax) | ω ($Wm^{-2}$) | τ ($Nm^{-2}$) | $\bar{v}$ ($ms^{-1}$) | Fr | Re × $10^7$ |
|---|---|---|---|---|---|---|
| Sarangkheda (A) | 24,750 | 74 | 18 | 3.50 | 0.33 | 40.42 |
| Gidhade (A) | 26,665 | 118 | 34 | 3.67 | 0.28 | 63.38 |
| Savkheda (A) | 24,856 | 373 | 263 | 3.67 | 0.30 | 54.02 |
| Burhanpur (A) | 26,883 | 338 | 104 | 4.54 | 0.34 | 82.44 |
| Teska (B)* | 12,771 | 1518 | 241 | 6.30 | 0.78 | 48.80 |
| Ghuttigarh (B)* | 10,000 | 602 | 188 | 5.39 | 0.44 | 82.19 |
| Dhanora (B)* | 9500 | 739 | 202 | 6.5 | 0.52 | 102.00 |

Qmax = maximum annual peak discharge; ω = unit stream power in $Wm^{-2}$; τ = boundary shear stress in $Nm^{-2}$; $\bar{v}$ = Mean velocity in $ms^{-1}$; Re = Reynolds number; Fr = Froude number; (A) = Alluvial; (B) = Bedrock; see Fig. 1 location of sites; * = Based on hydraulic modeling; Source = Hire, 2000 and Kale & Hire, 2004

the Tapi River and its tributaries can produce much superior values of power per unit area during disastrous flood flows (Table 6).

Froude numbers (Fr) for all the stations of the Tapi Basin are below 1 (Fr < 1). This in turn suggests that the flood flows on the Tapi River and its tributary mainly remains subcritical (Table 6). The fluvially sculpted bedrock erosional landforms in the upper reaches of the Tapi River are the indications of Froude number reaching close to 1 during the infrequent large magnitude flood (Hire, 2000). The values of Reynolds number advocate degree of turbulence during large magnitude floods on the Tapi River and its tributaries. Geomorphic efficacy is greatly affected by degree of turbulence. The bedrock reaches at Dhanora (Fig. 1; Table 6) generated the uppermost values of Reynolds number. Such high values can give an idea about erosion of bedrock at these locations. The presence of knick points, inner channels, large boulder berms, and plunge pools are the examples of erosional power of infrequent floods of higher magnitude. Another interrelated measure of great erosional power of high flows is the critical velocity for the inception of cavitation (Vc). The Vc, measured in $ms^{-1}$, is advocated by Baker (1973) and Baker and Costa (1987). Neither Tapi River nor its tributaries have achieved the values Vc during the large magnitude floods. However, water surface velocities in the alluvial reaches of the Tapi River vary between 3.7 and 5.5 $ms^{-1}$ for the great floods. Moreover, a dam failure flood in the upper reaches of the river under review has produced surface water velocities from 6.6 to 11 $ms^{-1}$.

## 4 Summary and Conclusions

The investigations of analysis hydrological data reveal that the Tapi River and its major tributary are influenced by seasonal monsoonal rainfall; therefore, the annual maximum discharges are greatly variable. Analyses of the AMS data display

noteworthy interannual fluctuations in the discharges of flows on the river under review. The 1968 flood with the peak discharge of 42,450 $m^3s^{-1}$ at the Ukai discharge gauging station in the lower reaches of the Tapi River is the highest ever recorded flood. High variability is also reflected by the Cv (63% to 94%) and the FFMI. Generally, the Qmax are 2 to 5 times greater than the Qm. High unit discharges (0.27 and 3.14 $m^3s^{-1}$ $km^{-2}$) and great FFMI values (0.24 and 0.43) demonstrate the great prospective of the river to cause high magnitude floods. The channel forms of the Tapi River, either in alluvial or bedrock, with flat bed and high banks are distinctive. Consequently, during the dry season and/or during low flows, the water spreads over the channel beds, and hence the water surface width is more and depth is low. Therefore, the width-depth quotient is more and the river reveals all the physiognomies of a shallow, widespread channel. Occurrence of torrential precipitation can be the source upsurge in channel and flow volume that governs the escalation in the depth of the flood flow. Subsequently, the value of width-depth quotient reduces and the hydraulic competence heightens substantially. The results of HG analysis advocate that the performance of the alluvial Tapi River is not truly alluvial but quasi-bedrock. The channel form of the Tapi River plays an important role in effectual transmission of monsoon flows through the adjustments in the hydraulic parameters with increasing discharge. The $\omega$ and $\tau$ values range from 74 to 1518 $Wm^{-2}$ and from 18 to 263 $Nm^{-2}$ correspondingly. Such greater values can erode alluvial channels of the Tapi River and its tributaries and transport boulders as bed load and cobbles and pebbles in suspension. Fr for all the stations of the Tapi Basin is below 1 ($Fr < 1$) suggesting subcritical flows. High values of Re advocate degree of turbulence during large magnitude floods on the Tapi River and its tributaries. Neither Tapi River nor its tributaries have achieved the values Vc during the large magnitude floods.

In addition to above characteristics of floods, the basin geology determines the nature of the Tapi's sediment. The Deccan Trap lava beds contribute coarse sediments (cobbles and boulders) in the gorge section of the upper Tapi River, as do the granite gneisses and the sandstones. The alluvial fill of the Tapi and the Purna basins contributes a large volume of silt and clay to the rivers during monsoon floods. Moreover, geotectonically, the elongated Tapi River basin forms a part of the Son-Narmada-Tapi (SONATA) lineament zone, a megatectonic feature (Ravi Shankar, 1991) with elongation ratio of 0.40. Such elongated basin with high bifurcation quotient and highly unequal flood flow path lengths produce comparatively lower peaks of flood hydrograph but more sustained flow.

Summarizing, it can be mentioned that the Tapi River of western India displays all classical characteristics of monsoonal flood hydrology, hydraulics, and hydrodynamics. Besides this, the basin geology determines the nature of the Tapi's sediment during monsoon floods and an elongated Tapi Basin produce comparatively lower peaks of flood hydrograph but more sustained flow.

**Acknowledgments** The results presented in this chapter are based on studies carried out by PSH during his PhD research. The authors are grateful to Professor Vishwas S. Kale for his guidance, comments, and suggestions during preparation of draft of this chapter. Thanks are due to the

Central Water Commission (CWC), New Delhi, for providing discharge data. PSH thanks the University Grants Commission (UGC), New Delhi, for its financial support by awarding teacher fellowship.

## References

Abbi, S. D. S., & Jain, B. C. (1971). A study of major rainstorms of Tapi basin for evaluation of design storm. *Indian Journal of Meteorology and Geophysics, 22*, 203–212.

Baker, V. R. (1973). Erosional form and processes for the catastrophic Pleistocene Missoula floods in eastern Washington. In M. Morisawa (Ed.), *Fluvial geomorphology* (pp. 123–148). George Allen and Unwin.

Baker, V. R. (1977). Stream channel response to floods with examples from Central Texas. *Geological Society of America Bulletin, 88*, 1057–1070.

Baker, V. R. (1988). Flood erosion. In V. R. Baker, R. C. Kochel, & P. C. Patton (Eds.), *Flood geomorphology* (pp. 81–95). Wiley Interscience.

Baker, V. R., & Costa, J. E. (1987). Flood power. In L. Mayer & D. Nash (Eds.), *Catastrophic flooding* (pp. 1–21). Allen and Unwin.

Baker, V. R., & Kale, V. S. (1998). The role of extreme floods in shaping bedrock channels. In K. J. Tinkler & E. E. Wohl (Eds.), *Rivers over rock: Fluvial processes in bedrock channels* (Geophysical monograph series) (Vol. 107, pp. 153–165). American Geophysical Union.

Costa, J. E. (1974). Response and recovery of a piedmont watershed from tropical storm Agnes, June 1972. *Water Resources Research, 10*(1), 106–112. https://doi.org/10.1029/WR010i001p00106

Costa, J. E., & O'Connor, J. E. (1995). Geomorphologically effective foods. In J. E. Costa, A. J. Miller, K. W. Potter, & P. R. Wilcock (Eds.), *Natural and anthropogenic influences in fluvial geomorphology* (Geophysical Monograph) (Vol. 89, pp. 45–56).

Deodhar, L. A., & Kale, V. S. (1999). Downstream adjustments in allochthonous rivers: Western Deccan Trap upland region India. In A. J. Miller & A. Gupta (Eds.), *Varieties of fluvial form* (pp. 295–315). Wiley.

Dhar, O. N., & Nandargi, S. (1995). On some characteristics of sever rainstorms of India. *Theoretical and Applied Climatology, 50*, 205–212. https://doi.org/10.1007/BF00866117

Erskine, W. D., & Livingstone, E. A. (1999). In-channel benches: The role of floods in their formation and destruction on bedrock-confined rivers. In A. J. Miller & A. Gupta (Eds.), *Varieties of fluvial form* (pp. 445–475). Wiley.

Goswami, D. C. (1985). Brahmaputra River, Assam, India: Physiography, basin denudation and channel aggradation. *Water Resources Research, 21*, 959–978. https://doi.org/10.1029/WR021i007p00959

Gunjal, R. P. (2016). *Rainfall characteristics of the Tapi basin*. Unpublished Ph.D. Thesis, Tilak Maharashtra Vidyapeeth, Pune.

Gupta, A. (1983). High-magnitude floods and stream channel response. In J. D. Collinson & J. Lewin (Eds.), *Modern and ancient fluvial systems* (pp. 219–227). Blackwell Publishing Ltd. http://scholarbank.nus.edu.sg/handle/10635/114225

Gupta, A. (1988). Large floods as geomorphic events in the humid tropics. In *Flood geomorphology* (pp. 301–320). Wiley-Interscience.

Gupta, A. (1995). Magnitude frequency and special factors affecting channel form and processes in the seasonal tropics. In J. E. Costa, A. J. Miller, K. W. Potter, & P. Wilcock (Eds.), *Natural and anthropogenic influences in the fluvial geomorphology* (Monograph 89) (pp. 125–136). American Geophysical Union.

Gupta, A., Kale, V. S., & Rajaguru, S. N. (1999). The Narmada River, India, through space and time. In A. J. Miller & A. Gupta (Eds.), *Varieties of fluvial form* (pp. 113–341). Wiley.

Hire, P. S. (2000). *Geomorphic and hydrologic studies of floods in the Tapi Basin*. Unpublished PhD Thesis, University of Pune, Pune (India). https://doi.org/10.13140/RG.2.2.29414.86084.

Hire, P. S., & Hire, P. P. (2021). Changes in hydraulic variables with discharge on the Tapi River India: Role of channel geometry. *Transactions of the Institute of Indian Geographers, 43*(1), 21–30.

Kale, V. S. (2007). Geomorphic effectiveness of extraordinary floods on three large rivers of the Indian Peninsula. *Geomorphology, 85*(3), 306–316. https://doi.org/10.1016/j.geomorph.2006.03.026

Kale, V. S., Ely, L. L., Enzel, Y., & Baker, V. R. (1994). Geomorphic and hydrologic aspects of monsoon floods on the Narmada and Tapi Rivers in Central India. *Geomorphology, 10*(1–4), 157–168. https://doi.org/10.1016/0169-555X(94)90014-0

Kale, V. S., & Gadgil, A. (1997). *Evaluation of the flood hydrology in the Upper Tapi Basin*. Unpublished Report submitted to the Department of Science and Technology New Delhi.

Kale, V. S., & Hire, P. S. (2004). Effectiveness of monsoon floods on the Tapi River India: Role of channel geometry and hydrologic regime. *Geomorphology, 57*(3–4), 275–291. https://doi.org/10.1016/S0169-555X(03)00107-7

Kale, V. S., & Hire, P. S. (2007). Temporal variations in the specific steam power and total energy expenditure of a monsoonal river: The Tapi River India. *Geomorphology, 92*(3–4), 134–146. https://doi.org/10.1016/j.geomorph.2006.06.047

Kale, V. S., Hire, P. S., & Baker, V. R. (1997). Flood hydrology and geomorphology of monsoon-dominated rivers: The Indian Peninsula. *Water International, 22*(4), 259–265. https://doi.org/10.1080/02508069708686717

Kochel RC (1988) Geomorphic impact of large floods: Review and new perspectives on magnitude and frequency. In: Baker VR, Kochel RC, Patton PC (eds) Flood geomorphology. John Wiley and Sons, New York P 169–187.

Leopold, L. B., & Maddock, T. (1953). The hydraulic geometry of stream channels and some physiographic implications. United States Geological Survey, Professional Paper-252, 1–57. https://doi.org/10.3133/pp252.

Leopold, L. B., Wolman, M. G., & Miller, J. P. (1964). *Fluvial processes in geomorphology*. Dover Publications.

McMohan, T. A., Finlayson, B. L., Haines, A. T., & Srikanthan, R. (1992). Global runoff – continental comparisons of annual flows and peak discharges. In M. M. TA, B. L. Finlayson, A. T. Haines, & R. Srikanthan (Eds.), *Catena paperback*.

Mutreja, K. N. (1995). *Applied hydrology*. Tata McGraw-Hill Publishing Company Ltd..

Patil, A. D., Bramhankar, G. W., & Hire, P. S. (2018). At-a-station hydraulic geometry of the Mahi River with special implication to annual maximum series. *International Journal of Scientific Research in Science and Technology, 5*(1), 101–105.

Petts, G. E., & Foster, I. D. L. (1985). Rivers and landscape. *Earth Surface Processes and Landforms, Edward Arnold London, 11*(5), 579–579. https://doi.org/10.1002/esp.3290110515

Shankar, R. (1991). Thermal and crustal structures of SONATA. A zone of mid continental rifting in the Indian shield. *Journal of Geological Society of India, 37*, 211–220.

Sakthivadivel, R., & Raghupathy, A. (1978). Frequency analysis of floods in some Indian rivers. *Hydrology Review, 4*, 57–67.

Shaligram, V. M., & Lele, V. S. (1978). Analysis of hydrologic data using Pearson type III distribution. *Hydrology Research, 9*(1), 31–42. https://doi.org/10.2166/nh.1978.0004

Viessman, W., Lewis, G. L., & Knapp, J. W. (1989). *Introduction to hydrology* (pp. 149–355). Harper and Row.

Ward, R. C. (1978). *Floods: A geographical perspective* (pp. 205–231). Macmillan.

Wohl, E. E. (1993). Bedrock channel incision along Piccaninny Creek, Australia. *The Journal of Geology, 101*(6), 749–761. https://doi.org/10.1086/648272

Wolman, M. G., & Miller, J. P. (1960). Magnitude and frequency of forces in geomorphic processes. *The Journal of Geology, 68*(1), 54–74. http://www.jstor.org/stable/30058255

# Geomorphological Analysis of the Ukhma River Basin from the Northern Foreland of Peninsular India


**K. Chaubey, S. Singh, S. Kanhaiya, and P. Singh**

## 1 Introduction

Fluvial landforms are primarily shaped by river systems (Vandenberghe, 2002; Corenblit et al., 2007). Previous studies have concentrated on geometric characteristics and practices, including quantitative investigation of the drainage basin's texture, shape, pattern, relief, and topography (Schumm, 1986; Burbank et al., 2000; Huggett & Cheesman, 2002; Rai, 2017).

The drainage pattern reflects the surface expression of underlying lithology and typical physiographic features (Pophare et al., 2014). Any hydrological investigation, including groundwater efficiency estimation and management, requires its morphometric analysis of the river basin (Waikar, 2014; Mustafa, 2016).

The morphometric analysis, with the support of the digital elevation model (DEM) and remote sensing data, ensures accurate information on the stream network. It also helps to understand the geomorphological and geology of the basin (Kumar et al., 2011; Rai, 2017). The morphometric variables such as slope, area, altitude, volume, profile, and texture of landforms include important study parameters (Rai et al., 2014; Singh et al., 2018a, b; Kanhaiya et al., 2019a, b, c; Prakash et al., 2019; Singh et al., 2020).

The morphometric investigation estimates the channel's relief, aerial, linear, and gradient (Singh et al., 2018a, b). Numerous researchers have utilized GIS and

K. Chaubey · P. Singh
CAS in Geology, Institute of Science, Banaras Hindu University, Varanasi, India

S. Singh (✉)
Department of Geology, Institute of Earth and Environmental Sciences, Dr. Rammanohar Lohia Awadh University, Ayodhya, India

S. Kanhaiya
Department of Earth and Planetary Sciences, Prof. Rajendra Singh (Rajju Bhaiya) Institute of Physical Sciences for Study and Research, V. B. S. Purvanchal University, Jaunpur, India



S. Kanhaiya et al. (eds.), *Rivers of India*,
https://doi.org/10.1007/978-3-031-49163-4_14

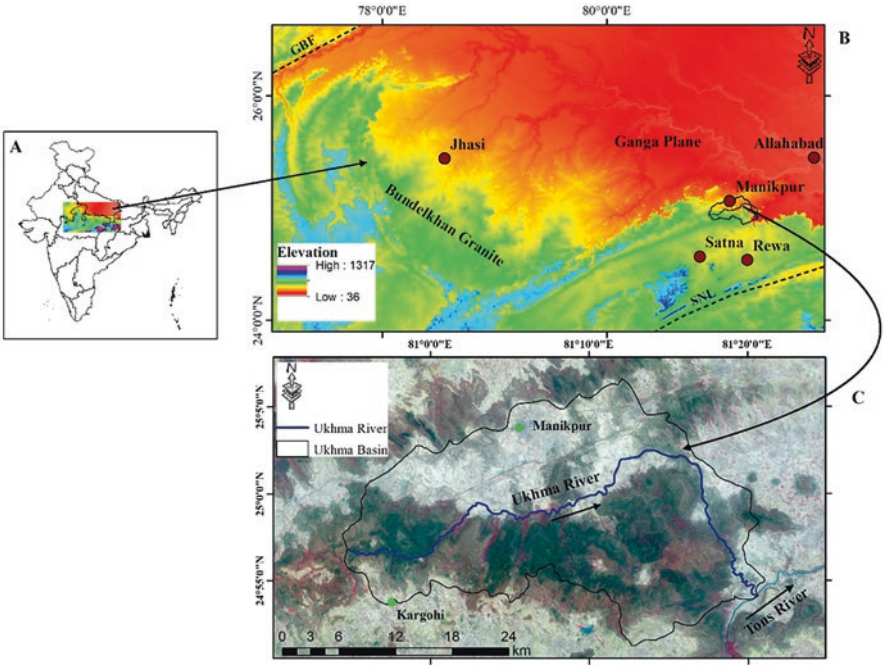


**Fig. 1** The map shows the location of the Ukhma river basin (Singh et al., 2022)

remote sensing techniques to investigate the morphometric analysis of river basins in recent and previous years (Horton, 1945; Strahler, 1957; Babar & Kaplay, 1998; Kaplay et al., 2004; Babar, 2001, 2002, 2005; Sreedevi et al., 2009; Singh et al., 2013; Jadhav & Babar, 2014; Singh & Kanhaiya 2015; Rai, 2017; Prakash et al., 2019; Solangi et al., 2019a, b, Singh et al., 2021).

The present study focuses on the characterization of the Ukhma river basin using GIS and remote sensing techniques (Fig.1a–c). The morphometric parameters, in conjunction with morphotectonics, have undergone comprehensive analysis and discussion to delineate the river basin's structure. This exploration aims to ascertain its effectiveness in water harvesting and groundwater management.

## 2 Geology of the Area

The Ukhma river is the tributary of the Tons River. It flows through districts such as Rewa and Satna of Madhya Pradesh, Central India (Fig. 1a–c). A typical seasonal river, the river Ukhma, joins the Tons River near Deokhar Village in the Satna district and originates from Ledari Village. The area of the Ukhma basin lies on Vindhyan rocks, covering an area of about 745 km$^2$.

The Ukhma basin covers one of the most dominant stratigraphic horizons in Central India, viz., Vindhyan Supergroup. Two distinct groups within the Vindhyan Supergroup are distinguished by distinct regional unconformity: Kaimur, Rewa, and Bhander Groups make up the Upper Vindhyan and the Lower Vindhyan (Semri Group) (Auden, 1933; Chakraborty & Chaudhuri, 1990; Chakraborty et al., 1998; Chakraborty, 2006; Shukla et al., 2014; Verma & Shukla, 2020). The maximum part of the study area is covered by the Rewa Group of rock, which consists of sandstone and shale, followed by the Kaimur Group.

The Aravalli-Delhi orogenic belt confines the Vindhyan Basin to the west and the Satpura orogenic belt to the south. According to Roy and Bandyopadhyay (1990), Verma (1991), and Verma (1996), the Mahakoshal Supergroup and the Bijawar Supergroup are low-grade metamorphic rocks to the east. The Vindhyan Basin's southern tectonic boundary is marked by the Son-Narmada lineament. It is accepted that this structural design appeared during the Archean and has stayed dynamic all through its geologic past (Naqvi & Rogers, 1987; Kaila, 1986; Kaila et al., 1989) (Fig. 1b). A southerly dipping reverse fault separates the Vindhyans from the Satpura mobile belt further south of this lineament (Tewari et al., 2001).

This fault appears to have generated deformations in the sedimentary rocks occurring immediately to its North in the Son Valley. However, these deformations are untraceable to the west, possibly due to the cover of younger rocks (Rogers, 1986). It is believed that the mountain-building activity in the Satpura was underway during the early phases of deposition in the Vindhyan Basin. At a later stage, the folded rocks of the Satpura were transported onto the Vindhyan (Naqvi & Rogers, 1987). The Great Boundary Fault (GBF) at the western margin in Rajasthan roughly separates the Vindhyan from the Archean/Paleoproterozoic Aravalli/Delhi Foldbelt (Fig. 1b). Although it was earlier believed that the GBF was purely a pre-Vindhyan fault that bounded the Vindhyan from the pre-Vindhyan rocks, there is sufficient field evidence that indicates that it had abundant reactivations after the deposition of the Vindhyan (Banerjee & Singh, 1981; Kaila, 1986; Kaila et al., 1989; Srivastava & Sahay, 2003).

## 3 Methodology

The Ukhma Basin boundary has been delineated using Survey of India (SOI) topographical maps No. 63C/16, 63D/13, 63G/8,4, and 63H/1,5 at a 1:50,000 scale. The Universal Transverse Mercator (UTM) projection WGS 1984, Zone 44 North, serves as a georeference for the topographical maps. Arc GIS 10 software uses SOI topographical maps to extract the streams of the Ukhma Basin. The entire high-resolution advanced topographic database of the Earth's surface was created by the Shuttle Radar Topography Mission (SRTM), which collected elevation (height) data from all over the world. Geomorphological parameters like slope aspect and gradient were identified using the SRTM DEM. Deformation (structural) features like

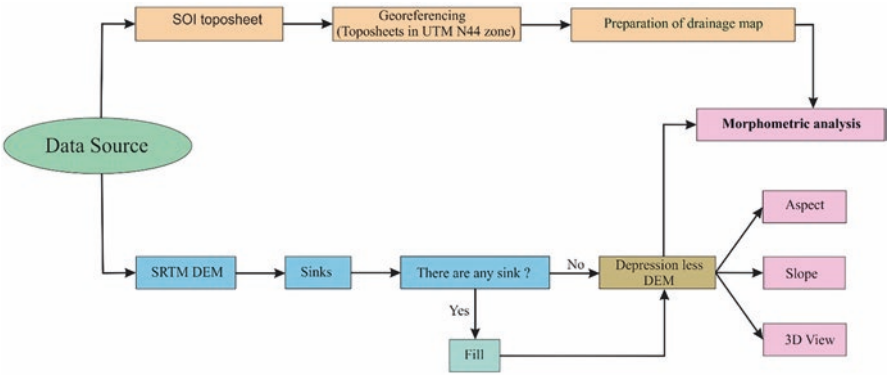


**Fig. 2** The flowchart depicts the in-depth methodology

joints, fractures, and drainage offset (linear features or lineaments) were determined

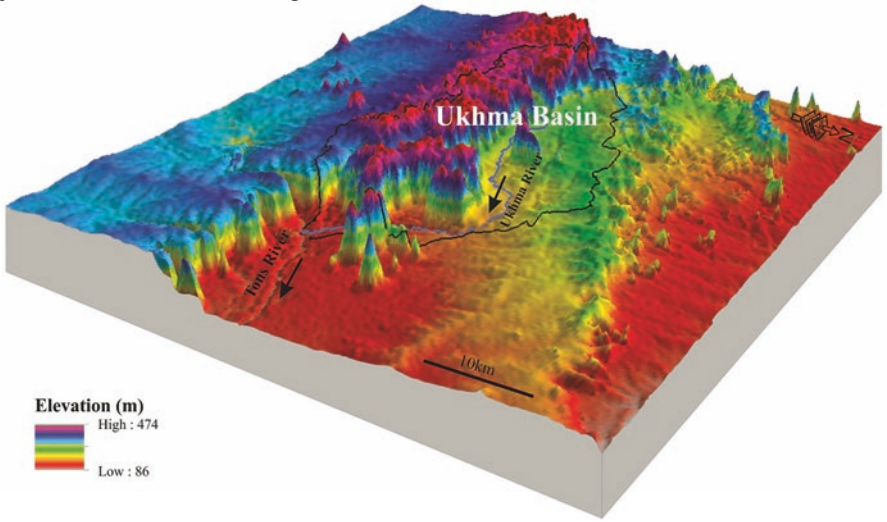


**Fig. 3** The digital elevation model of the Ukhma river basin drove from SRTM data. The elevation varies between 86 to 474 m in the study area

using Sentinal-2 images. The flowchart (Fig. 2) depicts the in-depth methodology.

The data from the SRTM DEM (Fig. 3) is used to highlight important geomorphological parameters like slope aspect and gradient (Fig. 4). This study used Strahler's (1964) stream order method. A mathematical approach and formula for calculating the basin morphometric parameters are presented in Table 1.

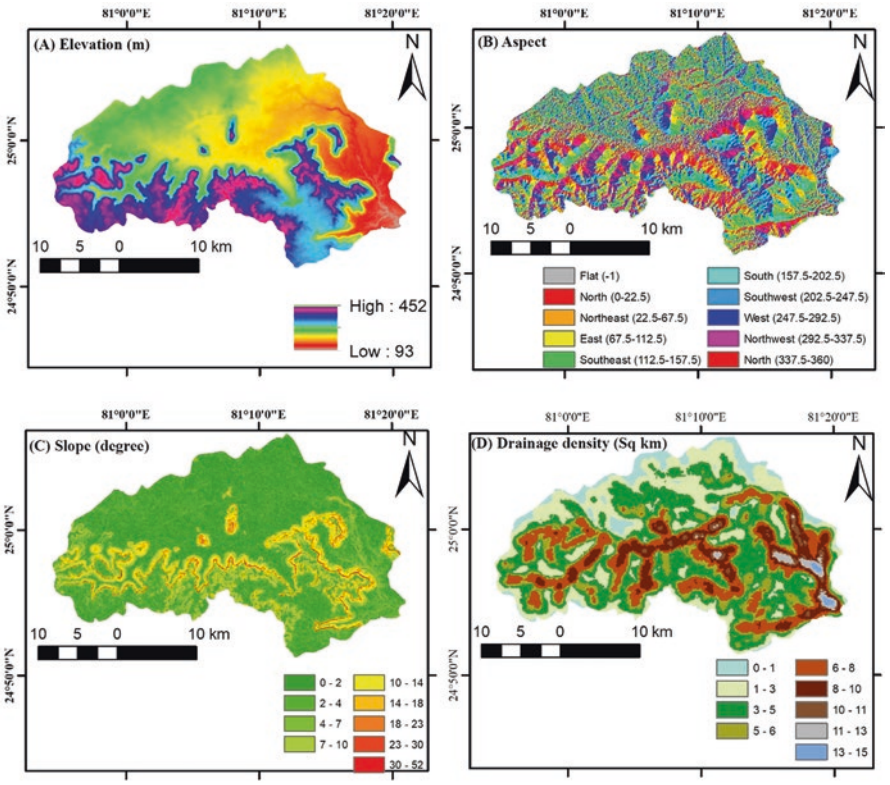


**Fig. 4** (**a**) Relief map, (**b**) aspect map, (**c**) slope map, and (**d**) drainage density map of the Ukhma river basin

## 4 Results

The morphometric analysis involves the measurement and analytical study of the river basin. Morphometric studies include basin area, altitude, volume, slope, profiles of the River, and drainage basin characteristics of the catchment zone concerned (Clark, 1966). Ukhma river basin is a six-order basin with fifth-order 10 subbasins, viz., Jiro, Gularha, Chhatan, Baridari, Bedhak, Dharkundi, Kakarhai, Terhwa, Jarera, and Karibarah subbasin are, shown in Fig. 5.

The characteristics of linear, areal, and relief perspectives have been examined and illustrated in the accompanying results, along with their respective features.

### *4.1 Drainage Pattern and Morphometric Aspects*

The drainage orientations (direction) of the Ukhma River basin (UW) show polymodal distribution (NE–SW, NW–SE, N–S, and E–W) (Fig. 5). The dendritic drainage pattern is primarily found in the lower part of the Ukhma river basin. The

**Table 1** Different parameters implemented for morphometric analysis

| | Parameter | Definition |
|---|---|---|
| Linear aspects | | |
| | Perimeter (P) (km) | |
| | Stream order (nu) | Strahler (1957) |
| | Stream length (Lu) (km) | Horton (1945) |
| | Bifurcation ratio (Rb) | Rb = Nu/N(u + 1), Horton (1945) |
| | Stream length ratio (Rl) | Rl = Lu/L(u−1), Horton (1945) |
| | Rho coefficient(R) | R = Rl/Rb, Horton (1945) |
| Areal aspects | | |
| | Area (A) ($km^2$) | |
| | Drainage density (Dd) (km km-2) | Dd = ∑Lt/A, Horton (1945) |
| | Length of overland flow (Lg) (km) | Lg = 1/2Dd, Horton (1945) |
| | Constant of channel maintenance (C) (km) | C = 1/Dd, Schumm (1956) |
| | Form factor (Ff) | Ff = A/Lb2, Horton (1945) |
| | Circularity ratio (Rc) | Rc = 4∏A/P2, Miller (1953) |
| | Elongation ratio (re) | Re = 1.128√A/Lb, Schumm (1956) |
| Relief aspects | | |
| | Basin relief (R) (km) | R = H-h, Schumm (1956) |
| | Relief ratio (Rr) | Rr = R/Lb, Schumm (1956) |
| | Relief ratio (Rr) | Rr = R/Lb, Schumm (1956) |
| | Gradient ratio (Rg) | Rg = Es-Em/Lb, Sreedevi et al.(2004) |
| | Melton ruggedness ratio (MRn) | MRn = H–h/$A^{0.5}$, Melton (1965) |

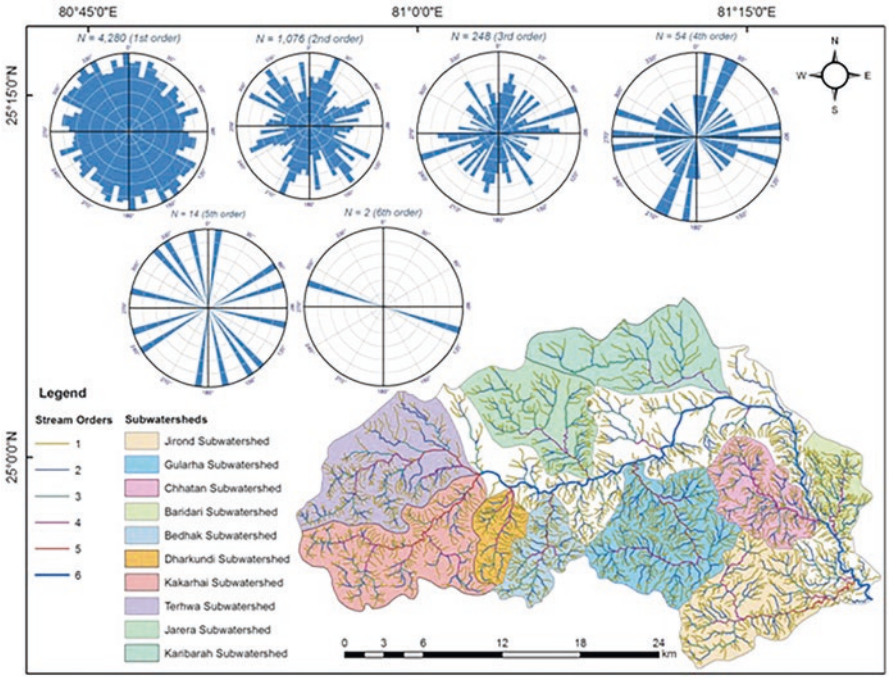


**Fig. 5** The drainage of the Ukhma river with 10 subbasins (Jirond, Gularha, Chhatan, Baridari, Bedhak, Dharkundi, Kakarhai, Terhwa, Jarera, and Karibarah)

dendritic patterns resemble a zone of similar lithologies. The elevation, aspect, slope, and drainage density map also have been prepared and shown in Fig. 4a–d. The elevation, aspect, slope, and drainage density map are beneficial to determine the distribution of vegetation, biodiversity in the basin area, morpho-conservation practices, etc. (Sreedevi et al., 2004).

## *4.2 Linear Characteristics of the Basin*

From head to mouth, stream network reveals the behavior of a stream and its tributaries and reflects the structural and lithological controls on the drainage basin. A drainage basin's perimeter, stream order, length, bifurcation ratio, stream length ratio, and rho coefficient are all important linear properties.

The Ukhma River basin is divided into ten 5th-order stream subbasins and has a perimeter of 139.74 kilometers (Table 2). The Dharkundi subbasin has a minimum perimeter of 20.31 km, while the Kakarhai subbasin has a maximum perimeter of 50.52 km. According to Leopold (1969), stream order demonstrates a stream's distinct position within a drainage basin. The Ukhma river basin is designated as the sixth-order stream in accordance with Strahler's stream ordering (Strahler, 1957, 1958).

For a given order, the length of the stream indicates the basin's contributing region (Horton, 1945). The length of stream segments is inversely proportional to the order of the streams (Fig. 6). It indicates that stream length increases with stream order and decreases in first-order streams (Fig. 7). Table 2 displays the average and total lengths of each stream. Hack (1957) depicts the relationship between basin territory and stream length, stating that head-ward erosion is the predominant river for drainage system expansion and improvement. The Dharkundi subbasin has the highest stream length ratio (0.66), indicating that structures and rock types influence the development of drainage patterns.

The bifurcation ratio is the proportion between the number of following higher-order streams and the number of streams of a given order (Strahler, 1964).

The bifurcation ratio ranges from 3 to 7, by which the geological structures control the drainage pattern. The typical Rb of the Ukhma Bowl is 4.75 (Table 2), which shows the undulating region with high surface runoff and moderate permeability of litho-units.

As defined by Horton (1945), the stream length ratio is the proportion of the stream's mean length to the following lower order of the stream segments. The stream length proportion among 10 subbasins varies from 0.49 to 0.66. According to Sreedevi et al. (2004), the RL values' variations are directly related to the topography and lithology. The high erosion activity indicates a higher stream length ratio. The stream length ratio increases from lower- to higher-order and is represented as an achievement of geomorphic development (Thomas et al., 2010; Prakash et al., 2016a, b, 2017; Singh et al., 2018a, b, 2020, 2021).

**Table 2** Morphometric parameters of the Ukhma river basin and its subbasins

| Linear aspects | Jirond subwatershed | Gularha subwatershed | Chhatan subwatershed | Baridari subwatershed | Bedhak subwatershed | Dharkundi subwatershed | Kakarhai subwatershed | Terhwa subwatershed | Jarera subwatershed | Karibarah subwatershed | Main watershed |
|---|---|---|---|---|---|---|---|---|---|---|---|
| Perimeter (P) (km) | 41.74 | 40.16 | 27.99 | 21.44 | 27.63 | 20.31 | 50.52 | 42.28 | 33.82 | 40.61 | 139.74 |
| Stream order (Nu) | 294 | 405 | 273 | 167 | 166 | 104 | 347 | 291 | 151 | 62 | 2837 |
| Stream length (Lu) (km) | 206.79 | 268.11 | 167.49 | 93.02 | 101.05 | 67.62 | 222.46 | 197.81 | 122.92 | 91.59 | 1995.38 |
| Bifurcation ratio (Rb) | 3.93 | 4.38 | 6.58 | 5.11 | 3.34 | 3.21 | 4.03 | 3.96 | 3.36 | 3.54 | 4.75 |
| Stream length ratio (Rl) | 0.601 | 0.558 | 0.499 | 0.585 | 0.627 | 0.667 | 0.582 | 0.497 | 0.491 | 0.625 | 0.562 |
| Rho coefficient(R) | 0.152 | 0.127 | 0.075 | 0.114 | 0.187 | 0.207 | 0.144 | 0.125 | 0.146 | 0.176 | 0.118 |
| *Areal aspects* | | | | | | | | | | | |
| Area (A) ($km^2$) | 69.91 | 81.51 | 43.79 | 24.01 | 30.19 | 20.96 | 82.21 | 84.89 | 60.17 | 66.74 | 745.84 |
| Drainage density (Dd) (km $km^2$) | 2.95 | 3.28 | 3.82 | 3.87 | 3.34 | 3.22 | 2.71 | 2.33 | 2.04 | 1.37 | 2.67 |
| Length of overland flow (Lg) (km) | 1.47 | 1.64 | 1.91 | 1.93 | 1.67 | 1.61 | 1.35 | 1.16 | 1.02 | 0.68 | 1.33 |
| Constant of channel maintenance (C) (km) | 0.33 | 0.3 | 0.26 | 0.25 | 0.29 | 0.31 | 0.36 | 0.42 | 0.48 | 0.72 | 0.37 |
| Form factor (Ff) | 0.34 | 0.61 | 0.5 | 0.37 | 0.38 | 0.38 | 0.4 | 0.41 | 0.4 | 0.26 | 0.4 |
| Circularity ratio (Rc) | 0.5 | 0.63 | 0.7 | 0.65 | 0.49 | 0.63 | 0.4 | 0.59 | 0.66 | 0.5 | 0.47 |

| | | | | | | | | | | | |
|---|---|---|---|---|---|---|---|---|---|---|---|
| Elongation ratio (Re) | 0.66 | 0.88 | 0.8 | 0.68 | 0.7 | 0.7 | 0.71 | 0.72 | 0.71 | 0.57 | 0.71 |
| *Relief aspects* | | | | | | | | | | | |
| Basin relief (R) (km) | 0.311 | 0.243 | 0.295 | 0.183 | 0.215 | 0.218 | 0.193 | 0.213 | 0.069 | 0.093 | 0.312 |
| Relief ratio (Rr) | 0.021 | 0.021 | 0.031 | 0.022 | 0.024 | 0.029 | 0.013 | 0.014 | 0.005 | 0.005 | 0.007 |
| Gradient ratio (Rg) | 0.021 | 0.02 | 0.031 | 0.021 | 0.023 | 0.029 | 0.013 | 0.014 | 0.005 | 0.005 | 0.007 |
| Melton ruggedness ratio (MRn) | 0.037 | 0.026 | 0.044 | 0.037 | 0.039 | 0.047 | 0.021 | 0.023 | 0.008 | 0.011 | 0.011 |

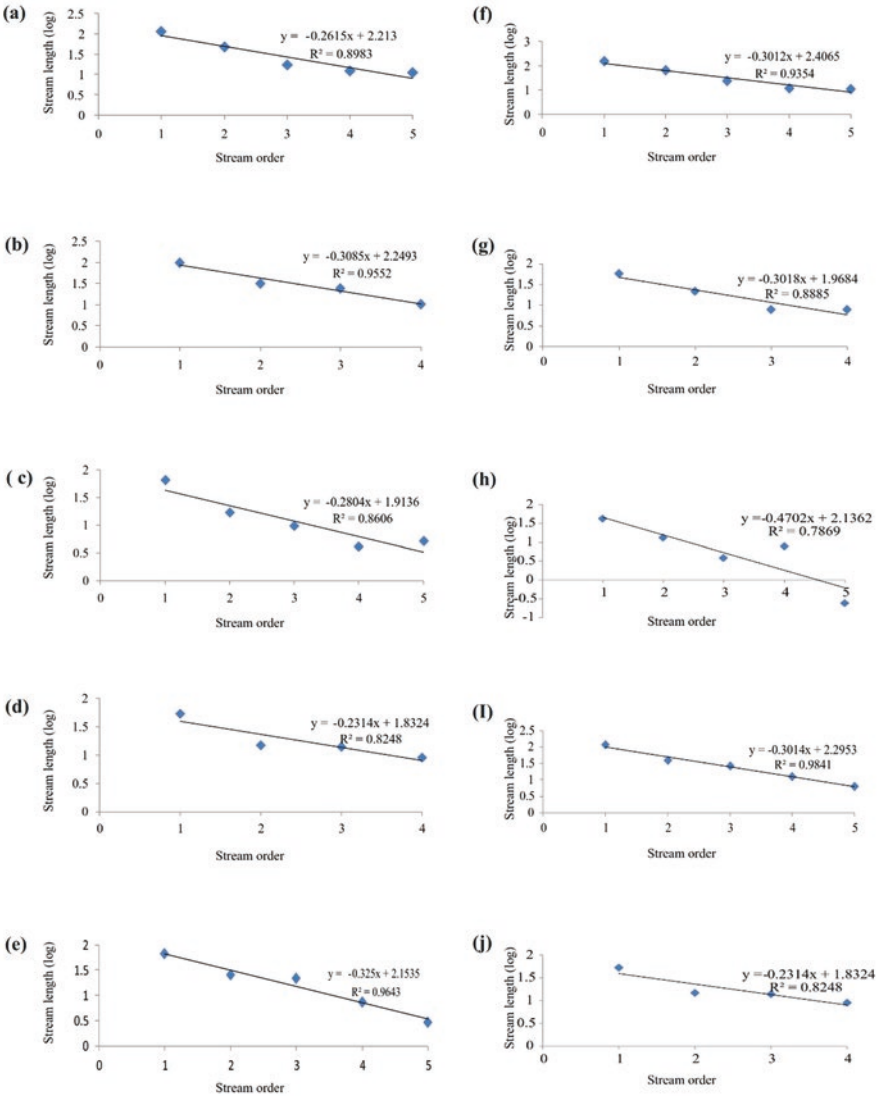


**Fig. 6** The relation between stream order and stream length (**a**) Jirond subbasin (**b**) Chhatan subbasin (**c**) Bedhak subbasin (**d**) Kakarhai subbasin (**e**) Jarera subbasin (**f**) Gularha subbasin (**g**) Baridari subbasin (**h**) Dharkundi subbasin (**i**) Terhwa subbasin (**j**) Karibar

The Rho coefficient is characterized as the proportion of the stream length ratio to the bifurcation ratio. For the subbasins, the rho coefficient varies between 0.07 and 0.21. It is an essential parameter relating drainage density to the physiography maturity of a basin. It is a crucial parameter that links drainage density to a basin's physiography maturity. The Rho coefficient is a valuable parameter for assessing the storage capacity limit of the drainage system (Horton, 1945). Higher hydrologic

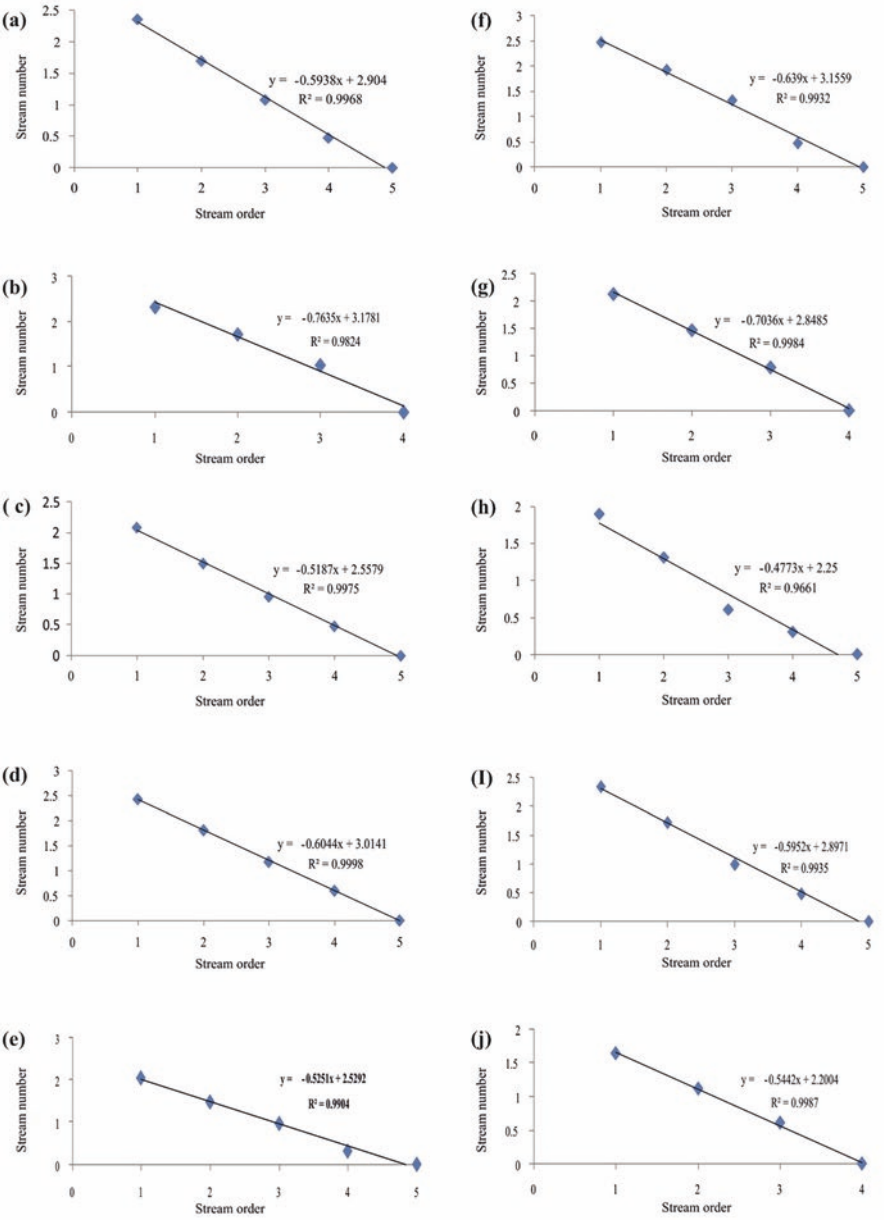


**Fig. 7** The relation between stream order and stream number (**a**) Jirond subbasin (**b**) Chhatan subbasin (**c**) Bedhak subbasin (**d**) Kakarhai subbasin (**e**) Jarera subbasin (**f**) Gularha subbasin (**g**) Baridari subbasin (**h**) Dharkundi subbasin (**i**) Terhwa subbasin (**j**) Karibara subbasin

storage during floods and decreased erosion during high discharge explain the higher Rho coefficient values found in the Dharkundi and Bedhak subbasins.

### *4.3 Areal Aspects of the Basin*

Geological structure, climatic conditions, lithology, and the basin's history of denudation are all revealed by the areal aspects of a drainage basin. Basin area, drainage density, overland flow length, constant channel maintenance, form factor, circulatory ratio, and elongation ratio are all aerial aspects of a drainage basin. The Ukhma basin occupies a 745.84 $km^2$ area in Central India. The areas of 10 subbasins are arranged and summarized in Table 2.

The ratio of total channel lengths within a basin to the basin's area is known as drainage density (Dd). It could also indicate how close the channels' spacing is (Strahler, 1964). Under dense vegetation and low relief, a low Dd is more likely to occur in a region with highly resistant and permeable subsoil. Mountainous relief, weak or impermeable subsurface material, and sparse vegetation all indicate a high drainage density. The Ukhma River basin has a drainage density of 2.67 per km, which indicates a moderate drainage density (Table 1). According to Rai (2017) and Thomas et al. (2010), the basin should have permeable subsoil and vegetative cover due to the moderate drainage density. Figure 4 depicts the Ukhma basin's drainage density map. The Karibarah subbasin's low drainage density is preferable to resistant lithology or extremely permeable subsoil beneath dense vegetation.

In contrast, the Baridari subbasin's high drainage density is supported in locations with weak or impermeable materials and minimal vegetation cover. The distance from the crest line at which the flow concentration occurs is used to calculate the overland flow length (Lg) (Horton, 1945, Rudraiah et al., 2008). According to Horton (1945), Lg is a significant parameter that influences the hydrological and physiographical developments of the drainage basin. Lg ranges between 0.68 and 1.93 in the study area (Table 2). The Baridari and Chhatan subbasins are characterized by an early stage of basin development, whereas other subbasins, such as the Ukhma basin, are assumed to have reached a mature stage.

Drainage density and the constant of channel maintenance (C) complement one another (Schumm, 1956). The basin's slope, permeability, climatic conditions, vegetation cover, erosional activity duration, and rock types influence the C. The C value of the Ukhma basin (UW) is 1.33 and differs from 0.25 and 0.72 for every 10 subbasins (Table 2). Subbasins with low C values are categorized as areas with few structural constraints. The stream's old saying is that a higher value of C indicates a higher invasion rate.

The drainage basin's shape and flow intensity are directly related to peak discharge by the form factor (Ff) (Gregory & Walling, 1973; Magesh et al., 2012). The higher Ff values of the Gularha and Chhatan subbasins (> 0.51) suggested that the peak flow was increased and lasted for a shorter time. In contrast, the Karibarah subbasin's lower value indicates shorter periods of insufficient peak flow.

According to Miller (1958), the circularity proportion (Rc) is the proportion of the basin area to the area of a circle with the same parameter as the basin. It is influenced by the basin's stream frequency (Fs), the land cover, the geological structures, the climate, the relief, and the steepness of the slope (Bali et al., 2012). Rc is a crucial parameter that indicates the stage of the basin (Sreedevi et al., 2004; Kumar & co., 2011). The Ukhma main basin has an Rc value of 0.47 (Table 2). The young and mature stages of basin development are represented by the Kakarhai subbasin's low Rc value of 0.41 and the Chhatan subbasin's high Rc value of 0.71, respectively.

The elongation ratio (Re), as defined by Schumm (1956), is the ratio of the basin's length to the diameter of a circle with the same area as the basin. The higher elongation ratio indicates the impervious surface's low relief. In contrast, the low value of the elongation ratio indicates similar geological materials that are strongly elongated and highly permeable (Reddy et al., 2004). The Re in the Ukhma basin ranges from 0.57 and 0.88 over a sufficient assorted atmosphere and topography with strong relief and steep slope.

## *4.4 Relief Aspects of the Basin*

The basin relief, relief ratio, gradient ratio, and melton ruggedness number were all relief aspects of a drainage basin. According to Schumm (1956), basin relief is the difference in elevation between the basin's maximum and minimum elevations. Basin relief provides a better understanding of the basin's denudational description, reveals the stream's gradient, influences the channel's capacity for transportation, and reveals flood patterns (Sreedevi et al., 2004).

According to Schumm (1956), the relief ratio, defined as the ratio of basin relief to basin length, is widely accepted as a valid measure of the basin's gradient aspects (Vittala & co, 2004). A relief ratio with a high value represents the hilly region. In contrast, the valley and Pedi-plain areas are characterized by a low value (Kumar et al., 2011, Magesh et al., 2012). The Chhatan subbasin has a maximum Rr value of 0.031 (Table 2), indicating higher relief and a steeper slope supported by rugged rocks.

From source to mouth and basin length, the gradient ratio is the ratio of the various elevations. A measure of channel slant, the gradient ratio (Rg), aids in determining the runoff volume (Sreedevi et al., 2004; Thomas et al., 2010; Prakash et al., 2016, 2017; Singh et al., 2018b). The Chhatan subbasin's high Rg value indicates a steep slope and increased runoff. In contrast, the Karibarah subbasin's low Rg value indicates less surface runoff and a greater likelihood of infiltration.

The ratio of basin relief divided by the square root of the basin's area is the melton ruggedness number (Melton, 1965). The melton ruggedness number of the Ukhma Bowl is 0.011 (Table 2).

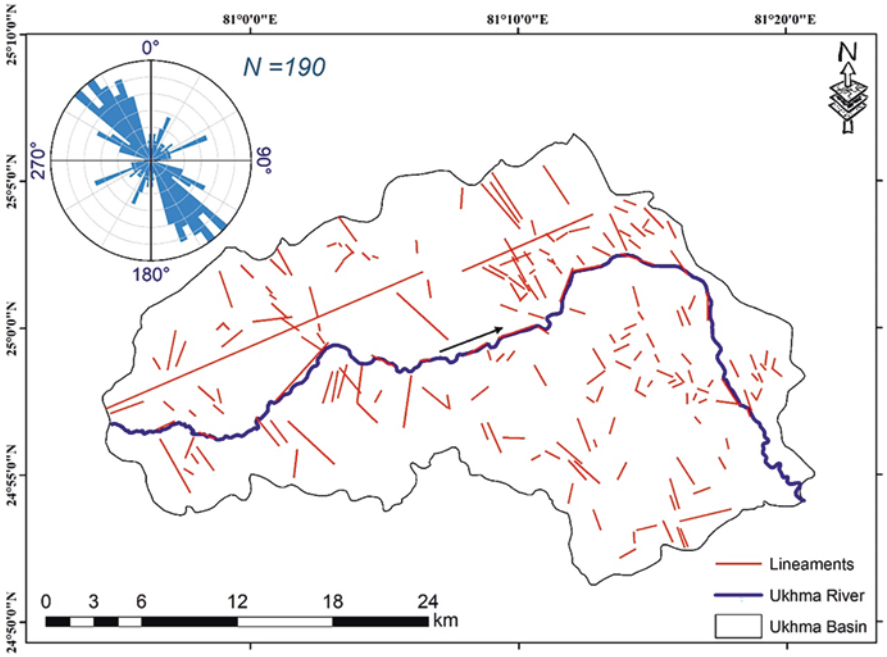


**Fig. 8** Figure showing different lineament directions in the Ukhma river basin

## *4.5 Lineaments Analysis*

According to Nur (1982), the lineaments are the essential components of the Earth's surface morphology and deformation. With the help of the Arc GIS-10 platform's sentinel-2 imagers, the lineaments were identified and further supported by in-depth field investigations. One hundred ninety lineaments have been mapped. Figure 8, a rose diagram, depicts the orientations of these lineaments. There are some NE–SW trending lineaments, and the NW–SE trending lineaments are relatively high. The fact that most lineaments do not follow the Son-Narmada lineament's regional trend suggests that secondary tectonics in and after the Son-Narmada lineament developed the basin. Figure 1b demonstrates that the faulting and fractures that occurred during the subsequent stage of basin development are distinct from the regional trend of the Son-Narmada lineaments.

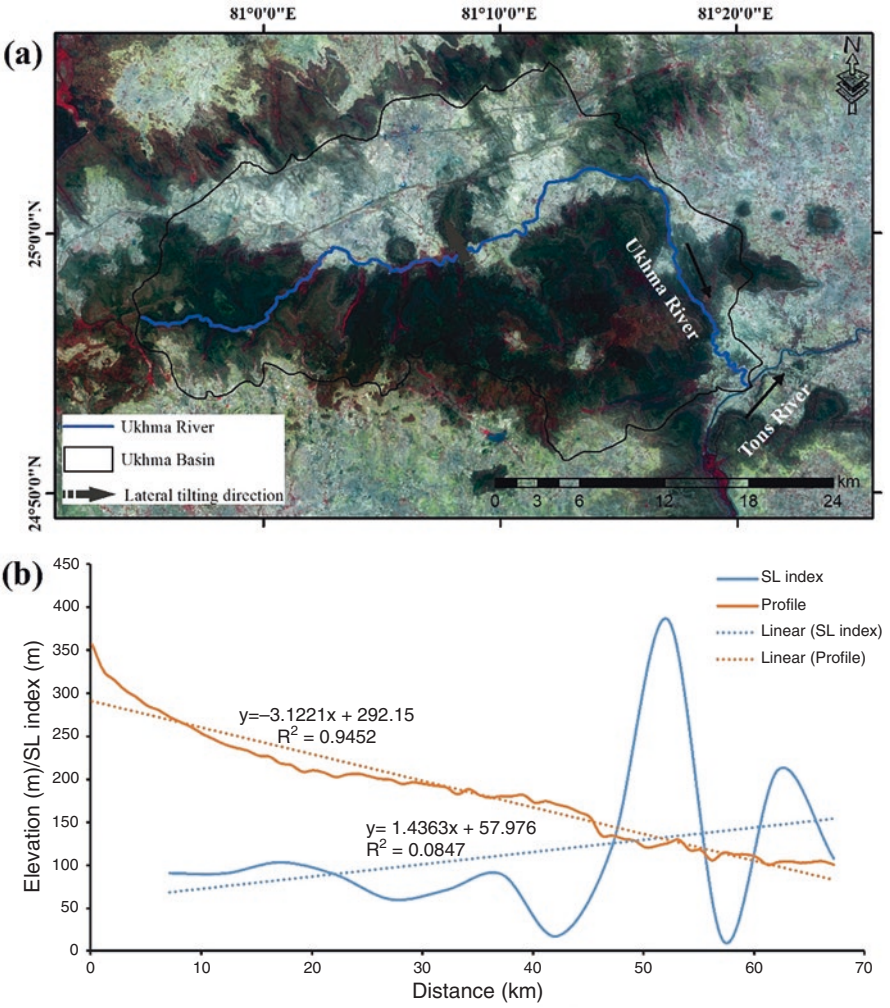


**Fig. 9** (**a**) The AF value of the Ukhma river is 52.65, which is greater than 50, suggesting that the basin has been tilted in the northward direction (left side of the river) (**b**) longitudinal profile of the Ukhma river

## *4.6 Longitudinal Profiles*

Longitudinal profiles of the river significance from the interaction between base-level change, fluvial incision, lithology, and tectonics (Brocard et al., 2003; Larue, 2008a, b). The variation in lithology of the region influences longitudinal

profile development as well (Duvall et al., 2004; Stock & Montgomery, 1999; Ritter et al., 2002). The Ukhma river has a variable of curves and gradients in its longitudinal profile (Fig. 9b). These deviations from the longitudinal profile may indicate either a harmonious stream in which the upstream retreat alters the base level of the upstream basin (Bishop et al., 2005) or, in some instances, a dynamic equilibrium between tectonic movements and fluvial processes (Snow & Slingerland, 1990). These knick points connect the lithological variation and outcomes of regional tectonics in the longitudinal profile of the Ukhma river.

### *4.7 Asymmetry Factor (AF)*

According to Cox et al. (2001) and Pinter (2005), AF is a crucial parameter for determining the directions of potential differential tectonism and tilting. A basin's lateral tilt concerning the river is indicated by this factor (Cox et al., 2001; Cuong & Zuchiewicz, 2001). The asymmetry factor is calculated as AF = 100 (Ar/At), where Ar is the area of the mainstream's right side and At is the drainage basin's total area. If AF exceeds 50, the river has tilted to the left of the basin in relation to the river (Molin et al., 2004), and if AF is greater than 50, the river has sunk to the right of the drainage basin (Molin et al., 2004). In the current review, the AF of the Ukhma Stream is 52.65 (Fig. 9a).

## 5 Discussion

The linear parameters provide information about the very high fraction of first-order stream, high infiltration rate, mature stage, and gentle slope. The areal parameters provide information about the value of circularity ratio (0.373), length of overland flow (1.337), drainage density (2.675), low water storage capacity, and concentration of peak discharge in the distal part of this basin (Table 1). The relief parameter gives information about the low value of relief ratio (0.007), relief (0.312), high infiltration rate, low surface runoff, and spreading of water within the basin (Table 1). The estimations of the bifurcation ratio for the Ukhma basin represent the basin's dismembered mountainous nature having mature geography.

The area with homogeneous lithologies and horizontal or gently dipping strata resembles the dendritic pattern. The basin's behavior during heavy rainfall, which may result in significant runoff and floods, is predicted using the morphometric parameters (Garde, 2006; (2010) (Perucca and Angilieri). According to Table 2, the Ukhma Basin's average Rb is 4.75, indicating a hilly area with moderate litho-unit permeability and high surface runoff. The drainage system's storage capacity limit can be determined and evaluated using the Rho coefficient. According to Horton (1945), it is utilized as a component of the drainage level of advance in a specific basin. Higher hydrologic storage during floods and decreased erosion during high

discharge explain the higher Rho coefficient values found in the Dharkundi and Bedhak subbasins. The Karibarah subbasin's low drainage density is preferable to resistant lithology or extremely permeable subsoil beneath dense vegetation. In contrast, the Baridari subbasin's high drainage density is supported in locations with weak or impermeable materials and minimal vegetation cover. Lg ranges between 0.68 and 1.93 in the area under study. The Baridari and Chhatan subbasins are characterized by an early stage of basin development, whereas other subbasins, such as the Ukhma basin, are assumed to have reached a mature stage. The higher Ff values (>0.51) of the Gularha and Chhatan subbasins suggested a shorter period of high peak flow. In contrast, the lower Ff value of the Karibarah subbasin suggested a more extended period of insufficient peak flow. The Son-Narmada lineament is not the most common of the lineaments (Figs. 1b and 9). Through its overall morphology and knick points, where the river gradient changes rapidly, the longitudinal profile of the Ukhma river reveals the influence of regional tectonism (Fig. 9b).

The Ukhma river has an AF value of 52.65, which is higher than 50 and indicates that the basin has been tilted to the North (left side of the river) (Fig. 9a). By identifying abnormally high SL index values, the SL index was used to identify neotectonic activity (Merritts & Vincent, 1989; Keller & Pinter, 1996).

## 6 Conclusion

1. The bifurcation ratio suggests that some geologies and structures control the drainage pattern of the Ukhma basin.
2. The very high fraction of first-order streams indicates uniform lithology and gentle slope, explaining the significant portion of precipitation flow as surface runoff. The overland flow length shows the drainage basin's physiographical development and geomorphic maturity.
3. Morphometric parameters are used to predict the behavior of the basin during heavy rains that can generate significant runoff and create flooding.
4. The lineament study and longitudinal profile of the basin suggest that the regional tectonics somehow controls the drainage dynamics of the Ukhma Basin. The asymmetry factor of the Ukhma river indicates left-side channel shifting, i.e., in the northward direction.

**Acknowledgments** S. Singh is thankful to the SERB (Project No. PDF/2018/004148), New Delhi, India, for financial support.

## References

Auden, J. B. (1933). Vindhyan sedimentation in the son valley, Mirzapur District. *Memoirs of the Geological Survey of India, 62*, 141–250.

Babar, M. D. (2001). Hydrogeomorphological studies by remote sensing application in Akoli watershed (Jintur) Parbhani dist., Maharashtra, India. *Spatial Information Tech Remote sensing and GIS-ICORG, 2*, 137–143.

Babar, M. D. (2002). Application of remote sensing in Hydrogeomorphological studies of Purna River basin in Parbhani District, Maharashtra, India. *Proceeding volume of the international symposium of ISPRS Commission VII on Resource and Environmental Monitoring, 34*, 519–523.

Babar, M. D. (2005). *Hydrogeomorphology, fundamental applications and techniques* (Vol. 1, p. 259). New India Publishing Agency.

Babar, M. D., & Kaplay, R. D. (1998). Geomorphometric analysis of Purna River basin Parbhani District (Maharashtra). *Indian Journal of Geomorphology, 3*, 29–39.

Bali, R., Agarwal, K., Nawaz, S. N., Rastogi, S., & Krishna, K. (2012). Drainage morphometry of Himalayan glacio-fluvial basin, India- hydrologic and neotectonic implications. *Environmental Earth Science, 66*, 1163–1174.

Banerjee, A. K., & Singh, H. J. M. (1981). Plaeogeography and sedimentation of Vindhyans in eastern Rajasthan. *Miscellaneous Publications of the Geological Survey of India, 50*, 89–94.

Bishop, P., Hoey, T. B., Jansen, J. D., & Artza, I. L. (2005). Knick point recession rate and catchment area: The case of uplifted rivers in eastern Scotland. *Earth Surface Processes Landform, 30*(6), 767–778.

Brocard, G. Y., van der Beek, P. A., Bourlès, D. L., Siame, L. L., & Mugnier, J. L. (2003). Long-term fluvial incision rates and postglacial river relaxation time in the French western Alps from 10Be dating of alluvial terraces with assessment of inheritance, soil development and wind ablation effects. *Earth and Planetary Sciences Letters, 209*, 197–214.

Burbank, D. W., & Anderson, R. S. (2000). *Tectonic geomorphology* (p. 274). Blackwell Science.

Chakraborty, C. (2006). Proterozoic intracontinental basin: The Vindhyan example. *Journal of Earth System Science, 115*(1), 3–22.

Chakraborty, P. P., Sarkar, S., & Bose, P. K. (1998). A viewpoint on intracratonic chenier evolution: Clue from a reappraisal of the Proterozoic Ganurgarh Shale, Central India. In B. S. Palliwal (Ed.), *The Indian Precambrians* (p. 61). Scientific Publishers.

Chakraborty, T., & Chaudhuri, A. K. (1990). Stratigraphy of the late Proterozoic Rewa Group and palaeogeography of the Vindhyan basin in Central India during Rewa sedimentation. *Journal of Geological Society of India, 36*, 383–402.

Clark, C. (1966). Morphometry from map, essay in geomorphology. *Amer Else Publishing Company New York.*, 235–274.

Corenblit, D., Tabacchi, E., Steiger, J., & Gurnell, A. M. (2007). Reciprocal interactions and adjustments between fluvial landforms and vegetation dynamics in river corridors: A review of complementary approaches. *Earth-Science Reviews, 84*(1–2), 56–86.

Cox, R. T., Van Arsdale, R. B., & Harris, J. B. (2001). Identification of possible quaternary deformation in the northeastern Mississippi embayment using quantitative geomorphic analysis of drainage-basin asymmetry. *Geological Society of America Bulletin, 113*(5), 615–624.

Cuong, N. Q., & Zuchiewicz, W. A. (2001). Morphotectonic properties of the Lo River fault near Tam Dao in North Vietnam. *Natural Hazards and Earth System Sciences, 1*, 15–22.

Duvall, A., Kirby, E., & Burbank, D. (2004). Tectonic and lithologic controls on bedrock channel profiles and processes in coastal California. *Journal of Geophysical Research, 109*, 1–18.

Garde, R. J. (2006). *River morphology*. New Age International.

Gregory, K. J., & Walling, D. E. (1973). *Drainage basin form and process a geomorphological approach*. Edward Arnold.

Hack, J. T. (1957). Studies of longitudinal stream profiles in Virginia and Maryland. *Unit States Geological Surface Professional Paper US Geological Survey, 294*(B), 45.

Horton, R. E. (1945). Erosional development of streams and their drainage basins hydrophysical approach to quantitative morphology. *Geological Society American Bulletin, 56*, 275–370.

Huggett, R., & Cheesman, J. (2002). *Topography and the environment*. Pearson Education.

Jadhav, S. I., & Babar, M. D. (2014). Linear and aerial aspect of Basin morphometry of Kundka sub-basin of Sindphana Basin (Beed), Maharashtra, India. *International Journal Geological Agriculture and Environmental Science, 2*, 2348–2354.

Kaila, K. L. (1986). Tectonic framework of Narmada–Son lineament: A continental rift system in central India from deep seismic soundings. In M. Brazangi & L. Brown (Eds.), *Reflection seismology: A global perspective* (Geodynamic series). AGU. 13 pp.

Kaila, K. L., Murthy, P. R. K., & Mall, D. M. (1989). The evolution of the Vindhyan basin vis-à-vis the Narmada–Son lineament, Central India, from deep seismic soundings. *Tectonophysics, 162*, 277–289.

Kanhaiya, S., Singh, B. P., Singh, S., Mittal, P., & Srivastava, V. K. (2019a). Morphometric analysis, bed-load sediments, and weathering intensity in the Khurar River Basin, Central India. *Geological Journal, 54*, 466–481.

Kanhaiya, S., Singh, S., Singh, C. K., Srivastava, V. K., & Patra, A. (2019b). *Geomorphic evolution of the Dongar River Basin, Son Valley, Central India*. Geology, Ecology, and Landscapes. https://doi.org/10.1080/24749508.2018.1558019

Kanhaiya, S., Singh, S., Singh, C. K., & Srivastava, V. K. (2019c). Pothole: A unique geomorphological feature from the bedrocks of Ghaggar River, Son valley, India. *Geology, Ecology, and Landscapes, 3*(4), 258–268.

Kaplay, R. D., Babar, M. D., Panaskar, D. B., & Rakhe, A. M. (2004). Geomorphometric characteristics of 30th September 1993 Killari Earthquake Area, Maharashtra (India). *Journal of Geophysics, 25*, 55–61.

Keller, E. A., & Pinter, N. (1996). *Active tectonics* (Vol. 1338). Prentice Hall.

Kumar, A., Jayappa, K., & Deepika, B. (2011). Prioritization of sub-basins based on geomorphology and morphometric analysis using remote sensing and geographic information system (GIS) techniques. *Geocarto International, 26*, 569–592.

Larue, J. P. (2008a). Effects of tectonics and lithology on long profiles of 16 rivers of the southern central Massif border between the Aude and the Orb (France). *Geomorphology, 93*, 343–367.

Larue, J. P. (2008b). Tectonic influence on the quaternary drainage evolution on the northwestern margin of the French Central Massif: The Cruese valley example. *Geomorphology, 93*, 398–420.

Leopold, L. B. (1969). *Fluvial processes in geomorphology*. Eurasia Publishing House.

Magesh, N. S., Jitheshlal, K. V., Chandrasekar, N., & Jini, K. V. (2012). GIS based morphometric evaluation of Chimmini and Mupily watersheds, parts of Western Ghats, Thrissur District, Kerala, India. *Earth Science Information, 5*, 111–121.

Melton, M. A. (1965). The geomorphic and paleoclimatic significance of alluvial deposits in southern Arizona. *Journal of Geology, 73*, 1–38.

Merritts, D., & Vincent, K. R. (1989). Geomorphic response of coastal streams to low, intermediate, and high rates of uplift, Medocino triple junction region, northern California. *Geological Society of America Bulletin, 101*(11), 1373–1388.

Miller, V. C. (1953). *A quantitative geomorphic study of drainage basin characteristics in the Clinch Mountain area, Virginia and Tennessee* (Vol. 3). Columbia University.

Miller, J. P. (1958). *High mountaineous streams effect of geology on channel characteristics and bed material, Mem*. New Maxi Bur Mines Mineral Resource.

Molin, P., Pazzaglia, F. J., & Dramis, F. (2004). Geomorphic expression of the active tectonics in a rapidly deforming forearc, sila Massif, Calabria, Southern Italy. *American Journal of Science, 304*, 559–589.

Mustafa, A. S. (2016). Drainage Basin morphometric analysis of Galagu Valley. *Journal Applied and Industrial Science, 4*, 2320–4609.

Naqvi, S. M., & Rogers, J. J. W. (1987). *Precambrian geology of India*. Clarendon Press/Oxford University Press. 233p.

Nur, A. (1982). The origin of tensile fracture lineaments. *Journal of Structural Geology, 4*(1), 31–40.

Pinter, N. (2005). Applications of tectonic geomorphology for deciphering active deformation in the Pannonian Basin, Hungary. In L. Fodor & K. Brezsnya'Nszky (Eds.), *Proceedings of the*

*workshop on "applications of GPS in plate tectonics in research on fossil energy resources and in earthquake hazard assessment", occasional papers of the geological institute of Hungary* (Vol. 204, pp. 25–51).

Pophare, A. M., Lamsoge, B. R., Katpatal, Y. B., & Nawale, V. P. (2014). Impact of over-exploitation on groundwater quality: A case study from WR-2 watershed, India. *Journal of Earth System Science, 123*(7), 1541–1566.

Prakash, K., Singh, S., & Shukla, U. K. (2016a). Morphometric changes of the Varuna River basin, Varanasi district, Uttar Pradesh. *Journal of Geomatics, 10*, 48–54.

Prakash, K., Mohanty, T., Singh, S., Chaubey, K., & Prakash, P. (2016b). Drainage morphometry of the Dhasan River basin, Bundelkhand Craton, Central India using remote sensing and GIS techniques. *Journal of Geomatics, 10*, 21–132.

Prakash, K., Singh, S., Mohanty, T., Chaubey, K., & Singh, C. K. (2017). *Morphometric assessment of Gomati River basin, middle Ganga plain*. Spatial Information Research. https://doi.org/10.1007/s41324-017-0110-x

Prakash, K., Rawat, D., Singh, S., Chaubey, K., Kanhaiya, S., & Mohanty, T. (2019). *Morphometric analysis using SRTM and GIS in synergy with depiction: A case study of the Karmanasa River basin, North central India*. Applied Water Science. https://doi.org/10.1007/s13201-018-0887-3

Rai, P. K. (2017). A GIS-based approach in drainage morphometric analysis of Kanhar River Basin, India. *Applied Water Science, 7*, 217–232.

Rai, P. K., Mishra, S., Ahmad, A., & Mohan, K. (2014). A GIS-based approach in drainage morphometric analysis of Kanhar River Basin India. *Applied Water Science*. https://doi.org/10.1007/s13201-014-0238-y

Reddy, G. P. O., Maji, A. K., & Gajbhiye, K. S. (2004). Drainage morphometry and its influence on landform characteristics in a basaltic terrain, Central India – A remote sensing and GIS approach. *Journal of Applied Earth Observation and Geoinformatics, 6*, 1–16.

Ritter, D. F., Kochel, R. C., & Miller, J. R. (2002). Process geomorphology wavel and press. In I. L. Long Grove, E. A. Keller, & N. Pinter (Eds.), *Active tectonics: Earthquakes uplift and landscape* (2nd ed., p. 362). Prentice Hall.

Rogers, J. J. (1986). The Dharwar craton and the assembly of peninsular India. *The Journal of Geology, 94*(2), 129–143.

Roy, A., & Bandyopadhyay, B. K. (1990). Cleavage development in Mahakoshal group of rocks of Sleemanabad-Sihora area, Jabalpur District, Madhya Pradesh. *Indian Miner, 44*(2–3), 111–128.

Rudraiah, M., Govindaiah, S., & Vittala, S. S. (2008). Morphometryusing remote sensing and GIS techniques in the sub-basins of Kagna River Basin, Gulbarga district, Karnataka, India. *Journal of Indian Society of Remote Sensing, 36*, 351–360.

Schumm, S. A. (1986). Alluvial river response to active tectonics. *Active Tectonics*, 80–94.

Schumm, S. A. (1956). Evolution of drainage systems and slopes in badlands at Perth Amboy, New Jersey. *Geological Society of American Bulletin, 67*, 597–646.

Shukla, T., Verma, A., Adnan, A., Pandey, M., & Shukla, U. K. (2014). Scarp sandstone: An example of estuarine sedimentation within the Mesoproterozoic Kaimur Group of the Vindhyan Basin, (Mirzapur, U.P.) India. *Journal of Paleontological Society of India, 59*, 45–58.

Singh, P., Thakur, J., & Singh, U. C. (2013). Morphometric analysis of Morar River basin, Madhya Pradesh, India, using remote sensing and GIS techniques. *Environmental Earth Science, 68*, 1967–1977.

Singh, S., & Kanhaiya, S. (2015). Morphometry of the Barakar River Basin, India. *International Journal of Current Research, 7*(7), 17948–17955.

Singh, S., Kanhaiya, S., Singh, A., & Chaubey, K. (2018a). Drainage network characteristics of the Ghaggar River Basin (GRB), Son Valley, India. *Geology, Ecology, and Landscapes*. https://doi.org/10.1080/24749508.2018.1525670

Singh, S., Kumar, S., Mittal, P., Kanhaiya, S., Prakash, P., & Kumar, R. (2018b). Drainage Basin parameters of Bagh River, a sub-basin of Narmada River, Central India: Analysis and Implications. *Journal of Applied Geochemistry, 20*(1), 91–102.

Singh, S., Prakash, K., & Shukla, U. K. (2020). Spatiotemporal migration of the River Ganga in middle Ganga Plane: Application of remote sensing and GIS technique. *Journal of the Indian Society of Remote Sensing*. https://doi.org/10.1007/s12524-020-01170-z

Singh, S., Singh, A. K., Kumar, P., & Jaiswal, M. K. (2021). Morphotectonic analysis of the Bihar River, Madhya Pradesh, India. In *Proceedings of the Indian national science academy*, 87, 163–174

Singh, S., Kanhaiya, S., Kumar, S., & Yadav, S. K. (2022). Spatial and temporal variation in NDVI and NDWI of the Ukhma River Basin, Central India. *Journal of Scientific Research, 66*(3), 62–65

Snow, R. S., & Slingerland, R. L. (1990). Stream profile adjustment to crustal warping: Nonlinear results from a simple model. *Geology, 98*, 699–708.

Solangi, G. S., Siyal, A. A., & Siyal, P. (2019a). Analysis of Indus Delta groundwater and surface water suitability for domestic and irrigation purposes. *Civil Engineering Journal, 5*(7), 1599–1608.

Solangi, G. S., Siyal, A. A., & Siyal, P. (2019b). Spatiotemporal dynamics of land surface temperature and its impact on the vegetation. *Civil Engineering Journal, 5*(8), 1753–1763.

Sreedevi, P. D., Owais, S., Khan, H., & Ahmed, S. (2009). Morphometric analysis of a watershed of South India using SRTM data and GIS. *Journal of Geological Society of India, 73*, 543–552.

Sreedevi, P. D., Subrahmanyam, K., & Shakeel, A. (2004). The significance of morphometric analysis for obtaining groundwater potential zones in a structurally controlled terrain. *Environmental Geological, 47*, 412–420.

Srivastava, D. C., & Sahay, A. (2003). Brittle tectonics and pore-fluid conditions in the evolution of the great boundary fault around Chittaurgarh, northwestern India. *Journal of Structural Geology, 25*, 1713–1733.

Stock, J. D., & Montgomery, D. R. (1999). Geologic constraints on bedrock river incision using the stream power law. *Journal of Geophysical Research: Solid Earth, 104*, 4983–4993.

Strahler, A. N. (1957). Quantitative analysis of watershed geomorphology. *Eos, Transactions American Geophysical Union, 38*(6), 913–920.

Strahler, A. N. (1958). Dimensional analysis applied to fluvially eroded landforms. *Geological Society of American Bulletin, 69*, 279–300.

Strahler, A. N. (1964). Quantitative geomorphology of drainage basin and channel networks. Section 4ii in *Handbook applied hydrology 4–39 to 4–76*.

Tewari, H. C., Murthy, A. S. N., Kumar, P., & Sridhar, A. R. (2001). A tectonic model of the Narmada region. *Current Science, 80*, 873–878.

Thomas, J., Joseph, S., & Thrivikramaji, K. P. (2010). Morphometric aspects of a small tropical mountain river system, the southern Western Ghats, India. *International Journal of Digital Earth, 3*, 135–156.

Vandenberghe, J. (2002). The relation between climate and river processes, landforms and deposits during the quaternary. *Quaternary International, 91*(1), 17–23.

Verma, A., & Shukla, U. K. (2020). Heterolithic lower Rewa sandstone of the Neoproterozoic Rewa group, Vindhyan Basin, U. P., India: An example of tidal point bar. *Precambrian Research, 350*, 105932. https://doi.org/10.1016/j.precamres.2020.105932

Verma, P. K. (1996). Evolution and age of the great boundary fault of Rajasthan. *Geological Society of India Memoirs, 36*, 197–212.

Verma, R. K. (1991). *Geodynamics of the Indian Peninsula and the Indian plate margin*. Oxford and IBH. 357pp.

Vittala, S. S., Govindiah, S., & Honne, G. H. (2004). Morphometric analysis of sub-watersheds in the pavagada area of Tumkur district, South India, using remote sensing and GIS techniques. *Journal of Indian Society of Remote Sensing, 32*, 351–362.

Waikar, M. L. (2014). Morphometric analysis of a Drainage Basin using geographical information system: A case study. *International Journal of Multidisciplinary and Current Research, 2*, 180–184.

# Index





S. Kanhaiya et al. (eds.), *Rivers of India*,
https://doi.org/10.1007/978-3-031-49163-4